QUANTIFICATION AND OPTIMISATION OF THE BENEFITS AND RISKS OF URBAN CYCLING

Ronan Doorley

A dissertation submitted to the University of Dublin in partial fulfilment of the requirements for the degree Doctor of Philosophy.

Department of Civil, Structural and Environmental Engineering
Trinity College Dublin

September 2017

DECLARATION

I declare that this thesis has not been submitted as an exercise for a degree at this or any other university and it is entirely my own work.

I agree to deposit this thesis in the University's open access institutional repository or allow the library to do so on my behalf, subject to Irish Copyright Legislation and Trinity College Library conditions of use and acknowledgement.

September 2017

_____

Ronan Doorley

SUMMARY

This thesis reports on a research project aimed at developing comprehensive methods for quantifying the benefits and risks of urban cycling, investigating the environmental exposures of cyclists and developing a tool for optimising the design of cycling infrastructure. These goals have been achieved through a combination of statistical modelling, mathematical programming and data collection and analysis. There are many good reasons to encourage urban cycling such as the reductions in the social costs of air and noise pollution and the promotion of active and healthy lifestyles. However, there are also risks associated with urban cycling such as traffic collisions and increased inhalation of air pollutants. Promotion of cycling also requires investment of resources such as capital and road space. For these reasons it is essential that all of these benefits and risks can be quantified in common units to enable evidence-based policy formulation. In order to mitigate the risks of cycling, the factors affecting the variability in these risks also need to be understood so that they can be mitigated. Finally, in order to design measures to promote cycling in such a way as to optimise for these impacts, it must be possible to model the change in travel behaviour and associated impacts resulting from such measures.

The first step taken in this thesis was to conduct a thorough review of the literature relating to quantification of health and environmental impacts of transportation, in-travel environmental exposures and modelling of travel behaviour. The literature review revealed that there was significant heterogeneity in the modelling techniques and a lack of studies which considered the variation in benefits and risks experienced by individual cyclists. A comprehensive framework was therefore developed to quantify the health, environmental and travel time impacts of cycling. Different mathematical models from the literature were used to quantify impacts related to physical activity, pollution inhalation, traffic collisions, noise, vehicle emissions and travel time. Using census data, this framework was applied to a case study of an increase in cycling in Dublin. It was shown that, at a societal level, the total net health and environmental impacts of increased cycling in Dublin would be strongly positive. When travel costs are also considered, the uncertainty becomes greater but the best estimate of the net impact is still positive. A framework was also developed for quantification of the expected benefits and risks experienced by an individual cyclist switching from driving to cycling. The application of this framework to a case study of Dublin was the first study to investigate the variation in health impacts of cycling experienced by individuals of different ages, genders and travel distances. A stochastic simulation approach was employed in order to calculate distributions of each health impact reflecting both the uncertainty in the model parameters and the variation among

individual characteristics. It was shown that for some groups, in particular males aged 20-30, cycling can have negative expected net health impacts.

The literature review also indicated that one particular health impact of cycling—in-travel pollutant inhalation—was relatively poorly understood in terms of the factors affecting its variation. In order to investigate this further using an exposure study, a new environmental sensing node—the BEE node—was first designed and built using relatively low-cost pollution sensors and electronics. The BEE node's gaseous pollutant measurements were calibrated and validated to a degree of accuracy comparable with much bulkier and expensive equipment. Using the BEE node, two studies of the environmental exposures of cyclists in Dublin were designed and carried out. Volunteer cyclists cycled through Dublin while collecting data about the pollution and noise they were exposed to. These data were analysed along with time-resolved information about the cycling facilities they used, the vehicle traffic volumes they interacted with and the weather conditions. The analysis produced new insights such as the observation that while segregated cycle lanes decreased pollution exposures, roadside cycle lanes and bus lanes actually increased exposures.

Having developed models for quantifying the benefits and risks of cycling, the next step was to develop a model for predicting the change in levels of cycling and driving which would result from a given intervention. This required a disutility function for cycling and while a small number of studies have previously suggested functional forms, no study had attempted to calibrate or validate such a function. A new method for calibrating a cycling disutility function was therefore developed. The method involves formulating the calibration problem as a Mathematical Programme with Equilibrium Constraints (MPEC) and solving the MPEC using a descent-based method. A new cycling disutility function—the DOC function—was also proposed based on previous research into the factors affecting cycling disutility. Using the newly developed calibration method, this function was calibrated and its accuracy was validated based on data from the Dublin network.

The final contribution of this thesis was a tool for systematically designing a cycle network in order to optimise the resulting net impacts to the network users and society. This Network Design Problem (NDP) is formulated as an MPEC and a solution approach is presented which is uses a genetic algorithm (GA) to find the optimal solution. The problem formulation and solution algorithm are tested using a numerical example and the GA algorithm was shown to efficiently converge to a near-optimal solution for the cycle network design.

ACKNOWLEDGEMENTS

Firstly, I would like to thank my supervisors Bidisha Ghosh and and Vikram Pakrashi for putting so much time and energy in advising and guiding me through my PhD and helping me to develop as a researcher.

Thanks also to all the other professors and staff at TCD who provided expert advice and assistance, especially Dr. Francesco Pilla, Dr. Kevin Ryan, Dr. Brian Caulfield, Dr. Aonghus McNabola, Patrick Veale, Dr. John Kennedy and David McAulay. Thanks also to Dr. Wai Yuen Szeto for his valuable advice.

This research would have been impossible without the financial support of the Environmental Protection Agency of Ireland. Special thanks also to Kevin Delaney and Micheal O'Dwyer for providing me with pollution data and helping me with my experiments.

Thanks to the National Transport Authority and especially Peter O'Sullivan and John Nott for very patiently walking me through their transport models and providing me with data. Thanks to all those at Dublin City Council who helped me to collect traffic and pollution data, particularly Dave Traynor, Karen Hosie and Martin Fitzpatrick.

I would like to thank all the students who helped me with my research, especially Conor de Courcy, Giacinto Rittgers and Patricia Nogueira.

Finally, a big thank you to my family for supporting me throughout this endeavour and only rarely making fun of my eternal student status.

TABLE OF CONTENTS

Declaration ii
Summary iii
Acknowledgements v
Table of Contents vi
List of Abbreviations viii
List of Figures xi
List of Tables xiv
Chapter 1: Introduction 1
1.1 Research Objectives 1
1.2 Organisation of thesis 2
Chapter 2: Literature Review 5
2.1 Quantification of the health impacts of active travel 5
2.2 Measurement and characterisation of environmental exposures of cycling 28
2.3 Models of cyclist travel behaviour 39
2.4 Evaluation and optimisation of cycle networks. 49
2.5 Scope of Research 53
Chapter 3: Quantifying the Benefits and Risks of Urban Cycling in Dublin; Total Societal Impacts 57
3.1 Case Study of Dublin 58
3.2 Estimation of Impacts 60
3.3 Results and Discussion 71
3.4 Conclusion 80
Chapter 4: Quantifying the Benefits and Risks of Urban Cycling in Dublin; Individual and Marginal Societal Impacts 83
4.1 Scenario Design 84
4.2 Estimation of Health Impacts 86
4.3 Results and Discussion 93
4.4 Conclusions 103
Chapter 5: Development of Environmental Sensing Node 105
5.1 Design Requirements 106
5.2 Development 108
5.3 Conclusions 127

Chapter 6: Environmental Exposure of Cyclists in Dublin 129
6.1 Introduction 129
6.2 Pilot Study: NO_x exposures of a cyclist on fixed routes in Dublin 129
6.3 Full Scale Exposure Study: exposure of commuter cyclists to NOx, CO, PM2.5 and Noise in Dublin 138
6.4 Conclusions 154
Chapter 7: A Cycling Cost Function; development, validation and calibration 157
7.1 The Combined Mode Choice and Traffic Assignment Problem 159
7.2 The Disutility of Cycling (DOC) Function 161
7.3 The Inverse Combined Mode Choice and Traffic Assignment Problem (I-CMC-TAP) 163
7.4 Solving the I-CMC-TAP 165
7.5 Numerical Experiment 166
7.6 Calibration of cost function for Dublin city network 175
7.7 Conclusions 191
Chapter 8: Optimal design of cycle networks 193
8.1 Introduction 193
8.2 Methodology 194
8.3 Numerical Example 199
8.4 Effect of GA parameters 208
8.5 Conclusions 212
Chapter 9: Conclusions 215
9.1 Main Contributions 215
9.2 Critical Assessment 217
9.3 Policy Implications and Directions for Future Research 219
Chapter 10: Appendices 221
10.1 Jacobians of KKT equations 221
10.2 Dissemination from thesis 225
10.3 Participant Information and Consent Form 226
References 230

LIST OF ABBREVIATIONS

Abbreviation	Explanation
ADC	Analogue to digital converter
ADT	Annual Daily Traffic
AIS	Abbreviated Injury Scale
APHEIS	Air Pollution and Health: A European Information System
BC	Black carbon
BEE	Bicycle Environmental Exposures
BIC	Bayesian Information Criterion
BLOS	Bicycle Level of Service
BOD	Burden of Disease
BPR	Bureau of Public Roads
CAF	Common Appraisal Framework
CBA	Cost Benefit Analysis
CMC-TAP	Combined Mode Choice and Traffic Assignment Problem
CO	Carbon Monoxide
CO_2	Carbon Dioxide
COPERT	A software tool used to calculate air pollutant and greenhouse gas emissions from road transport
CSO	Central Statistics Office
DALYs	Disability Adjusted Life Years
DAQ	Data acquisition system
DCC	Dublin City Council
DOC	Disutility of Cycling
DRF	Dose-response function
DUE	Determinstic User Equilibrium
EC	Elemental carbon
EPA	Environmental Protection Agency
FSM	Fixed site monitor
GA	Genetic Algorithm
GCoT	Generalised costs of travel
GDA	Greater Dublin Area
GDP	Gross Domestic Product
GHG	Greenhouse Gas
HEAT	Health Economic Assessment Tool
HEATCO	"Developing Harmonised European Approaches for Transport Costing and Project Assessment", EU FP6 project, runtime 2004-2006
HRM	Heart rate monitor
I-CMC-TAP	Inverse Combined Mode Choice and Traffic Assignment Problem

Abbreviation	Explanation
IMPACT	"Internalisation Measures and Policies for All external Cost of Transport", study on behalf of European Commission, runtime 2007-2008
IPAQ	International Physical Activity Questionnaire
ITAP	Inverse Traffic Assignment Problem
KKT	Karush-Kuhn-Tucker
MAPE	Mean Average Percentage Error
MET	Metabolic Equivalent of Task
MPEC	Mathematical Programme with Equilibrium Constraints
MS	Modal Split
NDP	Network Design Problem
NMVOC	Non-methane volatile organic compounds
NO_x	Nitrogen oxides
NPV	Net Present Value
NTA	National Transport Authority
O3	Ozone
OPC	Optical particle counter
PCT	Propensity to Cycle Tool
PCU	Passenger car units
$PM_{2.5}$	Particulate matter with aerodynamic diameter of 2.5µm or less
PNC	Particle number concentration
POWCAR	Place of Work – Census of Anonymised Records
POWSCAR	Place of Work, School or College – Census of Anonymised Records
RH	Relative humidity
RR	Relative Risk
RS	Reference scenario
RSA	Road Safety Authority
SB	Societal Benefit
SDM	System Dynamics Modelling
SIN	Safety in Numbers
SO_2	Sulphur dioxide
STRADA	Swedish Traffic Accident Data Acquisition
SUE	Stochastic User Equilibrium
TAP	Traffic Assignment Problem
TREMOVE	Policy assessment model and transport and environmental database, owned by the European Commission
TS	Test Scenario
UFPs	Ultra fine particles
USDHHS	United States Department of Health and Human Services
VE	Minute ventilation rate

Abbreviation	Explanation
VI	Variational Inequality
VOCs	Volatile Organic Compounds
VOLY	Value of a Life Year
VoT	Value of Time
VSL	Value of a Statistical Life
WHO	World Health Organisation
YLDs	Years of healthy Life lost to Disability
YLLs	Years of Life Lost

LIST OF FIGURES

Figure 1.1 Organisation of the thesis. Legend provides explanations of connections between chapters 4
Figure 2.1 Process Flow for Quantification of the Health Impacts of Active Travel 10
Figure 2.2 Dose Response Function (DRF) Process Flow 11
Figure 3.1 Commuters converted from driving to cycling in the case where all driving trips <5km are cycled. 75
Figure 3.2 Vehicle km avoided by converting trips from driving to cycling in the case where all driving trips <5km are cycled. 76
Figure 3.3 Summary of health and environmental impacts. Bars indicate upper and lower bounds. 77
Figure 3.4 Comparison of models for health impact of physical activity 77
Figure 3.5 Summary of less significant impacts of cycling uptake. 79
Figure 3.6 Summary of health, environmental and travel-cost impacts. Bars indicate upper and lower bounds. 79
Figure 4.1 Process of defining the reference scenario and test scenario in each iteration 86
Figure 4.2 Process of estimating individual and external health impacts resulting from one additional cyclist 87
Figure 4.3 Distributions of health impacts in the Current and Smarter Travel MS 95
Figure 4.4 Net individual health impacts and net marginal external health impacts in the Current and Smarter Travel MS 96
Figure 4.5 DALYs saved by male test subjects disaggregated by age 98
Figure 4.6 DALYs saved by female test subjects disaggregated by age 99
Figure 4.7 Relationship between DALYs saved and commute distance for male test subjects disaggregated by age 100
Figure 4.8 Relationship between DALYs saved and commute distance for female test subjects disaggregated by age 101
Figure 5.1 Alphasense NO2-B42F sensor (Alphasense, 2015a) 110
Figure 5.2 Raspberry Pi Miniature Computer (Raspberry Pi, 2016) 111
Figure 5.3: Screenshot from myTracks app 112
Figure 5.4 Functional diagram of sensing node 1st prototype 113
Figure 5.5 A cyclist carrying the sensing node 1st prototype in a backpack. 113
Figure 5.6 Collocated inlets of sensing node (red funnel) and DCC fixed site monitors (clear plastic) at Coleraine st. 115

Figure 5.7 NO_x values from DCC reference sensor vs NO_x values estimated from calibration model 115
Figure 5.8 Alphasense Optical Particle Counter OPC-N2 117
Figure 5.9 Microphone with wind shield mounted on backpack 118
Figure 5.10 Adafruit GPS module and antenna 119
Figure 5.11 Functional diagram of sensing node 2nd prototype 120
Figure 5.12 Comparison of time series data from Alphasense CO-B4 and EPA reference sensor 124
Figure 5.13 NOx values from reference sensor vs NOx values estimated from calibration model. 125
Figure 5.14 Recorded signal from sound calibrator 126
Figure 6.1 Pilot study routes with counter locations (Google Maps, 2015) 131
Figure 6.2 NOx concentrations measured in pilot study in Dublin city. 133
Figure 6.3 Google Street View of NOx hotspot close to Temple Bar area of Dublin (Google Maps, 2014) 134
Figure 6.4 Average NOx exposure concentrations by facility type in pilot study 134
Figure 6.5 Cycling facility types on both routes in the pilot study 135
Figure 6.6 Distributions of recorded pollution exposures in full scale study 144
Figure 6.7 All CO concentrations measured in full scale exposure study 145
Figure 6.8 All NO_x concentrations measured in full scale exposure study 146
Figure 6.9 All noise levels measured in full scale exposure study 147
Figure 6.10 All $PM_{2.5}$ concentrations measured in full scale exposure study 148
Figure 7.1 Sioux Falls Test Network 167
Figure 7.2 Map of Sioux Falls 168
Figure 7.3 Predicted and actual flows on unobserved links 175
Figure 7.4 The Greater Dublin Area (National Transport Authority, 2015a) 177
Figure 7.5 Components of the NTA Peak GDA Model (National Transport Authority, 2011b) ... 178
Figure 7.6 Comparison of (a) CSO Small Areas and (b) NTA zones and their centroids 180
Figure 7.7 Motor vehicle network and segregated cycle network of GDA 182
Figure 7.8 Motor vehicle network and segregated cycle network of Dublin city centre. 182
Figure 7.9 Links in city centre for which flow observations were available 183
Figure 7.10 Scatterplot of predicted vs observed flows on the links of the test set. 190
Figure 7.11 Prediction errors on test links; link widths shown are proportional to absolute percentage errors. 190

Figure 7.12 Empirical CDFs of absolute percentage errors on the test set using (i) shortest path assignment and (ii) assignment using the Disutility of Cycling (DOC) function. 191
Figure 8.1 Test network 200
Figure 8.2 Car traffic in base case (no cycling facilities). Link thickness is proportional to traffic volume. 204
Figure 8.3 Bicycle traffic in base case (no cycling facilities). Link thickness is proportional to traffic volume. 204
Figure 8.4 Societal benefit values at baseline (no cycle facilities) 205
Figure 8.5 Evolution of best-so-far fitness in initial run of GA 207
Figure 8.6 Cycle network design suggested by initial run of GA 207
Figure 8.7 Societal benefit values resulting from solution of initial GA run 208
Figure 8.8 Influence of GA parameters P_c and P_m on the optimum SB value found by the GA and the iterations taken to find it. 210
Figure 8.9 Best cycle network design found across all runs of GA 211
Figure 8.10 Value of P_c and P_m for the GA runs which found the overall best solution. The highlighted box shows the suggested interval. 211

LIST OF TABLES

Table 2.1 Summary of studies reviewed 8
Table 2.2 Health summary measures and monetisation in studies reviewed 13
Table 2.3 Summary of physical activity effects considered in studies reviewed 17
Table 2.4 Summary of pollution effects considered in studies reviewed 19
Table 2.5 Summary of road traffic collision analysis in studies reviewed 26
Table 2.6 Summary of studies which compare pollution exposure concentrations across modes 33
Table 2.7 Studies which analyzed factors affecting cyclist pollution exposure concentrations 35
Table 2.8 Studies using the ITAP to calibrate network model parameters. 47
Table 3.1 Commuter trips by car/van, bicycle, walking and public transport (PT) in county Dublin as per census, 2011 59
Table 3.2 Outline of models used to quantify and monetise impacts of active travel 61
Table 3.3 Unit costs for avoided external impacts 70
Table 3.4 Change in traffic collision casualties. 78
Table 4.1 Fatality and Injury risk factors by age and gender 92
Table 4.2 Mean YLLs and YLDs saved per year due to uptake of cycling by individual commuters. Positive values indicate health benefits. 94
Table 4.3 Mean change in Traffic Collision DALYs in each modal split stage 102
Table 5.1 Measurement capabilities of each prototype of the BEE node 108
Table 6.1 Summary of data collected in pilot study 133
Table 6.2 Parameters of the Linear Mixed Model of log(NOx Concentration) for the pilot study 137
Table 6.3 Parameters of the linear mixed model of ln(NOx Intake/metre) for the pilot study... 137
Table 6.4 Demographics of the study group of the full scale exposure study..... 139
Table 6.5 Summary of data collected by facility type in full scale exposure study 142
Table 6.6 Correlations between the observed data in the full scale exposure study 143
Table 6.7 Mixed Effects Model for log(CO Concentration)..... 149
Table 6.8 Mixed Effects Model for log(NO_x Concentration) 150
Table 6.9 Mixed Effects Model for Noise..... 150
Table 6.10 Mixed Effects Model for log($PM_{2.5}$ Concentration)..... 151
Table 6.11 Mixed Effects Model for log(CO Intake)..... 151
Table 6.12 Mixed Effects Model for log(NO_x Intake) 152
Table 6.13 Mixed Effects Model for log($PM_{2.5}$ Intake)..... 152

Table 7.1 Notation: Travel modes 158
Table 7.2 Notation: Sets 158
Table 7.3 Notation: Variables 158
Table 7.4 Notation–constants 159
Table 7.5 Upper and lower limits of each calibration parameter in the numerical experiment. 172
Table 7.6 Solving the I-CMC-TAP using the descent algorithm with sensitivity analysis 173
Table 7.7 Calibration results of the numerical experiment 175
Table 7.8 Upper and lower limits on model parameters. 186
Table 7.9 Solving the ITAP using the descent algorithm with empirical gradients 187
Table 7.10 Calibration of DOC function results 189
Table 8.1 Steps of the Genetic Algorithm for solving the MPEC 198
Table 8.2 Link characteristics of test network 200
Table 8.3 Route characteristics of test network 201
Table 8.4 Link traffic volumes in base case (no cycle facilities) 205

Chapter 1: Introduction

The overarching goal of this thesis was to develop models to quantify the benefits and risks of urban cycling and tools to allow these benefits and risks to drive infrastructure design and investment.

There are many reasons why it is important to quantify and optimise for the benefits and risks of urban cycling. Cycling as a mode of transport avoids the negative external costs of driving such as air pollution, carbon emissions and noise and can also reduce the public health costs associated with physical inactivity and obesity. However, there are also risks associated with urban cycling which should be managed. These risks include traffic collisions and in-travel inhalation of harmful air pollutants. Any measures to promote cycling such as infrastructure provision and financial incentives also have a monetary cost. Therefore, it is essential that the health and environmental benefits and risks of urban cycling can be quantified in order to inform evidence-based policy formulation.

Transportation engineers, urban planners and politicians cannot act to increase the modal shares of cycling directly. They can only implement measures which are expected to influence modal shares such as building new cycle lanes or offering tax relief on purchases of bicycles used for commuting. For this reason, there is also a need for models which can predict the changes in cycling modal shares and route choices which would result from particular interventions. The ideal solution would be an end-to-end tool allowing stakeholders to design cycling-focussed interventions in order to maximise the resulting societal benefit. With this overall goal in mind, the specific objectives of this thesis are outlined in the next section.

1.1 Research Objectives

The main objectives of this thesis are:

1. To develop a comprehensive framework for quantification of the health, environmental and travel time impacts of increases in urban cycling at a societal level and to demonstrate this framework with a case study.
2. To develop a framework for quantifying the health impacts of a single individual switching from driving to cycling and to assess whether or not the expected health impacts of cycling are positive for all age and gender groups.
3. To design and build a prototype environmental sensing node capable of being carried by a cyclist and monitoring their exposure to gaseous and particulate pollution.

4. To investigate the extent to which the environmental exposures of cyclists are affected by factors such as motor vehicle traffic, cycling facilities and weather conditions.
5. To develop a methodology for calibrating a disutility function for cyclists based on cyclist traffic observations on a small number of roads, and to use this methodology to produce and validate a suitable disutility function for cyclists.
6. To develop a tool capable of finding the optimal design for a cycle network in an existing road network, taking into account health, environmental and travel time impacts as well as infrastructure costs.

1.2 Organisation of thesis

The organisation of the rest of this thesis, which is illustrated in Figure 1.1 is as follows. Chapter 2 reviews the relevant literature in four research areas related to this thesis: quantifying the health and environmental impacts of cycling, monitoring of in-travel environmental exposures, analysis of travel-behaviour of cyclists and macroscopic modelling of transportation networks.

Based on the insights gained from Chapter 2, Chapter 3 develops models for comprehensively quantifying the total societal impacts of a given increase in the modal share of cycling. The framework is also applied to a case study of Dublin and the results are reported.

One of the findings from the literature review was that there has been a lack of research into the benefits and risks of cycling at an individual level. Chapter 4 describes a study carried out to addresses this need. Models are developed for quantifying the distribution of health benefits and risks experienced by individuals who switch from driving to cycling. A case study of Dublin is carried out and the results are reported.

One particular health impact of urban cycling—in-travel exposure to air pollution—was found in the literature review to be relatively poorly understood in terms of the factors affecting its variability. In order to address this problem using an exposure study, a custom environmental sensing node, suitable for use by urban cyclists, was developed and calibrated. This process is described in Chapter 5.

Chapter 6 describes the planning, implementation and results of two field studies which investigated the factors affecting the environmental exposures of cyclists. These studies made use of the sensing node developed in Chapter 5.

With models in place for quantifying the benefits and risks of given amounts of cycling, the next step was to develop a model for predicting the change in levels of cycling and driving which

would result from a given intervention, such as a new piece of infrastructure. Chapter 7 describes a study which achieved this by proposing a new disutility function for cycling, calibrating its parameters and validating its accuracy in predicting cyclist behaviour.

Chapter 8 builds on the foundations of all the previous chapters in order to develop a modelling framework and solution algorithm for the optimal design of cycle networks, taking into account the health and environmental impacts of cycling and driving.

Chapter 9 concludes the thesis by summarising the main contributions of the thesis, providing a critical assessment of the research, discussing the implications for research and policy and suggesting some directions for future research.

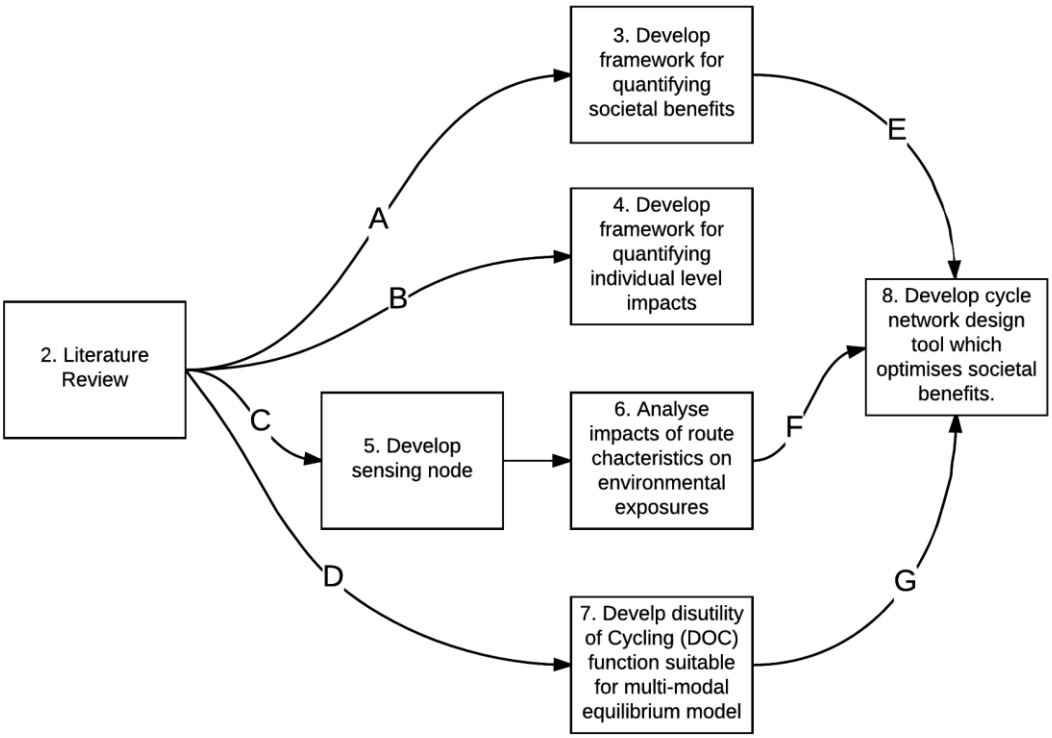

A: The literature lacked a consistent and comprehensive methodology for quantifying health and environmental impacts of cycling.
B. Previous studies had quantified the societal impacts of cycling but no studies had quantified the distribution of impacts impacts at an individual level.
C. Studies of route-level determinants of environmental exposures had inconsistent results where facilities and traffic levels were concerned. They also had not considered NOx.
D. Inclusion of cycling in a multi-modal equilibrium model requires a calibrated route disutility function for cyclist and no such function exists in the literature.
E. Framework developed in chapter 3 used in societal benefit calculation of the MPEC in chapter 8.
F. Concentration exposure factors found in chapter 6 used in societal benefit calculation of the MPEC in chapter 8.
G. Calibrated route disutility function developed in chapter 7 used in the equilibrium model of the MPEC in chapter 8.

Figure 1.1 Organisation of the thesis. Legend provides explanations of connections between chapters

Chapter 2: Literature Review

The research reported in this thesis lies at the intersection of several fields of research and, as such, builds on previous works in diverse fields. In particular, this thesis builds on previous studies in the following areas: quantifying the health and environmental impacts of transport, monitoring of in-travel environmental exposures, analysis of travel-behaviour of cyclists and macroscopic modelling of transport networks. The most relevant research to date in each of these areas is described in this chapter in order to provide context for the original work to follow.

2.1 Quantification of the health impacts of active travel

This contents of this section are based on work reported in Doorley et al. (2015b).

2.1.1 Overview of Studies

A comprehensive review was carried out of studies which quantitatively assessed the health impacts of real or simulated transport scenarios involving increased active travel and included health outcomes such as mortality, life expectancy or Burden of Disease (BOD). An overview of the 24 studies considered in this review is given in Table 2.1. Nine of the studies considered changes in walking and seventeen considered changes in cycling. The study designs in the papers considered can be grouped into five broad categories: studies where actual data from before and after an intervention were used; studies where a sub-population underwent a hypothetical change in travel behaviour; studies where the entire population underwent a hypothetical change in travel behaviour; studies where travel behaviour responses to a hypothetical intervention were simulated and one study which simulated the impacts of policy changes using System Dynamics Modelling (SDM).

The first type of study design simply used recorded data regarding traveller behaviours before and after an intervention. However, in many cases reliable data regarding use of active travel is unavailable. Bike share schemes are a notable exception as they can provide reliable disaggregate information on the cycling patterns of a population in response to the introduction of the scheme. The first quantitative assessment of health impacts of such a scheme was conducted by (Rojas-Rueda et al., 2011) to evaluate the public bike sharing initiative, Bicing, in Barcelona, Spain. It was assumed that 90% of the trips made by Bicing users were new cycling trips which would have otherwise been made by car. However, this assumption has been criticised by Fishman (2011) who states that the available data show that only 9.6% of Bicing

trips substitute for a car journey and so, that study probably overestimated the benefits of the scheme. Fishman (2011) also evaluated the benefits of the Bicing scheme but used publicly available reports to estimate not only the number of trips and distance travelled per day, but also the proportions of these trips which were new trips and which substituted for trips by walking, private bike and other modes. A more recent study by Woodcock et al. (2014) evaluated the London bicycle sharing system, taking advantage of detailed user data. The modal shift attributable to the use of the scheme was estimated from survey responses from registered users which prevented unrealistic assumptions about the proportion of trips which were replacing car trips.

The second and most commonly used approach for defining scenarios was to consider a situation where some portion of current or future trips undertaken by private car was shifted to active travel and/or public transport. This approach assumes that a small sub-population can make a fundamental change to their travel behaviour without any change to the behaviour of the rest of society. The third approach, taken by four studies, (Jarrett et al., 2012; Maizlish et al., 2013; Woodcock et al., 2009; Woodcock et al., 2013) considered more holistic changes in travel behaviour whereby, instead of an isolated sub-population switching from motorised travel to active travel, the distribution of times spent in active travel across the whole population was shifted positively. Current and hypothetical transport scenarios being considered were used to derive mean distances walked and cycled per year and per week. Lognormal distributions (because distributions of time spent walking and cycling are non-negative and are empirically known to have long tails on the positive side of the peak) were fit about these means to give age-specific and sex-specific active travel-time distributions. A characteristic of all of these hypothetical approaches is that they give the assessment little value as a policy formulation instrument as no consideration is given to the courses of action which may help policymakers to achieve the scenarios.

The fourth approach evaluated the impacts of travel behaviour changes resulting from specific interventions. Two studies (de Nazelle et al., 2009; Dhondt et al., 2013) simulated travel behaviours before and after the intervention. using activity based travel analysis (Axhausen and Gärling, 1992). de Nazelle et al. (2009) developed a custom MATLAB (The MathWorks Inc., 2016) model, BESSTE (Built Environment Stochastic Spatial Temporal Exposure), to simulate travel activity patterns before and after a built environment transformation. Activity diaries were generated for each simulated individual from the Environmental Protection Agency's (EPA) Consolidated Human Activity Database (CHAD). The home locations and locations of daily

activities were then decided by a stochastic selection process subject to a trip generation gravity model, which models attraction between origins and destinations by an analogy to Newton's gravitational formula (Sheffi, 1985). The mode choice taken to access each destination was then selected using a logit model.

Dhondt et al. (2013) simulated travel activity patterns before and after an increase in the cost of fuel using the FEATHERS (Forecasting Evolutionary Activity-Travel of Households and their Environmental Repercussions) model, whose activity scheduling engine is based on decision trees derived from activity diary data. FEATHERS uses these sequential decision trees to predict where and when individual activities are conducted and - if transport is required - the mode taken, for a simulated population. Origin-destination matrices and modal choices are then extracted from the simulated activity patterns, and iteratively assigned to the road network. These activity based models have greater potential for the evaluation of transport policies or interventions than methods which simply define hypothetical transport scenarios without considering the instruments which may affect such changes. However, they are much more data and resource intensive and so, may not be suitable for many practical applications. Schepers et al. (2015) estimated the impacts of increasing the density of cycle facilities in a hypothetical Dutch city. Previous research into the relationship between cycle lane density and cycling mode share was used to estimate how much additional cycling would take place due to the additional infrastructure.

Finally, Macmillan et al. (2014) used SDM to simulate three policy scenarios. SDM is a field which incorporates knowledge of strategic decision making and feedback loops into simulation of complex bounded systems (Richardson, 2011). Using this framework, Macmillan and colleagues developed equations to simulate the effects of three intervention policies based on quantitative and qualitative research and local data. Feedback effects such as improvements in infrastructure in response to increases in cycling rates were also incorporated into their simulation.

Having defined the scenario of interest, the health impacts of the increase in active travel relative to a baseline or counter-factual could be estimated. Figure 2.1 and Figure 2.2 show a guideline of the various processes which were used for translating these study scenarios and interventions into quantified health impacts. In order to keep the diagrams compact, not every variation in these processes has been shown but the figures should give the reader an idea of the modelled pathways. These processes are discussed in sections 2.1.2 and 2.1.3.

Table 2.1 Summary of studies reviewed

Study	Scenario	Study Location	Active modes
de Nazelle et al. (2009)	Hypothetical built environment transformation	Orange County, NC, USA	Walking
Woodcock et al. (2009)	Hypothetical transportation strategies to reduce greenhouse gas emissions.	London, UK Delhi, India	Walking Cycling
Gotschi (2011)	Three hypothetical transport scenarios involving higher modal shares of cycling	Portland, Oregon	Cycling
Hartog et al. (2011)	Hypothetical transition from car driving to cycling for 500,000 people for short daily trips	Netherlands	Cycling
Lindsay et al. (2011)	Hypothetical transition from car driving to cycling for short trips	Urban areas in New Zealand	Cycling
Rojas-Rueda et al. (2011)	Assessment of existing bicycle share scheme	Barcelona, Spain	Cycling
Fishman et al. (2012)	Assessment of existing bicycle share scheme	Barcelona, Spain	Cycling
Grabow et al. (2012)	Hypothetical elimination of short automobile trips and replacement of 50% with cycling.	Upper midwestern USA	Cycling
Holm et al. (2012)	Hypothetical transition from car driving to cycling for trips to place of work or education on weekdays	Copenhagen, Denmark	Cycling
Jarrett et al. (2012)	Seven hypothetical scenarios where changes in transport contribute to reductions in CO_2 emissions.	Urban areas in England and Wales	Walking Cycling
Rabl and de Nazelle (2012)	Hypothetical transition from car driving to walking or cycling for commuting to and/or from work.	Not location-specific	Walking Cycling
Rojas-Rueda et al. (2012)	Eight hypothetical transport scenarios involving replacement of car trips by active travel and public transport	Barcelona, Spain	Walking Cycling
(Dhondt et al., 2013)	Hypothetical increase in fuel price	Flanders and Brussels, Belgium	Walking Cycling
Maizlish et al. (2013)	Three hypothetical transportation strategies to reduce greenhouse gas emissions (GHGE).	San Francisco Bay	Walking Cycling
Olabarria et al. (2013)	Hypothetical scenario where people not meeting physical activity guidelines convert walkable driving trips to walking.	Catalonia, Spain	Walking
Rojas-Rueda et al. (2013)	8 hypothetical transport scenarios involving replacement of car trips by active travel and public transport	Barcelona, Spain	Walking Cycling
Woodcock et al. (2013)	3 hypothetical scenarios described by the Visions 2030 project involving increased levels of walking, cycling, public transport and electric vehicle use.	Urban areas in England and Wales outside of London	Walking Cycling
Deenihan and Caulfield (2014)	Hypothetical increase in cycling share due to construction of a segregated cycleway.	Leinster, Ireland	Cycling
Edwards and Mason (2014)	Lifetime impact of switching from driving to cycling for a 10km daily round trip	U.S.A.	Cycling
Macmillan et al. (2014)	5 hypothetical policy scenarios over the next 40 years.	Aukland, New Zealand	Cycling

Study	Scenario	Study Location	Active modes
Woodcock et al. (2014)	Assessment of existing bicycle share scheme	London, UK	Cycling
Buekers et al. (2015)	Estimated actual cycling on two new bicycle highways.	Flanders	Cycling
Schepers et al. (2015)	Estimated travel behaviour changes in response to increased density of cycle lanes	Hypothetical Dutch city	Cycling
Rojas-Rueda et al. (2016)	Hypothetical transitions to walking and cycling from other modes.	Six European cities: Barcelona, Paris, Prague and Warsaw, Basel and Copenhagen	Walking Cycling

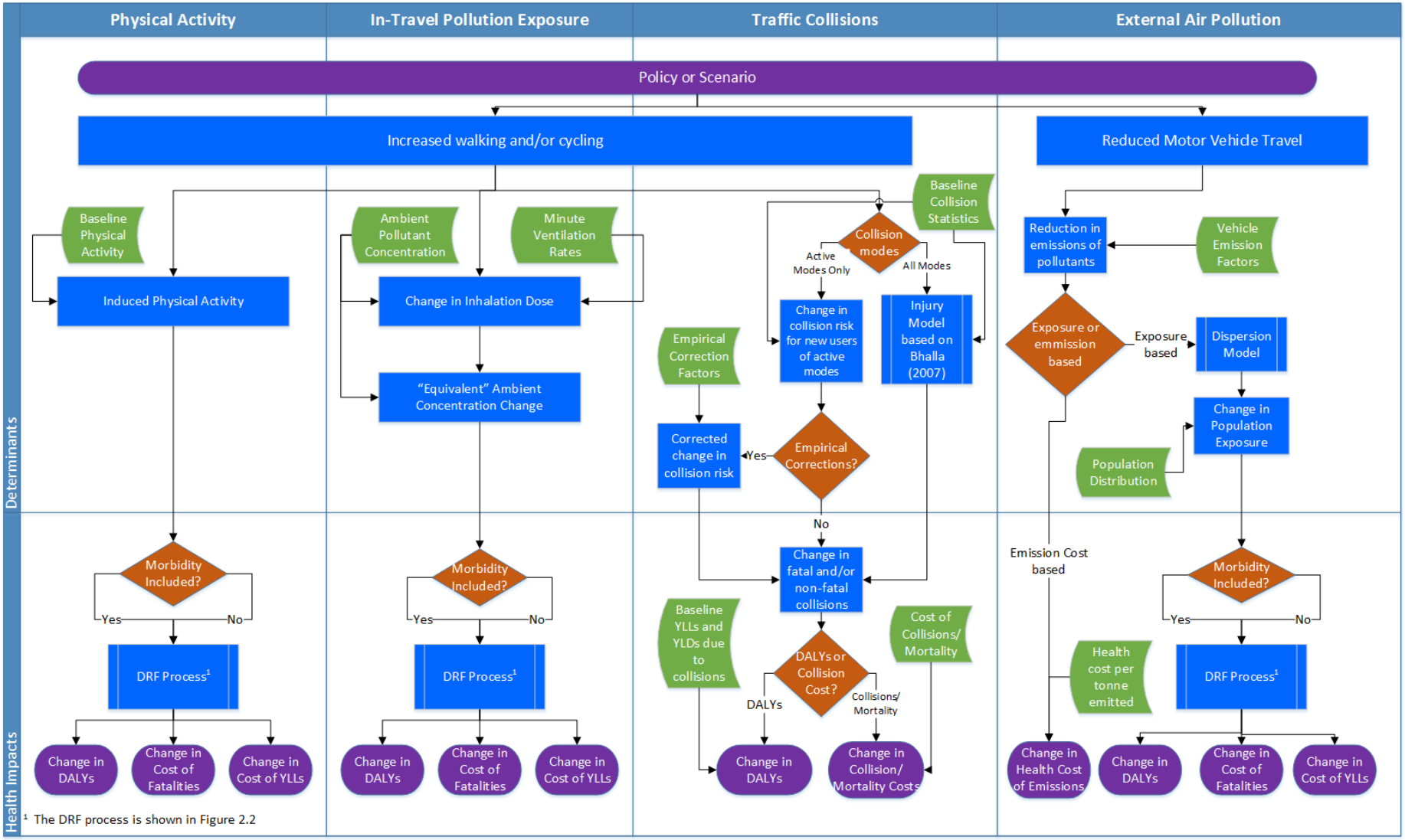

Figure 2.1 Process Flow for Quantification of the Health Impacts of Active Travel

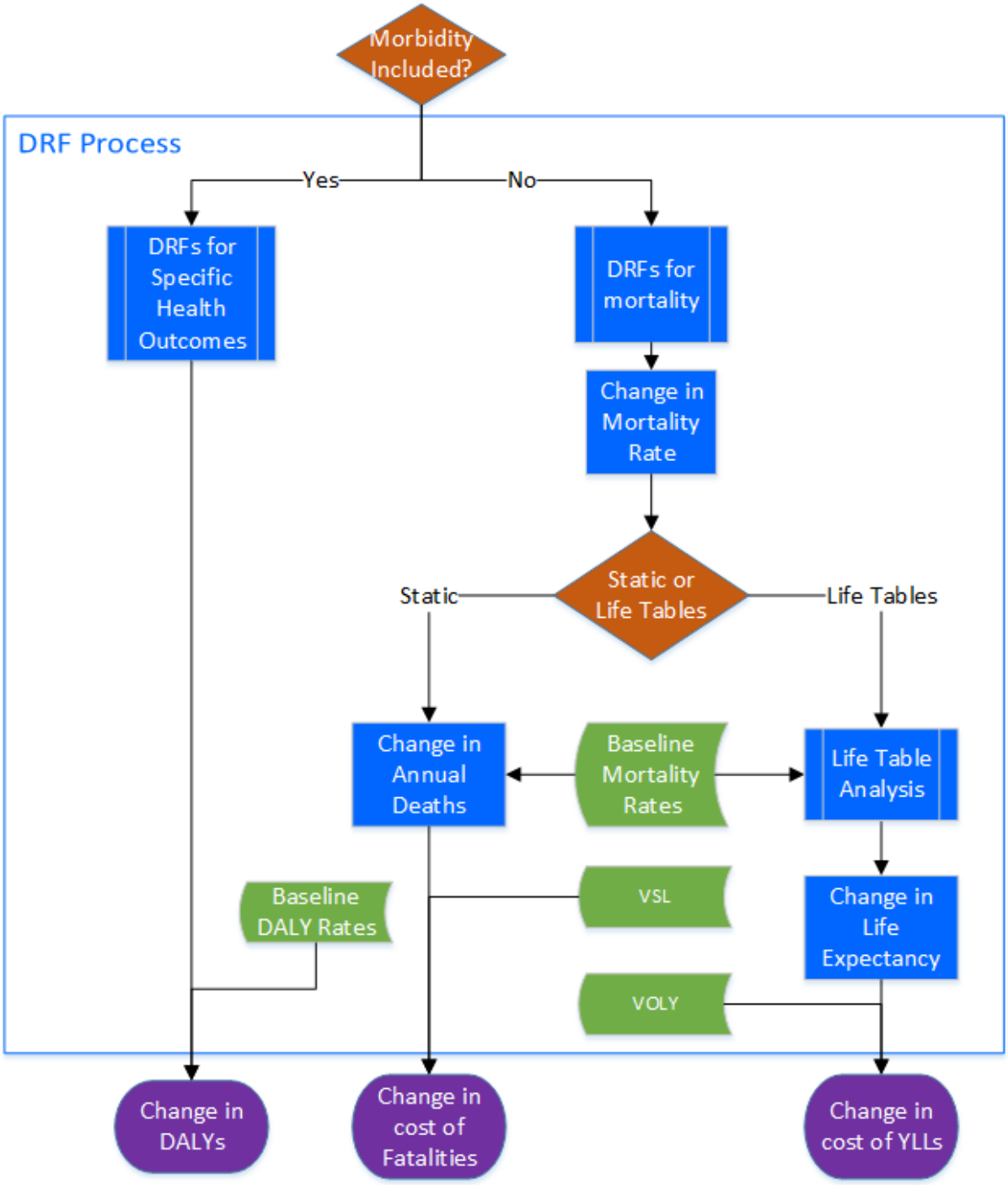

Figure 2.2 Dose Response Function (DRF) Process Flow

2.1.2 Outcome Variables

All studies reviewed used a health summary measure(s) as the outcome of interest which was (were) sometimes converted to a monetary equivalent. Table 2.2 and the bottom row of Figure 2.1 show the health summary measures which were the outcomes of interest in the studies reviewed. Although choice of transport mode can affect many aspects of both mortality and morbidity (Garber et al., 2011), many of the studies neglected morbidity. The Health Economic Assessment Tool (HEAT) released in 2011 (WHO, 2011) considers the economic value of reductions in mortality only and this was the most widely used tool for estimating the health effects of walking and cycling in the studies reviewed. As outlined in Rutter et al. (2013), evidence regarding all-cause mortality is considered to be more robust and so, the inclusion of morbidity would lead to greater uncertainty in the results of an assessment. Despite the apparent reliability of using all-cause mortality as the outcome variable, it can be expected that exclusion of the effects of morbidity in assessments of the health impacts of active travel may lead to underestimation of total health impacts. It should also be noted that in 2011, addressing morbidity was identified as the single most important improvement to be made to HEAT in future revisions (WHO, 2011) . However, focussing on mortality only may still be preferable in some cases. For example, when the aim is to influence policy, conservatism and transparency may be more important than precision. Several of the studies reviewed did consider morbidity as an outcome variable in addition to mortality. BOD is a summary measure of the impact of a disease on global health which takes into account both years lost and years spent in poor health. The BOD approach was taken by seven studies. It should be noted that BOD could produce more conservative results than mortality if the range of diseases considered is not comprehensive enough. For example, Rojas-Rueda et al. (2013) did not consider depression as an outcome but the studies of Woodcock and colleagues found significant increases in the BOD due to depression. Several other studies quantified individual health events such as hospitalisations or incidence of cancer.

Table 2.2 Health summary measures and monetisation in studies reviewed

Study	Health Summary	Unit of Measurement	Monetisation
de Nazelle et al. (2009)	-	-	-
Woodcock et al. (2009)	Disease-specific BOD	Deaths YLL YLD DALYs	-
Gotschi (2011)	All-Cause Mortality Cost of illness	Deaths Health care costs	VSL
Hartog et al. (2011)	All-Cause Mortality Disease-Specific Morbidity	Deaths Disease Incidence ER Visits School-loss days Worker Productivity	VSL "Damage Function" (BenMAP)
Lindsay et al. (2011)	All-Cause Mortality	YLLs	-
Rojas-Rueda et al. (2011)	Mortality Morbidity Health Care Costs Energy Expenditure	Deaths Restricted Activity Days Hospital Admissions kJ expended over baseline MET rate	VSL Cost per Health Event (HAPiNZ)
Fishman et al. (2012)	All-Cause Mortality	Deaths	-
Grabow et al. (2012)	Mortality Morbidity	Not Stated	Value per km of cycling Value per km of walking
Holm et al. (2012)	Disease-specific BOD	DALYs	-
Jarrett et al. (2012)	Incidence of specific diseases and injuries	Treatment Costs to National Health Service (NHS)	Estimates of disease treatment costs from PubMed search. Estimates of injury treatment costs from NHS and the Personal and Social Services Research Unit
Rabl and de Nazelle (2012)	All-Cause Mortality	Deaths YLLs	VSL VOLY
Rojas-Rueda et al. (2012)	All-Cause Mortality	Deaths YLLs	-
(Dhondt et al., 2013)	Mortality Morbidity	YLLs YLDs DALYs	-
Maizlish et al. (2013)	Disease-specific BOD	DALYs	-
Olabarria et al. (2013)	All-Cause Mortality	Deaths	VSL
Rojas-Rueda et al. (2013)	Disease-specific BOD	DALYs	-
Woodcock et al. (2013)	Disease-specific BOD All-Cause Mortality	DALYs Deaths	-
Deenihan and Caulfield (2014)	Mortality	Deaths	VSL

Study	Health Summary	Unit of Measurement	Monetisation
Edwards and Mason (2014)	Mortality	YLLs	-
Macmillan et al. (2014)	Mortality Morbidity Health Care Costs	Deaths Injuries Restricted Activity Days Hospital Admissions	Cost of bicycling fatal injury (NZTA) Cost of pollution mortality (HAPiNZ) Cost of cycling serious injury (NZTA) Restricted Activity Days (HAPiNZ) Hospitalisation Costs (HAPiNZ)
Woodcock et al. (2014)	Disease-specific BOD All-Cause Mortality	DALYs YLLs	-
Buekers et al. (2015)	All-Cause Mortality Disease-specific Morbidity	DALYs Medical Costs Productivity Losses	VOLY Estimates of medical costs and productivity losses from Flemish studies.
Schepers et al. (2015)	All-cause Mortality	Deaths YLLs	VSL
Rojas-Rueda et al. (2016)	All-Cause Mortality	Deaths	-

As shown in Figure 2.2, if mortality was the outcome variable; estimated changes to mortality rates could be used to directly estimate the reduction in number of deaths per year using a static approach or to calculate the resulting changes in life expectancy using a life tables approach. If BOD was the outcome variable, it was measured in Disability Adjusted Life Years (DALYs) (Murray and Acharya, 1997). DALYs can be considered as the sum of Years of Life Lost (YLL) and Years Lost Due to Disability (YLD). YLDs are calculated as the product of the duration of a condition in years and a "disability weight", where a weight of 0 implies perfect health and the worst disabilities approach a weight of 1. As shown in Table 2.2, several of the studies reviewed also calculated equivalent monetary benefits for the estimated health benefits. If the health outcome considered was static mortality rate, the reduction in mortality could be translated to an equivalent monetary benefit using the Value of a Statistical Life (VSL) (Mankiw, 2011). This is the method used in HEAT. An advantage of VSL is that it is the most commonly used measure in transport appraisals and so it provides coherence and consistency with other estimates of mortality impacts. If the life tables approach was employed, the equivalent monetary benefit could be calculated using the Value of a Life Year (VOLY) (Desaigues et al., 2011). None of the studies reviewed which considered DALYs, calculated an equivalent monetary benefit. As contended in Desaigues et al. (2011), VOLYs are a more appropriate measure of the cost of mortality due to air pollution and physical activity than VSL.

The strongest argument for this is that VSL is calculated with regard to accidental deaths which generally lead to many more years of life lost than deaths due to chronic pollution exposure or physical inactivity. Therefore, if VSL is used to monetise the mortality effects of pollution exposure or physical activity, the results are likely to be overestimated. This leads to the approach taken by Rabl and de Nazelle (2012) where the change in mortality due to air pollution and physical activity were monetised in VOLYs while deaths due to traffic collisions were monetised using VSL. The values used for VSL and VOLY are chosen at the discretion of the researcher and these values vary widely, particularly between Europe and North America. For example, Grabow et al. (2012) used a VSL of $7.4 million whereas Olabarria et al. (2013) used a VSL of € 1.3 million. In addition to the costs of morbidity and mortality, several studies quantified the impact on actual health care (Gotschi, 2011; Grabow et al., 2012; Jarrett et al., 2012; Lindsay et al., 2011). However, with the exception of Jarrett et al. (2012), health care costs were only considered alongside morbidity and mortality costs, which were generally the main focus of these studies.

2.1.3 Determinants of Health

2.1.3.1 Physical Activity

All studies reviewed included changes to physical activity levels as a determinant of health. As outlined in Table 2.3, physical activity levels could be described in terms of distance or time spent in active travel, metabolic equivalent of task (MET) hours or energy expenditure. These measures could relate to walking, cycling or engaging in any physical activity. The most suitable way of measuring physical activity depends on the data available as well as the Dose-Response Functions (DRF) to be used for estimation of health impacts. Various approaches were used across the studies to translate changes in physical activity to health benefits. The majority of these considered physical activity or walking and/or cycling as continuous variables and used published RRs and DRFs to determine the impact of the additional physical activity on a health summary measure as illustrated in Figure 2.1 and Figure 2.2. This includes eight studies which calculated reductions in all-cause mortality using the approach of HEAT (see Table 2.3) and several studies which calculated reductions in mortality using RRs and/or DRFs from other sources. Five studies (Maizlish et al., 2013; Rojas-Rueda et al., 2013; Woodcock et al., 2009; Woodcock et al., 2013; Woodcock et al., 2014) used the WHO's Comparative Risk Assessment (CRA) approach which involves estimating the change in DALYs due to specific diseases using RRs and DRFs. Conditions such as dementia, cardiovascular diseases, type II diabetes, breast cancer,

depression and colon cancer were considered. Since the exposure variable in these cases was total physical activity, it was necessary to also estimate non-travel physical activity.

2.1.3.1 Air Pollution

Pedestrians and cyclists do not produce any air pollution while travelling and thus, a modal shift towards active travel has the potential to decrease societal exposure to air pollution. However, persons switching from motorised travel to active travel may be exposed to higher inhalation doses of air pollution during travel time due to higher ventilation rates (McNabola et al., 2008). Therefore, both individual and external effects of air pollution should be considered in quantifying the health impacts of a modal shift. However, as shown in Table 2.4 most of the studies considered in this review only based their analysis on one or the other.

Exposures to a range of particulate and gaseous pollutants were considered as determinants of health in the studies reviewed, including $PM_{2.5}$, PM_{10}, carbon monoxide (CO), sulphur dioxide (SO_2), nitrogen dioxide (NO_2), ozone (O_3) and elemental carbon (EC). There is strong evidence that $PM_{2.5}$ exposure is associated with increased long term risks of all-cause, cardiopulmonary, and lung cancer mortality (Brook et al., 2010; Chen et al., 2008). There has also been some evidence of effects of gaseous pollutants such as CO, SO_2, NO_2 and O_3 on long term mortality. However, evidence has shown that, apart from SO_2, the effects of these gaseous pollutants on mortality become non-significant when controlling for PM2.5 exposure and other covariates (Brook et al., 2010; Chen et al., 2008). The recent decline in the use of high-sulphur coal for domestic heating has led to large reductions in levels of sulphur dioxide in the U.S.A. and many European countries (Clancy et al., 2002; WHO, 2005) and this may be why SO_2 was not considered in any of the studies reviewed. The most commonly considered pollutant in the studies reviewed was $PM_{2.5}$. However, some other pollutants were also considered as shown in Table 2.4. In sensitivity analysis, several studies (Hartog et al., 2011; Rojas-Rueda et al., 2011; Rojas-Rueda et al., 2012) analysed the effect of an air pollutant not considered in their main analysis.

The following two sub-sections discuss the methods used to quantify the impacts of external pollution and in-travel exposure to pollution respectively.

Table 2.3 Summary of physical activity effects considered in studies reviewed

Study	Unit of Measurement	Exposure-Response Relationship
de Nazelle et al. (2009)	Daily energy expenditure	Proportion of days exceeding USDHHS (1996) energy expenditure thresholds
Woodcock et al. (2009)	Physical Activity MET hours	Various published RRs of specific diseases for physical activity.
Gotschi (2011) Hartog et al. (2011)	Time spent cycling	HEAT for cycling
		Health care cost of inactivity proportional to number of inactive people
Lindsay et al. (2011)	Average distance cycled	HEAT for cycling
Rojas-Rueda et al. (2011)	Distance cycled	Range of RRs of mortality for cycling (0.5-0.90) based on published values
Fishman et al. (2012)	Average distance cycled	HEAT for cycling
Grabow et al. (2012)	Average distance cycled	HEAT for cycling
Holm et al. (2012)	Additional distance cycled Reduction in distance walked	Values per km walked/cycled from New Zealand Transport Agency (2010, Vol. 2)
Jarrett et al. (2012)	Physical activity categorised as sufficiently active, moderately active or inactive.	RRs of specific diseases between the physical activity categories from the WHO's Comparative Quantification of Health Risks study
Rabl and de Nazelle (2012)	Physical Activity MET hours	Various published RRs of specific diseases for physical activity. Assuming linear relationship with maximum threshold.
Rojas-Rueda et al. (2012)	Time spent cycling	Andersen RR of mortality for cycling with USDHHS (2008) DRF
(Dhondt et al., 2013)	Average distance cycled Average distance walked	HEAT for cycling HEAT for walking
Maizlish et al. (2013)	Physical Activity MET hours	RR of mortality for moderate physical activity from Woodcock (2011)
Olabarria et al. (2013)	Physical Activity MET hours	Various published RRs of specific diseases for physical activity.
Rojas-Rueda et al. (2013)	Time spent in new walking	HEAT for walking
Woodcock et al. (2013)	Average distance cycled Average distance walked	Various published RRs of specific diseases for physical activity.
Deenihan and Caulfield (2014)	Physical Activity MET hours	Various published RRs of specific diseases for physical activity. RRs of all-cause mortality for walking and total physical activity from Woodcock (2011) RRs of all-cause mortality from Andersen (2000) HEAT for walking HEAT for cycling
Edwards and Mason (2014)	Average distance cycled	HEAT for cycling
Macmillan et al. (2014)	Distance cycled	RR of mortality from Andersen (2000) only applied to ages >45.

Study	Unit of Measurement	Exposure-Response Relationship
Woodcock et al. (2014)	Cycling distance range	RR of mortality for cycling based on Andersen (2000) and Matthews (2007) with linear dose response vs. range of commuter cycling.
Buekers et al. (2015)	Physical Activity marginal MET hours	Various published RRs of specific diseases for physical activity. RRs of all-cause mortality for walking and total physical activity from Woodcock (2011). RR of mortality from HEAT (2014).
Schepers et al. (2015)	Time spent cycling	RR of mortality from Kelly et al. (2014)
Rojas-Rueda et al. (2016)	Cycling MET hours	RRs of disease-specific morbidity for physical activity from Woodcock (2013).

Table 2.4 Summary of pollution effects considered in studies reviewed

	In-travel exposure		External exposure	
Study	**Pollutant**	**Health Effects**	**Pollutant**	**Health Effects**
de Nazelle et al. (2009)	PM10 O_3	Proportion of days exceeding NAAQS thresholds	-	-
Woodcock et al. (2009)	-	-	PM2.5	RR of specific diseases from Ostro, 2004
Gotschi (2011)		-	-	-
Hartog et al. (2011)	-	-	PM2.5 O_3	Concentration response functions for PM2.5 from US EPA 2006 Regulatory Impact Analysis Exposure response functions for O_3 from NAAQS
Lindsay et al. (2011)	PM2.5 BS	RR of mortality for PM2.5 from Pope, 2002 RR of mortality for BS from Beelen, 2008	NO_2 PM10	RR of mortality from Tonne et al., 2008
Rojas-Rueda et al. (2011)	-	-	PM10 CO Benzene	Assumed impacts of air pollution estimated by HAPiNZ were proportional to vehicles kilometres travelled per square km
Fishman et al. (2012)	PM2.5	RR of mortality from Krewski 2009	-	-
Grabow et al. (2012)				
Holm et al. (2012)	PM2.5	RR of specific diseases for PM2.5 from Pope, 2002	-	-
Jarrett et al. (2012)	-	-	-	-
Rabl and de Nazelle (2012)	PM2.5	RR of mortality from Pope, 2002	PM2.5	RR of mortality from Pope, 2002
Rojas-Rueda et al. (2012)	PM2.5	RR of mortality from Krewski, 2009	PM2.5	RR of mortality from Krewski, 2009
(Dhondt et al., 2013)	EC	RR of mortality from Janssen et al 2011	EC	RR of mortality from Janssen et al 2011 RRs of CVD hospital admissions from Tolbert et al., 2007 and Peng et al.,

	In-travel exposure		External exposure	
Study	**Pollutant**	**Health Effects**	**Pollutant**	**Health Effects**
		RRs of CVD hospital admissions from Tolbert et al., 2007 and Peng et al., 2009		2009
Maizlish et al. (2013)	-	-	PM2.5	RR of specific diseases from Ostro, 2004
Olabarria et al. (2013)	-	-	-	-
Rojas-Rueda et al. (2013)	PM2.5	RR of various diseases	PM2.5	RR of various diseases
Woodcock et al. (2013)	-	-	PM2.5	RR of specific diseases from Ostro, 2004
Deenihan and Caulfield (2014)	-	-	-	-
Edwards and Mason (2014)	-	-	-	-
Macmillan et al. (2014)	-	-	PM10 CO	Modelled health outomes based on changes in light vehicle emissions using HAPiNZ Health Effects Model.
Woodcock et al. (2014)	PM2.5	RRs of specific diseases from Ostro, B. 2004	-	-
Buekers et al. (2015)	PM2.5	DRF based on WHO 2013 and Holland (2014)	PM2.5	Assuming linear relationship between YLLs per person per year and concentration of PM2.5
Schepers et al. (2015)	BC NO_2	DRF based on Hoek et al. (2013b)	-	-
Rojas-Rueda et al. (2016)	PM2.5	RR of mortality from Hoek G. et al. (2013)	-	-

2.1.3.1.1 External Impacts of Air Pollution

The first step taken in each study for calculating the avoided external cost of air pollution was to estimate the avoided emissions of various gaseous and particulate pollutants, usually using emission factors provided by an emissions prediction model as shown in Figure 2.1. A number of emissions modelling software packages were used in the studies reviewed but the most common was the COPERT 4 model; a software tool which calculates average emission factors and total mass of air pollution and greenhouse gas emissions from road transport (Kousoulidou et al., 2008) based on data such as fleet characteristics and meteorological information. Woodcock et al. (2013) took a more simplified approach to this step by using published emissions factors. The external impacts of the avoided emissions could be estimated directly from the emissions by using cost estimates from previous studies or by estimating the resulting exposure concentrations, as shown in Figure 2.1. Rabl and de Nazelle (2012) combined the emissions results from COPERT 4 with the results of the ExternE study of the external costs of energy (ExternE) which reported damage costs per tonnes of transport emissions for various cities. Lindsay et al. (2011) and Macmillan et al. (2014) estimated the total morbidity and mortality impacts of their study scenario by using the results of the HAPiNZ study (Fisher et al., 2007) which estimated the morbidity, mortality and health costs associated with road vehicle emissions in New Zealand. Other studies modelled the pollutant concentrations resulting from the change in emissions using an atmospheric dispersion model and estimated the impact of the change in population exposure. A range of commercial and non-commercial dispersion models were used but it is outside the scope of this thesis to discuss these in detail. Several reviews have already been devoted to the discussion of such models (Holmes and Morawska, 2006; Jerrett et al., 2005). Woodcock et al. (2013) used a simpler approach for this step, assuming that the change in transport related emissions would translate to a proportional change in ambient concentrations of primary $PM_{2.5}$ attributable to transport. The concentration changes (or population-weighted concentration changes) of pollutants, estimated by a dispersion model or another method, could then be used to calculate the impacts on mortality (Hartog et al., 2011; Rojas-Rueda et al., 2012) or BOD (Maizlish et al., 2013; Rojas-Rueda et al., 2013; Woodcock et al., 2009; Woodcock et al., 2013) using published RRs and DRFs for different levels of pollution exposure as in Figure 2.2 or by using specialised software (Grabow et al., 2012). Similar to the DRFs for physical activity, there were uncertainties associated with the published DRFs for pollution exposure used in these studies. In some cases, the responses of these models to variations in the RRs were tested using Monte Carlo simulation (Dhondt et al., 2013; Grabow et al., 2012; Rojas-Rueda et al., 2011; Rojas-Rueda et al., 2012) or by testing the upper and lower

confidence limits of the RRs directly (Holm et al., 2012). Rabl and de Nazelle (2012) created confidence intervals for the damage costs of air pollution analytically by assuming an approximately lognormal distribution, as described in (Spadaro and Rabl, 2008).

The use of a dispersion model and DRF for quantifying external pollution impacts may provide more precise results than using generic cost estimates but also requires significantly more data and modelling effort and so may not be suitable in many cases.

2.1.3.1.2 In-Travel Air Pollution Exposure

Several of the studies reviewed considered the impacts of a change to in-travel exposures to air pollution for the travellers changing their mode of travel. (Dhondt et al., 2013) calculated the change in "dynamic exposure" for the population by taking an average of the concentrations of each zone at each time step, weighted based on the proportions of each zonal population exposed to each concentration (Dhondt et al., 2012a). In the rest of the studies which considered in-traffic pollution exposures, the methods used (illustrated in Figure 2.1) were similar and based on inhaled dose rather than concentration. de Nazelle et al. (2009) estimated inhaled doses of PM_{10} and O_3 by simulated individuals by integrating the product of stochastically determined minute ventilation rate (VE) and modelled pollutant concentration level over time for each activity throughout each day. Other studies used similar approaches but estimated the VE and pollutant concentrations in different ways. The four studies by Rojas-Rueda and colleagues obtained average exposure concentrations for each mode from previous studies (de Nazelle et al., 2008; de Nazelle et al., 2011). Hartog et al. (2011) and Rabl and de Nazelle (2012) took typical urban European concentrations and applied scaling factors to account for differences in exposure concentrations between modes. Holm et al. (2012) assumed constant in-travel concentrations for all modes based on average values from two street monitoring sites. Woodcock et al. (2014) used data on 24-hour average $PM_{2.5}$ concentrations at $20m^2$ resolution to estimate in-travel $PM_{2.5}$ concentrations at the route-specific level and applied scaling factors to account for differences between each mode. A scaling factor was used for trips on the London Underground to account for the difference in potency between underground and surface-level $PM_{2.5}$ (Seaton et al., 2005). The four studies by Rojas-Rueda and colleagues also obtained ventilation rates for each mode from previous studies (de Nazelle et al., 2008; de Nazelle et al., 2011). Hartog et al. (2011) and Holm et al. (2012) estimated the ventilation rate during cycling to be 2.2 times that of driving or resting based on the average of ratios reported by two studies (Vanwijnen et al., 1995; Zuurbier et al., 2009). Rabl and de Nazelle (2012) and Woodcock et al. (2014) assumed ventilation rates were proportional to MET rates. These methodological differences were minor and mostly dictated by the data which was available to

the researchers. The health impacts of short time periods spent in differentially polluted environments and inhalation doses of pollutants have not been studied extensively. For this reason, all of the studies which estimated health impacts using inhaled dose did so by calculating an "equivalent" long-term change in average concentration using the ratio of the time-averaged inhalation doses for the alternative scenarios as shown in Figure 2.1. The impact on mortality or BOD could then be calculated as illustrated in Figure 2.2 using concentration-response functions for all-cause mortality or specific diseases from the literature (Beelen et al., 2008a; Krewski et al., 2009; Ostro, 2004; Pope et al., 2002). This meant that the inhalation dose during the non-travel daily activities also had to be estimated. This was done by assuming that non-travel time was spent in low intensity activities while exposed to typical ambient concentrations. Of the eleven studies which analysed in-travel pollution exposure, only three based their calculations on pollutant concentrations measured during travel in the study area (Rojas-Rueda et al., 2011; Rojas-Rueda et al., 2012; Rojas-Rueda et al., 2013). However, studies have shown that fixed monitoring stations can significantly underestimate or have little or no association with the exposure of commuters (Adams et al., 2001; Gulliver and Briggs, 2004). For this reason, future studies should consider taking in-travel measurements of pollution exposure where possible. Generally, the validity of using the "equivalent" concentration change is not totally clear but this seems to be the currently accepted approach in the literature.

2.1.3.2 Traffic Collisions

Increases in active travel affect collision risk for all users in a transport network. In this section, the quantification of collision risk is discussed first, followed by the quantification of the resulting benefits or detriments. In most transport environments, where modal share of active travel is low, pedestrians and cyclists face a greater risk of injury or death due to traffic collisions than motor vehicle users (Elvik, 2009) and cycling is perceived as being less safe than driving (Lawson et al., 2013). As shown in Table 2.5, many of the studies reviewed considered only the change in risk for the individuals who changed mode and assumed the risk was unchanged for those who did not. Eight studies (Edwards and Mason, 2014; Hartog et al., 2011; Holm et al., 2012; Rojas-Rueda et al., 2016; Rojas-Rueda et al., 2011; Rojas-Rueda et al., 2012; Rojas-Rueda et al., 2013; Woodcock et al., 2014) took this approach by using historical collision data to derive the risk of a collision per unit distance for each mode under study. Dhondt et al. (2013) and Buekers et al. (2015) used a similar method but stratified by conflict type. Such methods are unrealistic and likely to overestimate the increase in traffic collisions due to increased active travel for a number of reasons.

Research has consistently shown a “Safety in Numbers” (SIN) effect associated with active travel modes (Jacobsen, 2003; Robinson, 2005) meaning that as distances travelled by cycling and walking increase, the risk of road traffic injury for pedestrians and cyclists decreases. For example, Robinson (2005) reported that “If cycling doubles, the risk per kilometre falls by about 34%” and Jacobsen (2003) reported that “An individual’s risk while walking in a community with twice as much walking will reduce to 66%”. One study (Bhatia and Wier, 2011) has called into question the policy application of SIN given the small amount of empirical evidence supporting it. However, a later review (Elvik and Bjørnskau, 2017) of quantitative studies examining SIN found that the effect does indeed exist and that the model coefficient estimates found across different studies were highly consistent. Lindsay et al. (2011) accounted for the “Safety in Numbers” effect by first estimating the risk of traffic injuries and fatalities for motorised transport and cycling using historical collision data and then applying a correction factor to the cycling collision rates (see Figure 2.1) based on the aforementioned empirical estimate of Jacobsen (2003). However, this empirical correction does not account for the reduction in risk to the remaining users of all other modes due to the reduction in vehicle km travelled. Woodcock et al. (2009) and Jarrett et al. (2012) used an elaboration of a traffic injury model described by Bhalla et al. (2007) to estimate the absolute numbers of road traffic collisions at the city level for all modes of transport after a modal shift. A traffic injury matrix was constructed for each road type and level of injury severity where the cells of each matrix contained the historical number of traffic collisions for each pairwise combination of striking mode and victim mode (e.g. the number of pedestrians injured by cars). To estimate the numbers of injuries after a modal shift, it was assumed that the number of injuries for each striking-victim pair was proportional to the distance travelled by the striking mode and to the distance travelled by the victim mode. Although this approach accounts for changes in collision risk for all modes after a modal shift, the proportionality assumption ignores evidence of a non-linear relationship between distance travelled and road traffic injuries (Elvik, 2009). Woodcock et al. (2013) and Maizlish et al. (2013) took a similar approach but introduced non-linearity by using power transformations of the exposure variables (distances). As the degree of the non-linearity of injury risk is not well established, both studies tested the sensitivity of these models by using a range of exponents of the distances travelled. Macmillan et al. (2014) also elaborated on the model of Bhalla et al. but only considered collisions between light vehicles and bicycles, ignoring other modes. Based on longitudinal collision data for the study area, they assumed a linear relationship between cycling trips and cycling collisions up to a threshold modal share of 2.5% after which a SIN effect of half

that recommended by Jacobsen (2003) was applied. A power transformation based on Turner et al. (2010) accounted for the non-linear impact of the number of light vehicles.

Since most of the reviewed studies were based on hypothetical scenarios where cycling levels increased without any change in infrastructure, they did not consider the impact of cycling infrastructure on collision risk. The only study to consider this factor was (Schepers et al., 2015). The change in collision risk for cyclists resulting from provision of new cycle facilities was estimated using models from previous observational studies. A range of effect sizes was used for each facility type In order to account for uncertainty in the effects of changes in routing and overall numbers of cyclists.

Another factor which can confound predictions of road traffic injuries is underreporting of injuries in the baseline data. This is especially true for cycling as many cycling injuries are not recorded by police (Doherty et al., 2000). Woodcock et al. (2014) corrected their injury data for underreporting of injuries by applying London-specific scaling factors for each mode from published data comparing police data and hospitalisation rates. (Rojas-Rueda et al., 2013) also corrected their bicycle injury data in sensitivity analysis using generic European scaling factors recommended by the HEATCO (Developing Harmonised European Approaches for Transport Costing and Project Assessment) project (Bickel et al., 2006).

For studies where mortality was the health outcome considered and only fatal injuries were modelled, the calculation of health impacts from the change in traffic injuries was trivial. In several studies where BOD was the outcome considered (Holm et al., 2012; Maizlish et al., 2013; Woodcock et al., 2009; Woodcock et al., 2011; Woodcock et al., 2013), the proportional change in incidence of non-fatal injuries was used to estimate the change in YLDs due to traffic injuries from baseline levels and the change in incidence of fatal injuries was used to estimate the change in YLLs . Rojas-Rueda et al. (2013) calculated the increase in YLDs due to non-fatal injuries by assuming for avoided minor injuries, a disability duration and severity weight equal to that of a sprain diagnosis which were obtained from a previous study. For major injuries, an average duration and severity weight of severe injuries was assumed. Dhondt et al. (2013) took a more complex approach. For each predicted fatal injury, a specific age was sampled stochastically from within the broader age strata being used for the analysis and life-table analysis with age-specific mortality rates was employed to calculate the YLLs (Dhondt et al., 2012b). For each predicted non-fatal injury, first an injury diagnosis was sampled stochastically from injury distributions derived from national hospital data. Then an injury specific disability weight was assigned using values from a previous study (Haagsma et al., 2012). For temporary

injuries, a duration of 1 year was assigned and for long term injuries, the duration was assumed to be the remaining life expectancy.

Table 2.5 Summary of road traffic collision analysis in studies reviewed

Study	Travelers changing mode	Other travelers
de Nazelle et al. (2009)	-	-
Woodcock et al. (2009)	✓	✓
Gotschi (2011)	-	-
Hartog et al. (2011)	-	-
Lindsay et al. (2011)	✓	✓
Rojas-Rueda et al. (2011)	✓	✓
Fishman et al. (2012)	✓	-
Grabow et al. (2012)	-	-
Holm et al. (2012)	✓	-
Jarrett et al. (2012)	✓	✓
Rabl and de Nazelle (2012)	✓	✓
Rojas-Rueda et al. (2012)	✓	-
(Dhondt et al., 2013)	✓	✓
Maizlish et al. (2013)	✓	✓
Olabarria et al. (2013)	-	-
Rojas-Rueda et al. (2013)	✓	-
Woodcock et al. (2013)	✓	✓
Deenihan and Caulfield (2014)	-	-
Edwards and Mason (2014)	✓	-
Macmillan et al. (2014)	✓	-
Woodcock et al. (2014)	✓	✓
Buekers et al. (2015)	✓	-
Schepers et al. (2015)	✓	-
Rojas-Rueda et al. (2016)	✓	-

2.1.4 Results of reviewed studies

In this section, some trends which can be found in the results of these studies are discussed. In some studies such as Dhondt et al. (2013) and Grabow et al. (2012), it was unclear how much of the resulting impacts could be attributed to increases in walking and cycling. However, in the remaining studies, although the scenarios under study were different, some interesting commonalities and differences could be found. The overall results are discussed first, followed by discussion of the relative impacts of each determinant.

The total benefits of active travel outweighed the risks in all studies. However, Woodcock et al. (2014) found that the benefits for females were much lower than for males and that under certain modelling assumptions, there was no evidence of a benefit to women. This was partially due to the lower age distribution and baseline disease rate of women in this study as well as their higher background rate of fatal injuries from heavy goods vehicles.

In almost all studies where several determinants of health were considered, physical activity was the most significant, in most cases by a substantial margin, and always had a positive impact. Traffic collisions were the next most significant determinant, particularly in studies which included non-fatal traffic collisions in addition to fatalities. Some studies (Macmillan et al., 2014; Rabl and de Nazelle, 2012; Rojas-Rueda et al., 2013) even found that the change in cost of non-fatal collisions was more significant than the change in cost of fatal collisions. Although, in most cases, the cost of traffic collisions increased as a result of the increase in active travel, studies which considered the collision risk of motorised modes and the SIN effect yielded significantly more optimistic results than those which maintained the current injury rates for each mode. Woodcock et al. (2013) even found a reduction in the BOD due to traffic collisions in the increased active travel scenario. This was the only study to incorporate changes to freight and changes in travel distance in the more active scenario in their traffic collision model. Woodcock et al. (2009) found that the burden of road traffic injury increased for London but decreased for Delhi in the active travel scenarios, but it was noted that this difference in direction may indicate uncertainty. Holm et al. (2012) on the other hand, found the increase in health burden from traffic collisions to be comparable to the decrease in health burden due to physical activity.

In all studies, the health impacts of changes in external pollution were positive but relatively small and the health impacts of in-travel exposures to air pollution were negative and almost negligible.

2.1.5 Conclusions

In conclusion, assessments of the health impacts of active travel are invariably dominated by the health benefits of increased physical activity but there are also significant differences in the approaches used to quantify this impact and several studies have shown through sensitivity analysis that these modelling differences can drastically affect the scale of the estimated impact. The impacts related to individual and external air pollution are relatively small. The impacts of changes in traffic collision risk, however, tend to be negative and comparable in scale to the physical activity impacts. Failure to account for the SIN effect and the non-linearity of collision risk with respect to traffic volumes may produce estimates which are overly pessimistic and misleading.

This review also has identified several methodological challenges to be addressed in this thesis. Almost all of the studies reviewed focussed on evaluating the health impacts resulting from a modal shift but did not attempt to simulate the pathways which lead to model shift. This presents an opportunity to build on this work and increase the applicability of such studies to transport planning and policy formulation, through further research into the integration of these methods with travel demand forecasting models. Two of the studies integrated activity based modelling into their models. However, although activity based approaches are frequently used in academic settings, Urban Transport Planning (UTP) models (such as, the four-stage model) are more commonly used in practical demand forecasting applications. Integration of a health impact model with a UTP model would be an ideal way of incorporating health impacts into policy formulation and infrastructure planning processes and bridging this area of research with practice. Additionally, research into identifying the causes for the large discrepancies between the results of different models of the health impacts of physical activity is necessary. Physical activity has been consistently shown to be the most significant determinant of the health impacts of increased active travel but the magnitude of the impact is still difficult to quantify due to wide variations in the results of different models. A consensus on the best approach would increase the credibility and policy relevance of these studies.

2.2 Measurement and characterisation of environmental exposures of cycling

2.2.1 Air Pollution Exposure Concentrations of Cyclists

There have recently been considerable research efforts into measuring and characterising the air pollution exposures of urban cyclists. The pollutants considered have included PM, CO, NO_2, O_3, EC, black carbon (BC), volatile organic compounds (VOCs) and carbon dioxide (CO_2). As discussed

in a recent review (Bigazzi and Figliozzi, 2014), most of these studies have been based on roadside concentration measurements. However, in reality, pollution concentrations can vary greatly even on the scale of a few metres (McNabola et al., 2009) and so the concentrations at roadside may not reflect the exposures of cyclists. Numerical modelling of the spatial concentration field could be used to account for this variation but as discussed in Tiwary et al. (2011), the existing numerical modelling techniques suffer from significant limitations and consequently, they tend to under predict the exposures of cyclists and pedestrians. For these reasons, the rest of this section will focus on studies which directly measured cyclist exposures using portable sensors. Such studies are more difficult to carry out but have become more prevalent in recent years thanks to improvements in sensor technology, low-power electronics and location tracking systems (Kumar et al., 2015; Snyder et al., 2013; Steinle et al., 2013).

These designs of these studies can be broadly separated into two categories: modal comparison studies and studies of the factors which influence cyclist exposures. In modal comparison studies, exposure measurements are typically taken during multiple trips between the same origin and destination but using different modes of transport. In some cases the route is also fixed while in other cases, each traveller chooses their own route (Bigazzi and Figliozzi, 2014). Table 2.6 summarises the modal comparison studies to date and shows that there is considerable inconsistency as to whether cyclists experience higher or lower exposure concentrations than motorised modes. A recent review of this subject has suggested that likely reasons for the inconsistency include variations in cycling facilities and in intensity and proximity of motor traffic (Bigazzi and Figliozzi, 2014).

The second type of study uses multivariate analysis to determine the factors which influence the exposure concentrations of cyclists. As shown in Table 2.7, the most commonly considered factors include weather variables, presence of cycling facilities, and proxy measures of traffic volume. Wind has consistently been shown to be the most important weather variable as it increases dispersion of pollutants. Temperature has been less consistently associated with exposure concentrations and its effects are difficult to separate from those of humidity (Bigazzi and Figliozzi, 2014). Since the weather is out of our control, cycling facilities and traffic volume more important factors from a design or planning perspective.

Six of the studies reviewed considered the presence and/or type of cycle facilities as an explanatory factor. The presence of a cycle facility was consistently shown to decrease exposure concentrations and facilities with a higher degree of separation such as off-road bike trails provided the greatest benefits. Kingham et al. (1998) compared the exposures of cyclists on

roads and on cycle paths to benzene and particulates and found that the cyclists on the road had a higher exposure than the cyclists on the path. However, the sample size was small and only average concentrations for each trip were recorded. Hong and Bae (2012) measured the exposure of cyclists to black carbon (BC) on a single route at 1 minute intervals and found that the presence of a bicycle trail decreased BC exposure concentrations. Hatzopoulou et al. (2013) examined the impact of the presence of cycling facilities on the exposure of cyclists to UFPs, $PM_{2.5}$ and CO at 1 second intervals and to BC at 1 minute intervals. Cycling lanes were found to decrease exposure to all pollutants except for $PM_{2.5}$. Kingham et al. (2013) monitored exposures to PM_1, UFPs, and CO on predefined routes and found that on-road cyclists were exposed to higher concentrations of all pollutants than off-road cyclists. Bigazzi and Figliozzi (2015a) monitored exposure concentrations of cyclists to CO and VOCs at 1 second intervals and found that exposures on off-street facilities were lower than on-street riding with the exception of an off-street path through an industrial corridor. Finally, Hankey and Marshall (2015) monitored BC concentrations and particle number concentration (PNC) while cycling and found that mean concentrations on bike-lanes were slightly reduced compared to roads with no facility.

Almost all of the studies considered some measure of traffic intensity as a factor but in most cases real-time traffic data were not available so some proxy measure was used. Two studies aggregated Average Daily Traffic (ADT) data for a number of roads in an area to create a measure of traffic intensity for the area as a whole (Boogaard et al., 2009; Hong and Bae, 2012). Seven studies represented traffic intensity on routes using a binary distinction such as “heavy traffic” or light traffic”. Exposure concentrations in these studies were generally higher for high traffic intensities. Of course, such dichotomous variables cannot reveal the influence of variations in traffic along the same route or from day to day.

Eight studies incorporated real-time traffic volume data at the link level. Of these, six used observed real-time traffic volumes. McNabola et al. (2008) and McNabola et al. (2009) both obtained traffic counts from inductive loop detectors in Dublin for the sampling periods. McNabola et al. (2008) did not report any associations between traffic counts and pollutant concentrations but McNabola et al. (2009) found that the exposures of non-motorised modes of transport to $PM_{2.5}$ and VOCs were less influenced by traffic congestion than those of motorised modes. Kaur and Nieuwenhuijsen (2009) used hourly traffic volumes for the approximate exposure timings of the study and found that traffic counts explained little of the variability in $PM_{2.5}$ but had a greater influence of UFP and CO concentrations. Hatzopoulou et al. (2013) obtained 10-min traffic counts of total vehicles and diesel vehicles for sites along the cycling

routes during each sampling period. They found that 10 additional diesel vehicles per hour increased BC exposures of cyclists by 15%. Associations between all other pollutant concentrations (UFPs, $PM_{2.5}$ and CO) and vehicle counts were insignificant. Quiros et al. (2013) obtained 5-min traffic counts of various vehicle types for their sampling periods and calculated a variable called emissions-weighted traffic volume to account for the effects of higher and lower emitting vehicles. The emissions-weighted traffic volume was found to be quadratically related to UFP concentrations under parallel wind conditions only. This relationship was based on only eleven observations. Emissions-weighted traffic volume was not found to be related to $PM_{2.5}$. Hankey and Marshall (2015) used video recordings to take instantaneous counts of vehicles operating within one city block for a subset of the pollution sampling times. Additional trucks and buses on the city block had a greater impact on PNC and BC concentrations than additional passenger cars. Two studies did not have actual real-time traffic data but used the ADT of each link and accounted for temporal variation in other ways. Dons et al. (2013) estimated real-time traffic volumes from ADT for the sampling times using standard conversion factors (Jonkers and Vanhove, 2010). A positive linear relationship was found between BC exposure concentrations and estimated traffic volumes. Bigazzi and Figliozzi (2015a) used the ADT for each link and also included dynamic traffic data from 2 reference locations in the network to account for temporal variation. VOC and CO exposures both increased by 2% per 1000 ADT and CO exposure only was positively correlated with dynamic traffic intensity.

A number of key observations can be drawn from these studies. Firstly, it appears that the relationship between exposure concentrations and traffic intensity is more consistent when simplifications and modelling are used rather than actual traffic counts for the sampling period. Secondly, although traffic volumes and the presence of cycling facilities are likely to be highly correlated; only three studies to date have considered both real-time traffic and the presence of cycle facilities in their analysis. The results of these studies showed inconsistent effects of both of these variables on exposure concentrations of cyclists. These observations suggest that more research is required in order to characterize the influence of traffic volumes and the presence of cycling facilities on cyclist pollution exposures and the interactions between these variables.

An additional observation is that several important traffic-related pollutants such as NO_2 and NO_x have been overlooked in the studies to date. One reason for this may be that until recently, research had failed to uncover long term health effects of NO_x which were independent of the health impacts of particulates. However, evidence regarding health effects of NO_2 has strengthened substantially in recent years and the balance of probabilities now indicates that

NO_2 is itself responsible for adverse health impacts (COMEAP, 2015). Another possible reason is that, until recently, instruments capable of real-time measurement of gaseous pollutants were prohibitively large and expensive, making them unsuitable for mobile use. However, a new generation of low-cost highly-mobile mobile gas sensors capable of high temporal resolution measurements has become available in recent years (Kumar et al., 2015; Snyder et al., 2013; Steinle et al., 2013), making mobile measurement of NO_x exposures more achievable.

Table 2.6 Summary of studies which compare pollution exposure concentrations across modes

Author(s)	Location	Modes compared	Pollutant (s)	Cyclists exposures
Waldman et al. (1977)	Washington, D.C, U.S.A.	Cycling, Driving	CO, O_3, sulfates, nitrates, particulates	No significant difference
Vanwijnen et al. (1995)	Amsterdam, Netherlands	Cycling, Driving	CO, NO_2, VOCs	Lower than motorised
Kingham et al. (1998)	Christchurch, Zew Zealand	Cycling, Driving, Bus, Train	PM_{10}, Benzene	Lower than Driving. Relationship to other modes varied by pollutant.
Adams et al. (2001)	London, U.K.	Cycling, Driving, Bus, Underground Rail	$PM_{2.5}$	Lower than motorised
Adams et al. (2002)	London, U.K.	Cycling, Driving, Bus, Underground Rail	EC	Lower than motorised
Chertok et al. (2004)	Sydney	Cycling, Driving, Bus, Train, Walking	NO_2, VOCs	Lower than Driving. Relationship to other modes varied by pollutant.
Kaur and Nieuwenhuijsen (2009)	London, U.K.	Cycling, Driving Bus, Walking, Taxi Passenger	$PM_{2.5}$, CO	Lower than motorised
McNabola et al. (2008)	Dublin, Ireland	Cycling, Driving, Bus Walking	$PM_{2.5}$, VOCs	Lower than motorised
Boogaard et al. (2009)	Eleven medium-sized Dutch cities	Cycling, Driving	$PM_{2.5}$, PNC	Lower than motorised
Panis et al. (2010)	Three Belgian locations	Cycling, Driving	$PM_{2.5}$, PM_{10}, PNC	Insignificant or inconsistent differences.
de Nazelle et al. (2012)	Barcelona	Cycling, Driving, Bus, Walking	$PM_{2.5}$, CO, UFP, BC, CO_2	Lower than Driving. Relationship to Bus varied by pollutant.
Dons et al. (2012)	Flanders, Belgium	Cycling, Driving, Bus, Walking, Car Passenger, Train, Light Rail	BC	Lower than motorised except for Train.
Nwokoro et al. (2012)	London, U.K.	Cycling, Walking/Public Tranport	BC	Higher than Walking/Public Transport

Author(s)	Location	Modes compared	Pollutant (s)	Cyclists exposures
Yu et al. (2012)	Shanghai, China	Cycling, Bus, Walking, Taxi passenger, Underground Rail	PM_1	Higher than motorised
Kingham et al. (2013)	Christchurch, Zew Zealand	Driving, Bus	PM_{10}, $PM_{2.5}$, PM_1, UFPs, CO	Lower than motorised
Quiros et al. (2013)	Santa Monica, CA, U.S.A.	Cycling, Driving, Walking	$PM_{2.5}$, UFPs, CO_2	Insignificant or inconsistent differences.
Ragettli et al. (2013)	Basel, Switzerland	Cycling, Driving, Bus, Walking, Tram	UFPs	Insignificant or inconsistent differences.
Nyhan et al. (2014)	Dublin, Ireland	Cycling, Walking, Bus, Train	$PM_{2.5}$, PM_{10}	Higher than motorised
Namdeo et al. (2014)	Newcastle, UK	Cycling, Electric Vehicle, Bus	CO, PM_{10}	Lower than Bus
Goel et al. (2015)	Delhi, India	Cycling, Driving, Bus, Walking, Underground Rail, Motorcycle, Auto Rickshaw	$PM_{2.5}$	Insignificant or inconsistent differences.
Ramos et al. (2016)	Lisbon, Portugal	Cycling, Driving, Underground Rail, Bus, Motorcycle	PM_{10}, PM_4, $PM_{2.5}$, PM_1, CO, VOCs, CO_2, O_3	Insignificant or inconsistent differences.
Huang et al. (2012)	Beijing, China	Cycling, Bus, Taxi Passenger	$PM_{2.5}$, CO	Lower than Bus for both pollutants. $PM_{2.5}$ Higher than Taxi but CO lower than Taxi.

Table 2.7 Studies which analyzed factors affecting cyclist pollution exposure concentrations

		Factors Considered			
Author(s)	**Location**	**Traffic Intensity**	**Cycle Facilities**	**Others**	**Pollutant (s)**
Kleiner and Spengler (1976)	Boston, U.S.A.	Busy vs Light	-	Street Type Time of Day	CO
Kingham et al. (1998)	West Yorkshire, England	-	Use of bike path	Weather variables	Benzene PM10
Adams et al. (2001)	London, U.K.	-	-	Season Route Type	$PM_{2.5}$
Kaur et al. (2005a)	London, U.K.	Heavy vs Light	-		$PM_{2.5}$, UFPs, CO
McNabola et al. (2008)	Dublin, Ireland	Real-time traffic volumes from inductive loop detectors	-	Weather variables Time of Day	$PM_{2.5,}$ VOCs
Boogaard et al. (2009)	Eleven medium-sized Dutch cities	Traffic volume proxy based on AADT for a limited number of major roads	-	Road type Weather Variables Passing cars/mopeds	$PM_{2.5}$, PNC, Noise
Kaur and Nieuwenhuijsen (2009)	London, U.K.	Hourly traffic volumes from SCOOT for the approximate exposure timings.	-	Weather Variables	$PM_{2.5,}$ CO
McNabola et al. (2009)	Dublin, Ireland	Real-time traffic volumes from inductive loop detectors	-	Weather variables	$PM_{2.5,}$ VOCs

		Factors Considered			
Author(s)	**Location**	**Traffic Intensity**	**Cycle Facilities**	**Others**	**Pollutant (s)**
Weichenthal et al. (2011)	Ottawa, Canada	High vs. Low traffic	-	-	VOCs, UFPs, $PM_{2.5}$, CO
Cole-Hunter et al. (2013a)	Brisbane, Australia	High vs. low proximity to traffic	-	Weather Variables	UFP
Hong and Bae (2012)	Seattle, WA, U.S.	Traffic intensity proxy for buffer area based on AADT	Cycle Facility Types	Time of Day Length of each Road Type Land Use Variables Weather Variables Number of stops	BC
Huang et al. (2012)	Beijing, China	Wide High Traffic Route vs Narrow Congested Route	-	Time of Day Weather Variables	$PM_{2.5,}$ CO
Dons et al. (2013)	Flanders, Belgium	AADT converted to instantaneous traffic intensity using standard conversion factors.	-	Trip duration Degree of urbanization Road type Travel speed Road speed	BC
Hatzopoulou et al. (2013)	Montreal, Canada	Real-time 10-min traffic volumes	Cycle Facility Types	Weather Variables	$PM_{2.5,}$ CO, BC
Jarjour et al. (2013)	Berkeley, CA, U.S.A.	High vs. Low traffic	-	Weather Variables	
Kingham et al. (2013)	Christchurch, New Zealand	-	On-road route vs. cycleway route	-	PM_{10}, $PM_{2.5}$, $PM_{1,}$ UFPs, CO

		Factors Considered			
Author(s)	**Location**	**Traffic Intensity**	**Cycle Facilities**	**Others**	**Pollutant (s)**
Quiros et al. (2013)	Santa Monica, CA, U.S.A.	Categorised 5-min traffic counts	-	Time of Day Location Weather Variables	$PM_{2.5}$, UFPs, CO_2
Ragettli et al. (2013)	Basel, Switzerland	"High exposure" route vs "Low exposure" route	-	Time of Day Day of Week	UFPs
Bigazzi and Figliozzi (2015a)	Portland, OR, U.S.A	ADT for each link Continuous traffic data for 2 reference locations.	Location/facility dummy variables	Background concentration Weather Variables Road grade Intersection Stop-and-go riding	CO, VOCs
Hankey and Marshall (2015)	Minneapolis, MN, U.S.A.	Instantaneous categorised traffic volumes for a subset of observations	Presence of cycling facility	Street Type Distance from major roads Presence of nearby trucks	$PM_{2.5}$, BC, PNC

2.2.2 Air Pollution Inhaled Dose

Although there is a lack of consistency regarding the concentrations experienced by cyclists relative to motorised modes, studies have consistently shown that cyclists experience greater intake doses and uptake doses of pollutants while in traffic mainly due to their elevated exertion and breathing rates. The intake dose can be defined as the mass of pollutants which cross the body boundary through the mouth and nose and the uptake dose is the mass of pollutant which is not exhaled but incorporated into the body (Bigazzi and Figliozzi, 2014; Ott et al., 2006). The intake dose can be estimated by integrating the product of the exposure concentration and the ventilation rate over time. Therefore, in addition to exposure concentrations, it is influenced by how heavily the subject is breathing and the time during which the exposure takes place. A number of studies have compared the VE of subjects travelling by different modes and the ratio cyclist VE to driver VE has ranged between 1.9 and 4.9 (Bigazzi and Figliozzi, 2014). A number of studies have also directly measured the pollutant inhalation of cyclists in transit. However, as outlined in Bigazzi and Figliozzi (2014), most of these studies assumed a constant respiration rate. This would be a reasonable assumption if respiration rate and exposure concentration were independent but in reality, there is likely to be spatial correlation between these variables, particularly at locations such as intersections and hills. Two recent studies of particulate exposure used variable ventilation rates by trip (Cole-Hunter et al., 2013b) and at two minute aggregations (Nyhan et al., 2014) respectively but no studies of gaseous pollution exposure have been found which used variable ventilation rates.

Several studies have also measured the uptake of pollutants by cyclists. McNabola et al. (2008) and Nyhan et al. (2014) both modelled uptake of pollutants in the lungs by different modes based on a human respiratory tract model. Both studies found that cyclists had the highest uptake dose. Panis et al. (2010) modelled uptake of pollutants based on published deposition factor and also found that cyclists had the highest uptake. Nwokoro et al. (2012) measured biomarkers of long-term uptake of BC for London cyclists and non-cyclists and found that cyclists showed that the cyclists had signs of higher uptake than non-cyclists. Bergamaschi et al. (1999) measured biomarkers of VOC uptake in subjects before and after cycling on urban congested routes and on open rural routes. VOC biomarkers after urban cycling were significantly increased compared to before cycling.

2.2.3 Noise Exposure

Noise exposure of cyclists has not been studied as extensively as air pollution exposure but a few studies exist which analysed both air and noise pollution simulataneously. Boogaard et al. (2009)

measured both noise exposure and particulate exposure of cyclists in eleven Dutch cities. Moderate correlation was found between 1 minute averages of logged particle number concentrations and noise. Vlachokostas et al. (2012) measured the exposures of various modes to CO, VOCs and noise in Thessaloniki, Greece. Two combined exposure metrics were proposed to account for both air and noise pollution exposure: the Combined Exposure Factor (CEF) and the Combined Dose and Exposure Factor (CDEF). The CDEF takes into account the intake dose rather than just the exposure concentration. Cyclists were found to have a favourable CEF compared to other modes but cyclists and pedestrians had the least favourable CDEF due to their increased physical exertion levels. Dekoninck et al. (2013) monitored the noise and BC exposures of cyclists in Ghent, Belgium and developed noise indicators based on particular frequency bands to represent different physical sources such as engine noise, rolling noise and short term noise events. They found that a proxy for personal BC exposure could be developed based on a combination of these noise indicators and some weather variables.

Several other studies have simultaneously measured noise and air pollutant concentrations at fixed sites and found significant correlations between noise levels and air pollutants such as NO_x and primary particles (Allen et al., 2009; Can et al., 2011; Fernandez-Camacho et al., 2015; Tobías et al., 2001). According to one review (Chowdhury et al., 2015), noise levels have most consistent correlations with NO_x, UFPs and total suspended particles. They also found that lower wind speeds and longer averaging periods are associated with higher correlations between noise levels and pollutant concentrations. The level of correlation between air and noise pollution is important because both have been associated with mortality from cardiovascular and other causes (Babisch, 2014; Bluhm et al., 2007; Brook et al., 2010; Dzhambov, 2015; Hoek et al., 2013b) and it is unclear to what extent there is confounding between these two exposures.

2.3 Models of cyclist travel behaviour

This section describes the literature relating to modelling the travel behaviour of cyclists. Before discussing cyclist travel behaviour however, it is helpful to give some discussion of the state of the art in multi-modal traffic equilibrium modelling.

2.3.1 Multi-Modal Network Equilibrium

The formulation of the network equilibrium problem as an econometric equilibrium model was first described by Beckmann et al. (1956) in 1956. The application of the Frank and Wolfe algorithm to the solution of this problem was later suggested by Bruynooghe et al. (1969). However, in the intervening period, a sequential four-step paradigm had gained popularity which consisted of trip generation, trip distribution, modal split and traffic assignment. However,

each of these stages are interdependent and performing them in sequence leads to internal inconsistencies in the results of each stage. When researchers looked for ways to combine these steps into a method which would maintain internal consistency, they arrived back at Beckman's original formulation. Such models which combine several of the four stages into a single equilibrium model became known as combined models (Boyce and Bar-Gera, 2004).

The Frank and Wolfe algorithm introduced by Bruynooghe et al. (1969) allowed the deterministic user equilibrium (DUE) to be found for a network with a single mode of transport, fixed O-D demands and separable link cost functions. The assumption of separable cost functions was later relaxed to an assumption of symmetric cost functions by Dafermos (1971). This assumption requires that the Jacobian of the link-cost function is symmetric. However, even the assumption of no asymmetric link interactions is not always realistic. In particular, where multiple modes are involved it is reasonable to assume that the interactions between different modes on the same link may be asymmetric. Smith (1979) used the variational inequality (VI) to show the existence and uniqueness of traffic equilibrium under the weaker condition that the Jacobian of the link cost function is positive definite. This allows for asymmetric link interactions as long as the cost on each link is strictly increasing with the flow on that link and depends more strongly on its own flow than the flow on any other link. However, there is no known equivalent minimisation problem for this situation. The first solution to this problem was the diagonalisation method (sometimes referred to as the relaxation method) presented by Abdulaal and LeBlanc (1979). Other approaches to solving this problem include the projection method and decomposition methods such as the Gauss-Seidel algorithm (Nagurney, 1993).

In recent years, the flexibility of the variational inequality approach has led to it being used to model more complex transport scenarios using various solution algorithms. Florian et al. (2002) proposed a VI model for the combined modal split, trip distribution and assignment problem and a solution algorithm based on a block Gauss-Siedel decomposition method with the method of successive averages (MSA). The model and solution algorithm were tested using data from the road network of Santiago, Chile. Auto drivers, auto passengers, buses, taxis and pedestrians were included but cyclists were not. Li et al. (2015) proposed a model for a network problem with elastic demand, logit-based modal split and stochastic user assignment (SUE). The model included autos, buses and cyclists but it was assumed that there would be no interactions between cyclists and any other mode. A solution algorithm was proposed, also based on the Guass-Siedel decomposition approach with the MSA.

A key requirement for including any particular mode within a multimodal traffic equilibrium model is the availability of suitable functions to describe the travel costs of using this mode within the network. Previous efforts at developing such functions for cyclists are described in section 2.3.3.

2.3.2 Modal Share of Cycling

Mode choice in the context of cycling has been studied extensively, mainly using stated preference and revealed preference studies. Some studies examined factors affecting cycling modal share in the absence of any specific intervention while other studies were concerned with identifying the most effective interventions for increasing cycling levels. In this section, an overview of these studies is given. This section is not a comprehensive but further information can be found in reviews such as Pucher et al. (2010), Heinen et al. (2010) and Buehler and Dill (2016).

Wardman et al. (2007) collected revealed preference and stated preference data about mode choice of individuals travelling to work and developed a hierarchical logit model based on variables including demographic information, travel times and costs and environmental factors such as hilliness, noise and air pollution. It was found that provision of segregated facilities would significantly increase propensity to cycle but that the most effective policy would involve a combination of en-route facilities, a daily payment and comprehensive trip end facilities. Parkin et al. (2008) studied the determinants of bicycle mode share for the journey to work at the ward level using census data. A logistic regression model was developed and the variables found to be important predictors of cycling mode share included sociodemographic factors, traffic intensity, hilliness and off-road cycle paths. Dill and Voros (2007) conducted a phone survey of adults in Portland, Oregan to explore the relationship between cycling levels and demographic, environmental factors and attitudes. It was found that perceptions of the availability of bike lanes were associated with more cycling but the density of bike lanes within one quarter mile of the home address was not. It may be that density of cycle lanes within one quarter mile of one's address is not a good indicator of the availability of cycle lanes on the routes on which they would like to travel. The most common environmental barrier to cycling was "too much traffic". Vandenbulcke et al. (2011) studied the spatial determinants of cycling in Belgium at the municipal level. They found that flat terrain, high quality facilities and low accident risk can encourage cycling while town size, travel distance and demographics also had some effect. They also found that high traffic volumes had less impact on cycling rates in Flanders, where high quality infrastructure was more common, than in the rest of the study

region. This suggests an interaction effect between traffic volumes and cycling facilities on the propensity to cycle. Pucher and Buehler (2008) studied the success of the Netherlands, Denmark and Germany in promoting cycling in order to discover the key policies which have led to such high levels of cycling. They found that the most important factors are provision of separate cycling facilities on busy roads and at intersections and traffic calming in residential neighbourhoods.

Some studies have focussed in particular on the impact of cycle facilities on cycling mode share. Buehler and Pucher (2012) carried out a cross-sectional study of 90 American cities to explore the impact of cycling facilities and other explanatory variables on cycling levels. They found that the presence of both off-street paths and on-street lanes were associated with higher cycling levels. Buehler and Dill (2016) carried out a review of studies which considered the impact of cycling facilities on cycling levels. The cycling facilities considered ranged from individual lanes to entire bikeway networks and most studies reported positive associations between the infrastructure and cycling levels. They also found that separated facilities were preferred over on-road facilities and this was especially true when traffic levels were high. This also suggests an interaction effect between traffic volumes and facilities.

Pucher et al. (2010) carried out a comprehensive review of studies which examined the effectiveness of various interventions aimed at increasing cycling levels. The types of interventions considered included infrastructure improvements, end-of-trip facilities, integration with public transport, access programmes and legal interventions. Stated preference studies consistently found that cyclists preferred cycling in bike lanes than in mixed traffic. Revealed preference studies at the aggregate level also found positive associations between cycling facilities and bicycling but at the individual level, results were mixed. Some of the studies also suggested the importance of bicycle parking but the evidence for this was limited to a few cities. Similarly to Wardman et al. (2007), it was suggested that in order to significantly increase cycling levels, a comprehensive package of complimentary measures would be required.

In recent years, a different approach to understanding the choice to cycle has emerged based on an understanding of social and psychological factors (Heinen et al., 2010; Tapp and Parkin, 2015). One popular psychological model is the Theory of Planned Behaviour (Armitage and Conner, 2001) which suggests that intentions and subsequent behaviours are influenced by three factors: attitudes, subjective norms and perceived behavioural control. The attitude to a behaviour encompasses the expectation of the outcomes of the behaviour and the value of those outcomes. Dill and Voros (2007) found that cyclists indeed have more positive attitudes

towards cycling than non-cyclists. Subjective norms relate to the regulating influence of the beliefs of other individuals or groups. (Dill and Voros (2007)) for example, found that individuals are more likely to cycle to work if their co-workers do. Pooley et al. (2013) in a qualitative study of travel behaviours in four British towns found that travel by car is seen as more normal than travel by bicycle and that most people prefer to adopt such norms of behaviour and to fit in with those around them rather than to stand out. Perceived behavioural control relates to an individual's belief about their ability to perform a certain behaviour. Gatersleben and Appleton (2007) showed that individuals who do not cycle tend to perceive more barriers to cycling than individuals who do cycle. Bamberg et al. (2003) performed a longitudinal study to test an intervention—giving prepaid bus tickets to students—in the context of the Theory of Planned Behaviour. The results suggested that attitudes, social norms and perceptions of behaviour control with respect to mode choices are largely rational and can be influenced by interventions.

2.3.3 Route Choice of Cyclists

A number of studies have tried to identify and/or evaluate the importance of factors which contribute to the generalised travel costs of cyclists and thus influence their route choices. Both stated preference surveys and GPS tracking have been used in multiple studies. Sener et al. (2009) carried out a stated preference analysis on a survey of commuter and non-commuter cyclists in Texas and found that travel time and motorist volumes were the most important parameters for route choice. Winters and Teschke (2010) conducted a survey of current and potential cyclists using pictures of 16 routes. It was found that routes with traffic calming, bike lanes, paved surfaces, and no on-street parking were preferred. Tilahun et al. (2007) used a stated preference survey to show the value of different cycling facilities to bicycle users and showed that the most attractive facilities are segregated lanes followed by roads without parking. Dill (2009) used GPS tracking of cyclists and showed that disproportionately high numbers of cycling trips occurred on dedicated cycling infrastructure rather than roads without cycling infrastructure. Broach et al. (2012) used GPS tracking of cyclists in Portland, Oregan to estimate a bicycle route choice model and route choices were found to be affected by logged distance, turn frequency, slope, traffic signals and traffic volumes. Commuters were found to be more sensitive to time but less sensitive to other parameters than non-commuters. Hood et al. (2011) also used GPS tracking to study route choice of cyclists in San Francisco. Although distance, turn frequency, slope and traffic signals were again found to be significant, traffic volumes were not. The Highway Capacity Manual (TRB, 2000) suggested that the comfort of cyclists is also affected by presence of other cyclists due to the hindrance of passing and meeting manoeuvres. Bigazzi et al. (2016) considered the question of whether or not cyclists' route

choices are affected by air pollution levels. It was found that, in many situations, cyclists will tend to choose routes with the lowest inhalation doses but that this is due to a preference for low-traffic routes rather than a preference for low-pollution routes.

The preference of cyclists for lower traffic routes and segregation from vehicle traffic can be explained by the lower perceived risk associated with these conditions. Lawson et al. (2013) carried out a survey study of the perceptions of safety of cyclists in Dublin. The route-specific features which were found to increase perceptions of safety included quiet roads, streetlights and continuous cycling facilities. Parkin et al. (2008) explored the relationship between route characteristics and risk perceptions of cyclists using video clips from the perspective of the cyclist. It was found that volume, speed and composition of motor traffic influenced risk perceptions. In particular, traffic free routes significantly reduced risk perceptions. Cycling facilities which were off-road or adjacent to the road were more effective in reducing perceptions of risk than on-road cycle lanes.

Other studies have developed measures of link suitability or attractiveness for cyclists such as the Bicycle Level of Service (BLOS) (Landis et al., 1997) or Bicycle Compatability Index (BCI) (Harkey et al., 1998). Some studies also considered the level of service of a bicycle network as a whole. Klobucar and Fricker (2007) built on the BLOS concept by developing a tool for evaluating the level of service of an entire cycle network, taking into account both BLOS and route length.

Transport models in use by national or regional transport authorities typically do not model cyclist route choices or else model them based on simplistic models. Cyclists are often assigned to the shortest path based on arbitrarily chosen average speeds (Subhani et al., 2013). They also tend to ignore the impact of cycling facilities and the cross-modal impacts which cyclists and motorised traffic place on each other. For example, in the Regional Modelling System used by the NTA of Ireland, all cyclists are assigned to the shortest path and no cross-modal impacts are considered (National Transport Authority, 2011b). Similarly, in the UK, the WebTAG guidelines suggest that generalised costs for cyclists should be considered to be linearly dependent on O-D distance travelled via an average speed of 12km/hr (Department for Transport, 2017). Very little research effort has been devoted to developing a realistic bicycle link cost function which could be used in a traffic assignment model. One study did attempt to incorporate cycling into the Ottawa-Gatineau Transport Model (Subhani et al., 2013) using a link cost function based on the BLOS. This link cost function is sensitive to travel time, speed, level-of-stress, turn conditions at intersections and area type. The authors mention that validation of the function has taken place but the results of the validation are not reported in the paper (Subhani et al., 2013). Si et al.

(2011) suggested a multi-modal link cost function where travel impedance for any mode on any link depends on respective levels of congestion of each mode on the link. No attempt was made to validate the function. Lawson (2015) proposed a link cost function for cyclists which took into account car, bus and cyclist congestion as well as the presence of a cycling facility. However, the function was dependent on multiple parameters and no attempt was made to calibrate these parameters. Li et al. (2015) proposed path cost function for use of shared bicycle schemes; an additive function of rental prices, walking time, rider fatigue and additional travel time to return the bike to a station near the end point. It was assumed that there are no interactions with other modes and no attempt was made to validate the model.

In order to enable cycling to be modelled realistically in a network equilibrium modelling framework, there is a need to develop a bicycle link cost function which takes into account cyclist-specific considerations such as real-time traffic levels and cycling infrastructure and for the function to be validated with real world data. In order to improve the portability of the model and to ensure that calibration can be carried out, the function must also balance realism with simplicity. The development and calibration of such a link cost function will be addressed in the current study.

2.3.4 Calibration of Link Cost Functions

Link cost functions typically incorporate some parameters which must be calibrated. There have been two main approaches in the literature for calibrating the parameters of link cost functions (Garcia-Rodenas and Verastegui-Rayo, 2013). The first approach is calibration based on link data whereby links are considered in isolation in order to determine their speed-flow relationships. An advantage of such methods is that look-up tables of parameters can be developed based on functional characteristics of the link. A prime example of this is the Highway Capacity Manual (TRB, 2000) which lists parameterisations for the Bureau of Public Roads function (U.S. Department of Commerce and Bureau of Public Roads, 1964) to describe the speed-flow relationships for a number of link classes. Disadvantages of these methods are that the only travel cost they can account for is travel time and they also ignore the impact of other links on the link delay.

The second approach is calibration based on network data. In this approach, calibration is achieved by using the inverse traffic assignment problem (ITAP) which can be formulated as a mathematical program with equilibrium constraints (MPEC) (Luo et al., 1996), of which bilevel optimisation is a more specific case. The ITAP aims to find values of the model parameters which lead to the best possible agreement between the model outputs and corresponding network

observations. The ITAP has most often been used as a tool for estimating or updating the O-D demand matrix for a network. The use of the ITAP for the current problem where the O-D demand matrix is known and the parameters of a link-cost function need to be estimated is relatively unexplored but some previous studies exist. There also exist some studies which use the ITAP to estimate other parameters of a network model such as dispersion parameters of logit models and mode bias parameters. Table 2.8 gives a summary of studies which have estimated network parameters or simultaneously estimated network parameters and O-D demand matrices using the ITAP. Four of these studies estimated parameters of a link cost function. All four of these related to auto link cost functions and estimated the parameters based on an auto-only network assignment model. Suh et al. (1990) calibrated the link capacity parameter of the BPR function for vehicles in order to appropriately represent the Korean highway system. Xu et al. (2004) also estimated parameters of the BPR function while simultaneously updating the O-D demand matrix. Meng et al. (2004) simultaneously estimated link cost function parameters and updated the O-D demand matrix. Finally, Garcia-Rodenas and Verastegui-Rayo (2013) calibrated link cost function parameters where each link in the network was associated with different values for the parameters.

Table 2.8 Studies using the ITAP to calibrate network model parameters.

Author	Year	Estimated Parameters	Observed Data	Network Model			Calibration Algorithm
				OD Demands	Mode Choice	Route Choice	
Suh and Kim (1989)	1990	BPR function parameters	Link flows	Fixed	Auto only	DUE	Descent-type algorithm
Abrahamsson and Lundqvist (1999)	1999	Logit dispersion parameter Mode bias parameter Balancing factors of doubly constrained gravity model	Flow on each route by each mode	Doubly constrained gravity model	Binomial logit model with auto and transit	DUE	Upper level solved by maximum likelihood (MINOS optimisation package). Lower level solved by partial linearization (ref Boyce 1983)
Yang et al. (2001)	2001	O-D demand matrix Route-choice dispersion coefficient	Prior O-D demand matrix Link flows	Fixed	Auto only	SUE	Replaced logit model with equivalent differentiable constraint function. Solves as a nonlinear programming model.
Meng et al. (2004)	2004	Link cost function parameters	Link flows	Fixed	Auto only	DUE	Transformed into a nonlinear programming problem by constructing a gap function. Program solved using Augmented Lagrangian method.
Xu et al. (2004)	2004	BPR function parameters O-D demand matrix	Prior O-D demand matrix Link flows	Fixed	Auto only	SUE	Genetic Algorithm
García-Ródenas and Marín (2009)	2009	O-D demand matrix Nested logit parameters	Prior O-D demand matrix Link flows	Fixed	Logit model with auto, park 'n' ride, transit with walk/cycle access	DUE	MPEC converted to a unilevel optimisation model by replacing the VI with its equilibrium conditions and linearly approximating the path cost functions.
Garcia-Rodenas and Verastegui-Rayo (2013)	2013	Link cost function parameters	(a) Link flows (b) Links flows and O-D costs	Fixed	Auto only	DUE	Restricted problem developed using column generation algorithm. Solution algorithm of restricted problem unspecified.

No example could be found in the literature of calibration of a cycling link cost function with either the link based or network based approach. The network-based approach is more appropriate for this problem. This is because estimating parameters based on link data requires that the costs can be observed directly. This is not a problem for traditional link cost functions for motor vehicles as the cost to be observed is simply the travel time. However, based on the current literature relating to cyclist route preferences, it is clear that the disutility experienced by a cyclist travelling on a link is significantly affected by factors such as risks perceptions and segregation from traffic, independently of their effect on travel time. Such intangible costs cannot be directly observed. However, in the network-based approach, there is no need to directly observe the travel costs on the links; it is only necessary to observe the network utilisation at a macroscopic level.

2.3.5 Solution algorithms for the MPEC

In order to use the ITAP to calibrate network parameters, it must be modelled and solved as a MPEC. Multiple approaches to solving the MPEC can be found in the literature. These are generally categorised as extreme-point methods, KKT methods and descent methods (Kolstad, 1985). The first category, extreme-point methods, are only useful for linear problems and as such require no further discussion here. The second category, KKT methods—which include Branch-and-Bound and Complimentarity Pivoting—involve replacing the equilibrium problem by its KKT conditions. This replaces the MPEC by a single level problem which will not be convex due to the complimentarity constraint. Branch and Bound methods enumerate the different possibilities posed by the complimentarity constraint in order to find an exact solution. However, computation times increase rapidly with the size of the constraint region. In Complimentarity Pivoting, instead of minimising the objective of the MPEC, a feasible solution is found such that the objective function is below a certain upper bound. This is repeated with successively lower values for the upper bounds until no feasible solution can be found. This approach has only previously been used for linear and quadratic problems. Such KKT methods were not used in any of the studies in Table 2.8. The third type of algorithm, descent algorithms, relies on derivative information about the equilibrium problem with respect to the decision variables. If this information is available, then one of several descent algorithms can be used to find a local optimum of the MPEC. The sensitivity analysis of Fiacco (1983) or Tobin (1986) can be used to obtain this derivative information for a broad range of problems. A potential issue with using descent methods is that they do not guarantee a global solution. One of the studies in Table 2.8 used a descent-type algorithm to estimate parameters of a link-cost function (Suh et al., 1990). Descent algorithms have also been used to solve with other applications of MPECs

where the equilibrium problem is a traffic assignment model (Si et al., 2012; Si et al., 2011). Other solution algorithms which have been used with the ITAP to estimate cost function parameters but do not fit into these categories are genetic algorithms (Xu et al., 2004) and using a gap function to transform the problem into a single level nonlinear problem (Meng et al., 2004).

Since descent algorithms have been used successfully to solve bilevel programmes for several transport problems including calibration of a link cost function in a single-mode network; a descent-type algorithm is used in the main analysis in this study.

2.4 Evaluation and optimisation of cycle networks.

Policymakers and transport authorities often use tools and guidelines in order to aid them in the design and evaluation of cycling facilities. Some countries have national guidelines for designing and appraising transport projects. Cost Benefit Analysis (CBA) is the most commonly used tool in such appraisals (Mackie et al., 2014) and the methodologies, valuations and applications are broadly similar across different countries. In Ireland, the Common Appraisal Framework (CAF) (Department of Transport, 2016) sets out guidelines for the appraisal of transport projects. The first stage in the CAF appraisal process is the Preliminary Appraisal. In this stage, a problem is identified, and a number of possible interventions are designed: a Do-minimum option and at least three better-performing Do-something options. The CAF recommends that these options are subjected to a Multi-Criteria Analysis in order to select a smaller number of options to be analysed in the next stage, Detailed Appraisal. Multi Criteria Analysis involves the decision maker assigning scores and weightings to various impacts and this can add some subjectivity to the appraisal process. In the Detailed Appraisal step, transport projects are typically appraised using a CBA. This involves generating a list of all benefits and costs expected to arise over the lifetime of the project. Benefits and costs should be represented by market prices where possible and values based on revealed preference should be used where market prices are unavailable. The CAF also recommends parameters for evaluating value of time, vehicle operating costs, emission values, collision costs and active travel values. Net Present Value, Cost Benefit Ratio and Internal Rate of Return are used as the main measures for deciding on the preferred option.

In the UK, guidelines for transport appraisal are set out in WebTAG (Department of Transport, 2013). Similarly to the CAF, the process involves an initial 'Option Development' stage in which a number of possible interventions are outlined and sifted in order to find a smaller number of options to take forward to the 'Further Appraisal' stage. In this stage a smaller number of options are subjected to more complex appraisal including CBA, environmental assessment and

a Transport Business Case.

Some countries also have design guidelines specific to cycling facilities. The design guidelines of Ireland, the UK and other countries are strongly influenced by the Dutch cycling design guidance (CROW, 2007). The CROW guidelines identify coherence, directness, attractiveness, safety and comfort as the fundamental requirements for cycling infrastructure and these five dimensions are echoed in the National Cycle Manual of Ireland (National Transport Authority, 2011a) and the Handbook for Cycle Friendly Design (Sustrans, 2014) in the UK. These guidelines provide high level guidance for cycle friendly design as well as technical guidance and parameters such as minimum widths, turn radii and signal timings. This guidance can be used in order to aid in the design possible of interventions during the initial appraisal steps of the CAF or WebTAG appraisal process.

The effectiveness of the guidelines discussed above is limited by the number of possible interventions which can feasibly be appraised. In a real urban transport network, there are an effectively unlimited number of possible interventions and so, even in the initial appraisal stage, only a very small subset of possible interventions will be considered. An even smaller number of interventions will go through the full appraisal due to the human effort involved in carrying out such analysis.

In recent years there has been some research interest in designing software-based solutions in order to systematically identify suitable transport interventions for cycling. (Vandenbulcke et al. (2011)) built a regression model to predict the percentage of commuting by bicycle at the municipal level based on variables related to land use, urban structure, accident risk, traffic network and traffic volumes. By observing the residuals in the model for each municipality, they identified areas which were over-performing with respect to cycling levels and areas where there was still potential to develop the use of the bicycle for commuting. Lovelace et al. (2015) developed the Propensity to Cycle Tool (PCT) to identify O-D pairs in England with potential for increased cycling cycling levels. The PCT is uses a similar approach to (Vandenbulcke et al. (2011)) but on an O-D level rather than at the municipal level. The PCT is based on a logistic regression model which predicts cycling mode share for each O-D pair based on distance and hilliness of the fastest route. The tool was used to develop hypothetical scenarios with increased overall cycling levels whereby the increase in cycling between each O-D pair was determined by the propensity to cycle as predicted by the fitted model. The PCT is also available publicly as an open source web-tool. While the PCT is a useful tool for identifying O-D pairs with potential for greater cycling levels, it has limitations as a tool for aiding in the design of cycling infrastructure.

It does not consider the influence of some important factors such as motor traffic levels on the propensity to cycle nor does it consider the impacts of building new cycling infrastructure on other modes. It also works at the O-D level whereas infrastructure changes are ultimately made at the link level. For example, rather than designing a cycleway to cover an entire route, a cycle lane may be provided on a busy road which forms a small part of many routes.

There have also been some examples in the literature of using the network design problem (NDP) to aid in cycle network design. The NDP is a strategic decision-making problem which aims to find best use of limited resources such as land use and monetary budget in order to optimise the performance of a transport network while giving consideration to the behaviours of the network users in response to the strategy (Xu et al., 2016). Traditionally, the main objectives of the NDP in the literature have been to minimise traveller delays and maximise network reserve capacity (Bell and Iida, 1997; Boyce, 1984). The sustainable road NDP, however, in addition to economic considerations also includes environmental and/or social impacts. A review of the literature on the sustainable road NDP is given by Xu et al. (2016). The NDP is generally formulated as bilevel optimisation problem or MPEC where the objective function represents the decisions of the transportation authority and the equilibrium problem represents the behavioural responses of the users of the network. The decision variables may include discrete variables relating to the network topology (addition/removal of links, one-way restrictions etc.) as well as continuous variables relating to the parameterisation of the network (capacity enhancement, signal timing etc.) (Xu et al., 2016). Until recently there was a notable lack of NDP studies which aimed to optimise cycling networks. In the past six years, however, a number of studies have emerged which aimed to use the NDP to systematically design cycle facility layouts in multi-modal transport networks. These studies sought either a single optimal cycle network design or a set of pareto optimal designs. If a single solution was sought, it was necessary for all objectives such as functions of travel time or emissions to be expressed in common units or given relative weightings.

The cycle network design optimisation studies to date can be placed into two categories: studies which aimed to find the optimal placement of cycle infrastructure based on network structure alone and studies which aimed to find the optimal placement of cycle infrastructure given the predicted response of the network users to the new infrastructure.

In the first type of study, the problem is formulated as a single-level programming problem and the objective function is formed in relation to network characteristics. Lin and Yang (2011) used an integer nonlinear program to design the layout of public bicycle rental stations and bicycle

paths connecting them to optimise a function of travel costs (based on shortest-path, not traveller behaviour), setup costs, service coverage and bicycle stock costs. Smith and Haghani (2012) formulated a mixed integer programme to find pareto optimal layouts for cycle facilities in the centre of Baltimore in order to minimise path length and maximise bicycle LOS. Lin and Yu (2012) found a pareto set of bikeway layouts in a small area of Taipei City to optimise functions of risk, comfort and service coverage. Duthie and Unnikrishnan (2014) aimed to find the single lowest-cost solution to connect each O-D pair in the network by a fully connected path where each roadway segment and intersection exceeded a minimum bicycling LOS. Lin and Liao (2014) used a similar problem formulation to Lin and Yu (2012) but in addition to bikeways, it considered optimal placement of service stations.

In the second type of study, the problem is formulated as a bilevel programme or MPEC where the objective function represents the designer of the cycle facilities and the equilibrium problem represents the behavioural responses of the cyclists and/or other users of the network. Since these studies predicted the responses of users to the infrastructure, they could also take into account total travel costs in the system and/or the perceived benefits of travelling. Mesbah et al. (2012) formulated a bilevel programme to design the layout of cycle facilities where the top level optimised a function of distance cycled on cycle lanes and total travel time of autos and the lower level found the network equilibrium in response to the design. However, the cyclist and auto equilibrium solutions were found separately so that no interactions between the two modes were modelled. Li et al. (2015) developed a multi-modal equilibrium model including a public bicycle mode. They found the equilibrium for a small test network in response to a range of bicycle rental prices and emissions charges. Since only two design variables were considered, the solution which maximised the sum of consumer surplus and producer surplus could be found graphically. Bagloee et al. (2016) sought to find the optimal allocation of priority cycle links in the Winnipeg transport network by identifying links with latent misutilised capacity. A bilevel programming model was developed where the top level minimised the total system travel cost and the bottom level found the multi-modal traffic equilibrium in response to the design. The user equilibrium model included interactions between the cycling and driving modes but a simplified model of link congestion was used whereby each mode on a given link experiences the same delay.

Since most of the studies in both categories considered only discrete variables such as whether or not to add a cycle lane and did not consider capacity enhancement in a continuous sense, the problems had a combinatorial structure. For this reason a popular class of solution algorithm

were Branch and bound methods, which were used in three studies (Lin and Yang, 2011; Smith and Haghani, 2012; Bagloee et al., 2016). Other solution approaches included genetic algorithms (Mesbah et al., 2012) and various commercial solvers.

2.5 Scope of Research

A number of research gaps and opportunities can be identified based on this literature review and these are discussed below.

There have been many studies in recent years which have sought to quantify the total health and environmental impacts of cycling at a societal level. However, little attention has been given to the distribution of impacts experienced by cyclists at an individual level. This is important because if these impacts are only considered at an aggregate level; negative impacts by some sub-populations may be masked by positive impacts experienced by others. Chapter 4 will address this gap In the research.

Some of the studies which have quantified the health impacts of cycling included exposure to air pollution while travelling as a determinant of health. However, they have done so at a highly aggregate level, ignoring route specific considerations such as traffic volumes and presence of cycling facilities. Studies of the air pollution exposure of cyclists have found traffic levels and facilities to be important factors but only a small number of these have considered real-time traffic and presence of facilities in the same study these have shown inconsistent results. Also, none of these studies have measured NO_x, this may be because it was previously believed that NO_x exposure had no long term health impacts independently from PM exposure. However, the evidence now points towards an independent long term health impact of NO_x exposure (COMEAP, 2015). Therefore, there is a need for further research into the relationship between cyclist exposures to air pollution—including NO_x—and route specific characteristics such as traffic levels and presence of cycling facilities. This research gap will be address in Chapter 5 and 6.

Studies into the health and environmental impacts of cycling have focussed mainly on hypothetical scenarios where cycling mode shares are higher, with no consideration given to the policies which could achieve these scenarios. National guidelines such as the CAF and WebTAG offer guidelines on evaluating specific interventions but they are not suitable for properly evaluating cycling interventions as they cannot predict the change in travel behaviour of cyclists nor can they comprehensively quantify all of the expected impacts of changes in cycling levels. A software tool such as the PCT is useful for identifying areas with high potential for increased

cycling but it does not attempt to model how cycling behaviour would change in response to a new piece of infrastructure. There is a need for decision support tools which can help to identify infrastructure interventions with high potential for increasing cycling levels in such a way as to optimise the overall societal impacts. In this thesis, it is hypothesised that this can be achieved by combining quantification of impacts and network equilibrium modelling within an optimisation framework.

Econometric network equilibrium models assume that travel behaviour is governed simply by a desire to minimise one's expected disutility of travel. This ignores potentially important considerations such as social norms and attitudes which may be important in the context of cycling. However, equilibrium methods have many advantages such the ability to capture complex interactions between the transport network, route choice, mode choice and overall demand while maintaining internal consistency (Boyce and Bar-Gera, 2004). This advantage is particularly important when considering the impacts of an intervention which takes place at the link level on overall travel behaviour. The introduction of a new cycling facility can be expected to influence route choices of existing cyclists as well as to increase the modal share of cycling. The behaviour of other modes may also be influenced through changes in their interactions with cyclists and changes in the road capacity devoted to motor vehicles. All of these complex interactions can be readily accounted for in a combined equilibrium model. Also, the literature relating to cycling modal share suggests that the most consistently important determinants of cycling mode choice are route level characteristics such as traffic levels, topography and availability of facilities. This suggests that the choice to cycle is largely determined by the expected disutility of cycling on the most attractive cycling route. If these route-level characteristics can be captured in a measure of the disutility of cycling, then it should be possible to build and calibrate a combined model of mode and route choice based on route disutility alone with reasonable predictive accuracy. However, no studies in the literature to date have developed and calibrated such a disutility function for cyclists. Therefore, Chapter 7 addresses the challenge of developing and calibrating a disutility function for cycling. Since no suitable method exists for this calibration, a new calibration algorithm based on sensitivity analysis of the underlying equilibrium problem is proposed.

Chapter 8 then builds on the contributions of all the previous chapters in order to develop a tool for finding the optimal design for a cycle network, taking into account the responses of the network users to the intervention and the health, environmental and travel time impacts resulting from the changes in travel behaviour. In recent years, traditional appraisal methods for

transportation such as the CAF have been extended to consider impacts such as the health impacts of active travel. However, chapter 8 builds on this by integrating the impact calculations with modelling of the responses of cyclists to an intervention. This integrated approach is also placed in an optimisation framework so that rather than simply evaluating a particular existing design, an optimal design can be found automatically.

Chapter 3: Quantifying the Benefits and Risks of Urban Cycling in Dublin; Total Societal Impacts

Motorised modes of transportation have profound negative impacts on both the users of these modes and the surrounding population Per-km costs from IMPACT handbook (Korzhenevych et al., 2014). Dependence on motorised transport promotes physical inactivity, a leading cause of ill health which is responsible for 6% of deaths globally (WHO, 2010). In addition to personal impacts, motorised transport results in negative external impacts. In 2015, the transport sector was responsible for 37% of all energy-related carbon dioxide (CO_2) emissions in Ireland, more than any other sector (Sustainable Energy Authority of Ireland, 2016). Road transport is also the main source of emissions of particulate matter, nitrogen oxides, carbon monoxide and benzene in Ireland (Environmental Protection Agency, 2016). Motorised travel is often the only realistic option for essential trips. However many other trips, particularly in urban environments, are short and could easily be made by bicycle (National Transport Authority, 2015b; Pucher and Dijkstra, 2003). The replacement of motorised transportation by cycling can significantly mitigate the external costs of motorised transportation (Bickel et al., 2006) while also improving the health of end users through increased physical activity (Mueller et al., 2015). However, there are also additional risks associated with cycling such as increased vulnerability to road traffic collisions and increased in-travel exposure to air pollution. Although there is a growing understanding that the benefits of active travel significantly outweigh these risks, it is essential that these benefits can be appraised quantitatively in order to inform evidence based policy formulation and promote the uptake of cycling if appropriate. Quantification of the negative external costs of motorised travel also allows for internalisation of those costs through taxes and charges so that transport users will take these societal costs into account when making decisions. For these reasons, methods of quantification in common units of the total societal benefits and risks of cycling are needed.

As described in Chapter 2, a number of studies have previously quantified the impacts of increasing uptake of active modes of travel. However, many of these were not comprehensive in terms of the impacts considered. For example, the only reviewed study to consider noise and congestion impacts was Rabl and de Nazelle (2012) and they found these impacts to be highly significant. In addition, no study to date has included the change in travel costs to both the new cyclists and the rest of the network users alongside health and environmental impacts. Traditionally, travel costs have been the most important cost to be considered by transport

planners and so their exclusion is a major concern. This chapter aims to develop a framework for comprehensively quantifying the impacts of a modal shift in favour of cycling. This framework is also applied to a case study of work commuters in Dublin. In the next section, the scenario of interest in the case study is described. This is followed by a descriptions of the various models used to estimate the total societal impacts in monetary terms. The results are then presented, followed by a conclusion. The contents of this chapter are based on published work (Doorley et al., 2015a).

3.1 Case Study of Dublin

The scenario of interest in this study was one whereby all work commuter trips currently undertaken by car or van which would be considered as cycle-able are cycled. This is clearly an idealised scenario but it allows indicative estimates of the relative scale of the various benefits and risks of cycling to be made. For this purpose it was assumed that a journey of 5km or less each way is cycle-able. This was considered reasonable as a European study has suggested that cycling may be the fastest mode of transport for trips of 5km or less in urban environments (European Commission, 1999). The data for this study was sourced from the POWSCAR (Place of Work, School or College – Census of Anonymised Records), 2011 data (Central Statistics Office, 2011a; Central Statistics Office, 2011b). This dataset includes details of commuter trips made by all persons over the age of 4, resident in Ireland on Apr/10/2011, including home and work/school/college locations, journey times and journey modes. This study focussed on work trips because certain important variables such as age group are not reported for school or college trips in the data. A summary of the daily work trips in county Dublin based on these data is shown in Table 3.1. Since POWSCAR, 2011 only specifies journey times; the journey distances were estimated using average driving speeds. Trips were categorised based on their origins and destinations as being city trips, outside-city or combined trips. For outside-city and combined trips, average journey speeds of 25km/hr and 21km/hr were estimated based on POWCAR (Place of Work – Census of Anonymised Records), 2006 (Central Statistics Office, 2006) which included both journey times and journey distances. For city trips, this method was not used as a speed limit of 30km/hr was introduced in Dublin city centre in 2010. A conservative average driving speed of 15 km/hr was assumed for city trips. These average driving speeds are simplified estimates which ignore variations due to time of day, road types etc. No data were available on average cycling speeds in Dublin and so average cycling speed was estimated to be 14km/hour, consistent with the assumptions of the WHO's Health Economic Assessment Tool (HEAT) (WHO, 2014). The impacts of this modal shift were quantified for a single year—2012.

Table 3.1 Commuter trips by car/van, bicycle, walking and public transport (PT) in county Dublin as per census, 2011

		City Trips					Outside-city Trips					Combined Trips				
Gender	**Age**	**N**	**Car/Van**	**Bicycle**	**Walk**	**PT**	**N**	**Car/Van**	**Bicycle**	**Walk**	**PT**	**N**	**Car/Van**	**Bicycle**	**Walk**	**PT**
Male	15-19	458	18%	9%	34%	39%	666	42%	5%	31%	21%	409	37%	4%	7%	50%
	20-24	4349	21%	11%	38%	29%	4498	58%	5%	21%	16%	4031	44%	5%	3%	46%
	25-29	11443	21%	15%	39%	24%	9159	69%	5%	14%	11%	10837	48%	6%	3%	41%
	30-34	11266	26%	17%	32%	23%	10958	75%	5%	10%	8%	13452	53%	8%	2%	35%
	35-39	7865	33%	19%	25%	20%	9499	80%	5%	7%	7%	11477	58%	8%	1%	29%
	40-44	6054	41%	18%	21%	19%	7804	81%	5%	7%	5%	9400	63%	8%	1%	24%
	45-49	5424	46%	16%	18%	18%	6594	83%	4%	6%	4%	8283	67%	7%	1%	21%
	50-54	4804	48%	14%	19%	17%	5693	83%	4%	7%	5%	7291	67%	7%	1%	21%
	55-59	3607	48%	12%	19%	18%	4174	83%	4%	7%	4%	5478	69%	5%	1%	22%
	60-64	2287	52%	11%	18%	18%	2603	83%	4%	8%	4%	3103	72%	4%	1%	21%
	65-69	587	55%	6%	20%	17%	697	81%	2%	10%	5%	765	73%	3%	1%	22%
	70-74	177	57%	7%	14%	21%	256	79%	2%	14%	4%	234	74%	2%	1%	21%
	75+	116	47%	8%	32%	12%	111	77%	3%	17%	3%	140	75%	1%	4%	19%
Female	15-19	489	17%	2%	40%	41%	629	45%	1%	27%	28%	344	33%	0%	5%	62%
	20-24	6071	22%	4%	38%	36%	5692	61%	1%	20%	18%	5126	41%	1%	4%	53%
	25-29	15115	24%	7%	41%	28%	11491	70%	1%	16%	12%	12962	48%	2%	3%	47%
	30-34	13673	29%	8%	35%	28%	11575	78%	2%	12%	8%	14621	54%	2%	2%	41%
	35-39	9152	38%	7%	29%	25%	9182	81%	1%	11%	6%	11043	61%	2%	2%	35%
	40-44	7261	42%	6%	27%	24%	7556	81%	1%	12%	6%	8130	66%	3%	2%	29%
	45-49	6818	45%	5%	26%	24%	7705	79%	1%	13%	6%	7304	67%	2%	3%	28%
	50-54	5910	43%	4%	29%	24%	6896	75%	2%	16%	7%	6283	66%	2%	2%	29%
	55-59	4203	42%	3%	28%	26%	5134	74%	1%	18%	7%	4551	66%	1%	3%	30%
	60-64	2552	40%	3%	31%	26%	2705	70%	1%	21%	7%	2437	66%	1%	3%	30%
	65-69	570	43%	2%	29%	25%	571	72%	1%	21%	6%	453	65%	2%	3%	30%
	70-74	178	36%	2%	39%	24%	145	72%	3%	19%	6%	123	71%	0%	2%	27%
	75+	85	38%	6%	36%	20%	55	71%	2%	18%	9%	57	70%	0%	4%	25%

3.2 Estimation of Impacts

The impacts of increased cycling which were considered in this study included both those experienced by the cyclists themselves—health effects of physical activity, in-transit pollution exposure, traffic collisions and travel costs—and those experienced by the rest of society—traffic collisions, reduced emissions of air pollution and greenhouse gases, reduced noise and reduced congestion. Different models were used to quantify each of these impacts and convert them to equivalent monetary units. An outline of the methods used to quantify and monetise each impact is shown in Table 3.2 and each of these impacts is discussed in detail below. All monetary values from previous years were updated to 2015 values based on GDP per capita growth in Ireland (OECD Data, 2016). Since there are significant uncertainties associated with the models, upper and lower bounds are also calculated which take into account the main sources of uncertainty.

All impacts are calculated as deviations from the current or business-as-usual scenario and this is consistent with the prevailing approach taken in the studies reviewed in Chapter 2. However, it is worth noting that this paradigm implies that the net cost of the current transport scenario is zero when in fact, the level of motor vehicle traffic in a city such as Dublin has major consequences in terms of air pollution, congestion and other external impacts. It would be arguably more appropriate to calculate the costs of driving relative to cycling rather than to calculate the benefits of cycling relative to driving.

Table 3.2 Outline of models used to quantify and monetise impacts of active travel

Impact	Model	Units	Monetisation
Physical Activity influences risk of specific diseases	Dose-Response Functions based on Woodcock (Woodcock et al., 2009)	DALYs	VOLY
In-travel pollution exposure influences risk of specific diseases	Dose-Response Functions recommended by WHO (Ostro, 2004)	DALYs	VOLY
Traffic collision risk changes for entire network	Non-linear model based on Woodcock (Woodcock et al., 2013) with estimates of DALYs lost for each collision type	DALYs	VOLY
External air pollution emissions are reduced	Emission factors from TREMOVE (Breemersch et al., 2010)	Tonnes	Per-tonne costs from IMPACT handbook (Korzhenevych et al., 2014)
Greenhouse gas emissions are reduced	Per-km costs from IMPACT handbook (Korzhenevych et al., 2014)	Euro	-
External noise pollution is reduced	Per-km costs from IMPACT handbook (Korzhenevych et al., 2014)	Euro	-
Generalised cost of travel (GCoT) changes	GCoT modelled as the sum of time cost and operating costs	Euro	-
Congestion in network is reduced	Per-km costs from IMPACT handbook (Korzhenevych et al., 2014)	Euro	-

3.2.1 Health Impacts of Physical Activity

Cycling as a mode of travel is physical activity which is typically performed at a moderate intensity and such activities have positive long-term health impacts. As discussed in Chapter 2, the benefits of physical activity can be quantified in terms of mortality or BOD. In this study, the BOD approach is taken because, as outlined in Chapter 2, it is more appropriate for quantifying the health impacts of chronic exposure to air pollution and physical activity than mortality-based approaches. BOD is a summary measure of the impact of a disease on health, taking into account both Years of Life Lost (YLLs) and Years of healthy Life lost to Disability (YLDs). The sum of YLLs and YLDs gives the total Disability Adjusted Life Years (DALYs) lost. To calculate the change in DALYs due to physical activity, the average kms cycled by the additional cyclists in each age and gender group were first converted to Metabolic Equivalent of Task (MET) hours using a compendium of physical activity MET factors (Ainsworth et al., 2011). A MET factor of 6.8 was used for cycling, consistent with HEAT for cycling and several recent studies (Woodcock et al., 2013; Woodcock et al., 2014). Non-travel related physical activity MET hours also needed to be estimated. The proportions of people in each age and gender group having a physical activity level of, low, moderate or high on the International Physical Activity Questionnaire (IPAQ) scale could be obtained from the results of the recent Health Ireland survey (IPSOS MRBI, 2015). The MET hours per week associated with low, moderate and high activity levels were estimated to be 0, 10 and 28 based on the IPAQ guidelines (IPAQ Research Committee, 2005). The relationships between MET hours of physical activities and the risk of various health conditions were modelled based on a systematic review by Woodcock et al. (2009). The health conditions modelled were cardiovascular disease, breast cancer, colon cancer, dementia, depression and type II diabetes. It was assumed that the Relative Risks (RR) applied to both YLLs and YLDs. The RRs of this review were based on specific levels of weekly physical activity and so they needed to be adapted to the appropriate levels of physical activity in the current study. Similarly to Woodcock et al. (2013) this was achieved by assuming a log-linear relationship between risk of each condition and a power of 0·5 transformation of MET hours (power of 0.375 for diabetes). The baseline expected YLLs and YLDs for each age and gender group were obtained from the WHO global BOD estimates for 2012 (World Health Organization, 2014). The new cyclists were grouped by age, gender and level of baseline activity and the change in YLLs for each group due to each condition, *i*, were calculated using Eq. 3.1 to Eq. 3.3.

$$\Delta YLL^{i} = N \times YLL_{B}{}^{i}\left(1-\frac{RR_{C}{}^{i}}{RR_{B}{}^{i}}\right) \quad \text{Eq. (3.1)}$$

$$RR_{C}{}^{i} = RR_{Ref}{}^{i} \wedge \left(\frac{METS_{C}+METS_{B}}{METS_{Ref}{}^{i}}\right)^{\lambda^{i}} \quad \text{Eq. (3.2)}$$

$$RR_{B}{}^{i} = RR_{Ref}{}^{i} \wedge \left(\frac{METS_{B}}{METS_{Ref}{}^{i}}\right)^{\lambda^{i}} \quad \text{Eq. (3.3)}$$

Where *N* is the number of individuals in the group, ΔYLL^{i} is the change in expected YLLs due to condition *i*, $YLL_{B}{}^{i}$ is the YLLs expected at baseline, $METS_{B}$ is the MET hours of PA at baseline, $RR_{Ref}{}^{i}$ and $METS_{Ref}{}^{i}$ are the reference RR and reference MET hours associated with disease *i* in the systematic review of Woodcock et al. (2009), $METS_{C}$ is the additional MET hours of cycling and λ^{i} is the power transformation of the exposure. The change in the expected YLDs was calculated in the same way. The sum of all DALYs saved across all groups gave the central impact for total DALYs saved due to physical activity. This impact could be represented by a monetary value by multiplying the number of DALYs saved by the Value of a Life Year (VOLY). A VOLY of €94,794 was used based on an Irish study (Deloitte Access Economics, 2011). To calculate upper and lower bounds based on this model, the analysis was repeated, replacing the reference RRs with limits of the 95% confidence intervals as reported by Woodcock et al. (2009).

Since previous studies have shown that physical activity is the most important determinant of the impacts of cycling and also that the choice of model can have a significant effect on the results, some additional analysis of this impact was carried out for comparison using three different models: quantifying deaths using the 2014 version of the Health Economic Assessment Tool (HEAT) for cycling; quantifying YLLs using HEAT 2014; and quantifying deaths using the 2011 version of the HEAT.

As discussed in Chapter 2, the HEAT for cycling is the most widely used model for quantifying the mortality impacts of the physical activity of cycling. This tool was developed by the WHO as a user-friendly tool for anyone to conduct an economic assessment of the health benefits of cycling by estimating the value of the reductions in mortality resulting from the cycling. The first secondary model of this study was based on the most recent version of this tool, released in 2014, which predicts the decrease in all-cause mortality due to increased cycling in a population after a build-up period of 5 years based on Eq. (3.4).

$$\Delta D_{PA} = N \times MR_B \times \left(1 - RR_{Ref}\right) * \left(\frac{d}{d_{Ref}}\right) \quad \text{Eq. (3.4)}$$

where ΔD_{PA} is the change in deaths per year due to the cycling physical activity, *N* is the number of subjects, MR_B is the baseline mortality rate, RR_{Ref} is the reference Relative Risk (RR) from the underlying studies in the HEAT meta-analysis, d_{Ref} is the reference cycling distance from the underlying studies and d is the average distance cycled in the scenario of interest. Baseline mortality rates associated with each 5-year age group in Ireland were obtained from the WHO Mortality Database (WHO). The resulting avoided fatalities were converted to an equivalent monetary value using the Value of a Statistical Life (VSL). The VSL of €5,128,420 suggested by the WHO for use in Ireland was used. As with the main model, the limits of the 95% confidence interval for the reference RR were used to calculate upper and lower bounds.

In another secondary model, the RRs estimated using the HEAT, 2014 model were applied to the baseline all-cause YLLs per year to find the change in YLLs per year as a result of the physical activity. The economic impact of this reduction in YLLs was estimated using the VOLY. As with the main model, the limits of the 95% confidence interval for the reference RR were used to calculate upper and lower bounds. The final secondary model was based on the 2011 version of HEAT, 2011. As discussed in Chapter 2, this older version of HEAT, released in 2011, was widely used and discussed in studies which assessed the benefits and risks of cycling (Deenihan and Caulfield, 2014; Grabow et al., 2012; Lindsay et al., 2011; Rojas-Rueda et al., 2011; Rojas-Rueda et al., 2012) before the 2014 version was released. However, the base of epidemiological evidence for HEAT, 2011 was not as comprehensive as that of the 2014 version (WHO, 2014).

3.2.2 Traffic Collisions

Cyclists are generally at higher risk of being involved in road collisions than drivers and passengers of cars. However, evidence has consistently shown that there is a "Safety in Numbers" effect associated with cycling whereby increases in levels of walking and cycling lead to a reduction in the risk of collision for pedestrians and cyclists (Elvik, 2009; Robinson, 2005). Furthermore, the reduction in distance travelled by motorised modes in the network leads to a reduction in collision risk for users of all modes. For these reasons, the relationship between the distance travelled by a particular mode in a transport network and the collision risk for that mode is strongly non-linear (Elvik, 2009) and is also affected by the distance travelled by other modes. In this study, the change in the incidence of fatal and non-fatal collisions for each mode in response to the modal shift was modelled by using a non-linear model similar to that used by

Woodcock et al. (2013). For each pairwise combination of striking mode and victim mode, the number of fatal injuries and the number of non-fatal injuries were calculated using Eq. (3.5).

$$\Delta I = I_B \times \left(\left\{ \frac{d_s}{d_{s_B}} \right\}^{\beta} \times \left\{ \frac{d_v}{d_{v_B}} \right\}^{\alpha} - 1 \right) \qquad \text{Eq. (3.5)}$$

where ΔI is the change number of in injuries (fatal or non-fatal) per year, I_B is the number of injuries of the particular severity and striking/victim mode combination at baseline, d_{s_B} and d_{v_B} are the respective distances travelled by the striking and victim mode at baseline, d_s and d_v are the respective distances travelled by the striking and victim mode in the study scenario and α and β are power transformations of the distance travelled which account for the non-linear relationship between road traffic injuries and distances travelled. These power transformations vary by mode and were obtained for this study from Elvik (2009) and Woodcock et al. (2013). The baseline distances travelled by each mode were estimated using a similar method to Short and Caulfield (2014). The baseline collision data was obtained from the Road Safety Authority (RSA) Road Collision Factbook 2011 and 2012 (Road Safety Authority, 2011, 2012). It was assumed that the apportionment of non-fatal injuries to victim-striking mode combinations in Dublin County was the same as in Ireland as a whole. It was also assumed that the ratio of serious injuries to minor injuries for each combination of modes in Dublin was the same as the ratio of serious injuries to minor injuries in Ireland as a whole.

It is well documented that traffic collisions are significantly underreported, particularly minor collisions and collisions involving active modes. In Ireland the road collision information accumulated by the RSA is based on reports by the police service, An Garda Síochána. One study has estimated that the true number of cycling collisions in Ireland is six times greater than the police reported number (Short and Caulfield, 2014). In order to account for such underreporting, the baseline collision data from RSA was scaled using mode and severity specific correction factors provided by the HEATCO study (Bickel et al., 2006), a European study which developed a framework for consistent monetary valuation of transport projects. The scaled and unscaled results provided upper and lower bound estimates for the change in traffic collision casualties and the average of these was taken as the central estimate.

In order to represent the change in traffic collisions in monetary terms, it was necessary to first estimate the resulting change in DALYs. The monetary cost could then be quantified based on the VOLY. It was assumed that the DALYs lost due to a fatal injury would be equal to the

remaining life expectancy of the casualty at the time of the collision. The average DALYs per fatal collision was therefore assumed to be equal to the average remaining life expectancy among the 20-64 age group in the population of Dublin (CSO, 2015) . This resulted in an average of 42.5 DALYs lost per collision. To estimate the YLDs lost due to serious and minor injuries, no suitable data from Ireland was available so reference was made to a recent study (Tainio et al., 2014) which estimated YLDs lost in traffic collision injuries based on data from the Swedish Traffic Accident Data Acquisition (STRADA) database. Values were estimated for each injury severity on the Abbreviated Injury Scale (AIS): minor, moderate, serious, severe, critical and maximal. The RSA collision statistics in Ireland do not clarify what is meant by a "serious" or "minor" injury or how these relate to the AIS so it was assumed that RSA minor injuries include those which would be classified as minor or moderate on the AIS and RSA serious injuries include those which would be classified as serious, severe, critical or maximal on the AIS. To estimate the YLDs lost for each RSA injury type, a weighted average was taken of the estimated YLDs for each corresponding AIS injury type, where the weighting was based on the relative frequency of these injury classes in STRADA.

3.2.3 Health Impacts of In-travel Pollution Exposure

Although pedestrians and cyclists do not produce air pollutants which are directly harmful to human health while travelling, they are exposed to higher inhalation doses of toxic pollutants, mainly due to their elevated ventilation rates (McNabola et al., 2008; Panis et al., 2010; Zuurbier et al., 2010). $PM_{2.5}$ is commonly considered as the most important pollutant for predicting the long term health impacts of traffic related air pollution (Chen et al., 2008). To estimate the impact of the increased inhalation dose of travellers switching from car travel to active travel, an approach similar to Hartog et al. (2011) was taken. First, the ratio of yearly inhaled dose of $PM_{2.5}$ between the hypothetical and baseline scenarios was calculated. The ratio of inhalation doses, R_d was calculated using Eq. (3.6).

$$R_d = \left(\frac{w}{365}\right) \times \frac{C_C \times t_C \times MET_C + t_S \times MET_S + \left(T - t_A - t_S\right) \times MET_O}{C_D \times t_D \times MET_D + t_S \times MET_S + \left(T - t_D - t_S\right) \times MET_O} + \left(\frac{1-w}{365}\right) \quad \text{Eq. (3.6)}$$

where w is the number of work days per year (221), the subscripts *C*, *S*, *O* and *D* denote the activities driving, sleeping, cycling and other; *C* is the concentration factor for the activity, *MET* is the estimated MET factor for the activity, *t* is the average time spent in the activity daily and T is 24 hours. The concentration factor accounts for the relative exposure concentration experienced by different modes using the same routes due to vehicle type and road position. Similarly to a recent study (Woodcock et al., 2014), concentration factors of 0.8, 1 and 1.3 were used for

pedestrians, cyclists and drivers respectively based on a systematic review of air pollution exposure by different modes of transport in Europe. The MET factors, sourced from a compendium of MET factors (Ainsworth et al., 2011) were used to account for the relative ventilation rates between each travel mode. For non-travel time, a concentration factor of 1 and MET factors of 0.95 for sleeping (8 hours) and 1.5 for the rest of the day were assumed, similarly to Woodcock et al. (2014). It was then assumed that the health impact to these travellers of the increase in inhaled dose would be equivalent to the impact of an increase in average ambient $PM_{2.5}$ concentration of the same proportion. The baseline average annual $PM_{2.5}$ concentration used for this calculation was estimated at 10μg/m^3 based on the EPA of Ireland Air Quality Report 2012 (Environmental Protection Agency, 2012). The health impacts of changes in ambient $PM_{2.5}$ concentrations have been studied extensively. In this study, the results of the APHEIS (Air Pollution and Health: A European Information System) study (Boldo et al., 2006) were used to estimate the changes in YLLs from cardiorespiratory diseases and lung cancer of the new cyclists due to their change in $PM_{2.5}$ exposure. This study found that a 10 μg/m^3 increase in mean $PM_{2.5}$ concentration was associated with RRs of 1.09 and 1.14 for cardiopulmonary and lung cancer mortality respectively. The change in YLLs could be modelled using Eq. 3.7 and Eq. 3.8:

$$\Delta YLL^i = N \times YLL_B{}^i \left(1 - RR_C{}^i\right) \quad \text{Eq. (3.7)}$$

$$RR_C{}^i = RR_{Ref}^{i\ \Delta C_{eq} / \Delta C_{Ref}} \quad \text{Eq. (3.8)}$$

Where ΔYLL^i is the change in the individual's expected YLLs due to condition *i*, $YLL_B{}^i$ is the individual's baseline expected YLLs due to condition *i*, RR_{Ref}^i is the reference RR for condition *i*, ΔC_{Ref} is the reference concentration change for condition *i* and ΔC_{eq} is the equivalent change in concentration of $PM_{2.5}$. Since cardiovascular disease risk is influenced by both physical activity and pollution exposure, the impacts of the two exposures were modelled multiplicatively. To calculate upper and lower bounds based on this model, the analysis was repeated, replacing the reference RRs with limits of the 95% confidence intervals from the APHEIS study (Boldo et al., 2006).

3.2.4 External Pollution Impacts

Emissions of air pollutants by motor vehicles have negative societal impacts in the form of human health effects and damage to crops and eco-systems (Korzhenevych et al., 2014). In this study, the impacts of the decrease in toxic air pollution attributable to the reduction in vehicle km travelled was quantified in two steps. First, the reduction in emissions of $PM_{2.5}$, nitrogen oxides (NO_x), non-methane volatile organic compounds *(*NMVOC) and sulphur dioxide (SO_2) were estimated and then the external impacts of these reductions were estimated. In the first step, estimates of the average emissions of each pollutant per km travelled by the Irish fleet were obtained from the TREMOVE v3.3.2 (Breemersch et al., 2010) database, a widely used source of aggregate emission factors based on COPERT v4 (Gkatzoflias et al., 2007). The avoided emissions of each pollutant in the study scenario could then be easily calculated based on the avoided vehicle km (vkm) travelled. The external impacts of these avoided emissions were calculated by reference to the updated IMPACT Handbook (Korzhenevych et al., 2014). The Handbook gives cost estimates per tonne of each pollutant, differentiated by country as well as by type of locality—rural, suburban or metropolitan. It was assumed that emissions from city trips were 100% urban. For the central estimates, trips which had one end in the city centre were assumed 50% urban and 50% suburban and trips with both ends outside of the city centre were assumed 50% suburban and 50% rural. These assumptions were made due to a lack of data concerning the routes taken. These proportions were varied in the sensitivity analysis as described later in this section.

To estimate the avoided cost of greenhouse gas (GHG) emissions due to the avoided vehicle km, the updated IMPACT Handbook was referenced again. The Handbook provides per-km GHG costs based on an avoidance cost per tonne of CO_2 equivalent of €90, corresponding to efforts required to stabilise global warming at 2°C. The costs are differentiated by fuel type, technology class, engine size and locality type. In order to calculate the average per-km GHG cost of the Irish fleet, the apportionment of the Irish fleet to each fuel, technology class and engine size therefore needed to be estimated. This was estimated using the Irish Bulletin of Vehicle and Driver Statistics (Department of Transport Tourism and Sport Ireland, 2012). Trips were allocated to metropolitan, suburban and rural as described above.

The avoided costs of noise pollution were also calculated using the updated IMPACT Handbook (Korzhenevych et al., 2014). Costs estimates are provided by locality and by type of traffic—thin or dense. For the central estimate, the average of the per-km cost estimates for dense and thin traffic was used.

In estimating each of the external pollution impacts, the allocation of trips to locality types and traffic levels was a significant source of uncertainty. Therefore, these choices were varied in calculating the lower and upper bound estimates. For all the lower bound estimates, trips with one end in the city centre were assumed 100% suburban and trips with both ends outside of the city centre were assumed 100% rural. For the upper bound estimates, trips with one end in the city centre were assumed 100% urban and trips with both ends outside of the city centre were assumed 100% suburban. In calculating the lower and upper bound estimates of avoided noise costs, traffic was assumed to be dense and thin respectively. Additionally, for the lower and upper bound avoided GHG cost estimates, the lower and upper bound unit costs per tonne of CO_2 equivalent (€48 and €168) were used. The assumptions made regarding avoided external costs and the resulting unit costs values used for the central, lower and upper estimates are shown in Table 3.3.

Table 3.3 Unit costs for avoided external impacts

Central Estimate								
Trip type	**Assumed Locality Type**	**Costs avoided (€/vkm)**						
		GHGs	**Noise**	**Congestion**	**$PM_{2.5}$**	**NO_x**	**NMVOC**	**SO_2**
City Trips	100% Metro/Large-Urban	0.030	0.019	1.894	0.003	0.002	4.9E-04	1.3E-05
Combined Trips	50% Metro/Large-Urban and 50% Suburban/Small-Urban	0.030	0.010	1.539	0.002	0.002	5.7E-04	1.3E-05
Outside-City Trips	50% Suburban/Small-Urban and 50% Rural	0.024	0.001	0.782	0.000	0.002	3.5E-04	9.2E-06
Lower Bound								
	Assumed Locality Type	**Costs avoided (€/vkm)**						
		GHGs	**Noise**	**Congestion**	**$PM_{2.5}$**	**NO_x**	**NMVOC**	**SO_2**
City Trips	100% Metro/Large-Urban	0.016	0.011	1.779	0.003	0.002	4.9E-04	1.3E-05
Combined Trips	100% Suburban/Small-Urban	0.016	0.001	0.008	0.001	0.002	6.5E-04	1.2E-05
Outside-City Trips	100% Rural	0.010	0.000	0.005	0.000	0.001	4.6E-05	6.0E-06
Upper Bound								
	Assumed Locality Type	**Costs avoided (€/vkm)**						
		GHGs	**Noise**	**Congestion**	**$PM_{2.5}$**	**NO_x**	**NMVOC**	**SO_2**
City Trips	100% Metro/Large-Urban	0.056	0.027	3.055	0.003	0.002	4.9E-04	1.3E-05
Combined Trips	100% Metro/Large-Urban	0.056	0.027	3.055	0.003	0.002	4.9E-04	1.3E-05
Outside-City Trips	100% Suburban/Small-Urban	0.056	0.002	2.902	0.001	0.002	6.5E-04	1.2E-05

3.2.5 Travel Costs

A modal shift from driving to cycling impacts both the travel costs of individuals who alter their mode and the rest of society. The individuals who begin cycling experience a change in their generalised cost of travel while other users of the transport network are affected by a reduction in total congestion in the network. In this study, generalised costs of travel (GCoT) were assumed to be a combination of time expended in traveling and vehicle operating costs. For drivers, a Value-of-Time (VoT) of €19/hr and car operating cost of €0.103/km were assumed, consistent with the National Transport Model (National Roads Authority, 2014) of Ireland. The VoT for cyclists has not been studied extensively but a Swedish study (Börjesson and Eliasson, 2012) has estimated the VoT for cycling on streets and on cycle paths respectively to be greater than the VoT of the next preference mode by factors of 1.83 and 1.21. As cyclists in Dublin use a combination of shared streets and cycle paths, the driving VoT was scaled by the average of these two factors to estimate the cycling VoT. For the upper bound and lower bound estimates, the cycle-path factor and the on-street factor were used respectively. It was assumed that bicycle operating costs were negligible.

The external congestion costs were estimated based on the updated IMPACT Handbook which provides per-km marginal congestion costs differentiated by locality type, road type, and current congestion level—free flow, near capacity or over capacity. The same assumptions regarding locality type described in section 3.2.4 were used. The average of the unit costs for main roads near-capacity and other roads near-capacity was used for each locality type. For the upper and lower bound estimates, the locality type was varied as in section 3.2.4. Also, for the upper bound estimate, it was assumed that all roads were over-capacity. For the lower bounds, it was assumed that suburban and rural roads were at free-flow. The unit congestion costs used can be seen in Table 3.3.

3.3 Results and Discussion

The impact of converting all driving trips under 5km to cycling on the numbers of cycling commuters is shown in Figure 3.1. The vehicle km avoided in this scenario are shown in Figure 3.2. The modal share of cycling would increase from 8.85% to 21.5% for city trips, from 3.4% to 14.4% for outside-city trips and from 4.5% to 7.3% for combined trips. Figure 3.1 shows that there were more females than males driving for trips inside Dublin City and outer Dublin County which could be cycled. Figure 3.2 also shows that the conversion to cycling of trips by females would lead to a greater number of vehicle km avoided than conversion of trips by males. For both males and females, the greatest potential for conversion of car trips was in the 25-29 and

30-34 age groups. The youngest and oldest age groups had the lowest potential for trip conversion. In terms of location, there was greatest potential for avoidance of vehicle kms in outer Dublin County. Trips between Dublin City and Dublin County had the lowest potential for conversion to cycling and avoidance of vehicle kms. These findings suggest that in order to reduce vehicle traffic in Dublin by encouraging cycling, policies aimed at females aged 25-34 and improvement of cycling infrastructure outside of Dublin city centre have the greatest potential for positive impact.

3.3.1 Health, Environmental and Travel Time Impacts

Figure 3.3 summarises the health and environmental impacts of the modal shift envisioned in this study. Clearly, the positives outweigh the negatives and in particular, the physical activity benefits are significantly greater than any of the other impacts. This result is consistent with previous studies into the health and environmental impacts of increased cycling (Mueller et al., 2015). The secondary analysis of the physical activity benefits produced even more positive results. As shown in Figure 3.4, both of the models based on HEAT 2014 predicted significantly higher benefits of physical activity than the main BOD model. More surprisingly, the HEAT, 2011 model predicted benefits approximately five time greater than the main model. Previous studies have shown that different models of the health impacts of physical activity can produce significantly different results but this is the first study to have compared both versions of HEAT. The model which used the RRs from HEAT, 2014 to quantify the change in YLLs was slightly more conservative than the model which quantified deaths based on HEAT, 2014 model. However, the influence of quantifying YLLs rather than fatalities was much less dramatic than the influence of using a different model to calculate the RRs. In the analysis that follows, only the results of the BOD model are considered in order to maintain consistency with the other health impact estimates and because these were the most conservative estimates.

The only one of the impacts which was significantly negative was the change in road traffic collisions. Further insights can be gained by examining the predicted changes in traffic collisions for individual combinations of striking mode and victim mode. As shown in Table 3.4, there was a decrease in the total car driver fatalities and non-fatal casualties. There was also a decrease in the number of fatalities where cars were the striking vehicles. Total pedestrian fatalities and non-fatal casualties both decreased despite an increase in pedestrians being injured by cyclists. All of these results can be attributed the reduced distances driven by cars in the road network. However, for cyclists, the numbers of fatal and non-fatal victims were both increased. This increase in cycling casualties was much more significant than the reductions in driver and

pedestrian casualties. Of particular concern is the large increase in the number of non-fatal cyclist injuries. These large increases are due to the significant increase in distance travelled by cyclists in the network. Clearly, the benefits of the reduction in vehicle kms driven and the "Safety in Numbers" effect were not sufficient to offset the relative vulnerability of cyclists to traffic collisions. The overall impact on traffic collisions was a significant cost, largely due to the increase in minor cyclist casualties. The scale of the cost of minor cyclist casualties is particularly concerning due to the high level of underreporting of this type of incident. The HEATCO study estimated that in Europe minor cyclist injuries are underreported by a factor of 8. If underreporting of minor cyclist injuries is not accounted for when considering projects to promote cycling, the benefits of such projects may be significantly overestimated. It should also be noted that the underreporting factors provided by the HEATCO study were broad estimates for Europe as a whole and—while recent research in Ireland suggests that underreporting of cyclist injuries is of a similar scale (Short and Caulfield, 2014) —meaningful cost-benefit analysis will only be possible with more accurate collision data. The only other negative impact of the increased cycling in this study was due to the in-travel pollution exposure of cyclists and the scale of this impact was insignificant when compared to the physical activity and traffic collision impacts. However, it is worth noting that the pollution exposure estimates were not based on measured concentrations but on a simple exposure model which did not take into account variability due to traffic levels, time of day or available cycling facilities.

As shown in Figure 3.5, the positive external impact of reduced air pollution was of a similar scale to the negative individual pollution exposure impact. The benefit of the reduction in greenhouse gases was the greatest environmental impact. The uncertainty in the value of the GHG reduction is high due to the uncertainty in the per-tonne avoidance cost of a CO_2 equivalent. The value of the external noise reduction was greater than the value of the avoided air pollution, despite air pollution usually receiving much more attention than noise as a negative impact of motorised transport.

Up to this point, only the health and environmental impacts of cycling have been considered, similarly to most recent studies into the benefits and risks of cycling. However, arguably the most important impact to consider in appraising any transport project or policy is the impact on the cost of travel itself, both to the new cyclists and the other users of the network. As shown in Figure 3.6, these impacts are both very significant in the study scenario, but as the increase in GCoT of the cyclists is almost equal to the decrease in congestion costs in the network as a whole, there is little change in the central estimate of the total net impact. However, there is

considerably uncertainty in both estimates, particularly with regard to the VoT associated with time spent cycling. This causes the lower estimate of the total net impact to be negative. No previous studies of the total benefits and risks of cycling have predicted negative net impacts, even in sensitivity analysis. However, no previous studies have considered GCoT in their calculations, despite this being traditionally the most important cost to consider in appraising transport projects.

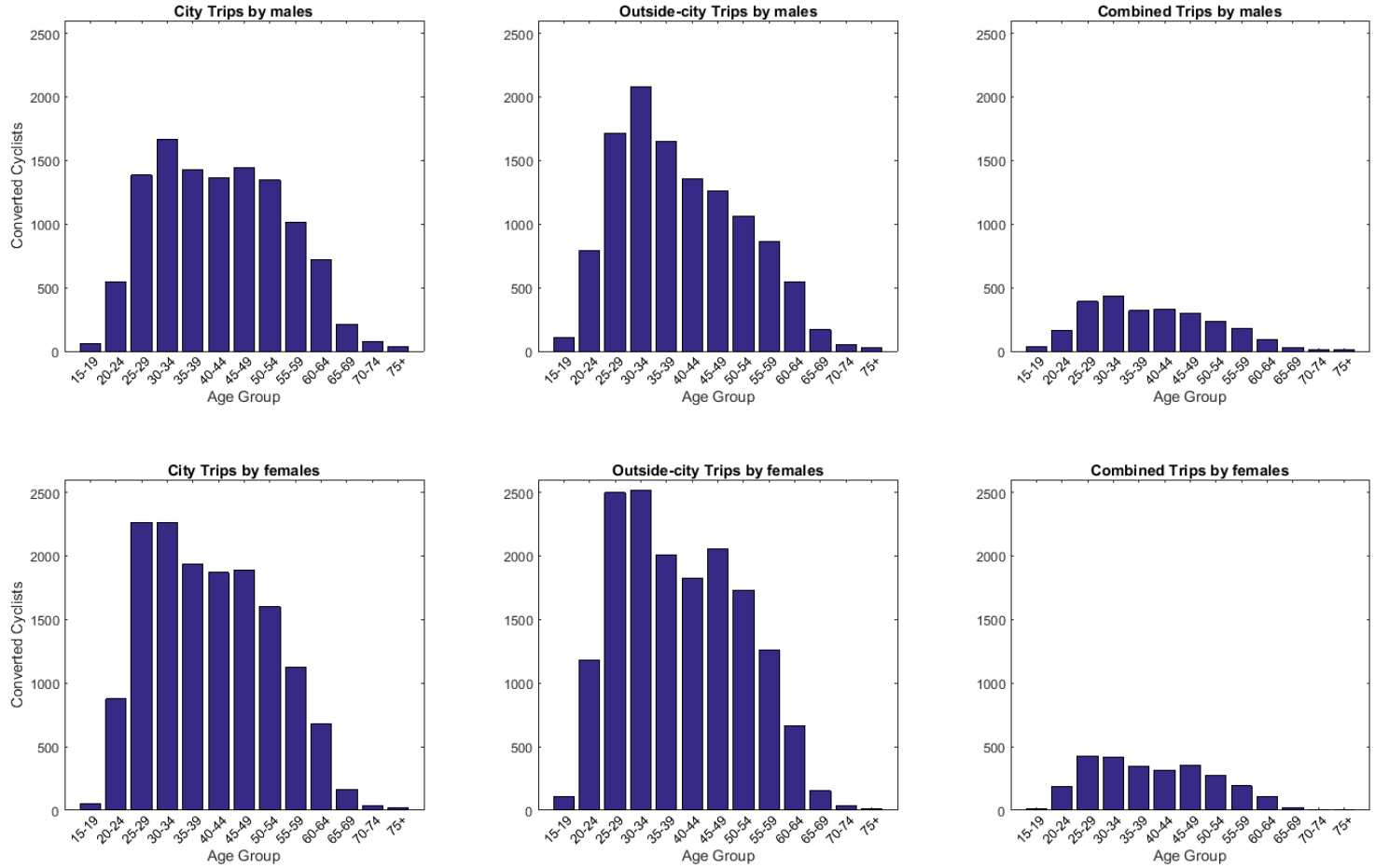

Figure 3.1 Commuters converted from driving to cycling in the case where all driving trips <5km are cycled.

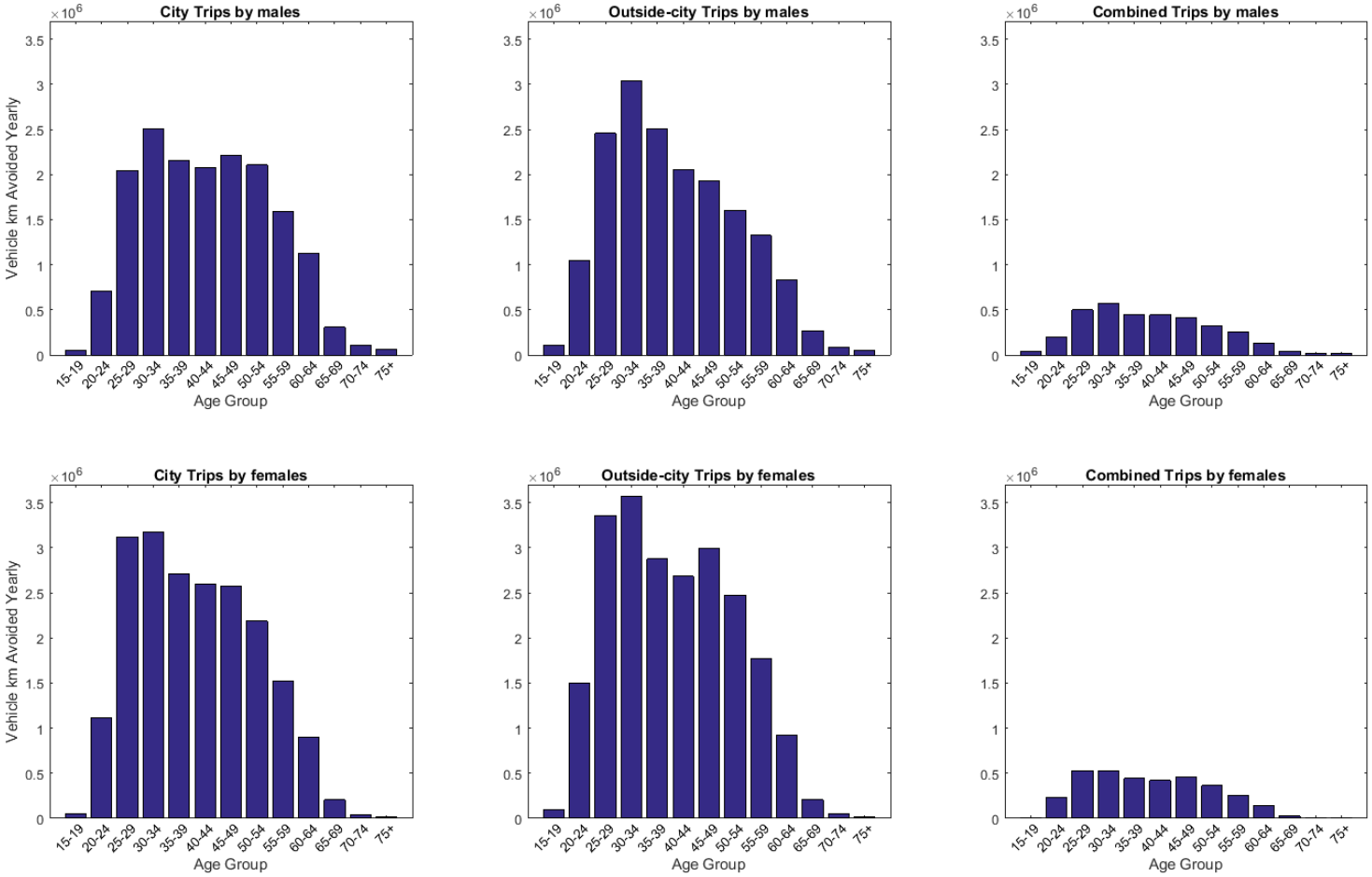

Figure 3.2 Vehicle km avoided by converting trips from driving to cycling in the case where all driving trips <5km are cycled.

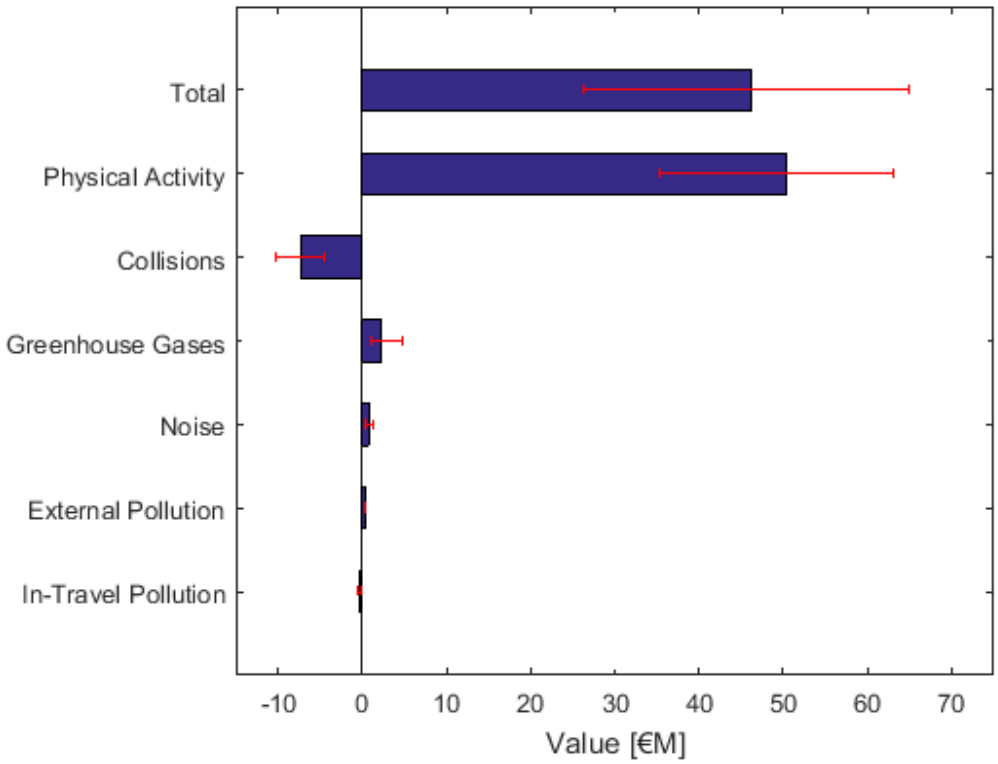

Figure 3.3 Summary of health and environmental impacts. Bars indicate upper and lower bounds.

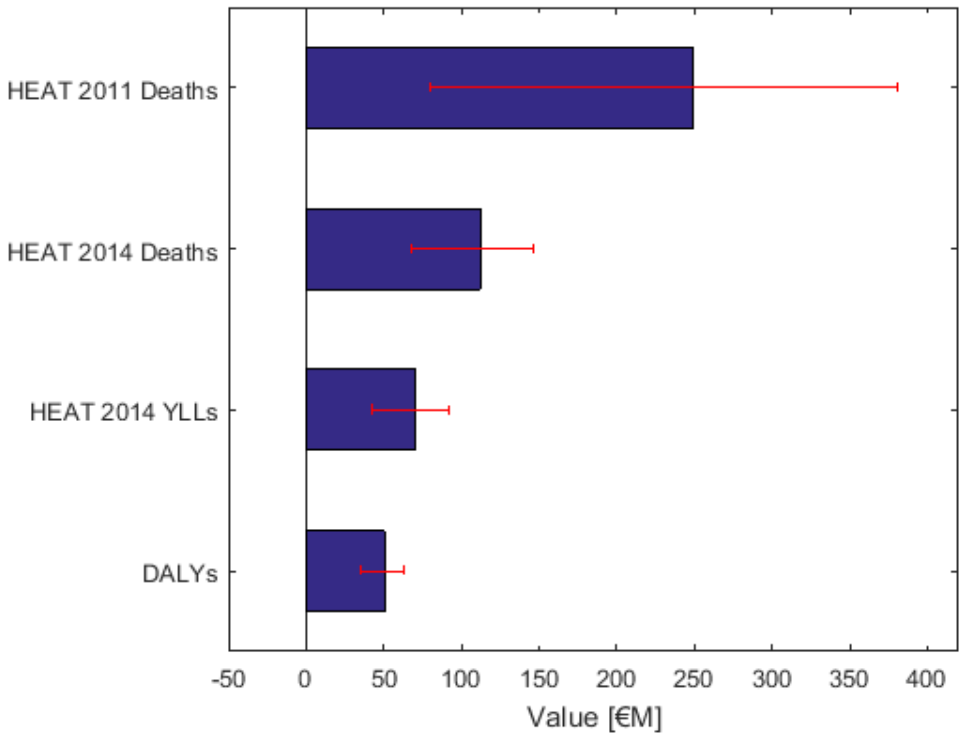

Figure 3.4 Comparison of models for health impact of physical activity

Table 3.4 Change in traffic collision casualties.

Change in fatalities					
Striking \ Victim	Car	Bicycle	Pedestrian	Total	Cost of fatalities
Car	-0.02	0.00	-0.04	-0.06	
Bicycle	0.00	0.00	0.00	0.00	
Pedestrian	0.00	0.00	0.00	0.00	
Other	0.00	0.25	0.00	0.25	
No other vehicle	-0.05	0.47	0.00	0.42	
Total	-0.07	0.72	-0.04	0.61	€2,927,610
Change in serious non-fatal casualties					
Striking \ Victim	Car	Bicycle	Pedestrian	Total	Cost of casualties
Car	-0.93	5.66	-0.20	4.52	
Bicycle	0.00	0.14	0.15	0.28	
Pedestrian	0.00	0.00	0.00	0.00	
Other	-0.18	1.31	0.00	1.13	
No other vehicle	-0.33	1.04	0.00	0.72	
Total	-1.44	8.15	-0.06	6.65	€3,096,652
Change in minor non-fatal casualties					
Striking \ Victim	Car	Bicycle	Pedestrian	Total	Cost of casualties
Car	-16.84	183.72	-3.95	162.93	
Bicycle	0.00	4.51	2.85	7.36	
Pedestrian	0.00	0.00	0.00	0.00	
Other	-3.30	42.55	0.00	39.25	
No other vehicle	-5.87	33.82	0.00	27.96	
Total	-26.01	264.61	-1.11	237.50	€1,315,609

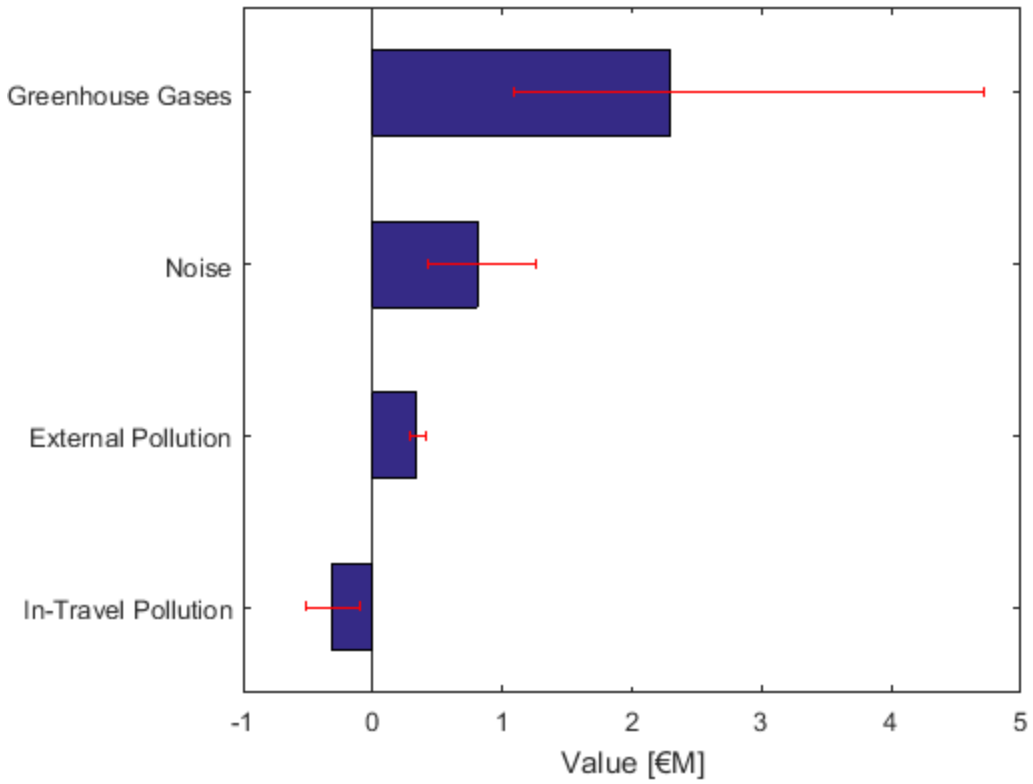

Figure 3.5 Summary of less significant impacts of cycling uptake.

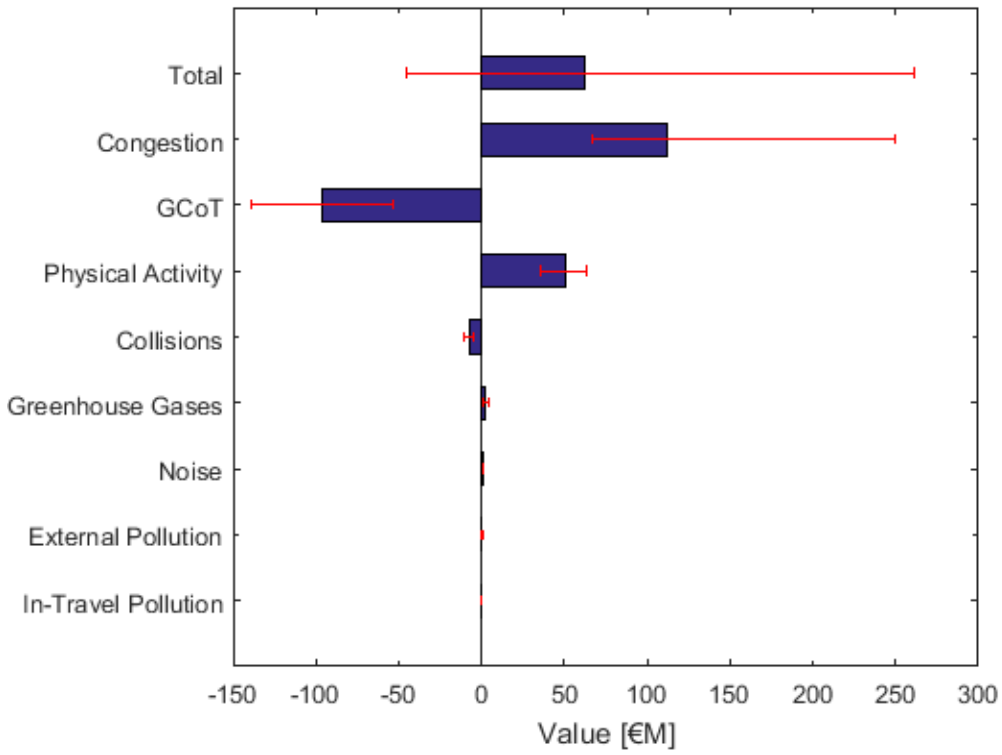

Figure 3.6 Summary of health, environmental and travel-cost impacts. Bars indicate upper and lower bounds.

3.3.2 Study Limitations

A limitation of this study is that the hypothetical scenario under consideration was not realistic and there was no consideration given to how this scenario might be realised. No consideration was given to the possibility of trip chaining or the existence of major barriers to cycling for some individuals such as physical limitations or the need to escort children to school. Even without such barriers, the conversion of all trips less than 5km would represent a major change to the transport environment and it would be unrealistic to assume that such a change could occur without major interventions. However, the purpose of this study was simply to provide indicative estimates of the relative scale and direction of the various impacts which would be achieved if a modal shift in favour of cycling took place. Since all of the impacts under consideration increase linearly (or close to linearly) with the amount of driving converted to cycling, the relative scale of the positive and negative impacts can be expected to be relatively consistent for smaller, more realistic modal shifts. As discussed in Chapter 2, many previous studies which quantified the health and environmental impacts of cycling were based on similarly unrealistic scenarios (Grabow et al., 2012; Holm et al., 2012; Rojas-Rueda et al., 2012; Rojas-Rueda et al., 2013). In the model presented in Chapter 8, this limitation is addressed by making the intervention leading to the modal shift endogenous to the model.

3.4 Conclusion

Overall, this study suggests that the health and environmental impacts of increased cycling in Dublin would be strongly positive. Although the scenario considered was highly idealised, the conclusions are consistent with the studies reviewed in Chapter 2 and this adds credibility to the results. When travel costs are also considered, the uncertainty becomes greater but the best estimate of the net impact is still positive. The largest sources of uncertainty are related to the marginal congestion of travel by car and the VoT associated with cycling. In future studies, the uncertainty regarding congestion could be reduced by using a bottom-up estimation based on speed-flow curves or simulations for the study area (Korzhenevych et al., 2014). Estimates of the cycling VoT could be improved by means of choice modelling experiments with the local population. These results show that if commuters making trips of less than 5km are interested in maximising utility or minimising cost for society as a whole, they should cycle if possible, rather than drive. However, if commuters are viewed as rational consumers, they can be expected to be interested in maximising their own individual utility, and the balance of these benefits and costs may look very different. Additionally these results do not address the possibility that the benefits and risks of cycling are unevenly spread across participants of different demographics

and that some cyclists may even experience a net negative impact. The next chapter of this thesis focusses on addressing these questions.

Chapter 4: Quantifying the Benefits and Risks of Urban Cycling in Dublin; Individual and Marginal Societal Impacts

In Chapter 3, a framework was developed for quantifying the total societal benefits and risks of urban cycling and a case study of cycling in Dublin was carried out. The framework developed was largely consistent with best practices in the literature to date but special attention was paid to uncertainty analysis and ensuring that all significant types of impacts were included.

Although estimating the total societal impacts of a modal shift is a useful tool for transport planners and policymakers, this has limited value in understanding the decisions and experiences of individual transport users for a number of reasons. Firstly, a positive net impact on society does not necessarily indicate that the net expected impacts for the individuals who switch from driving to cycling are positive. It is possible that expected external benefits simply outweigh the expected negative impacts on the cyclists. Secondly, the benefits and risks may be unevenly distributed across different demographic groups so that some groups of cyclists experience positive impacts on average while others experience negative impacts. Finally, changes in modal split (proportions of trips in the network using each transport mode) happen incrementally and the marginal health impacts (health impacts resulting from a unit increment) of motorised transport use are generally not equal to the average health impacts (European Commission, 2014) because these health impacts are influenced by the current modal split. Therefore, the expected individual and marginal external impacts of each individual switch from driving to cycling can be expected to be different from each other and from the averaged impact of a large cohort switching to cycling. Quantifying the individual and marginal external impacts of switching to cycling at the level of individual decisions has not been attempted in the literature to date and requires a different approach to those used to quantify total societal impacts.

This chapter describes a study which aims to determine whether or not the benefits to an individual taking up cycling in Dublin outweigh the risks for all ages, genders and trips. Another objective is to examine how the individual and marginal external impacts of each additional cyclist vary with the overall level of cycling modal share. A model is developed for estimating both the individual and marginal external impacts of a single user unilaterally switching from driving to cycling for their commute in various modal splits, taking into account age and gender specific effects. A clear distinction is made between the impacts experienced by the individual cyclist and by the rest of society. This study focusses on health impacts only as these are highly

variable across age and gender and they have been the focus of much interest in the literature to date. The BOD approach is used once again to quantify health impacts for the reasons outlined in Chapter 3 and because age and gender specific variations are key considerations in this study and BOD takes into account the life expectancy at the time of death.

The procedure described in this study also takes a different approach to uncertainty analysis by sampling key model parameters from appropriate probability distributions. In this way, the analysis accounts for variations in individual characteristic as well uncertainties in the health impact models. The contents of this chapter are based on published work (Doorley et al., 2017).

4.1 Scenario Design

In this study, the range of health impacts resulting from an individual—the test subject —switching from driving to cycling are quantified using health impact models from the literature. The approach used involves defining a reference scenario where the test subject drives and a test scenario where the test subject cycles and quantifying the difference in expected BOD between these scenarios. This process is repeated many times for different test subjects and modal splits. The procedure can be described as follows. Three modal split (MS) stages were first defined:

- The Current MS: the modal shares of walking, cycling, private car and public transport for commuter trips are 14·5%, 5·8%, 56·1% and 22·4% respectively as per the 2011 census (Central Statistics Office, 2011b)

- The Smarter Travel MS: the modal shares of walking and public transport remain at 14·5% and 22·4% but the modal share of cycling has increased to 10% while private car share has fallen to 51·9%. This represents the achievement one of the goals of the National Cycle Policy Framework 2009-2020—to have 10% of work trips made by cycling (Smarter Travel, 2009).

- The Intermediate MS: the modal shares of walking and public transport remain at 14·5% and 22·4% and the modal shares of cycling and private car are halfway between those of the Current and Smarter Travel MSs—7·9% and 54% respectively.

The procedure that follows was repeated for each of the three MS stages as the target MS. The procedure was to create a reference scenario (RS) in which the target MS had been realised and a test scenario (TS) which only differed from the RS in that additional one additional private car user—the test subject—had switched to cycling for their commute. The individual and marginal

external benefits of the additional cycling were then estimated by finding the difference between the health impacts in each scenario. The procedure was repeated multiple times to produce distributions of estimates, illustrating the influence of individual characteristics and the uncertainties in the models for estimating the impacts. The scenarios were informed by the POWSCAR, 2011 data (Central Statistics Office, 2011a; Central Statistics Office, 2011b). Similarly to the study described in Chapter 3, journey distances were estimated based on reported journey times and estimated average driving speeds and it was assumed that current driving trips of 6km or less each way could be considered as cycle-able trips. Similarly to Chapter 3, this is a simplification as it ignores the possibility of trip-chaining and trips which could not realistically be cycled for reasons other than distance. Using MATLAB (The MathWorks Inc., 2016), the following steps were followed as illustrated in Figure 4.1:

1. From the individuals aged 20 to 64 who make cycle-able trips to and from work by private car, randomly select (with equal selection probability and without replacement) the required numbers of individuals to switch to cycling in order to meet the target MS. These individuals are assigned to the *Converted* group. In the case of the Current MS, a single individual is selected to switch to cycling and is the only individual added to the *Converted* group. Call the scenario in which the entire *Converted* group has made the change to cycling the Case scenario (CS).

2. Randomly select a single *test subject* from the *Converted* group. Call the scenario in which the entire *Converted* group except for the *test subject* makes the change to cycling the Reference Scenario (RS).

3. Calculate the individual health impacts to the test subject as a result of switching to cycling during one year by estimating the difference in expected DALYs lost by that individual between the CS and RS. Three determinants of individual health impacts were considered: physical activity (PA), individual exposure to air pollution during transit (AP_{In}) and traffic collision risk (TC_{In}). The details of these calculations are presented in 4.2.

4. Calculate the expected marginal health impacts to the rest of the population in the study area as a result of the test subject switching to active travel during one year by estimating the difference in DALYs lost by the rest of the population between the CS and the RS. Two determinants of marginal external health impacts were considered: reductions in external air pollution (AP_{Ex}) and traffic collision risk (TC_{Ex}). The details of these calculations are presented in 4.2.

5. Repeat steps 1 to 4 for 50,000 iterations. This number was considered appropriate because increasing the iterations by an order of magnitude did not make any appreciable difference to the results.

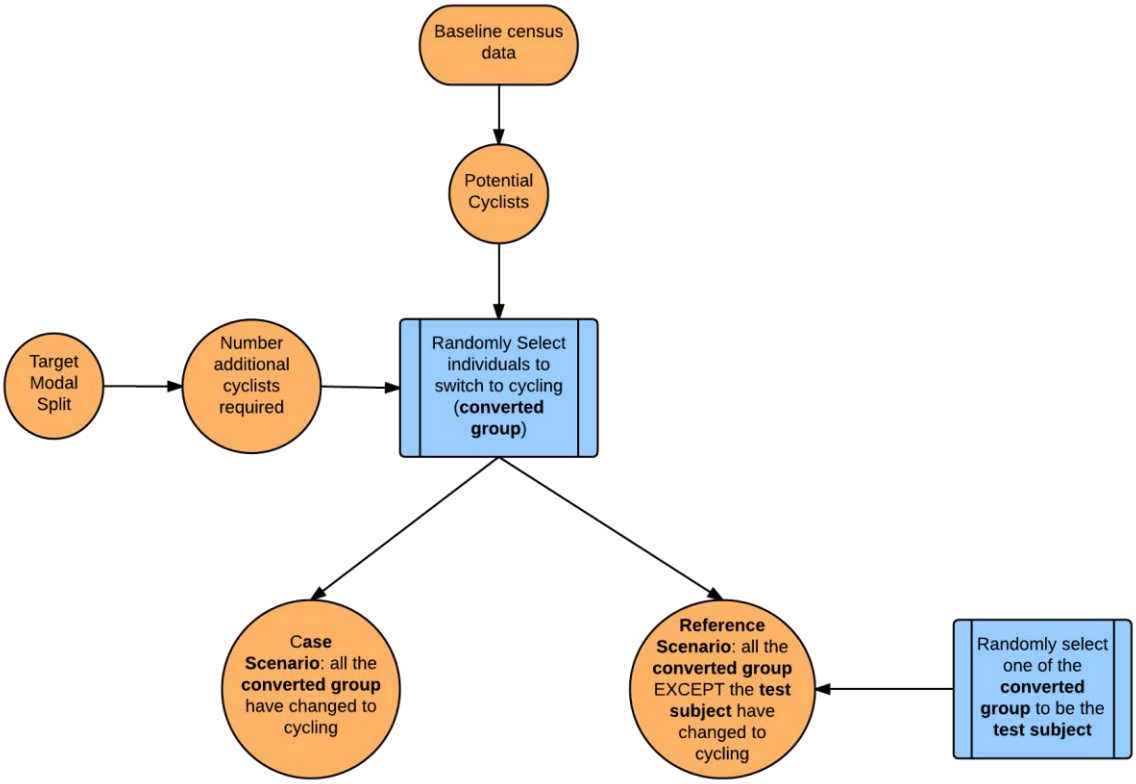

Figure 4.1 Process of defining the reference scenario and test scenario in each iteration

4.2 Estimation of Health Impacts

All health impacts in this study were modelled using a BOD approach. The health impact to an individual or group was defined as the change in the statistical expectation of DALYs lost by that individual or group in a single year. The calculation of the change in DALYs associated with each of the individual health determinants considered in this study is illustrated in Figure 4.2 and discussed in detail below.

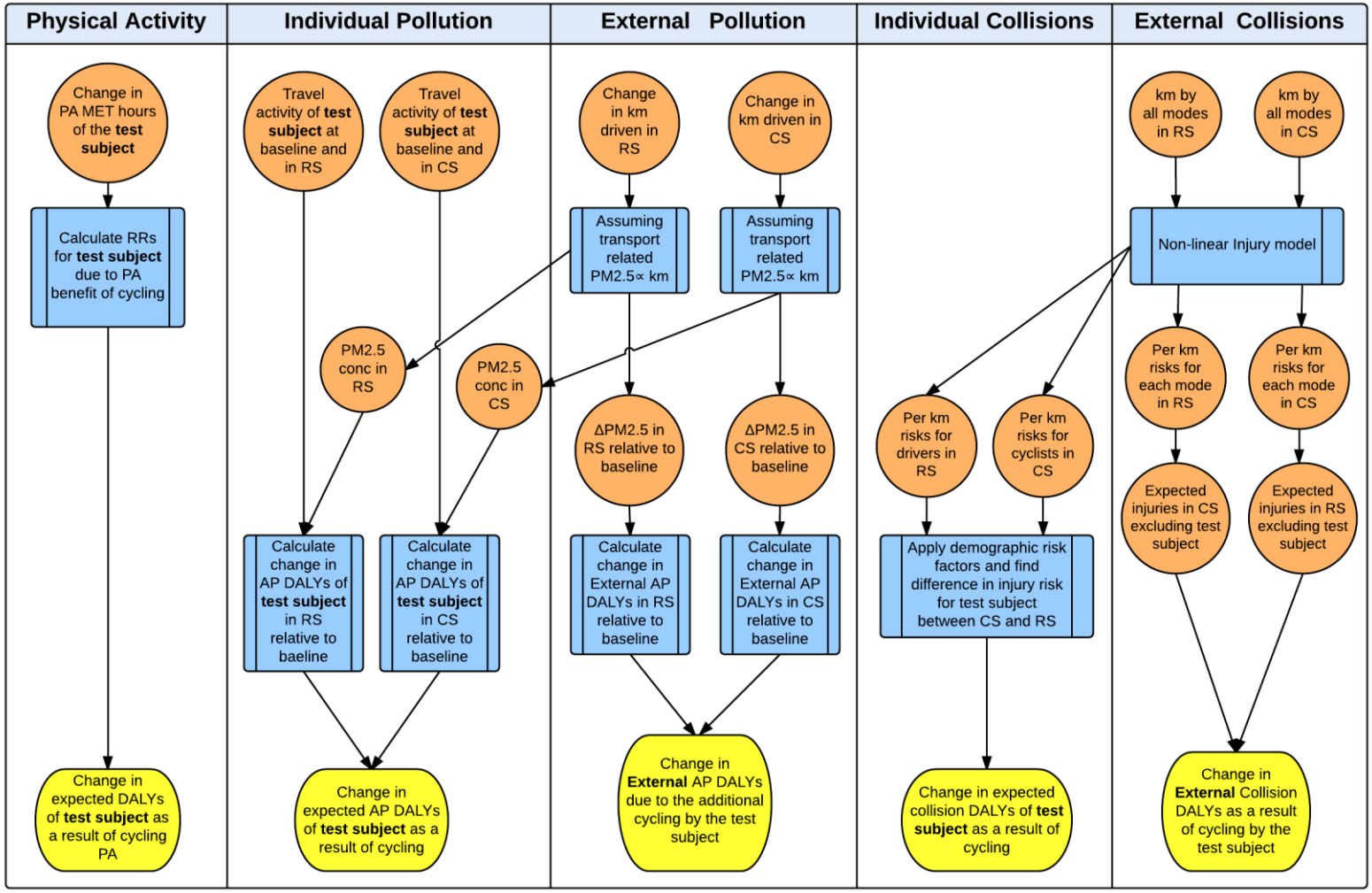

Figure 4.2 Process of estimating individual and external health impacts resulting from one additional cyclist

4.2.1 Health Impacts of Physical Activity

The additional kms cycled by the test subject in the CS were first converted to Metabolic Equivalent of Task (MET) hours using a compendium of physical activity MET factors (Ainsworth et al., 2011). A MET factor of 6.8 was used for cycling, consistent with HEAT for cycling and several recent studies (Maizlish et al., 2013; Woodcock et al., 2013; Woodcock et al., 2014). Non-travel related physical activity MET hours also needed to be estimated. The probability of an individual in each age and gender group having a physical activity level of, low, moderate or high on the International Physical Activity Questionnaire (IPAQ) scale could be obtained from the results of the recent Health Ireland survey (IPSOS MRBI, 2015). At each iteration, the activity level of the test subject was sampled from a discrete distribution based on these probabilities. The MET hours per week associated with low, moderate and high activity levels were estimated to be 0, 10 and 28 based on the IPAQ guidelines (IPAQ Research Committee, 2005). The relationships between MET hours of physical activities and the risk of various health conditions were modelled based on a systematic review by Woodcock et al. (2009). For each health condition and iteration, a reference relative risk (RR) was sampled from a lognormal distribution with mean and 95% confidence interval (CI) equal to the mean and CI found in the review (Woodcock et al., 2009). Lognormal distributions are appropriate because RRs are ratios and so the log of a RR is normally distributed. The health conditions modelled were cardiovascular disease, breast cancer, colon cancer, dementia, depression and type II diabetes. No confidence intervals were available for the RR of depression, so the mean RR was used directly. It was assumed that the RRs applied to both YLLs and YLDs. The RRs of this review were based on specific levels of weekly PA and so they needed to be adapted to the appropriate level of PA for each test subject in the current study. Similarly to Woodcock et al. (2013) this was achieved by assuming a log-linear relationship between risk of each condition and a power of 0·5 transformation of MET hours. For diabetes, a power transformation of 0·375 was used. The baseline expected YLLs and YLDs of the test subject for a given year were assumed to be equal to the per capita YLL and YLD rates of the same age and gender group in Ireland in 2012 which were obtained from the World Health Organisation (WHO) global BOD estimates for 2012 (World Health Organization, 2014). The change in the expected YLLs of the test subject due to each condition, *i*, was calculated using Eq. (4.1) to Eq. (4.3).

$$\Delta YLL^{i} = YLL_{B}{}^{i}\left(1-\frac{RR_{C}{}^{i}}{RR_{B}{}^{i}}\right) \qquad \text{Eq. (4.1)}$$

$$RR_C^{\,i} = RR_{Ref}^{\,i} \wedge \left(\frac{METS_C + METS_B}{METS_{Ref}^{\,i}} \right)^{\lambda^i} \quad \text{Eq. (4.2)}$$

$$RR_B^{\,i} = RR_{Ref}^{\,i} \wedge \left(\frac{METS_B}{METS_{Ref}^{\,i}} \right)^{\lambda^i} \quad \text{Eq. (4.3)}$$

Where ΔYLL^i is the change in expected YLLs due to condition *i*, $YLL_B^{\,i}$ is the YLLs expected at baseline, $METS_B$ is the MET hours of physical activity at baseline, $RR_{Ref}^{\,i}$ and $METS_{Ref}^{\,i}$ are the sampled reference RR and reference MET hours associated with disease *i* in the systematic review of Woodcock et al. (2009), $METS_C$ is the additional MET hours of cycling and λ^i is the power transformation of the exposure. The change in the expected YLDs was calculated in the same way.

4.2.2 Health Impacts of External Pollution Exposure

The marginal external air pollution health impact of a single additional cyclist was found by estimating in parallel, the societal air pollution health impacts in the CS and RS as shown in Figure 4.2. It was assumed that a reduction in the vehicle km travelled in Dublin would lead to a proportional reduction in $PM_{2\cdot5}$ emissions attributable to vehicular transport. It was also assumed that the change in ambient $PM_{2\cdot5}$ concentration would be proportional to the change in the total $PM_{2\cdot5}$ emissions. According to the Central Statistics Office (CSO) of Ireland, (Central Statistics Office, 2012), transport accounted for 31% of $PM_{2\cdot5}$ emissions in Ireland in 2010. In order to estimate the percentage reduction in motorised transport it was necessary to estimate the total baseline km travelled including non-commute trips. This was estimated from the National Transport Authority (NTA) travel survey of 2012 (National Transport Authority, 2013). For each RS and CS, the change in $PM_{2\cdot5}$ concentration was estimated. The health impact models based on the APHEIS model (Boldo et al., 2006), described in Chapter 3 were then used to calculate the RRs of cardiovascular diseases, respiratory diseases and lung cancer for the population in the CS and for the RS. Similarly to the physical activity models, for each health condition and iteration, a reference relative risk (RR) was sampled from a lognormal distribution with mean and 95% CI equal to the mean and CI found in APHEIS study. The age and gender structure of the population of Dublin was available from the CSO (Central Statistics Office, 2011a) and the baseline YLLs and YLDs lost due to each condition in Ireland in 2012 were available for each age and gender group from the WHO (World Health Organisation, 2013).The

change in YLLs for each condition, *i*, in each age and gender group could then be calculated using Eq. (4.4) and Eq. (4.5).

$$\Delta YLL^{i,p} = N_p * YLL_B^{\,i,p}\left(1 - RR_C^{\,i}\right) \quad \text{Eq. (4.4)}$$

$$RR_C^{\,i} = RR_{Ref}^{i\ \Delta C / \Delta C_{Ref}} \quad \text{Eq. (4.5)}$$

Where $\Delta YLL^{i,p}$ is the change in expected YLLs lost due to condition, *i*, by the exposed age/gender group *p*, N_p is the number of individuals in the age/gender group *p*, $YLL_B^{\,i,p}$ is the baseline expected YLLs associated with condition *i* and group *p*, RR_{Ref}^{i} is the sampled reference RR for condition *i*, ΔC_{Ref} is the reference concentration change for condition *i* and ΔC is the change is concentration of $PM_{2.5}$ in μg/m^3. The marginal change in external air pollution YLLs was calculated by finding the difference between the changes in YLLs in the RS and the CS.

4.2.3 Health Impacts of Individual Pollution Exposure

To estimate the impact of the increased inhaled dose of the test subject switching from private car travel in the RS to cycling in the CS, first the ratio of the subject's yearly inhaled dose of $PM_{2.5}$ compared to baseline was calculated for both the CS and RS using the same method outlined in Chapter 3. It was assumed that the health impact of the increase in inhaled dose would be equivalent to the impact of an increase in average ambient $PM_{2.5}$ concentration which would lead the same increase in inhaled dose. As with the external health impacts of air pollution, the RRs of cardiovascular diseases, respiratory diseases and lung cancer were calculated for the test subject in the CS and in the RS based on the reference RRs of the APHEIS study. The baseline expected YLLs and YLDs of the test subject for a given year were assumed to be equal to the per capita YLL and YLD rates of the same age and gender group in Ireland in 2012. The individual's change in expected yearly YLLs due to the conditions could be estimated for the CS and RS using Eq. (4.6) and Eq. (4.7).

$$\Delta YLL^{i} = YLL_B^{\,i}\left(1 - RR_C^{\,i}\right) \quad \text{Eq. (4.6)}$$

$$RR_C^{\,i} = RR_{Ref}^{i\ \Delta C_{eq} / \Delta C_{Ref}} \quad \text{Eq. (4.7)}$$

Where ΔYLL^{i} is the change in the individual's expected YLLs due to condition *i*, $YLL_B^{\,i}$ is the individual's baseline expected YLLs due to condition *i*, RR_{Ref}^{i} is the sampled reference RR for

condition *i*, ΔC_{Ref} is the reference concentration change for condition *i* and ΔC_{eq} is the equivalent change in concentration of $PM_{2\cdot5}$. Since cardiovascular disease risk is influenced by both physical activity and pollution exposure, the impacts of the two exposures were modelled multiplicatively. The expected change in individual air pollution YLLs was calculated by finding the difference between the changes in air pollution DALYs in the RS and the CS.

4.2.4 Individual Traffic Collisions

The traffic collision model used in Chapter 3 was used to find the per-km risks for each mode of being a victim of a fatal, serious or minor collision in the RS and the CS. This model assumes that the number of traffic collisions between each pairwise combination of modes is non-linearly related to the total distance travelled by each of these modes in the network. The degree of non-linearity of the relationship between distance travelled and number of collisions is unclear and likely to vary between different transport environments. Therefore, instead of using the constants of non-linearity suggested by Woodcock et al. (2013), each constant in each iteration was sampled from a normal distribution with a mean of the value suggested by Woodcock et al. (2013) and coefficient of variation of 0·5. The baseline collision data used in the model were obtained from the RSA Road Collision Handbook, 2011 and 2012 (Road Safety Authority, 2011, 2012). The collision data were also corrected for underreporting using the correction factors provided by the HEATCO study (Bickel et al., 2006). The baseline distances travelled by each mode were estimated using the same method as in Chapter 3.

The modal per-km risks calculated in this way were generic values for all users of the mode in that scenario. However, it is well documented that age and gender have a significant impact on the likelihood of an individual using a particular mode being involved in a traffic collision (Short and Caulfield, 2014; Woodcock et al., 2014). Mindell et al. (2012) has estimated the risk of fatality and hospitalisation for different age groups and genders per km travelled by driving and by cycling in England. No similar estimates could be found for Ireland so these results were used to estimate scaling factors for each age/gender group representing the ratio of their risk of fatality or injury to the risk of fatality or injury for the general population. The estimated scaling factors are shown in Table 4.1. These factors were used to correct the per-km risks from the traffic collision model, based on the age and gender of the test subject. The expected numbers of each type of collision for the test subject were then calculated for the RS and CS by multiplying the appropriate modal per-km risk by the kms travelled annually. The change in collision risk for the test subject due to the switch to cycling could then be calculated by comparing the expected numbers of each type of injury between the CS and RS.

Table 4.1 Fatality and Injury risk factors by age and gender

		Driver		Cyclist	
Gender	**Age Group**	**Fatality Factor**	**Injury Factor**	**Fatality Factor**	**Injury Factor**
Male	20-24	2.6	1.8	0.7	0.8
Male	25-29	2.6	1.8	0.7	0.8
Male	30-34	0.9	0.8	0.9	0.7
Male	35-39	0.9	0.8	0.9	0.7
Male	40-44	0.5	0.5	0.5	0.5
Male	45-49	0.5	0.5	0.5	0.5
Male	50-54	0.5	0.5	1.4	0.7
Male	55-59	0.5	0.5	1.4	0.7
Male	60-64	0.5	0.5	1.7	0.8
Female	20-24	0.9	1.4	0.4	0.6
Female	25-29	0.9	1.4	0.4	0.6
Female	30-34	0.3	0.8	0.7	0.6
Female	35-39	0.3	0.8	0.7	0.6
Female	40-44	0.3	0.5	0.7	0.6
Female	45-49	0.3	0.5	0.7	0.6
Female	50-54	0.4	0.6	0.8	0.9
Female	55-59	0.4	0.6	0.8	0.9
Female	60-64	0.7	0.8	1.0	1.4

In order to convert the change in expected incidence of injuries to a change in expected DALYs, the lost YLLs and YLDs associated with each type of injury needed to be estimated. For fatal injuries, the YLLs lost were assumed to be equal to the remaining life expectancy of the test subject. The average remaining life expectancy for an individual in each five-year age and gender group was obtained from the CSO (Central Statistics Office, 2009). For serious and minor non-fatal injuries, the average YLDs per injury used were the same as those used in Chapter 3.

4.2.5 External Traffic Collisions

The traffic collision model described in Chapter 3 was also used to estimate the change in injury risk for other users of the network as a result of the test subject switching from driving to cycling. The km travelled by each mode excluding the test subject was constant between the CS and RS but the per-km risk of each type of injury was not. For both the CS and RS, the external injuries of each severity level in each mode were found multiplying the per-km injury risk by the km travelled by that mode excluding the test subject. The change in external traffic injuries could be calculated by taking the difference between the external injuries in the CS and RS. The lost YLLs associated with an external traffic fatality were found by calculating the average remaining

life expectancy among the20-64 age group in the population of Dublin. The YLDs associated with serious and minor injuries were the same as those used for injuries to the individual cyclist.

4.3 Results and Discussion

The procedure described was carried out 50,000 times for each target MS, producing distributions of health impacts for each MS. The mean impact on YLDs and YLLs are shown for each health condition in Table 4.2. Negative values indicate increases in the YLLs or YLDs lost. For the health impacts to the individual cyclist, the changes in YLDs and YLLs are also expressed as percentages of the individual's baseline expected YLDs and YLLs for each health condition. The most significant positive benefit for all MSs was due to a reduction in YLLs due to cardiovascular disease. Other significant impacts related to PA include a reduction in YLDs due to depression and diabetes and a reduction in YLLs due to breast cancer and colon cancer. On average, the test subject's expected YLLs and YLDs due to traffic collisions increased by factors of 23 and 15 when they switched from private car to cycling in the Current MS but these factors decreased slightly in the Intermediate and Smarter Travel MS. These factors are higher than the typical ratio of cycling injury risk to driving injury risk (Elvik, 2009) and this difference can be attributed to the incorporation of underreporting and demographic risk factors in this study. As a result of these large increases in collision risk, there was a negative mean impact on TC DALYs for the cyclists themselves in each MS. However, a single driver switching to cycling in any MS had a positive mean impact on TC DALYs for the rest of the network. There was little difference in the AP_{Ex} estimates between the Current Intermediate and Smarter Travel MSs but this is to be expected as the marginal external AP costs of transport tend to be similar to the average external air pollution costs (European Commission, 2014). Further insights can be gained by examining not just the mean values but the distributions of total DALYs saved across all subjects tested. The distributions are shown for the Current MS and the Smarter Travel MS in Figure 4.3.

The histograms of all of the impacts look similar between the Current and Smarter Travel MS. In each case, the physical activity health impact is the most significant impact and is non-negative. The histograms of the AP_{In} impact and the AP_{Ex} impact respectively are entirely negative and entirely positive in both the Current and Smarter MS. Overall, the AP_{In} and AP_{Ex} impacts are not significant when compared to the other impacts. The histogram of the TC_{In} impact was entirely negative whereas the TC_{Ex} impact estimates are almost entirely positive. The distribution of TC_{In} impacts shifted positively in the Smarter MS relative to the Current MS while the distribution of TC_{Ex} impacts is shifted negatively. These were the only impacts which showed an obvious difference due to the change in background modal split.

Table 4.2 Mean YLLs and YLDs saved per year due to uptake of cycling by individual commuters. Positive values indicate health benefits.

		Current		Intermediate		Smarter	
		Mean Change	Mean % Change	Mean Change	Mean % Change	Mean Change	Mean % Change
Individual Physical Activity							
Breast Cancer	10^{-3} YLDs	0.03	9.18	0.03	10.71	0.03	10.75
	10^{-3} YLLs	0.35	9.18	0.36	10.71	0.35	10.75
Colon Cancer	10^{-3} YLDs	0.01	10.70	0.01	19.20	0.01	19.22
	10^{-3} YLLs	0.33	10.70	0.33	19.20	0.33	19.22
Cardiovascular Diseases	10^{-3} YLDs	**0.61**	19.18	**0.62**	18.16	**0.62**	18.13
	10^{-3} YLLs	**2.59**	19.18	**2.60**	18.16	**2.61**	18.13
Dementia	10^{-3} YLDs	0.13	18.17	0.13	17.00	0.13	17.00
	10^{-3} YLLs	0.03	18.17	0.03	17.00	0.03	17.00
Depression	10^{-3} YLDs	**2.30**	17.00	**2.30**	15.88	**2.29**	15.86
	10^{-3} YLLs	0.00	17.00	0.00	15.88	0.00	15.86
Diabetes	10^{-3} YLDs	**0.51**	15.86	**0.51**	0.00	**0.51**	0.00
	10^{-3} YLLs	0.12	15.86	0.12	0.45	0.12	0.45
Individual Pollution Exposure							
Respiratory Diseases	10^{-3} YLLs	-0.01	0.45	-0.01	0.45	-0.01	0.45
Cardiovascular Diseases	10^{-3} YLLs	-0.07	0.68	-0.07	0.68	-0.07	0.68
Lung Cancer	10^{-3} YLLs	-0.04	0.00	-0.04	0.00	-0.04	0.00
External Pollution Exposure							
Respiratory Diseases	10^{-3} YLLs	0.08	*	0.08	*	0.08	*
Cardiovascular Diseases	10^{-3} YLLs	0.41	*	0.41	*	0.41	*
Lung Cancer	10^{-3} YLLs	0.17	*	0.17	*	0.17	*
Individual Collision Risk	10^{-3} YLDs	**-1.99**	**1506.5**	**-1.82**	**1375.9**	**-1.68**	**1272.3**
	10^{-3} YLLs	**-0.73**	**2214.6**	**-0.68**	**2075.1**	**-0.65**	**1971.5**
External Collision Risk	10^{-3} YLDs	**1.49**	*	**1.33**	*	**1.21**	*
	10^{-3} YLLs	0.37	*	0.33	*	0.29	*

* Percentage changes for external impacts are not informative so they are omitted.

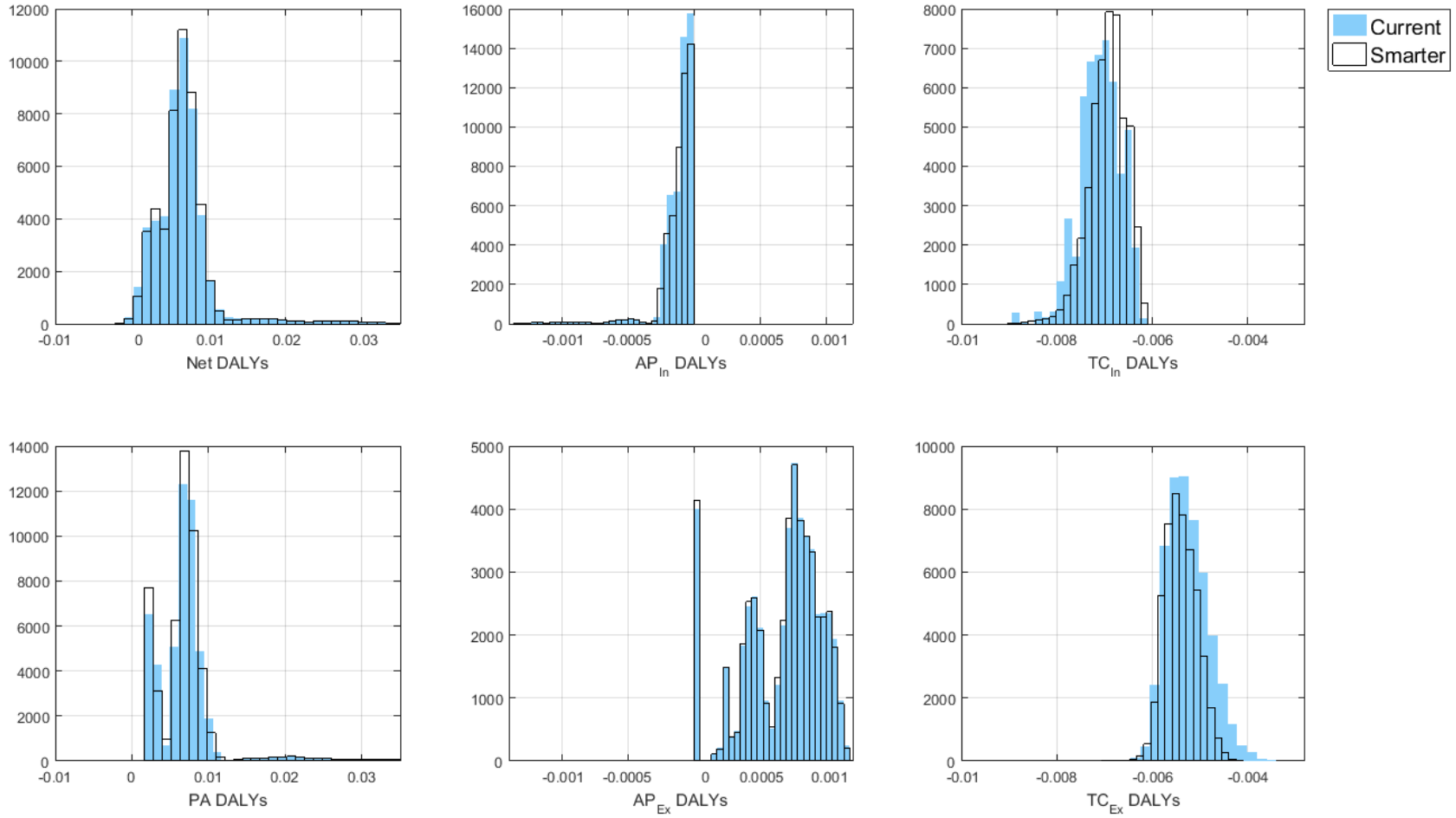

Figure 4.3 Distributions of health impacts in the Current and Smarter Travel MS

4.3.1 Net Individual and External Impacts

The histogram of Net DALYs shows that the total expected public health impact of the switch from driving to cycling was positive in almost all cases. In both the Current and Smarter Travel MS the total expected health impact was negative in less than 1% of cases. By grouping the impacts into individual and marginal external impacts, we can see more clearly how both the individual new cyclists and the rest of society were affected. Figure 4.4 shows the net impact to individuals due to the sum of the PA, AP_{In} and TC_{In} impacts and the net marginal external impact due to the sum of the AP_{Ex} and TC_{Ex} impacts. When the net individual DALYs are considered in isolation, negative impacts are expected in a higher proportion of cases than when total Net DALYs were considered —8% and 6% in the Current and Smarter Travel MS respectively. This means that, within the bounds of the model uncertainties considered in this study, cycling may have a negative net health impact for individuals of certain broad characteristics. The net marginal impact to society, however, was almost always positive and was generally higher in the Smarter Travel MS. These observations show that, in some cases, if individual and external impacts are considered in aggregation, a negative expected impact to the individual may be masked by a positive expected external impact.

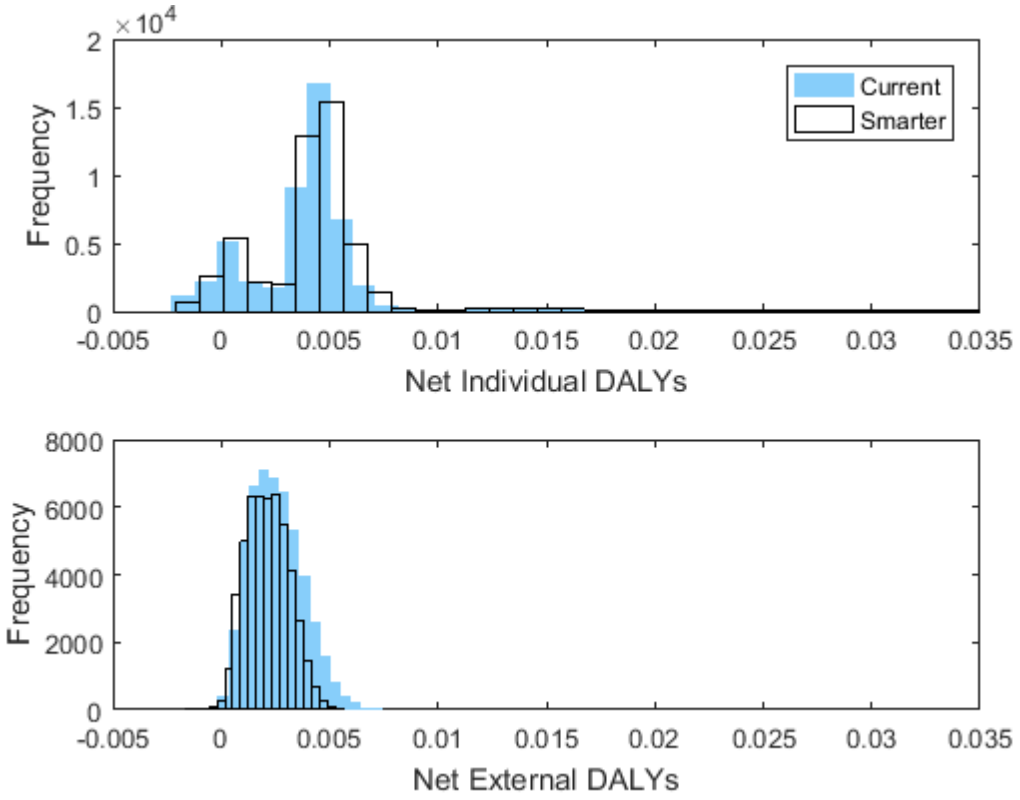

Figure 4.4 Net individual health impacts and net marginal external health impacts in the Current and Smarter Travel MS

4.3.2 Effects of Age and Gender

The specific cases in which negative individual health impacts may be expected were found to be closely related to age and gender. This is illustrated by Figure 4.5 and Figure 4.6 which show the distributions of Net individual DALYs and their two most significant components, PA DALYs and TC $DALYs_{In}$ in each age and gender group. Only the Current MS results are shown but the results in the other MS stages were similar. In both genders, the DALYs saved due to PA were lowest for the 20-29 age groups and highest for the 60-64 age group. This is because the lowest age groups have a relatively low baseline risk of the health conditions considered, whereas the higher age groups have higher baseline disease risks. The increase in collision risk was also relatively significant for the highest age groups. However, the over 60 age group experienced the greatest net health benefits as this relatively high increase in injury risk seems to have been outweighed by their large reduction in disease risk. The 20-29 age groups were the only groups where some individuals experienced negative net heath impacts as the health benefits they gained from physical activity were not enough to counteract their increase in collision risk. This observation that the benefits of cycling may not outweigh the harms in the case of young people is in agreement with another recent study which also considered age-specific health effects (Woodcock et al., 2014). The effect of gender is most clear for the youngest and oldest age groups. Older males experienced greater positive health impacts than older females due to their higher baseline DALY rates but younger males also experienced greater negative health impacts than younger females due to their increased risk of traffic injuries.

The individual net health benefits were also correlated with distance travelled. Figure 4.7 and Figure 4.8 show that, for ages 20-29, net individual DALYs were negatively correlated with distance and net negative impacts only occurred for longer trips. This can be explained by observing that individual collision risk increases linearly with distance travelled while the health benefits of physical activity increase log-linearly. Effectively, this means that a large part of the health benefits of cycling can be attained with a small amount of cycling per week and after this the physical activity benefits increase more slowly while the traffic collision risk continues to increase linearly. Above the age of 29, net individual DALYs were not strongly correlated with commute distance.

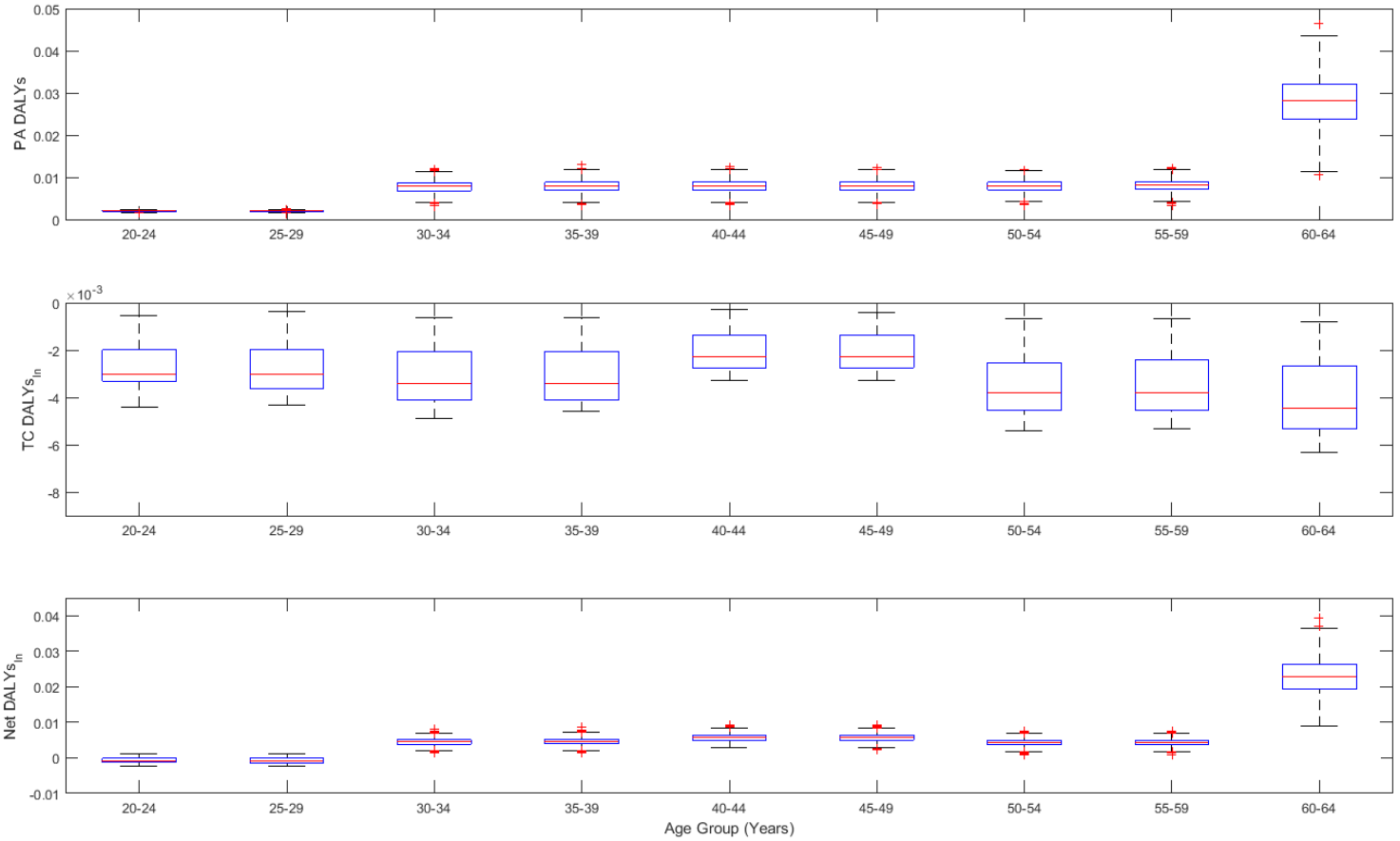

Figure 4.5 DALYs saved by male test subjects disaggregated by age

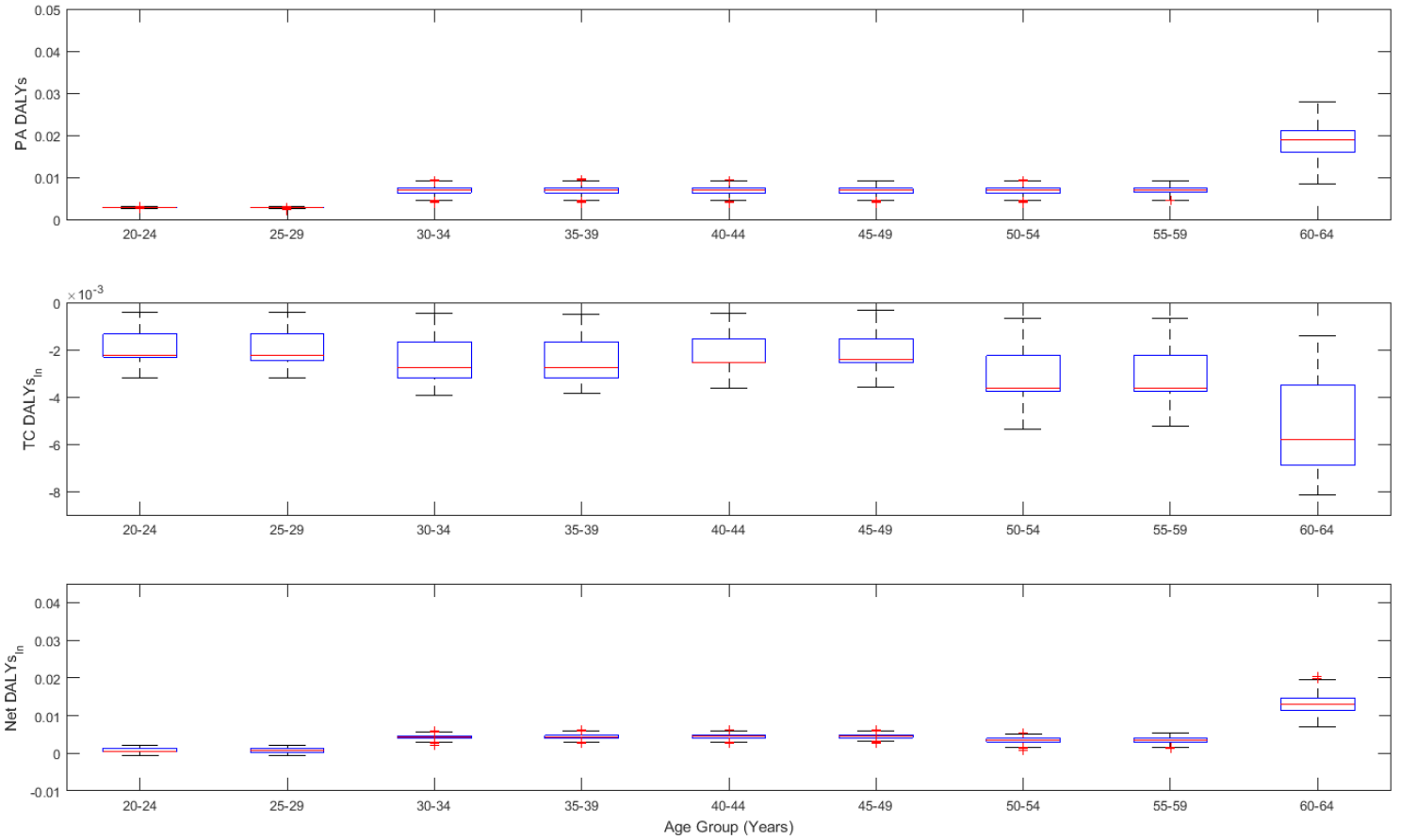

Figure 4.6 DALYs saved by female test subjects disaggregated by age

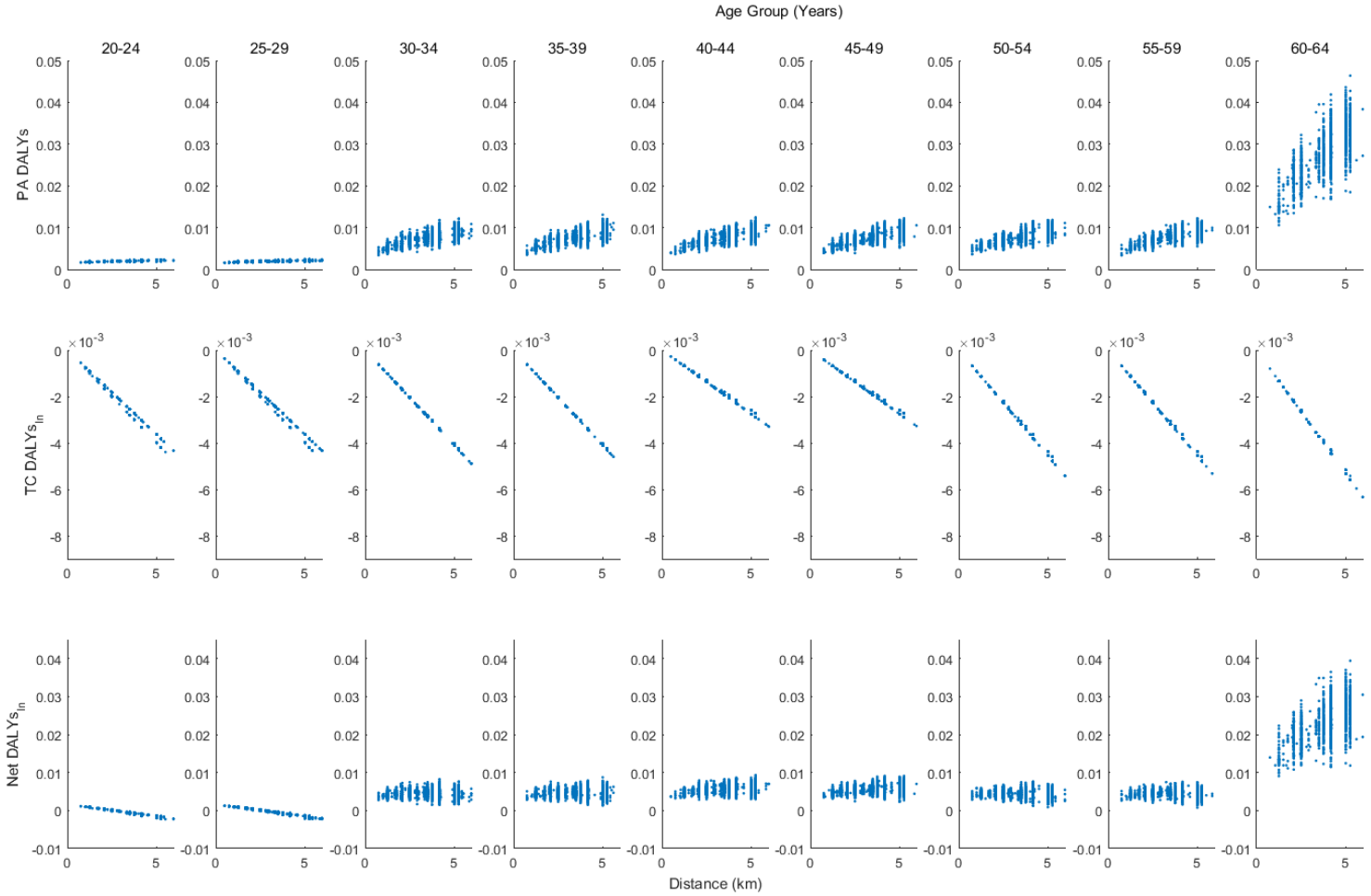

Figure 4.7 Relationship between DALYs saved and commute distance for male test subjects disaggregated by age

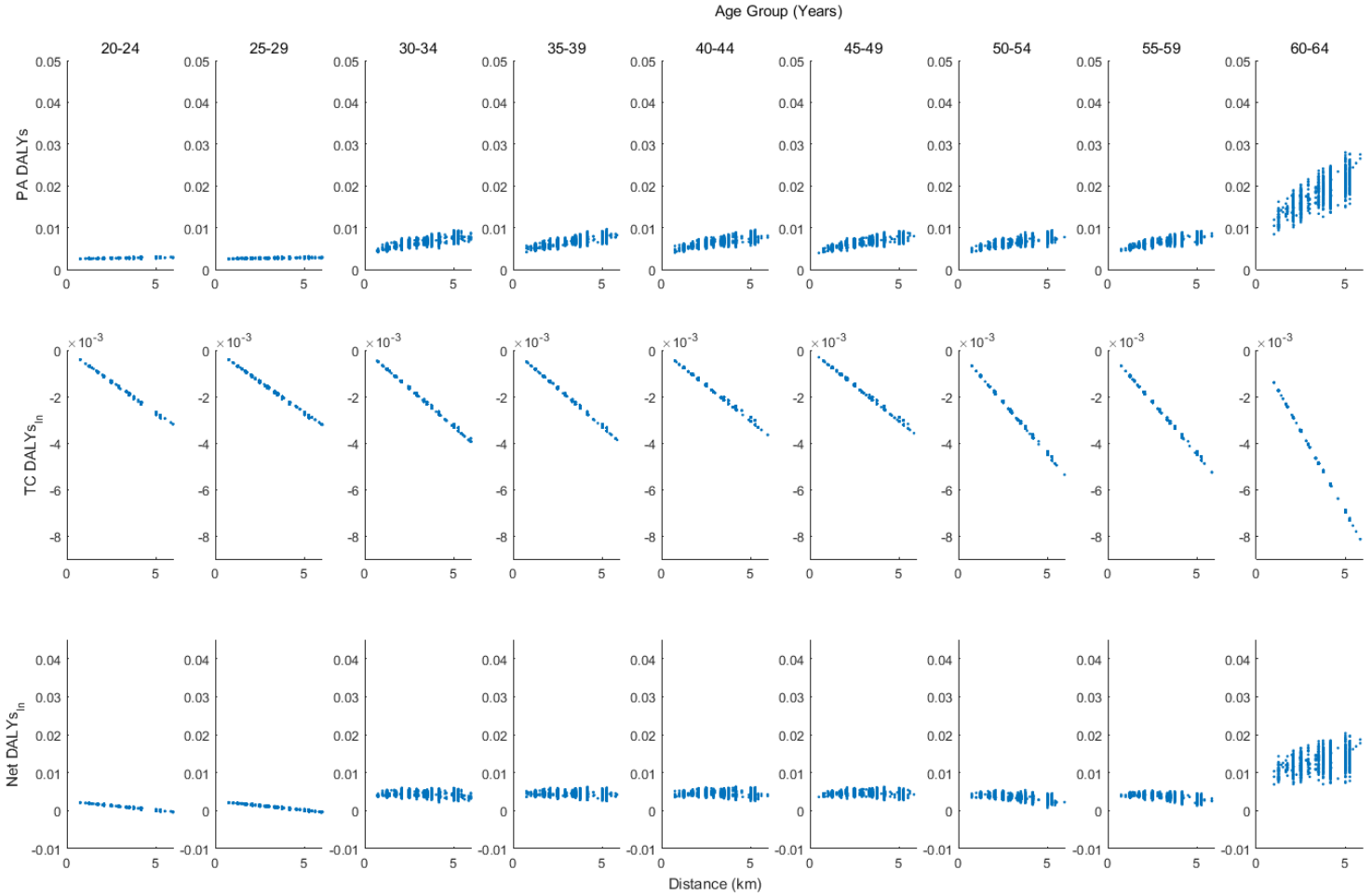

Figure 4.8 Relationship between DALYs saved and commute distance for female test subjects disaggregated by age

4.3.3 Effect of Modal Split

While net individual health impacts did not appear to depend strongly on the MS, the net external health impacts shifted negatively in the Smarter MS. The difference in the distribution of marginal external impacts between the Current and Smarter MS was mainly due to the difference in the distribution of TC_{In} and TC_{Ex}. The change in the TC_{In} and TC_{Ex} impacts between the MS stages can be seen more clearly in Table 4.3 which shows the mean of each impact in the Current, Intermediate and Smarter Travel MS. As the modal split changes in favour of more cycling and less private car use, the mean TC_{In} moves positively while the mean of TC_{Ex} moves negatively. This shows that as cycling increases, the negative impact on TC risk of the individual is mitigated by the "Safety in Numbers" effect (Elvik, 2009). However, the positive impact on TC risk for the rest of the users of the transport network is also slightly reduced. This indicates that in terms of improving the safety of the rest of the network, the marginal returns from replacing private cars with bicyclists diminish with increasing modal share of cycling.

Table 4.3 Mean change in Traffic Collision DALYs in each modal split stage

Modal Split	Mean Individual TC DALYs	Mean External TC DALYs
Current	-2.73E-03	1.86E-03
Intermediate	-2.50E-03	1.66E-03
Smarter	-2.33E-03	1.50E-03

4.3.4 Strengths and Weaknesses

This study was based on highly reliable individualised census data for the study area and included age and gender specific effects and, as such, the results are more specific than studies based on population level data. However, for certain parameters such as the constants of non-linearity in the collision model, no local estimates were available so estimates from other studies which were not location-specific were used. The use of local data where possible data increases the reliability of the findings of this study but also may make it more difficult to generalise these findings to other study areas. The method used to design the scenarios in order to estimate individual and marginal health impacts is a novel approach which allowed a unique perspective on the impacts of increments in cycling. In addition, the stochastic sampling of model parameters increases the robustness of the findings. The use of the models provided by Woodcock et al. (2009) and Boldo et al. (2006) allowed the health impacts to be broken down by individual health conditions, giving more specific insights than results based on mortality alone. Since there may be other conditions not included in these models which are relevant to cycling, it is possible that the PA and/or AP impacts are underestimates. However, it is unlikely that

other health conditions would have comparable impacts at the low levels of cycling being considered in this study (Woodcock et al., 2014).

4.3.5 Implications and Future Work

There are important policy implications of the finding that the external benefits of cycling may come at the expense of the individual cyclists. Firstly, economic incentives for commuter cyclists such as Ireland's Bike to Work scheme are justified in principal since society gains from additional commuters switching to cycling whereas, in some cases, the new cyclists themselves may not. Secondly, it should be noted that the only significant negative health impact for the individuals who switch to cycling is due to the large increase in traffic collision risk. This suggests that in order to ensure that the net health impacts of switching from driving cycling are positive, the risk of traffic collisions for cyclists in the Dublin network must be reduced. This could be achieved through provision of adequate infrastructure and improving driver awareness and perception of cyclists (Pucher and Dijkstra, 2003). As this study was focussed on behavioural change, it was assumed that in the scenarios involving increased cycling, the infrastructure remained the same. However, if improvements in infrastructure lead to increased cycling or vice versa, the impact of increases in cycling on traffic collisions are likely to be more positive. Future studies which incorporate this possible correlation would provide further useful information for both the health and transportation sectors. The histogram of individual net impacts in the Smarter Travel modal shift was shifted slightly positively in comparison to the Current Modal shift implying that in a less motorised transport network, the benefits experienced by an individual who begins cycling would be higher. It is likely that the reverse would also be true and that the net health impact experienced by someone who begins cycling in a highly congested city would be less positive. This should be considered by policymakers considering measures to promote cycling in highly congested cities. Finally, the observation that younger individuals benefit less from switching to cycling than older individuals and may even experience negative health impacts on average is highly substantial. The results of Chapter 3 showed that many younger individuals drive for short trips and therefore, policies aimed at encouraging them to cycle may be most effective. However, these results suggest that caution should be taken in encouraging younger people to cycle.

4.4 Conclusions

In this chapter and the last, two different approaches to quantifying the benefits and risks of cycling have been explored. In Chapter 3, the societal benefits and risks of a large scale modal shift from driving to cycling were quantified. This chapter focussed on health impacts only and

quantified the impacts of individual changes from driving to cycling and the influence of personal characteristics on the impacts experienced. One of the key conclusions of the Chapter 3, similarly to many other recent studies on this subject, was that the total societal benefits of increased urban cycling outweigh the detriments. However, many individuals who choose to cycle do so in order to benefit their own health and this chapter has shown that for some individuals, particularly young people, the expected health impact of cycling may be negative. If the health impacts had been considered at an aggregate level, these negative individual health impacts would have been masked. This underscores the importance of distinguishing between individual and external health impacts and considering age-specific effects.

In both studies, it was noted that the only significant negative impact of cycling is the increased risk of traffic collisions. The health impact of exposure to air pollution was relatively insignificant. However, a weakness of both of these studies as well as many other recent studies which have quantified the benefits and risks of cycling, has been a lack of measurement or detailed modelling of in–travel pollution exposure (Hartog et al., 2011; Rabl and de Nazelle, 2012; Rojas-Rueda et al., 2016; Rojas-Rueda et al., 2011; Rojas-Rueda et al., 2012; Rojas-Rueda et al., 2013). For this reason, Chapter 5 is focussed on developing an environmental sensing node capable of measuring the exposure of a cyclist to harmful pollution. In Chapter 6, this node is applied to a study of the environmental exposures of cyclists in Dublin.

Chapter 5: Development of Environmental Sensing Node

In chapters 3 and 4, methods were developed for quantifying the benefits and risks of cycling, based on best practices in the literature and novel simulation techniques. When applied to case studies of the Dublin area, it was found that the exposure of individuals to air pollution during transit was insignificant when compared to benefits such as increases in physical activity. This was consistent with the results of other studies on the benefits and risks of cycling. However, it was also noted that the estimation of air pollution exposure in this and many previous studies was either highly simplistic or absent entirely. In most cases, in-transit pollutant exposure concentrations were not measured but estimated based on ambient concentration data from fixed site monitoring (FSM) stations, sometimes applying a "concentration" factor to account for differences in exposure arising from different modes of travel. However, research has shown that air quality measurements from FSM stations can significantly underestimate or have little correlation with the pollution exposure of commuters (Adams et al., 2001; Gulliver and Briggs, 2004). Additionally, such methods ignore route specific variables such as traffic levels and infrastructure which as discovered in Chapter 2, can be expected to influence pollution exposure. In order to accurately characterise the pollution exposures of cyclists and inform future studies on the benefits and risks of active travel, it must be possible to measure air pollution exposure of cyclists directly.

In recent years, a new approach to air pollution monitoring has been emerging, whereby data from sparsely located FSMs are supplemented with data from low cost sensors which can be more finely distributed or mobile (Snyder et al., 2013; Steinle et al., 2015). This shift is being driven by advances in the technology of low-cost mobile pollution sensors, low-power electronics and communication networks. In addition to enhancing the spatial resolution of urban air quality data, such sensors can be used to assess the personal exposures of individuals wearing personal monitors. However, when using compact air quality sensors, the quality of data is an important concern as such sensors are emerging technologies which have not yet been subjected to rigorous field testing. Therefore, before such sensors can be used, their accuracy must be validated (Snyder et al., 2013; Steinle et al., 2015).

This chapter reports the development and validation of the Bicycle Environmental Exposure (BEE) node, a prototype mobile sensing node incorporating low-cost air quality sensors, capable of measuring cyclist exposure to air pollution as well as noise. Two iterations of the prototype are described. The prototypes were later applied to two studies into the air and noise pollution

exposure of cyclists in Dublin, which are reported in Chapter 6. The rest of this chapter is organised as follows. The functional requirements of the BEE node are first described and justified. The development of each iteration of the prototype is then described in turn, including the calibration of the sensors. The chapter concludes with some comments on the advantages and limitations of the BEE node for personal exposure monitoring of cyclists.

5.1 Design Requirements

The first stage in the development process was to determine the functional requirements of the sensing node including the pollutants which should be measured. These are described below

5.1.1 Measure concentrations of gaseous pollutants

The gaseous pollutants initially considered for inclusion in the measurements of the node were NO_x, CO, SO_2 and O_3 as all of these pollutants are present in urbans areas and are associated with adverse health outcomes.

NO_x is composed of nitric oxide (NO) and nitrogen oxides (NO_2). Exposure to NO_2 has been linked to increased risk of cardio-respiratory and all-cause mortality (Beelen et al., 2008b; Hoek et al., 2013a) and NO_x also acts as a precursor to formulation of particulates and O_3. NO_x concentrations are also highly spatially variable and the dominating source of NO_x is vehicle traffic (Andersen et al., 2008; Environmental Protection Agency, 2015). As noted in Chapter 2, NOx measurements have not been included in studies of cyclist exposure to air pollution, possibly because there was not enough evidence for health impacts of NO_x, independently of particulate matter. However, evidence regarding the health effects of NO_2 has strengthened substantially in recent years and the balance of probabilities now indicates that NO_2 is itself responsible for adverse health impacts (COMEAP, 2015). These factors make NO_x measurements an important functional requirement of the BEE node.

High concentrations of CO have been linked to short-term increases in total and cardiovascular mortality (Samoli et al., 2007). CO concentrations vary significantly in space and time and their main source of CO in Ireland in from motor vehicles. Highly trafficked areas therefore have higher concentrations of CO (Environmental Protection Agency, 2015). CO measurements were therefore considered an important requirement of the BEE node.

Exposure to SO_2 has been shown to be associated with increases in mortality from lung cancer, cardiovascular and all-cause mortality (Brook et al., 2010; Chau et al., 2002). However, the recent decline in the use of high-sulphur coal for domestic heating has led to large reductions in levels of SO_2 in the U.S.A. and many European countries (US EPA; WHO, 2005). In Dublin in

particular, the marketing, sale and distribution of bituminous coals has been banned since 1990 (Clancy et al., 2002). The decreased use of coal in favour of fuels which are low in SO_2 production, such as natural gas, has led to consistently low concentrations of SO_2 in Dublin over the past 10 years (Environmental Protection Agency, 2015). For these reasons, SO_2 measurements were not considered to be a requirement of the Bee node.

Exposure to ground-level O_3 can decrease lung function and aggravate symptoms in individuals with respiratory conditions such as asthma and lung cancer. However, ground-level O_3 is depleted through reactions with traffic-related pollutants and O_3 concentrations are therefore reduced in urban areas, particularly close to street level (Environmental Protection Agency, 2015). For this reason, O_3 measurements were not considered to be required.

5.1.2 Measure concentrations of particulate matter

Long-term exposure to PM in the ranges currently common in both developed and developing countries has been consistently shown to be associated with a range of adverse health outcomes including long-term risk of lung cancer, cardiopulmonary disease and all-cause mortality (Brook et al., 2010; Chen et al., 2008; Pope and Dockery, 2006; Stieb et al., 2002). Concentrations of both respirable particles (PM_{10}) and fine particles ($PM_{2.5}$) are commonly used indicators of PM. While PM_{10} particles are small enough to enter the thoracic region, $PM_{2.5}$ particles are particularly harmful as they have a high probability of deposition in the smaller conducting airways and alveoli. $PM_{2.5}$ is also considered by the World Health Organisation (WHO) as the most relevant measure of PM (WHO, 2005). Measurement of $PM_{2.5}$ was therefore considered to be essential to the sensing node while measurement of other size fractions such as PM_{10} and ultrafine particles (PM_1) would be considered as useful but not essential.

5.1.3 Measure noise

Long term exposure to noise pollution has been linked to hypertension, cardiovascular disease and type II diabetes (Babisch, 2014; Bluhm et al., 2007; Dzhambov, 2015). However, although it is reasonable to assume that cyclists experience higher noise exposure than drivers while in transit, this noise exposure has not previously been considered in studies of the health impacts of cycling. This is possibly because the majority of dose response functions used for air pollution exposure have not been adjusted for noise. Also, the extent of correlation between cyclist exposure to traffic-related noise and traffic-related pollution is unclear. Therefore, if both impacts were considered in such studies there may be risk of double-counting. However, it is likely that an independent impact of traffic related noise exposure exists. Furthermore, the

inclusion of noise measurements in the BEE node would allow insights into the relationship between cyclist exposure to noise and air pollution to be generated.

5.1.4 Mobility

A key requirement of the sensing platform is that measurements can be recorded in high spatial and temporal resolution in urban environments. This means that the node must be compact and battery-powered so that it can be easily carried through an urban environment by a cyclist. The time and location of each observation must also be recorded. Finally, the node must be protected from the variable weather conditions of Dublin. In addition to protecting the electronic components from water, it must be ensured that variations in wind speed and direction do not affect the consistency of the air quality measurements.

5.2 Development

Two iterations of the BEE node were developed and the features of each are summarised in Table 5.1. The development of each prototype is discussed in detail below.

5.2.1 Sensing node prototype 1

The purpose of the 1st prototype was to allow a pilot study into the exposures of cyclists in Dublin to take place. This pilot would inform the design of a more comprehensive study and also inform the design of further iterations of the BEE node. For this reason, it was not necessary for the 1st prototype to have all of the functional requirements described in section 5.1. The 1st prototype is described in this section.

Table 5.1 Measurement capabilities of each prototype of the BEE node

	Prototype 1		**Prototype 2**	
Measurement	**Units**	**Sensor**	**Units**	**Sensor**
NOx	ppb	Alphasense NO2-B42F	ppb	Alphasense NO2-B42F
CO	ppb	-	ppb	Alphasense C-B4
PM2.5	ug/m3	-	ug/m3	Alphasense OPC-N2
PM10	ug/m3	-	ug/m3	Alphasense OPC-N2
Noise	dBA	-	dBA	Zoom Handy Recorder H4N & Pro Signal NPA415-OMNI
Location	[lat, long] (WGS_1984)	Vodafone 975	[lat, long] (WGS_1984)	Adafruit Ultimate GPS
Speed	knots	Vodafone 975	m/s	Adafruit Ultimate GPS
Temperature	°C	TI LM35	°C	-

5.2.1.1 Air Quality Sensors

The most important function of the node was to record air quality measurements and thus the most important design decision was the choice of air quality sensors. This choice informed the design of all other aspects of the node. A number of models of miniature gas sensors were considered, including sensors from Figaro, e2v and Alphasense. Many of these small sensors however, were not suitable for low parts per billion (ppb) range detection. For example, the Figaro TGS2442 sensor—the CO sensor incorporated in the popular Waspmote sensing platform—has a detection range of 30-1000 parts per million (ppm). However, in Dublin, urban CO concentrations are often below 30ppm (Environmental Protection Agency, 2015). The only sensors which were found to be sufficiently mobile and to have acceptable detection ranges were the Alphasense B4 range of sensors. These are a range of miniature electrochemical sensors capable of detection of gas concentrations at low ppb levels. The sensors and accompanying circuit boards measure the local concentration of the target gas by generating voltages between 0V and 5V on two electrodes, the Working Electrode (WE) and the Auxiliary Electrode (AE). The voltage on the WE increases in proportion to the concentration of the target gas and the voltage on the AE can be used to correct for the influence of changes in temperature. The product range includes sensors for NO, NO_2, CO and other pollutants. For the first prototype, a single gas sensor was included, a beta version of the Alphasense NO2-B42F, shown in Figure 5.1. According to the datasheet, the NO2-B42F responds linearly to NO_2 concentrations between 0 and 5ppm with errors of within ±1ppb (Alphasense, 2015a). An individual factory calibration equation is provided with each Alphasense sensor which allows the concentration of the target gas to be calculated from the voltages of the two electrodes. The beta version of this NO_2 sensor had 100% cross-sensitivity to NO and so it was used in the BEE node to measure total NO_x. Similarly to most other miniature electrochemical gas sensors, the NO2-B42F requires a warm-up period before it can give accurate measurements. It must be powered for 90 minutes before the first valid measurement. The 1st prototype of the BEE node did not include a PM sensor as it was not required for the pilot study.

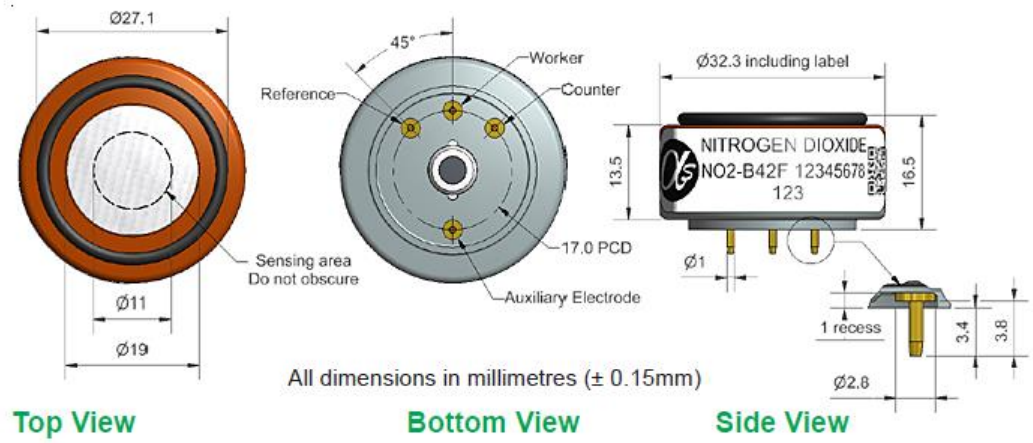

Figure 5.1 Alphasense NO2-B42F sensor (Alphasense, 2015a)

5.2.1.2 Data Acquisition System

In order to provide power to and capture and record the measurements produced by the NO_x sensor, a data acquisition (DAQ) system was required. The most widely used platform for prototyping of electronic sensor systems is the open-source, single-board Arduino platform. However, the Arduino was found to be unsuitable for use with the Alphasense sensors because the resolution of the voltage measurements was too low for the very small voltages produced by the Alphasense sensors. The Arduino analogue voltage measurement system uses a 10-bit analogue-to-digital converter (ADC). This divides the voltage range of 5V into measurement intervals of 4.88mV ($5V/2^{10}$). The NO2-B42F used with the sensing node, however, had a sensitivity of 0.571mV/ppb according to the factory calibration. This means that the measurement intervals of the Arduino ADC would correspond to NO_x concentration intervals of 8.5ppb. This would be a significant loss of measurement accuracy. An alternative to the Arduino platform is the Raspberry Pi (Raspberry Pi, 2016) shown in Figure 5.2. The Raspberry Pi is a credit-card sized computer based on the Broadcom BCM2835 System-on-a-Chip, which can run a Linux operating system. Although the Raspberry Pi does not include a built-in ADC, it can be combined with an external ADC. The ADC Pi is a 17-bit ADC which can be mounted to the Raspberry Pi in order to allow recording of analogue voltages between 0V and 5V at a resolution of 5e-17V. The Raspberry Pi and ADC Pi were therefore used as the DAQ system for the sensing node. A custom Python script was created to record voltage observations from the NO2-B42F at a frequency of 0.5Hz and save these values along with a timestamp to a csv file. The Raspberry Pi was powered using a battery-bank designed for mobile charging of smart phones.

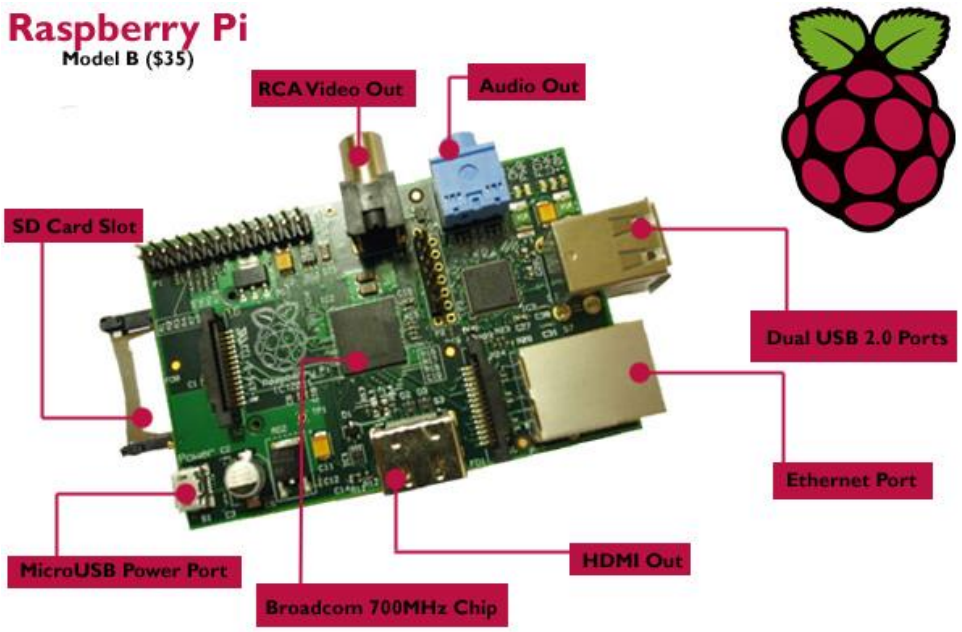

Figure 5.2 Raspberry Pi Miniature Computer (Raspberry Pi, 2016)

5.2.1.3 Temperature Sensor

Many compact pollution sensors, including the Alphasense B4 range, are sensitive to changes in temperature. For this reason, it is important that in calibrating and using the sensors, the local temperature is monitored so that if a dependence is noted during the calibration, the values recorded later can be corrected to remove the effects of temperature. Therefore, a Texas Instruments LM35 temperature sensor was added to the sensing node to provide temperature measurements concurrent to the air quality measurements. This sensor produces a voltage proportional to the ambient temperature, which was measured by the Raspberry Pi and saved to the csv file along with the measurements of the NO_x sensor.

5.2.1.4 GPS

For the first iteration of the BEE node, location and speed information were recorded by a stand-alone smart-phone, the Vodafone 975. The MyTracks app, running on the phone, retrieved coordinate and speed observations from the GPS satellites and saved them to a csv file in the phone's local storage. A screenshot of the myTracks app is shown in Figure 5.3.

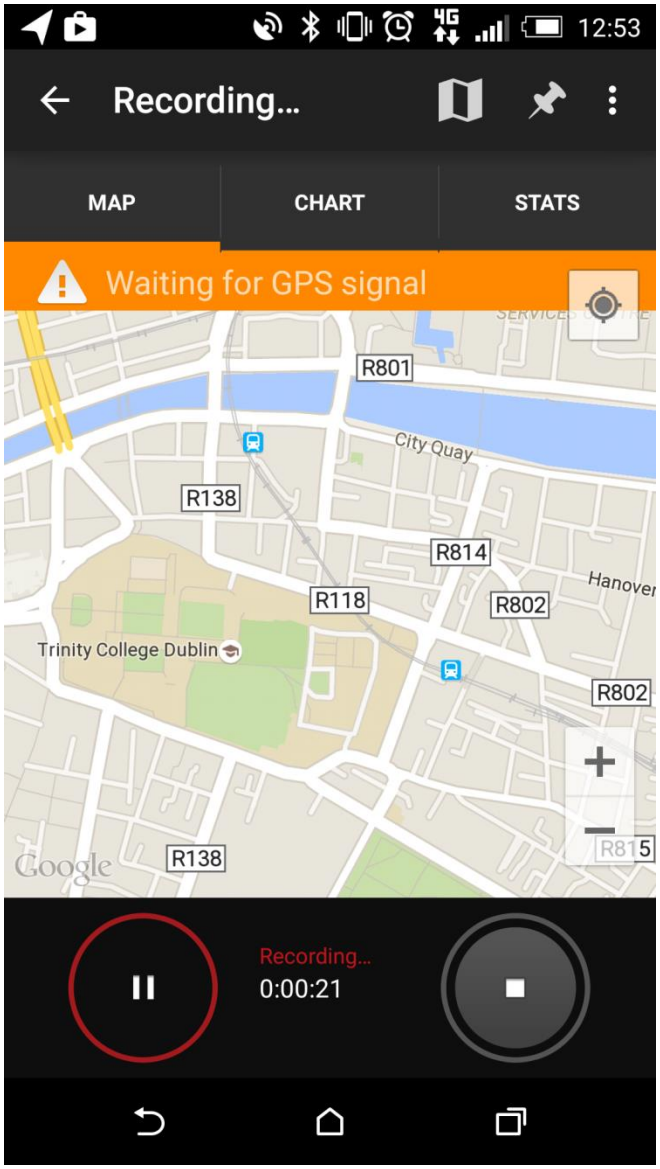

Figure 5.3: Screenshot from myTracks app

5.2.1.5 Enclosure and Pump

In order to protect the sensors and electronics from water damage and provide the sensors with a consistent flow of air, they were placed in an airtight ABS plastic enclosure which was connected to silicon tubing at both ends. As shown in Figure 5.4, one of the tubes led to a vacuum pump which forced air out of the enclosure and the other tube could be placed in the microenvironment to be sampled. This created an air flow of 4L/minute through the enclosure. The sensing node could be easily carried in a small backpack as shown in Figure 5.5.

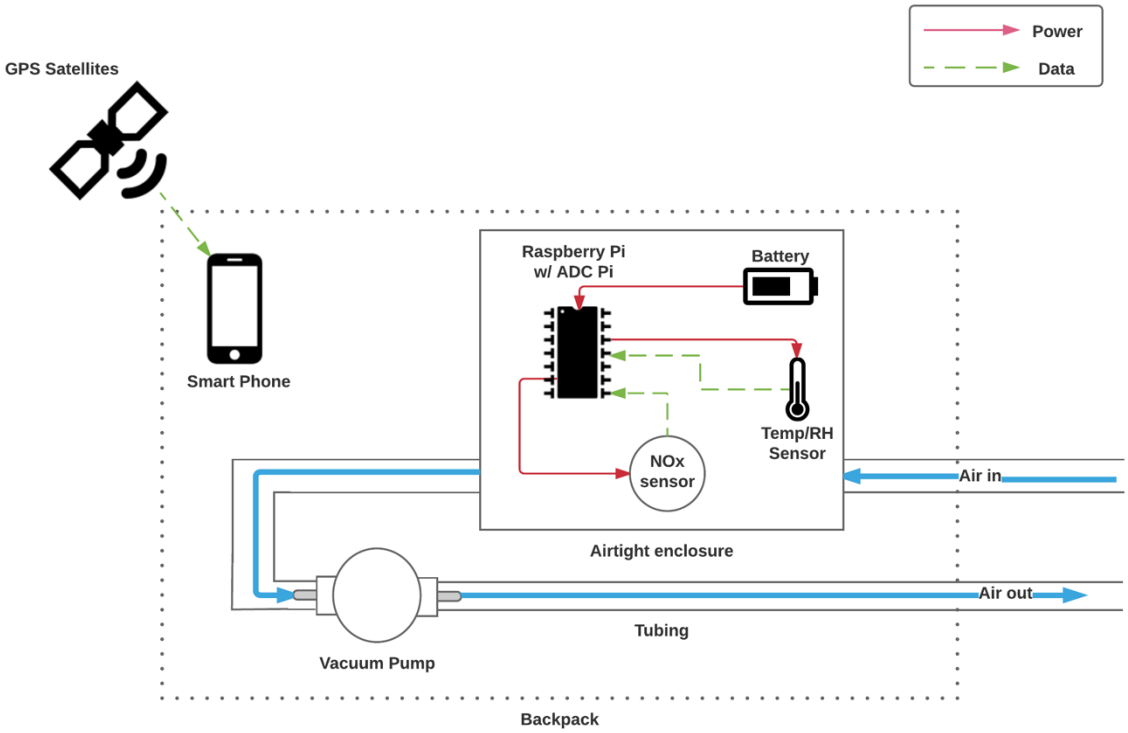

Figure 5.4 Functional diagram of sensing node 1st prototype

Figure 5.5 A cyclist carrying the sensing node 1st prototype in a backpack.

5.2.1.6 Calibration

In order to validate the accuracy of the NO_x sensor, the 1st prototype was collocated with the monitoring inlet of the Dublin City Council (DCC) FSM station at Coleraine St., about 20m from a regional road in Dublin city. The test was carried out for 2 weeks during December, 2014. The collocated inlets of the sensing node and the FSM station are shown in Figure 5.6. The reference

instrument was a Thermo Electron Corporation Model 42i NO_x analyser which is used to monitor ambient NO_x concentrations at accuracy levels suitable for reporting to the European Commission for compliance purposes. Hourly NO_x measurements of the reference instrument were compared to 1 hour averages of the factory calibrated NO_x sensor and the temperature sensor. Hourly averages were used because higher frequency measurements were not available from the reference sensor. It should be noted that taking hourly averages can be expected to filter out some temporal variability in the sensor readings and so ideally, the calibration model would have been developed using a higher temporal resolution. A linear regression model was fitted to estimate actual NO_x from the factory calibrated sensor readings. The collocated measurements were randomly split into a training set (70%) and test set (30%). The following model was fit to the data using the training set only:

$$NOx = 298 + 1.39 * NOx_{\alpha} \tag{5.1}$$

Where NOx is the true concentration of NO_x in ppb as measured by the reference instrument and NOx_{α} is the factory calibrated reading of Alphasense sensor. The correlation between the Alphasense sensor and the reference instrument was very high with an adjusted R^2 of 0.96 over the training set. The test set was used to test the predictive accuracy of the fitted model. The mean average percentage error (MAPE) over the test set was 17% showing that the fitted model generalised well to new data. A scatter plot of the reference instrument NO_x measurements vs. the NO_x estimates based on the fitted model is shown in Figure 5.7. In order to test whether changes in temperature were influencing the sensor readings, a multivariate linear regression model which included both temperature and the factory calibrated NO_x readings as predictors was also considered. However, the inclusion of temperature as a predictor did not improve the adjusted R^2 of the calibration model. Therefore, the simple linear model based only on the factory-calibrated NO2-B42F sensor readings was used.

Figure 5.6 Collocated inlets of sensing node (red funnel) and DCC fixed site monitors (clear plastic) at Coleraine st.

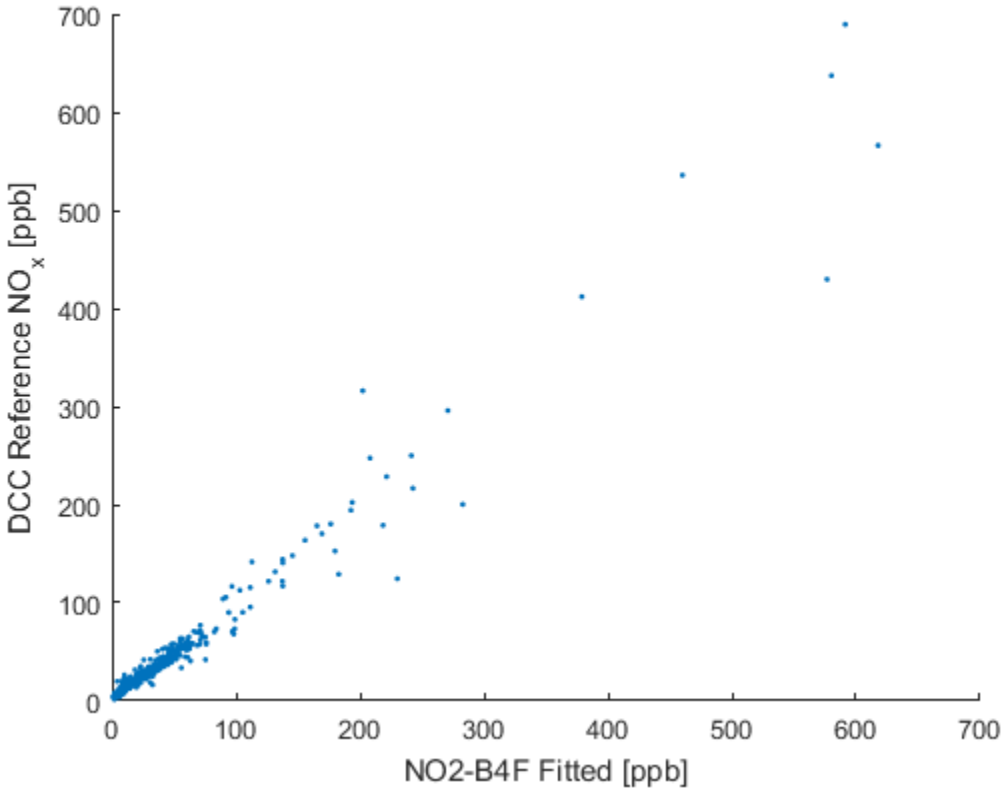

Figure 5.7 NO_x values from DCC reference sensor vs NO_x values estimated from calibration model

5.2.1.7 Limitations of 1st prototype

The 1st prototype was used for the pilot study described in section 6.2. This early prototype was missing some features which were considered essential. These included measurement of PM, CO and noise. Another limitation was that the location and speed measurements were recorded by a separate device to the main DAQ. This meant that when beginning and ending a recording, multiple devices needed to be turned on and off. The data from both devices also needed to be merged. As the speed and location observations were not sampled at exactly the same times as the rest of the data, it was necessary to average or interpolate the speed and GPS data before the data streams could be merged. Based on these limitations, a number of improvements were made to the design and these were incorporated into the 2nd prototype.

5.2.2 Sensing Node Prototype 2

5.2.2.1 Additional functionality

The most significant additional functionality of the 2nd prototype was the addition of a PM sensor. A number of PM sensor models were considered. Some models, such as the Aerocet 531, were found to be too bulky to be integrated into a mobile sensing platform. Others such as the Sharp GP2Y1010AU0F were not accurate enough and/or did not allow measurement of particular PM size fractions. The only sensor which was found that had sufficient accuracy and size selectivity was the Alphasense OPC-N2 (Alphasense, 2015b). This sensor is an optical particle counter (OPC) which measures the light scattered by individual particles which are carried in the sample stream of air stream through a laser beam. The size of each particle is estimated based on the degree of light scattering. The sensor is compact as shown in Figure 5.8 and a further attractive feature is that it is possible to send and receive data over a Serial Peripheral Interface (SPI) connection. This allows the sensor to work as an integrated component of the BEE node rather than as a standalone sensor. Since the OPC features an integrated pump, it did not need to be stored within the same enclosure as the gas sensors. Instead, it was placed in a smaller enclosure for protection from water damage. This smaller enclosure could be placed in the microenvironment to be sampled such as on the strap of a backpack.

Figure 5.8 Alphasense Optical Particle Counter OPC-N2

The Alphasense CO-B4 sensor was also added to the 2nd prototype to provide CO sensing capability to the sensing node. The CO-B4 operates similarly to the NO2-B42F and measures CO between 0 and 1000ppm with noise of 4ppb.

Another additional feature of the 2nd prototype was sound pressure level (SPL) measurement capability. In order to capture the entire audible frequency spectrum, it was necessary to record sound at a sampling rate of 44.1kHz which required a separate DAQ system with a sound card. The DAQ system chosen was a Zoom Handy Recorder H4N. It was out of the scope of this work to integrate this DAQ with the main DAQ system of the sensing node and so the noise recording system was stand-alone. Although the Zoom features built-in microphones, an external electret microphone was used so that it could be placed at head height while the Zoom remained protected in the backpack. The microphone used was the Pro Signal NPA415-OMNI. A recent study has shown that such consumer electret microphones can correlate well with type 1 microphones (Van Renterghem et al., 2011). In order to prevent interference from wind noise, the microphone was fitted with a wind shield as shown in Figure 5.9. Recorded signals could be converted to A-weighted equivalent sound pressure level (dBA) using a Matlab script with a scaling factor calculated in the calibration described in section 5.2.2.3.3.

Figure 5.9 Microphone with wind shield mounted on backpack

5.2.2.2 Improvements to existing functionality

In addition to the added functionality some improvements were made to the existing functionality of the 1st prototype. In the first prototype, position and speed information had been captured by a stand-alone smart phone. In the 2nd prototype, this information was instead captured by a dedicated GPS module, the Adafruit Ultimate GPS. Since the GPS module features serial communication pins, it is easy to send and receive data between it and any DAQ system. This meant that the GPS measurements could be integrated into the BEE node instead of being captured by a standalone system. Also, the module was fitted with a GPS antenna, shown Figure 5.10 which improved the signal reception from the GPS satellites.

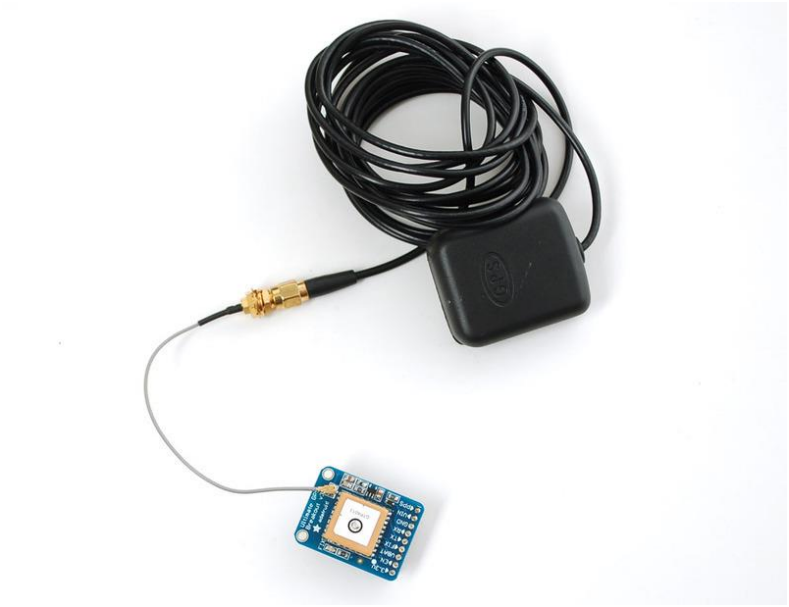

Figure 5.10 Adafruit GPS module and antenna

In order to make possible the recording of information from the gas sensors, OPC and GPS receiver using a single device, the main DAQ system was upgraded from the Raspberry Pi to the Intel Galileo. The Galileo is a compact microprocessor board based on Intel x86 architecture, designed for use in "Internet-of-Things" projects. The Galileo is also software compatible with the Arduino Software Development Environment. This was important as communication with the OPC was only possible using SPI communication and this is simple to implement using an Arduino sketch. A custom Arduino sketch was created which created one observation every 2 seconds which consisted of NOx, CO and PM2.5 concentrations as well as GPS coordinates, speed and a timestamp. All observations were saved to a csv file on the on-board SD card. Similarly to the Raspberry Pi, the Galileo was powered using a battery-bank designed for mobile charging of smart phones.

The 2nd prototype is illustrated in Figure 5.11. This version of the sensing node meets all of the functional requirements specified in section 5.1. Additionally, all of the measurements except for SPL are integrated in a single system. This system has a single power source and all of the sensors begin recording when the system is turned on.

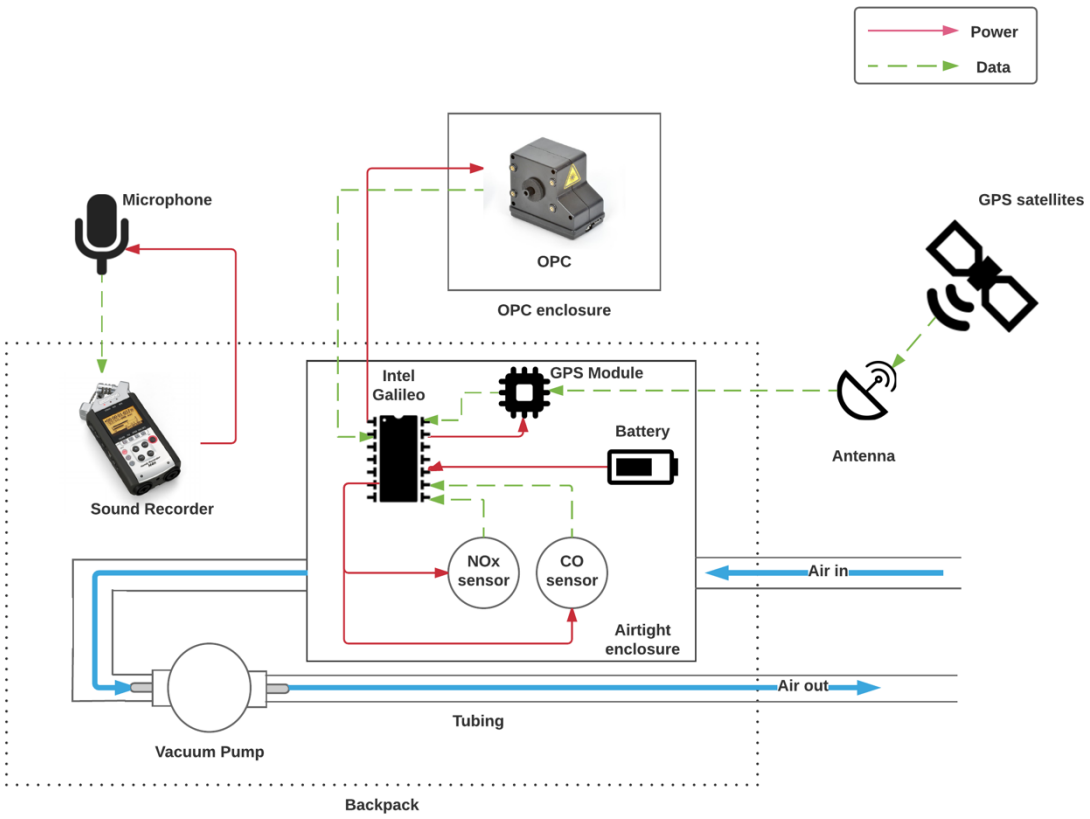

Figure 5.11 Functional diagram of sensing node 2nd prototype

5.2.2.3 Calibration

The additional environmental sensors of the second prototype needed to be validated and calibrated before use. The NO_x sensor was also recalibrated using a reference instrument with higher temporal resolution.

5.2.2.3.1 OPC Calibration

The Alphasense OPC-N2 is a nephelometer-type device which operates by measuring the scattering of light as it passes through a sample stream of air. It is well documented that these types of devices

are sensitive to environmental variables such as relative humidity (RH) and temperature (Chakrabarti et al., 2004; Nyhan et al., 2014). Therefore, these variables must be controlled for during calibration. Even so, if a nephelometer is used in a location where the range of temperature and RH is very different to that of the location where the calibration took place, the calibration may not be valid. During the development of the BEE node, there was an opportunity to use the sensors for an exposure study in Chennai, India. This required the OPC to be calibrated in the local environment. Although the resultsof the Chennai exposure study are

outside the scope of this thesis, the results of the local calibration are informative. Therefore, the results of Chennai calibration are reported in this section followed by the results of the main calibration which took place in Dublin.

In Chennai, the OPC was collocated with a Grimm portable aerosol spectrometer (PAS) 1.108. The Grimm PAS is also a nephelometer and so, it is not an ideal reference instrument. However, it was considered to be a higher fidelity instrument than the OPC as it has been used extensively in the literature (Hall et al., 2002; Peters et al., 2001) including one study which validated its performance (Teikari et al., 2003). The collocated test was run for 20 hours on 6/Apr/2015 to 7/Apr/2015 and for 48 hours on 17/Apr/2015 to 19/Apr/2015 on the roof of a FSM station at the edge of the campus of the Indian Institute of Technology, Madras. Minute by minute $PM_{2.5}$ concentrations recorded by the Grimm PAS were compared to minute averages of the OPC $PM_{2.5}$ measurements. Temperature (°C) and RH (%) measurements recorded by the FSM were also available. The data from 6/Apr and 17/Apr were aggregated and randomly allocated to a training set (70%) and a test set (30%). Using the training data, regression models were fitted in order to predict the Grimm PAS $PM_{2.5}$ observations based on the OPC $PM_{2.5}$ measurements, temperature and RH. Interactions between the predictor variables were also considered. The best fitting model for PM2.5 used the OPC measurements, RH and the product of the OPC measurements and RH as predictors. The fitted model was as follows:

$$C_{PM2.5} = 2.4 \times OPC_{PM2.5} + 0.12 \times RH - 0.02 \times (OPC_{PM2.5} \times RH) - 1.35 \quad (5.2)$$

Where $C_{PM2.5}$ was the concentration of $PM_{2.5}$ as measured by the Grimm PAS, $OPC_{PM2.5}$ was the $PM_{2.5}$ concentration as measured by the OPC and RH is the percentage relative humidity. The adjusted R^2 was 0.82 and the MAPE on the test set was 22%. It is interesting to note that the coefficients of OPC2.5 and RH were both positive but the coefficient of OPC2.5*RH was negative, indicating a complex influence of RH on the agreement between the OPC and the reference instrument. This may because both instruments were affected by RH. The final model does not include temperature as a predictor because temperature was not a significant predictor in any of the candidate models.

The best fitting model for PM10 in Chennai used the OPC measurements as the only predictor. The fitted model was as follows:

$$C_{PM10} = 0.2 \times OPC_{PM10} + 17.3 \quad (5.3)$$

The accuracy was lower than that of the PM2.5 model with an adjusted R2 of 0.38 and a MAPE on the test set of 53%.

In Dublin, the OPC was collocated with the inlets of an EPA FSM station in Rathmines, close to a main road just outside the city centre of Dublin. The reference instrument at the FSM station was a Thermo Scientific TEOM 1405-DF. This monitor is a candidate US EPA equivalent sampler for $PM_{2.5}$ and also has the advantage of producing continuous samples at 1 hour intervals, unlike gravimetric measurements which typically only produce one measurement per day. Since the OPC was to be used in applications requiring high temporal resolution; calibration using the TEOM sampler was considered to be most appropriate. Hourly weather data including temperature (°C), RH (%) and precipitation (mm) were available from a nearby weather station at the Phoenix Park. Conditions of very high RH and/or rainfall can be expected to influence the OPC measurements significantly (Chakrabarti et al., 2004; Nyhan et al., 2014). Therefore, in both the calibration process described here and the field measurements described in the next chapter, the OPC data recorded during hours of rainfall and/or RH of 95% or greater were discarded. The remaining valid data were randomly allocated to training (70%) and test (30%) sets. Regression models were fitted to predict the hourly measurements of the TEOM sampler from the hourly averages of the OPC, the temperature measurements and the RH measurements. Interactions between predictor variables were also considered. The best fitting model used the OPC measurements, RH and the product of the OPC measurements and RH as predictors. The fitted model was as follows:

$$C_{PM2.5} = 0.54 \times OPC_{PM2.5} + 0.24 \times T - 1.003 \quad (5.4)$$

Where $C_{PM2.5}$ is the concentration of $PM_{2.5}$ as measured by the EPA TEOM sampler, $OPC_{PM2.5}$ is the $PM_{2.5}$ concentration as measured by the OPC and T is the temperature. The adjusted R^2 was quite low at 0.15 and the MAPE on the test set was moderately high at 53%. The best fitting model for PM10 was as follows:

$$C_{PM10} = 0.41 \times OPC_{PM10} + 0.36 \times T - 3.005 \quad (5.5)$$

The accuracy was better than the PM2.5 model with a R2 of 0.34 and a MAPE of 36.3%. Based on these results, it would appear that the OPC-N2 is suitable for no more than rough indicative measurements of PM exposure. Additionally, there were significant differences between the calibrations in the two cities. In Chennai, RH was significant in predicting the PM2.5 measurements of the reference instrument and temperature was insignificant. In Dublin, temperature was a significant predictor but RH was not. The differences in calibration results show that even when environmental variables are controlled for, the performance of the OPC in one environment may be very different to its performance in another environment. This may be explained by differences in particle composition or density, differences in the performances of the reference instruments or some other factor. However, it is clear that if a low-cost PM sensor such as the OPC-N2 is to be used for measurements in a specific location, it should be tested and calibrated in that location during a range of typical meteorological conditions. Furthermore, in order test the performance of the sensor at a more general level, ideally, tests in multiple locations with differing environments and PM sources should be carried out.

Overall, it appears that there is some level of agreement between the OPC-N2 and other higher fidelity PM monitors. However, since the OPC-N2 could not be validated to a high degree of accuracy during the testing in Dublin; the PM measurements reported in Chapter 6 should be treated as rough indicators only.

5.2.2.3.2 Gas Sensors Calibration

In order to validate the CO-B4 sensor, a collocated test was carried out with an EPA FSM station at Portlaoise, a town about 80km from Dublin city. The reference instrument of the FSM station was an Enviro Technology CO Analyser Model 300E. Hourly CO measurements of the reference instrument were compared to 1 hour averages of the factory calibrated CO sensor and the temperature sensor. The time series of readings from the factory calibrated Alphasense CO sensor and the EPA CO analyser are shown in Figure 5.12.The measurements from the EPA monitor were quantised in steps of 250ppb and so it was not possible to calculate an accurate measure of correlation between the two series. However, the Mean Average Percentage Error (MAPE) between the two series was 12%, a reasonably low value. It can also be seen from Figure 5.12 that there is generally good agreement between the two sensors and much of the deviation between the series seems to be resulting from the quantisation of the values from the EPA sensor. Based on these results, there was no reason to suspect that the factory calibration provided by Alphasense needed to be corrected.

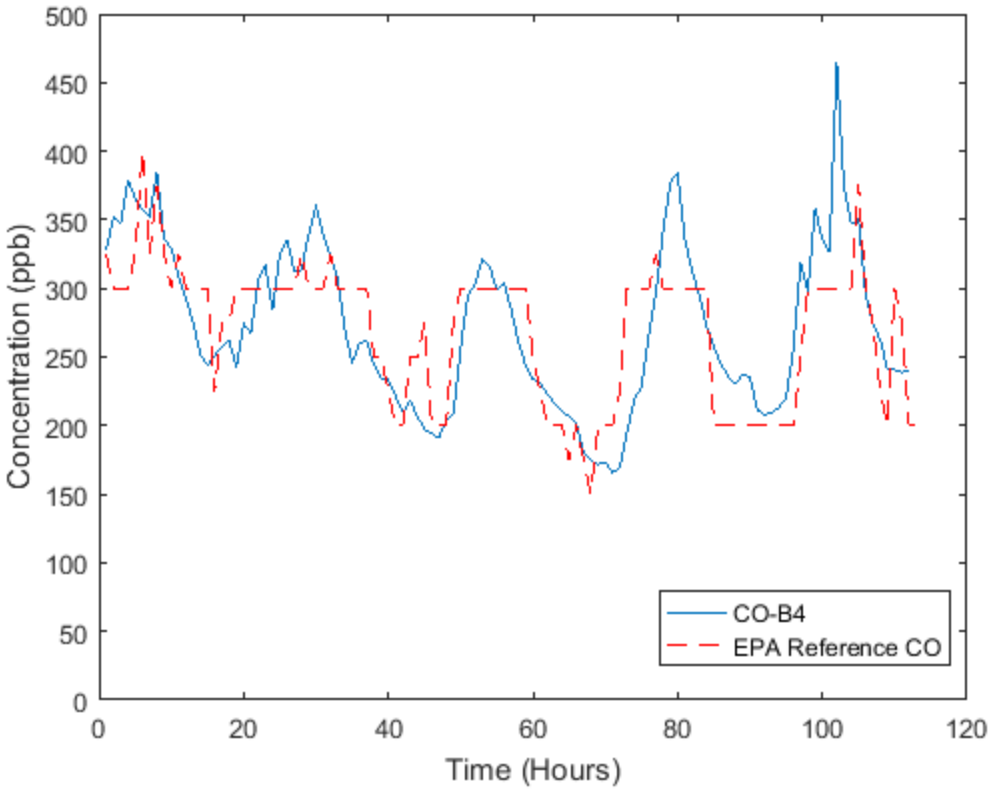

Figure 5.12 Comparison of time series data from Alphasense CO-B4 and EPA reference sensor

The NO2-B42F sensor had already been validated and recalibrated in the development of the first prototype. However, when developing the 2nd prototype, a reference instrument was available which could provide NOx measurements at a higher frequency. The calibration was therefore repeated using this reference instrument. The sensing node was collocated with the reference instrument, an Enviro Technology Chemiluminescence NO_x Analyser Model 200E, in Trinity College for 4 days from 24/Jul/2015 to 27/Jul/2015. Both devices were sampling air from Pearse st.—a highly trafficked street adjacent to the college—through an open letterbox. Measurements taken by the reference instrument at 15 minute intervals were compared to 15 minute averages of the NO2-B42F sensor readings.To predict NO_x concentration from the sensor readings, linear regression models were considered using different predictors, including the factory calibrated measurements and the raw voltage readings from the WE and the AE. A linear model of NO_x concentration vs WE voltage was chosen as it had the highest adjusted R^2 on the training set. The model was as follows:

$$NOx = 1275 * V_{WE} - 310 \tag{5.6}$$

Where V_{WE} was the measured voltage on the WE. A comparison of the reference instrument NO_x measurements and the NO_x estimates based on this model is shown in Figure 5.13. The MAPE on the test set was 11.5%. The voltage on the AE, which is meant to help control for the influence of temperature on the sensor readings did not improve prediction accuracies. This may be because extremely high or low temperatures were not encountered during the testing. However, during the test, the ambient temperature varied between 8°C and 18°C and temperatures outside of this range were expected to occur rarely during the planned exposure studies. The calibration model based on the WE voltage alone was therefore considered to be appropriate.

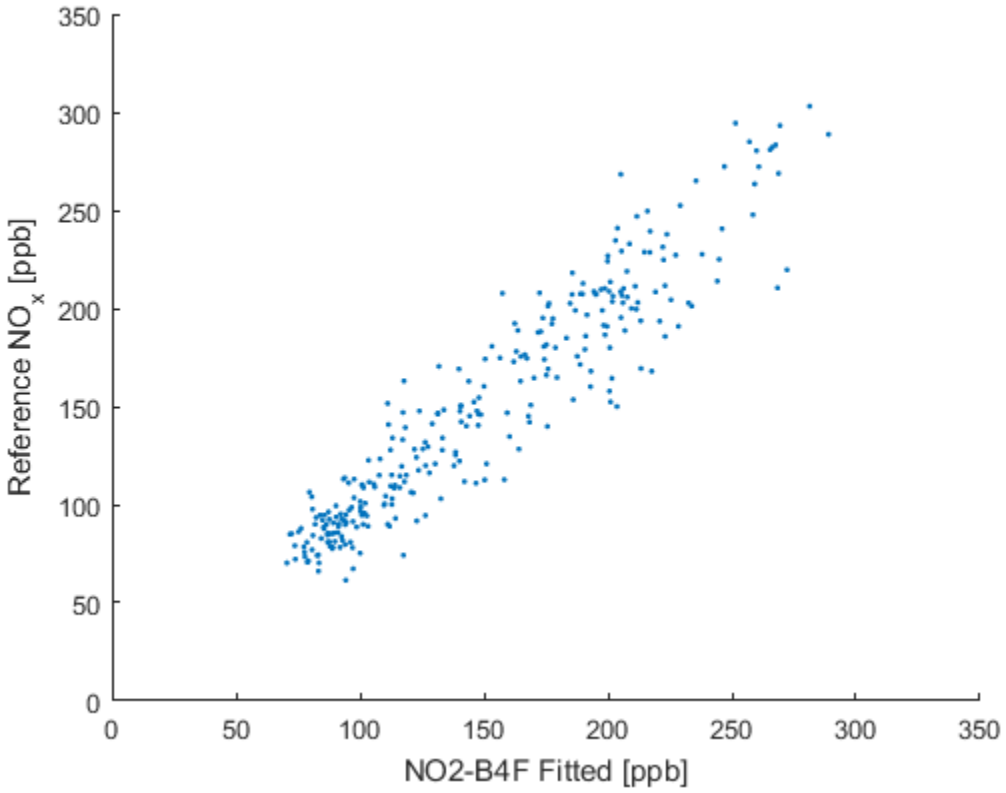

Figure 5.13 NOx values from reference sensor vs NOx values estimated from calibration model.

5.2.2.3.3 Sound Recorder Calibration

The microphone and sound recorder combination was calibrated using a microphone calibrator. The Brüel & Kjær Sound Calibrator Type 4231 was used for this purpose. Following the manufacturer's instructions, the microphone was placed into the calibrator and the calibrator delivered a stable calibration pressure of 1 Pascal (Pa) for a period of 20s. The sound was recorded at a sampling rate of 44.1kHz by the sound recorder. The recorded signal is plotted in Figure 5.14. The Root Mean Square (RMS) value of the recorded signal was then calculated and a scaling factor to convert RMS voltage to RMS Pa was determined. The scaling factor could later be used to calculate the RMS sound pressure of any recorded signal. The sound pressure level (SPL), measured in decibels (dB) of the signal could then be calculated using the following formula (Hansen and Sehrndt, 2001) :

$$L_p = 20 * \log_{10}(P_{rms} / P_0) \tag{5.7}$$

Where L_p is the SPL in dB, P_{rms} is the RMS sound pressure and P_0 is the reference sound pressure. The value of the reference sound pressure is the auditory threshold of 20 µPa.

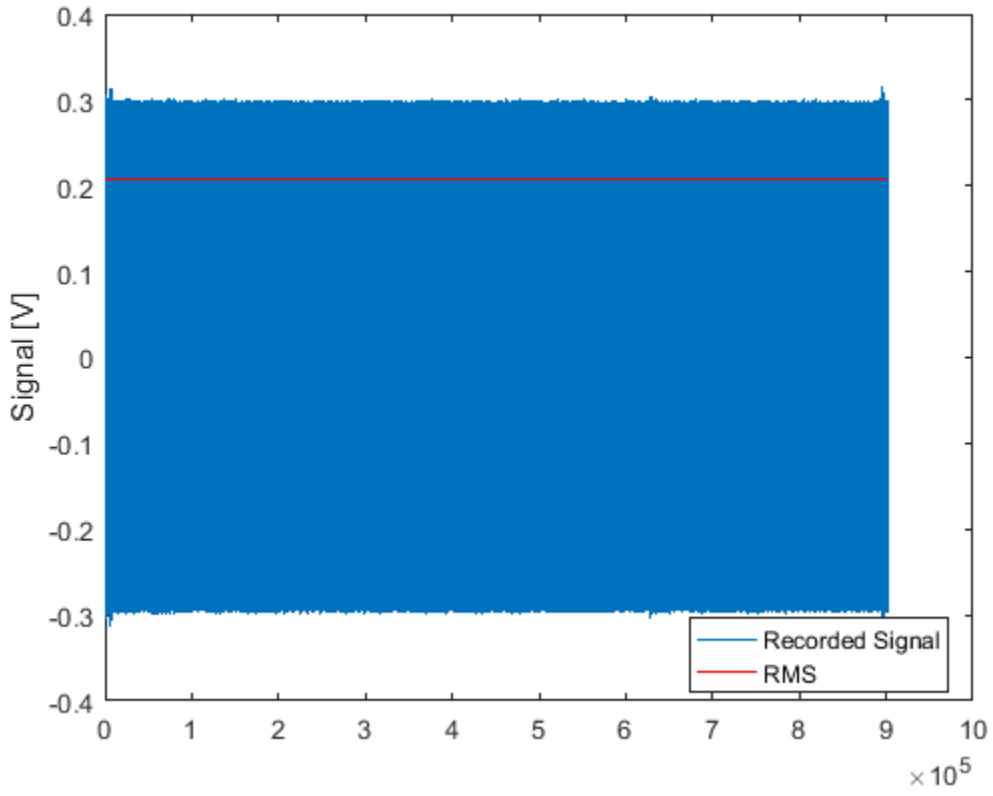

Figure 5.14 Recorded signal from sound calibrator

5.3 Conclusions

This chapter has reported the development of a low-cost mobile environmental sensing node capable of being used as a personal monitor by a cyclist. The node can record spatially resolved measurements of $PM_{2.5}$, CO, NO_x and SPL at high sampling rates. The node is inexpensive relative to traditional monitoring methods and simple to assemble and use. Although reliability of data is considered to be one of the main challenges in the use of low-cost pollution sensors, the accuracy of each of the low-cost sensors has been validated by means of collocated tests with high-fidelity instruments.

A number of limitations of the design are noteworthy. One limitation is that the SPL measurements are recorded by a different device to the air quality measurements. This means that if SPL measurements are required, two separate devices must be turned on and off when taking measurements and recorded data must also be retrieved from two devices. Also, in the current design, all data is simply recorded to an on-board SD card which must later be removed to retrieve the data. This was sufficient for the studies described in Chapter 5 but for future studies, it may be advantageous for the recorded measurements to be periodically uploaded to an online database over a mobile data connection.

Chapter 5 describes two studies which use the BEE node for the characterisation of cyclist exposure to environmental pollution while commuting.

Chapter 6: Environmental Exposure of Cyclists in Dublin

6.1 Introduction

In Chapters 3 and 4, it was noted that the approach used for quantifying the health impacts of environmental exposures—which was similar to the accepted approach in the literature—used approximations of exposure based on average concentrations from fixed site monitors. Therefore, the degree to which the health impacts of pollution exposure while cycling vary by route is unclear. As shown in Chapter 4, considering health impacts at a highly aggregated level may obscure the negative impacts to some individuals. In particular, this aggregate approach could not account for variations in exposure due to weather conditions or route-specific factors such as traffic levels or presence of cycling facilities. Based on the literature review discussed in Chapter 2, it can be reasonably expected that such factors would significantly influence pollution exposures but there are still significant gaps in the research. Of the many studies of cyclists' exposures discussed in Chapter 2, only three considered presence of cycling facilities and link level traffic volumes in the same study and none of these considered NO_x concentrations (Bigazzi and Figliozzi, 2015a; Hankey and Marshall, 2015; Hatzopoulou et al., 2013) or uptake dose of any pollutants. Also, very little research has considered the factors affecting the variation in noise exposure of cyclists.

This chapter reports two studies of the pollution exposures of cyclists in Dublin. The aforementioned gaps in the literature are addressed by analysing the impact of traffic volumes, presence of traffic facilities and weather variables on exposure concentrations and intake doses of CO, NO_x and $PM_{2.5}$ and on exposure to noise. The first study was a pilot study which used the first iteration of the BEE node of Chapter 5 and aimed to generate insights to improve the design of both the BEE node and the exposure study. The second study was a larger scale study which used the second iteration of the BEE node. The study design and results are presented below for each study in turn. The chapter concludes with a discussion of the limitations of the studies and the implications of the results.

6.2 Pilot Study: NO_x exposures of a cyclist on fixed routes in Dublin

A pilot study was carried out using the first prototype of the BEE node in order to (i) inform a later larger study and (ii) to identify potential improvements to the BEE node. In this pilot study, the NO_x concentrations to which a cyclist was exposed to while cycling along two fixed routes in Dublin city were measured. Simultaneous measurement of heart rate allowed respiration rate to

be modelled in real time in order to estimate pollution intake rate. Linear mixed effects models (Pinheiro and Bates, 2000) were then used to explore the impacts of a range of traffic network, meteorological and behavioural variables on NO_x exposure and intake. The study design is described in detail below followed by reporting of the results.

6.2.1 Study Design

The sampling was conducted on 9 days between February and March, 2015 in Dublin city, Ireland. A healthy male, aged 24, cycled along two fixed routes while carrying instrumentation for measurement of local NO_x concentration, heart rate, position and speed. The two routes were chosen to cover common commuter routes and to include the four categories of cycling facilities common to Irish cities: on-road (no cycling facility), bus lane, cycle lane adjacent to road with no separation and separated cycle lane. The total length of unique road sampled was 26.5km. Each route took approximately 45 minutes to cycle once and each route was cycled 3 times during on-peak hours (between 4pm and 7pm) and 2 times during off-peak hours. Motor vehicle traffic counts during the sampling periods were provided by Dublin City Council at 15 minute resolution. Figure 6.1 shows the two routes with the locations of the traffic counters. The first prototype of the BEE node described in Chapter 5 was used to measure the NO_x concentrations and GPS locations. It was carried by the participant in a small backpack as shown in Figure 5.5 in the previous Chapter. The heart rate of the participant was measured simultaneously using a CamNTech Actiheart monitor.

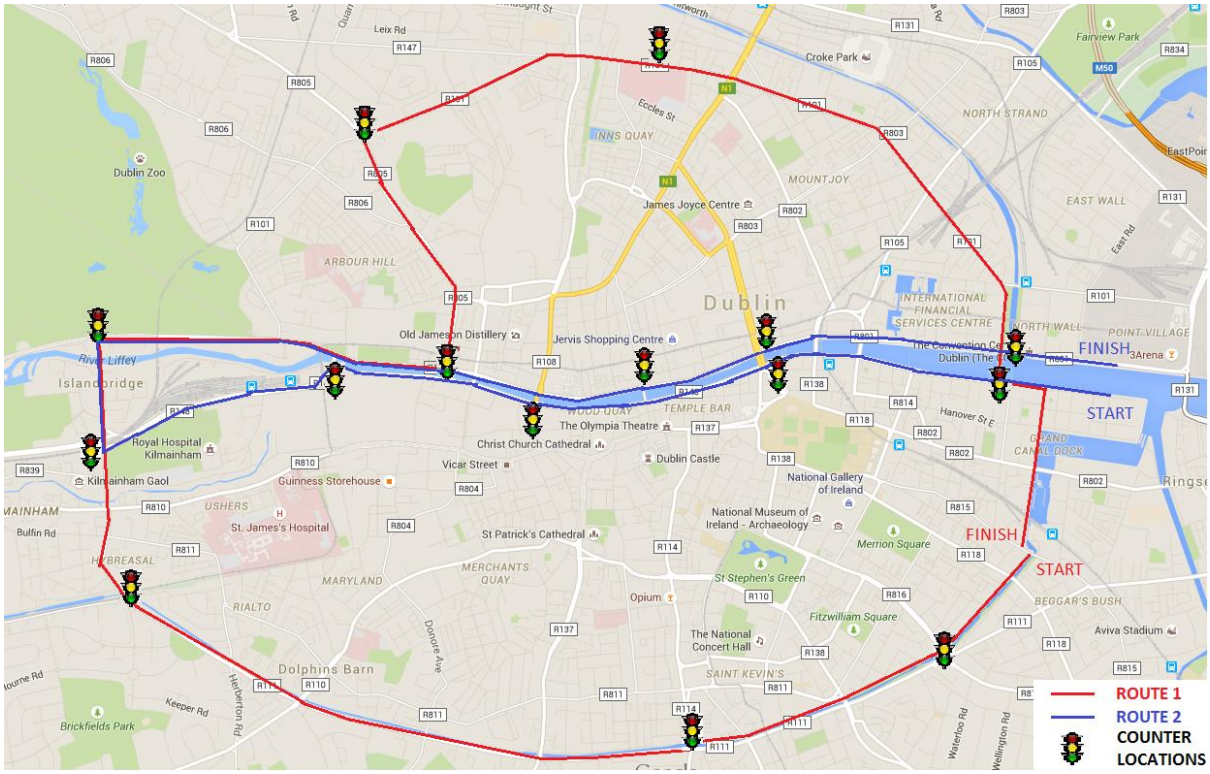

Figure 6.1 Pilot study routes with counter locations (Google Maps, 2015)

6.2.2 Data Analysis

For the purpose of analyzing the relationship between NO_x exposure and explanatory variables relating to cyclist behaviour, weather and the traffic network; 30 second averages of all the measured data were taken. Taking time-averaged gas concentrations when considering health impacts is typical practice in assessing in-transit exposure to pollutants (Bean et al., 2011; Kaur et al., 2005b; Kaur et al., 2007; Rakowska et al., 2014). Since the speed readings from the GPS system were not equally spaced, the averaging was weighted by the time since the previous measurement. As the health impacts of pollution exposure depend not just on the exposure concentration but on the intake dose, the minute ventilation rate (VE) of the subject also needed to be estimated. VE was estimated from the subject's measured heart rate (HR) using the empirical model estimated by Zuurbier et al. (2009).

$$VE = \exp(c + m \times HR) \qquad \text{Eq. (6.1)}$$

where c and m are constants (1.03 and 0.021 respectively for males). The rate of NO_x Intake per metre travelled could then be found by multiplying VE by NO_x Concentration and dividing by Average Cycling Speed in metres per minute.

Linear mixed-effects (LME) models were used in the analysis with fixed and random effects of a number of explanatory variables. The fixed effects were associated with all observations and the

random effects were associated with each Trip ID. The inclusion of random effects allows for unobservable heterogeneities between different trips to be accounted for by treating them as normally distributed random variables with zero mean. An LME model with a single level of grouping can be expressed as (Pinheiro and Bates, 2000):

$$y_i = X_i\beta + Z_i b_i + \varepsilon_i, \qquad \forall i = 1, 2, \ldots M$$

$$b_i \sim N(0, \Sigma), \quad \varepsilon_i \sim N(0, \sigma^2 I)$$

Eq. (6.2)

Where M is the number of groups, y_i are the observations in group i, X and Z are the fixed and random design matrices, β is the *p*-dimensional vector of fixed effects, b_i is the *q* dimensional vector of random effects, ε_i are the residuals, Σ is the variance-covariance matrix of the mixed-effects vectors, σ is the standard deviation of the residuals and I is the identity matrix. The *nlme* package was used with the R software package to fit linear mixed-effects models. The dependent variables considered were NO_x Concentration (ppb) and NO_x Intake per metre travelled (µg/metre). The independent variables considered for fixed effects were Traffic Volume (vehicles/hr), Facility Type (no facility, bus lane, adjacent cycle lane or separated cycle lane), Background NO_x Concentration (ppb) (as measured by a DCC fixed site monitoring station in a nearby public park, St. Annes' Park), Wind Speed (knots), Rainfall (mm/hr), Temperature (° C), Relative Humidity (%) and Average Speed (m/s). The weather data from a weather station at Dublin airport were obtained from the Irish National Meteorological Service (Met Éireann, 2016). Logged versions of all continuous variables were also considered. Random intercept terms associated with the Trip ID were also considered in order to allow for the possibility that unobserved differences between the conditions of each trip may have affected the exposure concentrations.

6.2.3 Description of dataset

Sampling was carried out during a total of 12 trips giving 919 observations over approximately 8 hours of cycling. Table 6.1 shows descriptive statistics for the sampled dataset. Route 2 which stayed close to the city centre had a higher mean traffic volume and slightly higher mean NO_x concentration.

The temporal and spatial resolution of the sampled data allows the NO_x concentrations on key commuter routes in Dublin city to be visualised as shown in Figure 6.2. This allows pollution hotspots to be identified in way which is not possible with traditional static monitoring. In

particular, Figure 6.2 shows very high NO_x concentrations on parts of Wellington Quay on route 2, adjacent to the popular tourist area of Temple Bar. A Google Street View image (Google Maps, 2014) of the location is shown in Figure 6.3. These very high levels should be interpreted with caution as, during the calibration process, no values were recorded as high as these and therefore the linearity of the sensor cannot be guaranteed at these levels. However, it is clear that the NO_x exposure concentrations were relatively very high at these locations. Further insights can be gained by looking at the average recorded NO_x concentration on each type of cycling facility. As shown in Figure 6.4 and Figure 6.5, bus lanes had the highest average NO_x concentrations followed by on-road cycling, adjacent cycle lanes and separated cycle lanes. The effect of different cycling facilities on pollution exposure will be further explored in the next section.

Table 6.1 Summary of data collected in pilot study

Route	N	NO_x Concentration (ppb)		NO_x Intake rate (µg/m)		Traffic Volume (vehicles/hr)	
		Mean	SD	Mean	SD	Mean	SD
Route 1	499	204.5	151.4	0.29	2.09	408.3	318
Route 2	420	283.3	217.4	0.12	0.4	807.6	526.7

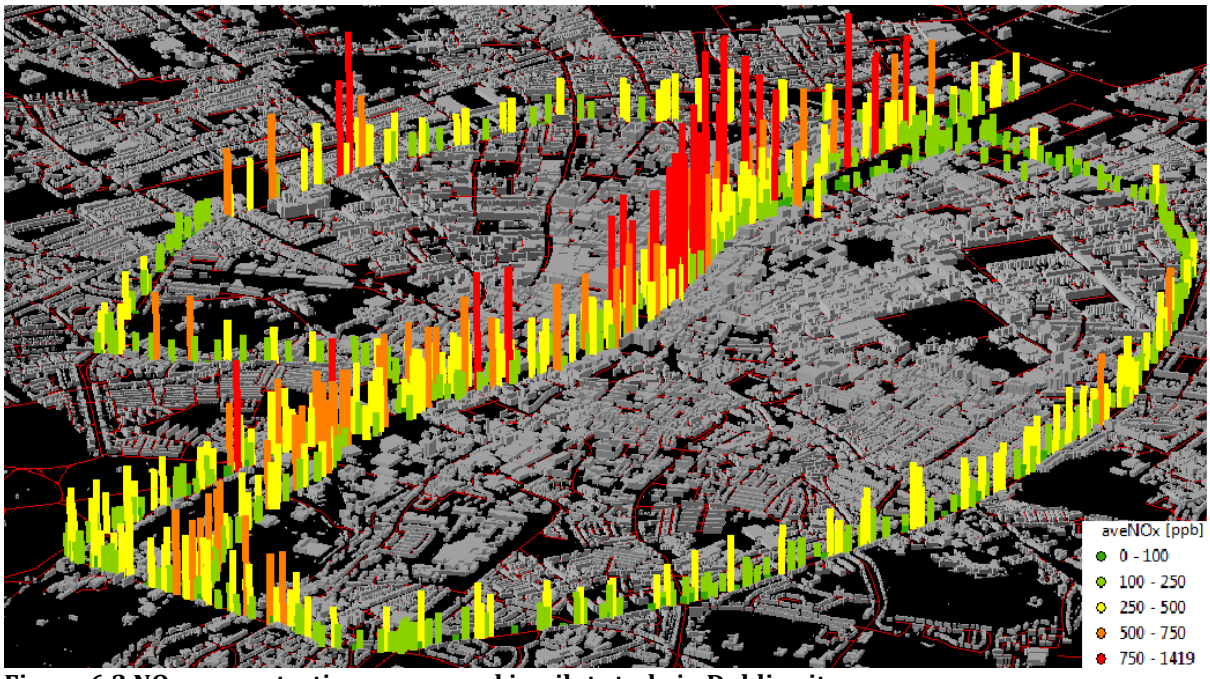

Figure 6.2 NOx concentrations measured in pilot study in Dublin city.

Figure 6.3 Google Street View of NOx hotspot close to Temple Bar area of Dublin (Google Maps, 2014)

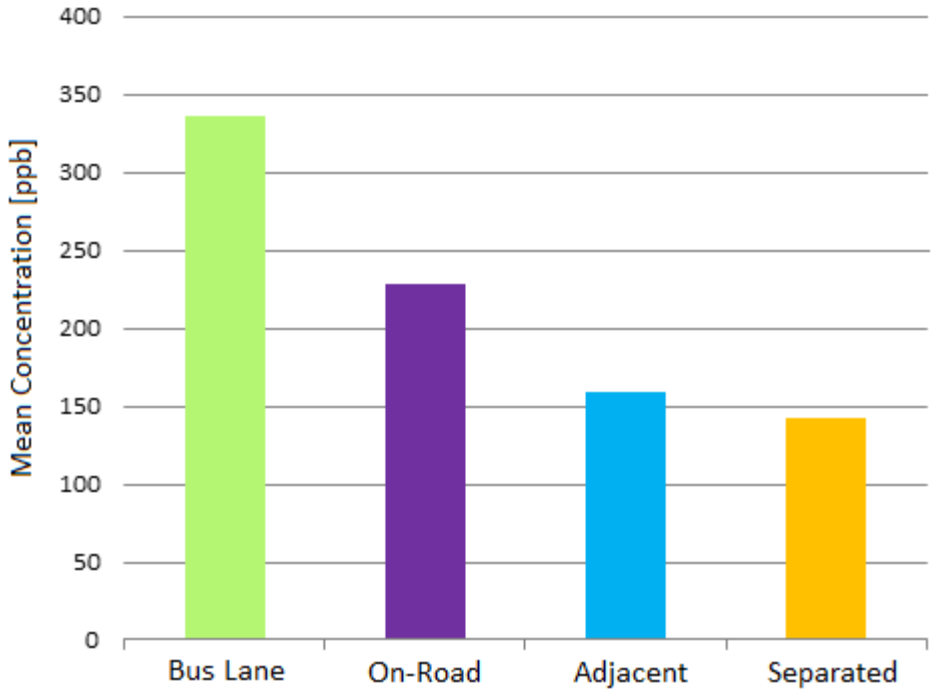

Figure 6.4 Average NOx exposure concentrations by facility type in pilot study

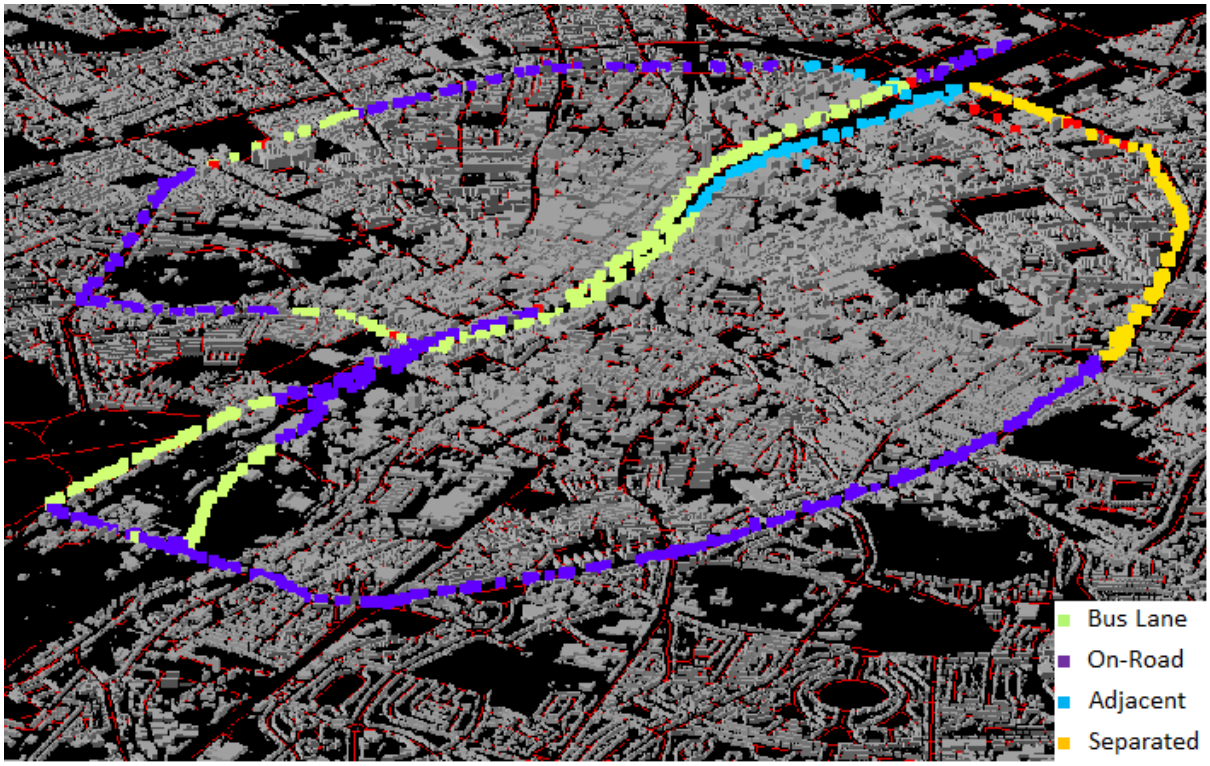

Figure 6.5 Cycling facility types on both routes in the pilot study

6.2.4 Results of Analysis

Linear mixed models were fit to the dependent variables on ln(NO_x) and ln(NO_x Intake/metre). Log transformations were used because the distributions of the raw variables showed high positive skew whereas the log transformed distributions were close to normal. To determine the best combination of fixed effects for each mixed effects model, a process of backwards elimination was followed whereby, in the first instance, all possible variables were included and then non-significant variables were eliminated one at a time, ensuring that the Bayseian Information Criterion (BIC) improved with each variable removed. In fitting the mixed effects model for NO_x concentration, it was found that the best model was a model of ln(NO_x) with fixed effects for ln(Hourly Traffic), Facility Type, ln(Background NO_x) and Wind Speed and random effects of Trip ID on the intercept. The other weather variables and Average Speed were all found to be insignificant. The model parameters are shown in Table 6.2. In fitting a mixed effects model for NO_x Intake/metre, it was found that the best model was a model of ln(NO_x Intake/metre) with fixed effects for ln(Hourly Traffic) and Wind Speed and random effects of Trip ID on the intercept. The model parameters are shown in Table 6.3. As expected, logged hourly traffic volume was positively associated with both NO_x concentration and NO_x Intake per metre travelled. Facility type was found to be linked to NO_x concentration but not to NO_x inhalation rate. Since the dependent variable is log transformed, the exponentiated coefficient of each facility type gives an estimate of the ratio of the expected value of NO_x concentration for that facility vs the expected value of NO_x concentration for the reference facility (on-road). Interestingly, bus lanes were associated with a 12% increase in NO_x concentration compared to no facility. This may suggest that in terms of pollution exposure, the separation from main traffic offered by bus lanes is outweighed by the higher emissions from buses compared to other traffic. Cycle lanes adjacent to the road and separated cycle lanes are associated with 32% and 17% decreases in NO_x concentrations. Similarly to other studies of cyclist and pedestrian pollution exposure, Wind Speed is the only significant weather variable. However, in this case NO_x concentrations seem to be increasing with Wind Speed whereas most previous studies have shown that pollution concentrations decrease with increasing wind speed (Bigazzi and Figliozzi, 2014; Greaves et al., 2008; Kaur et al., 2007). For the second model with NO_x Intake per metre as the dependent variable, logged Hourly Traffic and Wind Speed had similar impacts. However, neither Facility nor Background NO_x were found to be significantly associated with intake per metre. This is not what would be expected since NO_x intake is proportional to NO_x concentration and NO_x Concentration was found to be significantly associated with both of these variables. However, it appears that since NO_x intake per metre also depends on Heart Rate and

Average speed, the proportions of the total variance which could be explained by Background Concentration and Facility were lower, leading to non-significant associations. If this explanation is accurate, analysis of a larger sample size should show significant associations between these variables. The standard deviations of the random effects terms are sufficiently large to suggest that there were significant differences between the different sampling sessions which were not accounted for by the measured variables. These differences may be due to the effects of traffic, meteorological or behavioural variables not considered here.

Since only a single subject participated in this study, it was not possible to say whether the results relating to the intake dose would be similar for an individual with different level of cycling ability or cardiovascular fitness. Since measurements were only taken on two routes, it is possible that the model results were influenced by a correlation between facility type and traffic volumes. These concerns will be addressed by the second study in this chapter which features multiple participants and a larger sample size of routes with a variety of traffic levels and facility types.

Table 6.2 Parameters of the Linear Mixed Model of log(NOx Concentration) for the pilot study

	Variable	Estimate	Standard Error	p-Value
Fixed Effects	(Intercept)	2.66	0.44	0.00
	log(Hourly Traffic)	0.06	0.02	0.00
	Facility: Bus Lane*	0.12	0.04	0.00
	Facility: Adjacent*	-0.39	0.06	0.00
	Facility: Separated*	-0.18	0.07	0.00
	Wind	0.10	0.01	0.00
	log(Background NO_x)	0.31	0.06	0.00
Random Effects	**Variable**	**Standard Deviation**		
	(Intercept)	1.15		
	Residual	0.43		

* Relative to Facility: No Facility

Table 6.3 Parameters of the linear mixed model of ln(NOx Intake/metre) for the pilot study

	Variable	Estimate	Standard Error	p-Value
Fixed Effects	(Intercept)	-4.77	0.41	0.00
	log(Hourly Traffic)	0.12	0.02	0.00
	Wind	0.07	0.02	0.00
Random Effects	**Variable**	**Standard Deviation**		
	(Intercept)	0.95		
	Residual	0.97		

6.3 Full Scale Exposure Study: exposure of commuter cyclists to NOx, CO, PM2.5 and Noise in Dublin

The full study differed from the pilot study in a number of ways. Firstly, the second iteration of the BEE node was used so that exposures to CO, $PM_{2.5}$ and Noise could also be monitored. Secondly, instead of measuring the exposures of a single participant cycling on two fixed routes, a group of volunteers were recruited to cycle their own regular commutes. The study design is described in detail below followed by reporting of the results.

6.3.1 Study Design

Volunteer cyclists of all ages, genders and cycling experience levels were recruited to participate in the study using a number of avenues. In order to recruit regular cyclists, posters were placed in local cycling shops and contact was made with local cycling communities. Individuals who cycled infrequently were also recruited through personal contacts and by contacting businesses located in Dublin. Each participant completed an online survey prior to participating in order to record basic personal characteristics. Each participant was also required to read a participant information form which explained the study procedure and to sign the form indicating that they understood the information and consented to take part in the study. This form can be found as an appendix of this thesis. In addition, a Risk Assessment Statement was written by the author and reviewed and approved by technicians in the department of Civil, Structural and Environmental Engineering, of Trinity College Dublin. A formal ethics approval for the study was not judged to be necessary as the volunteers would not incur any significant additional risk as a result of their participation in the study. 22 volunteers participated in the study. The demographics of the study group are summarised in Table 6.4. The sampling protocol for the study was designed in order to develop a realistic representation of the pollution exposures faced by commuter cyclists in Dublin. Volunteers participated in the study by simply completing their usual commute as normal while carrying the monitoring equipment. Each volunteer completed between 1 and 4 trips with the equipment. Sampling was carried in both directions, on weekdays only. Before their first recorded trip, each participant was trained in the use of the monitoring equipment. After the measurements were completed, the equipment was collected and the recorded data were retrieved. As discussed in Chapter 5, air samplers which use light scattering methods are known to be unreliable during precipitation so if precipitation occurred at any time during the recording, the data were discarded.

Table 6.4 Demographics of the study group of the full scale exposure study

Variable	Category	Frequency	%
Age Group	18 - 30	6	27.3%
	31 - 44	11	50.0%
	45 +	5	22.7%
Gender	Male	13	59.1%
	Female	9	40.9%
Physical Activity Level	Sedentary: Little or no physical exercise	5	22.7%
	Active: Engage in moderately intense or vigorous physical exercise 2 - 5 times per week	10	45.5%
	Fitness Enthusiast: Engage in moderately intense or vigorous physical exercise more than 5 times per week	7	31.8%
Main Mode of Transport	Walking	1	4.5%
	Cycling	19	86.4%
	Private Car	1	4.5%
	Public Transport	1	4.5%

The equipment carried by the volunteers during each recorded trip included the second iteration of the BEE node described in Chapter 5 and a heart rate monitor (HRM). The BEE node allowed concentrations of CO, NOx, and PM2.5, location, speed and noise level to be recorded. The HRM used was a Zephyr HxM Bluetooth Heart Rate Monitor. The data from the HRM was logged in real time to a Samsung Galaxy Ace II smart phone via Bluetooth connection using the MyTracks app. This HRM was less cumbersome for the volunteers than the CamNTech monitor used in the pilot study. Additionally, the HRM data logged by the MyTracks app could also be accompanied by a GPS timestamp. This allowed the heart rate data to be accurately synchronized with the data collected by the BEE node which also used GPS timestamps.

Similarly to the first exposure study, linear mixed models were used to study the relationship between the exposure variables and the explanatory variables. The exposure data were analysed at 2 second intervals—the sampling rate of the BEE node. The seven exposure variables considered were CO exposure (ppb), NOx exposure(ppb), $PM_{2.5}$ exposure ($\mu g/m^3$), Noise Level (dBA), Inhaled CO (µg), Inhaled NOx (µg) and inhaled $PM_{2.5}$ (µg). The explanatory variables were Traffic Volume (veh/hr), Facility Type (no-facility, bus lane, roadside lane or separated cycle lane), Wind Speed (knots), Temperature (° C) and Relative Humidity (%). Because of the scale of this study and the variety of road sections covered by the volunteers, it would have been

impractical to obtain the Traffic Volume and Facility Type information manually as done for the first exposure study. Instead, this information was obtained using GIS software. A shape file was provided by the National Transport Authority (NTA) which contained all cycling facilities in the Dublin network and included information on the facility type and direction. Using the ArcMap GIS software, the closest cycling facility to every sampled data point could be found. In order to allow for possible inaccuracies in the GPS coordinates, a search radius of 20m was used. This value was chosen after testing several values and checking for clear errors. If a cycling facility was found in the search radius of a sampling point, which allowed travel in the same direction of travel as the cyclist at the sampling point, it was assumed that the cyclist was using the facility. There may have been some instances where a cyclist cycled alongside a facility without using it but, since the cyclists were all very familiar with their routes, this would be expected to be uncommon.

The NTA also provided vehicle network specification files for the Greater Dublin Area Transport Model. These files included the spatial coordinates of each junction in the network and the details of the links joining the nodes. The spatial information was used to create a shape file in ArcMap. However, since only the end points of each link were specified, curved links in the actual network were approximated by straight lines in the shape file. Some minor links were also not included in the model. The closest vehicle link to each data point was found using the ArcMap GIS software with a search radius of 50m. This larger search radius was used in order to allow for the aforementioned inaccuracies in the shape file. The NTA also provided hourly traffic volume estimates produced by the model for each link during the peak period. The traffic volume estimates were available for three 1-hour periods: 7-8am, 8-9am and 9-10am. Where traffic volume estimates were required for other time periods, the estimates were corrected to the appropriate time period using the expansion factors of the National Road Authority (National Roads Authority, 2012). For each data point where a vehicle link was found in the search radius, the Traffic Volume variable was given the value of the estimated traffic volume on that link for the appropriate time period. For two-way links, the sum of the estimated traffic volumes in both directions was used.

6.3.2 Description of dataset

Sampling was carried out during a total of 47 trips giving 38,544 observations over approximately 22 hours of cycling. The size of the dataset is comparable to other studies of cyclist multi-pollutant exposure. For example, Bigazzi and Figliozzi (2015b) recorded 20 hours of exposure to VOCs and 24 hours of exposure to CO. Table 6.5 shows descriptive statistics for the

sampled dataset, categorised by the type of cycling facility. Equipment malfunctions occurred on some trips so that the number of observations was not the same for each exposure variable. As shown in Table 6.6, there were significant correlations between some of the observed variables. CO and NO_x were the most highly correlated air pollutants. Noise was more correlated with NO_x than any other pollutant, similarly to previous studies (Chowdhury et al., 2015; Davies and Van Kamp, 2012). As expected, temperature was inversely related to RH. CO and $PM_{2.5}$ were both positively correlated with temperature (and inversely correlated with RH). Speed, HR and Noise were correlated with one another. The correlation between HR and Speed is easily explained as greater exertion is generally required to cycle at higher speeds. The correlation between these variables and Noise is less obvious. It may be that the noise produced by the bicycle itself was louder during faster cycling. It may also be that loud events such as overtaking cars caused temporary increases in heart rate due to the cyclist's perception of risk. There were only moderate correlations between the air pollution exposures and Traffic Volume. This is likely because the pollutant levels were significantly influenced by many other factors such as time of day, facility type and density of other nearby roads.

The distributions of the recorded pollution exposure variables, CO concentration (ppb), NO_x Concentration (ppb), Noise (dBA) and $PM_{2.5}$ Concentration ($\mu g/m^3$) are shown in Table 6.5. Only the noise data appears to conform to a normal distribution; the air pollutant data appear to be closer to log-normal distributions. In order to examine the spatial variability of the data, maps were produced using ArcScene. All recorded data for CO, NO_x, Noise and $PM_{2.5}$ are displayed in Figure 6.7, Figure 6.8, Figure 6.9 and Figure 6.10 respectively. Clearly, CO and NO_x concentrations were much higher in the city centre than outside, as would be expected due to the higher traffic density and taller buildings. The Noise data also show relatively high values in the city centre but the pattern is not as clear. This is also to be expected as noise pollution disperses much more quickly than air pollution. Therefore, the level of noise produced by sources in the immediate vicinity to the cyclist (such as road traffic on the same road) are much more important than the density of other sources in the wider neighbourhood. The $PM_{2.5}$ data do not show any clear spatial patterns. It may be that the variability in $PM_{2.5}$ concentrations was more influenced by other factors such as time of day and proximity to traffic. However, it was noted in Chapter 5 that the $PM_{2.5}$ sensor was not validated to a high degree of accuracy and so the data may not be very accurate.

Table 6.5 Summary of data collected by facility type in full scale exposure study

	No Facility			Separated Cycle Lane			Bus Lane			Adjacent Cycle Lane		
	N	Mean	StDev	N	Mean	StDev	N	Mean	StDev	N	Mean	StDev
CO Concentration (ppb)	18356	1018.1	322.7	5371	1013.0	237.7	4495	1176.7	378.4	9923	1079.5	357.7
NOx Concentration (ppb)	18507	84.0	77.4	5384	81.6	50.3	4529	136.5	96.7	10124	115.8	96.2
Noise (dBA)	13248	66.9	5.8	3618	68.5	6.7	3311	69.0	5.0	7694	69.5	5.1
$PM_{2.5}$ Concentration ($\mu g/m^3$)	14843	4.56	4.83	4832	6.07	4.60	4252	4.46	3.62	8734	4.61	3.57
Heart Rate (bpm)	18262	126.2	33.2	5257	139.2	22.2	4313	131.3	33.7	9973	133.8	27.0
Cycle Speed (knots)	18506	8.24	5.63	5384	11.63	5.24	4529	8.88	5.55	10124	9.49	5.39
CO Intake (µg)	18111	1.76	1.24	5244	2.15	1.04	4279	2.27	1.54	9772	2.10	1.36
NOx Intake (µg)	18262	0.24	0.24	5257	0.28	0.21	4313	0.42	0.37	9973	0.35	0.28
$PM_{2.5}$ Intake (µg)	14610	0.01	0.01	4705	0.01	0.01	4036	0.01	0.01	8593	0.01	0.01
Traffic Volume (veh/hr)	18507	771.4	806.2	5384	1286.5	1163.5	4529	961.4	651.6	10124	941.8	590.3
Temperature (°C)	18507	12.5	4.3	5384	12.7	2.6	4529	12.4	4.2	10124	11.6	3.9
Relative Humidity (%)	18507	75.1	13.8	5384	77.1	10.9	4529	74.6	15.2	10124	73.4	13.0
Wind Speed (knots)	18507	10.28	4.65	5384	9.57	2.54	4529	9.51	3.54	10124	10.72	5.14

Table 6.6 Correlations between the observed data in the full scale exposure study

	CO Conc	NO_x Conc	Noise	$PM_{2.5}$	HR	Speed	CO Intake	NO_x Intake	$PM_{2.5}$ Intake	Traffic Volume	Temp	RH	Wind
CO Concentration (ppb)	1.00	0.38	0.10	0.08	-0.02	-0.06	0.52	0.31	0.07	0.11	0.37	-0.33	-0.06
NO_x Concentration (ppb)	0.38	1.00	0.20	0.04	-0.04	0.01	0.14	0.73	-0.02	0.08	0.14	-0.16	-0.02
Noise (dBA)	0.10	0.20	1.00	0.16	0.14	0.23	0.18	0.25	0.22	0.18	0.00	0.02	0.10
$PM_{2.5}$ Concentration ($\mu g/m^3$)	0.08	0.04	0.16	1.00	0.11	0.09	0.14	0.09	0.79	0.11	0.24	-0.07	-0.07
Heart Rate (bpm)	-0.02	-0.04	0.14	0.11	1.00	0.36	0.70	0.45	0.47	0.00	0.02	-0.01	-0.17
Cycle Speed (knots)	-0.06	0.01	0.23	0.09	0.36	1.00	0.24	0.19	0.25	0.07	0.04	0.05	-0.09
CO Intake (µg)	0.52	0.14	0.18	0.14	0.70	0.24	1.00	0.58	0.53	0.11	0.17	-0.12	-0.14
NOx Intake (µg)	0.31	0.73	0.25	0.09	0.45	0.19	0.58	1.00	0.30	0.10	0.04	-0.07	-0.10
$PM_{2.5}$ Intake (µg)	0.07	-0.02	0.22	0.79	0.47	0.25	0.53	0.30	1.00	0.15	0.20	0.00	-0.15
Traffic Volume (veh/hr)	0.11	0.08	0.18	0.11	0.00	0.07	0.11	0.10	0.15	1.00	0.05	-0.05	0.03
Temperature (degC)	0.37	0.14	0.00	0.24	0.02	0.04	0.17	0.04	0.20	0.05	1.00	-0.58	-0.17
Relative Humidity (%)	-0.33	-0.16	0.02	-0.07	-0.01	0.05	-0.12	-0.07	0.00	-0.05	-0.58	1.00	-0.12
Wind Speed (knots)	-0.06	-0.02	0.10	-0.07	-0.17	-0.09	-0.14	-0.10	-0.15	0.03	-0.17	-0.12	1.00

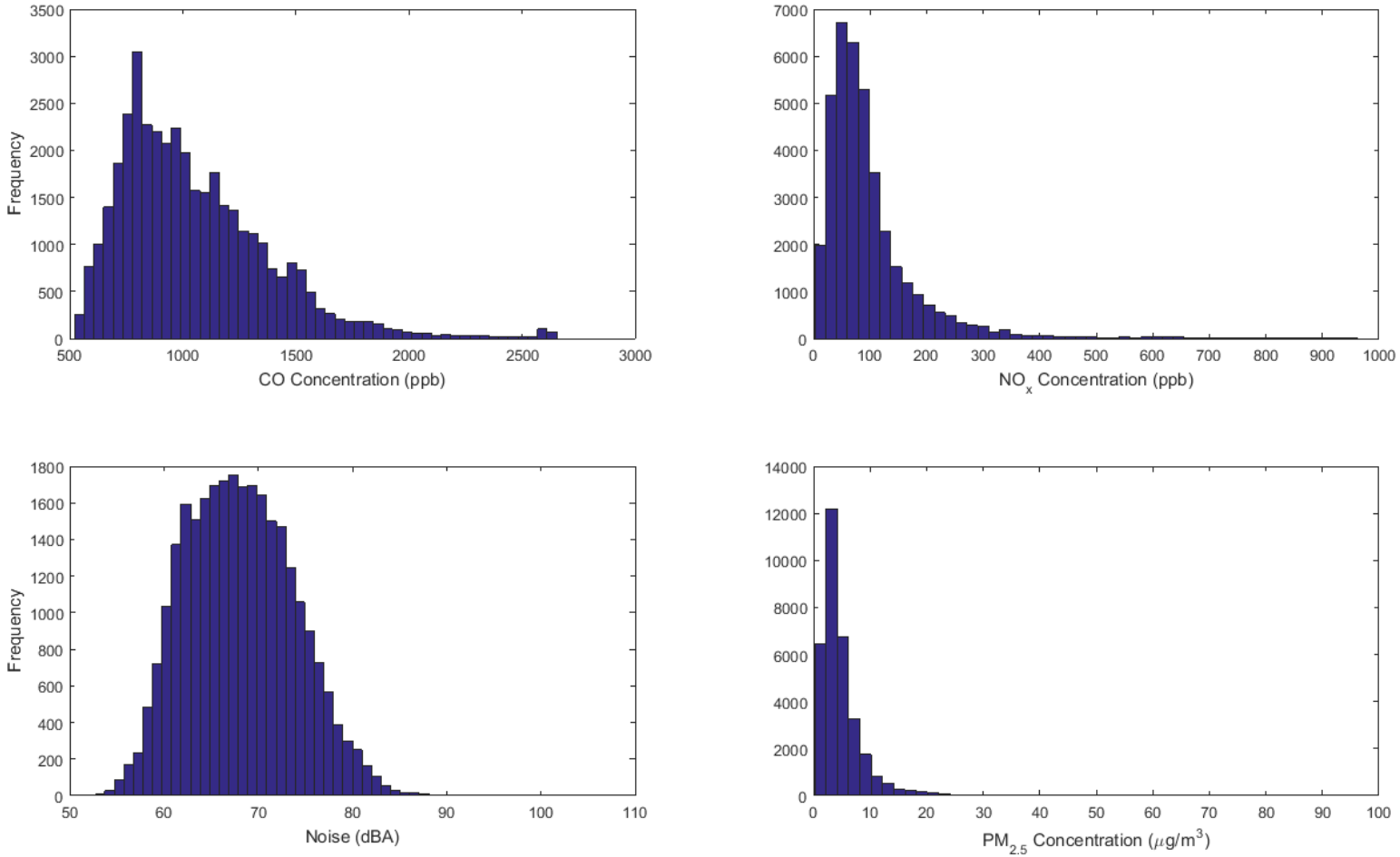

Figure 6.6 Distributions of recorded pollution exposures in full scale study

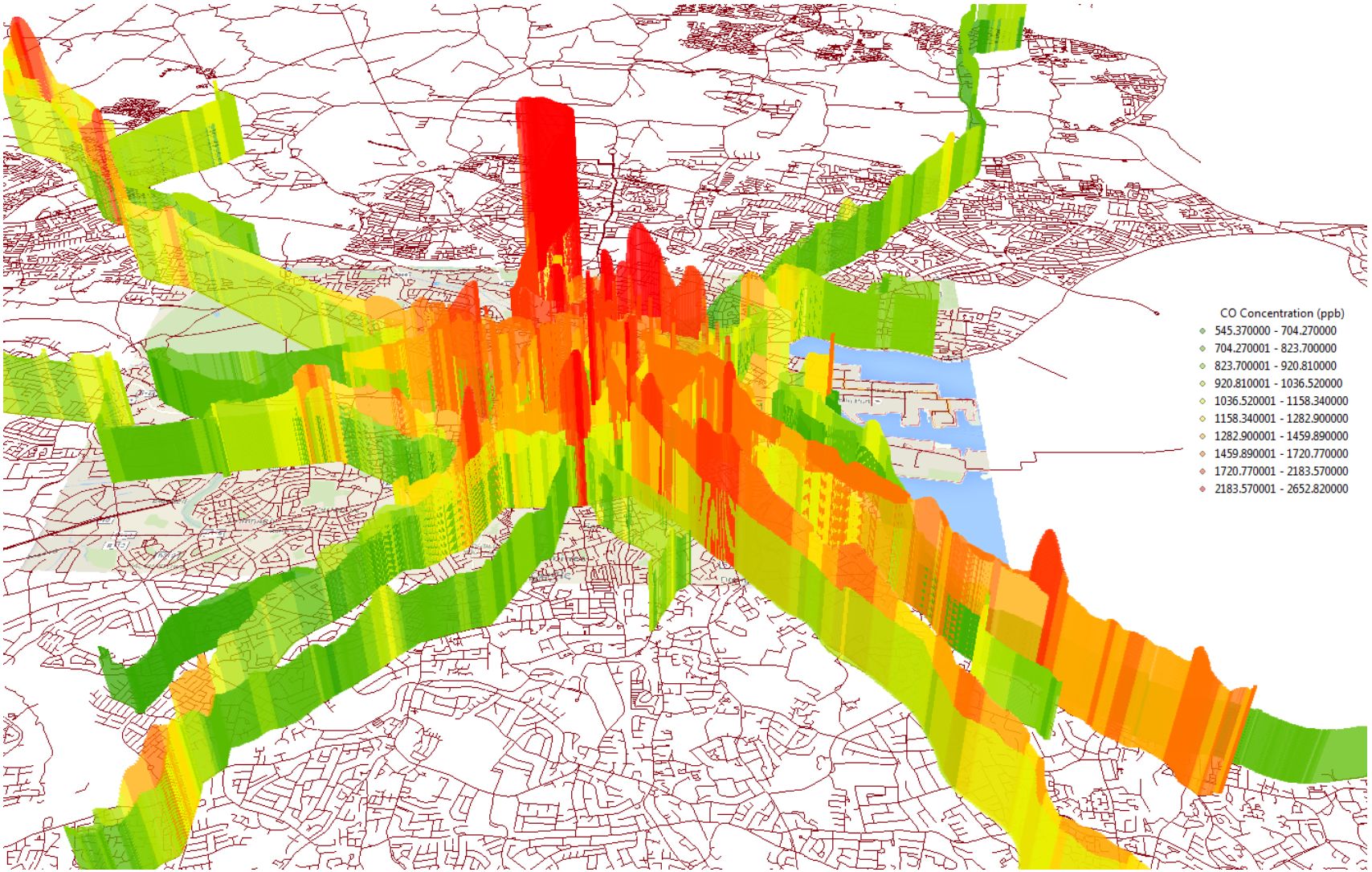

Figure 6.7 All CO concentrations measured in full scale exposure study

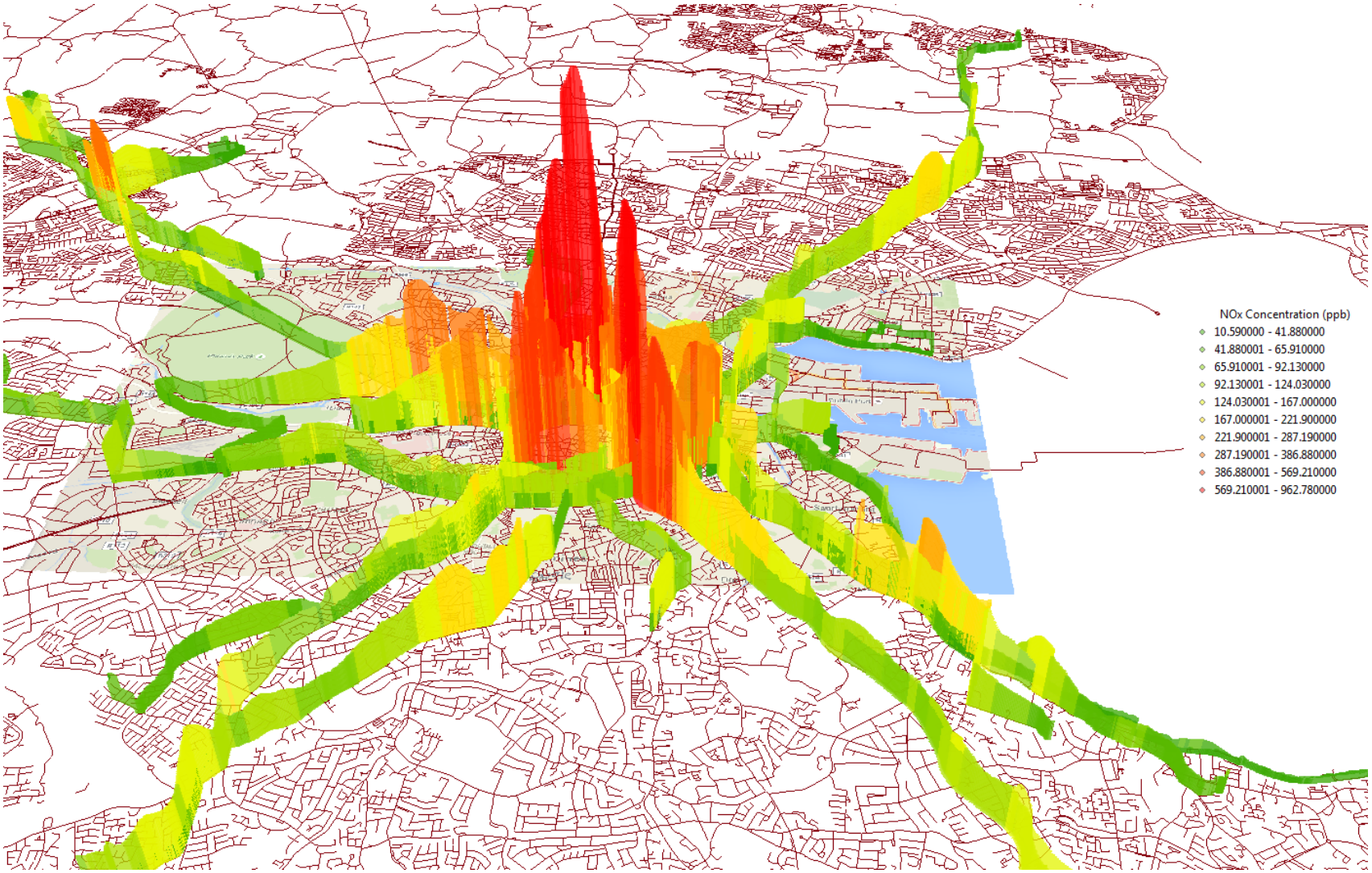

Figure 6.8 All NO_x concentrations measured in full scale exposure study

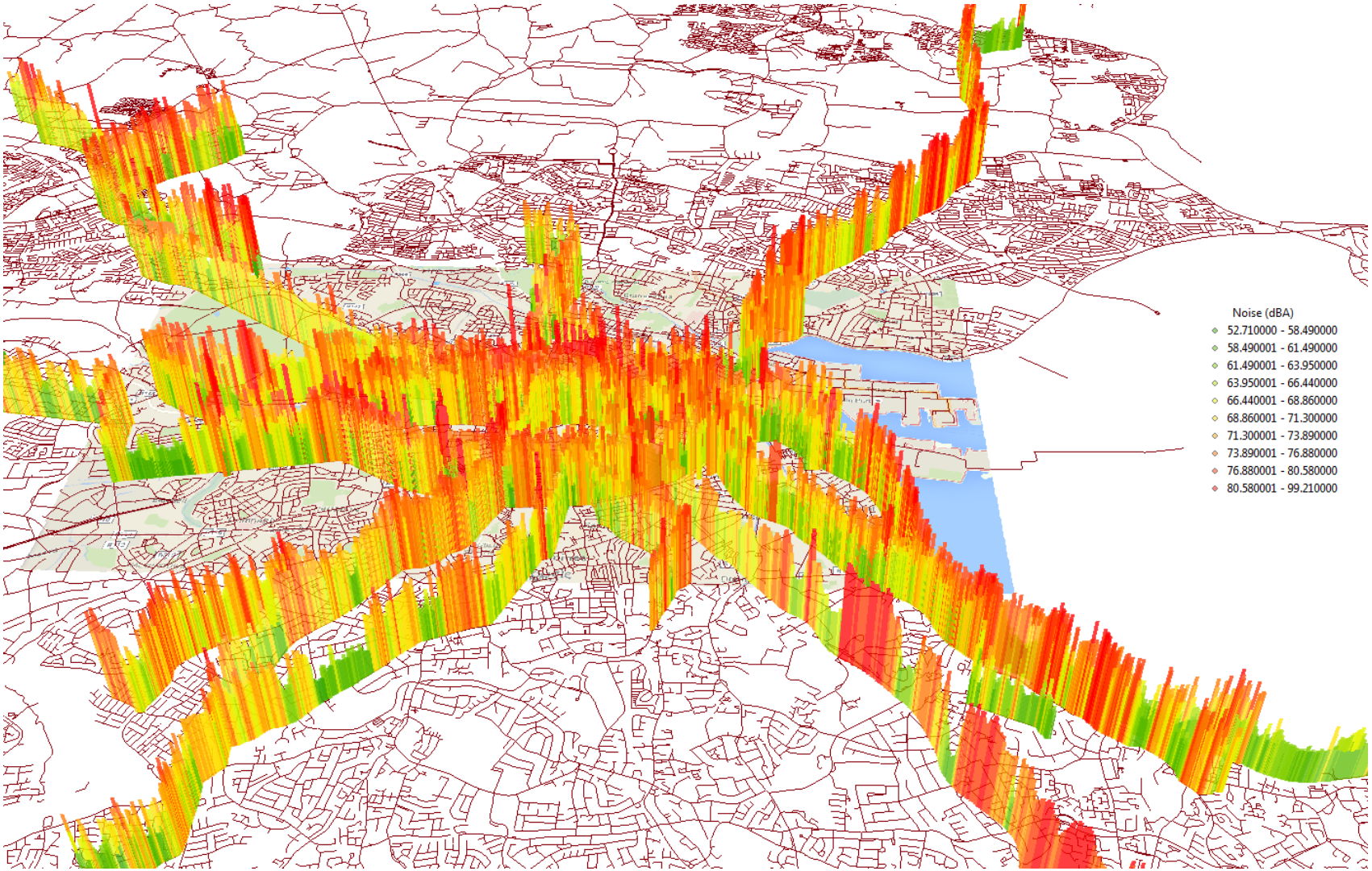

Figure 6.9 All noise levels measured in full scale exposure study

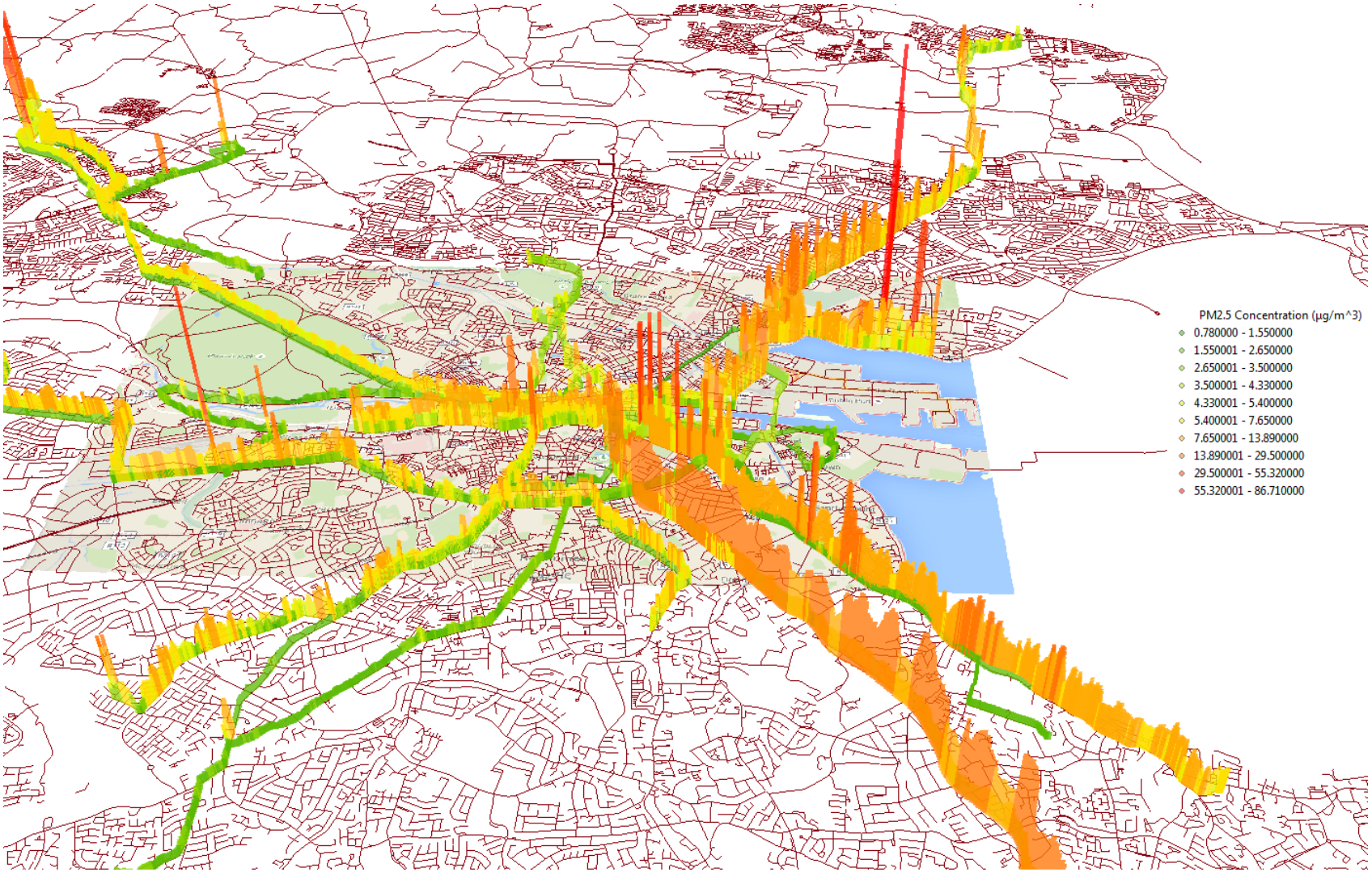

Figure 6.10 All $PM_{2.5}$ concentrations measured in full scale exposure study

6.3.3 Results of Analysis

Similarly to the pilot study, the exposures of the cyclist were analysed using linear mixed models. The 2 second intervals at which the BEE node logged measurements were analysed without further aggregation. Models were developed for seven exposure variables: log(CO Concentration), log(NO_x Concentration), Noise, log($PM_{2.5}$ Concentration), log(Inhaled CO), log(Inhaled NO_x) and log(Inhaled $PM_{2.5}$). Logged versions of the air pollution exposure variables were used because they were closer to normally distributed than the raw variables. Noise was not log transformed as the dBA scale is itself a logged scale and the distribution was already reasonably close to normal. The explanatory variables considered were Traffic Volume, Facility, Temperature, RH and Wind Speed. Log transformed Traffic Volume was also considered as an alternative. For the inhalation models, an additional variable, Cycling Speed (knots), was also considered. The model results are shown in Table 6.7 to Table 6.13.

Table 6.7 Mixed Effects Model for log(CO Concentration)

	Variable	Estimate	Standard Error	p-Value
Fixed Effects	(Intercept)	7.460	0.100	0
	log(Hourly Traffic)	0.003	3.37E-04	0
	Facility: Separated*	-0.037	0.002	0
	Facility: Bus Lane*	0.054	0.002	0
	Facility: Road Marking*	0.031	0.002	0
	Temperature	-0.016	0.004	0
	RH	-0.004	0.001	0
	Wind	-0.003	0.002	0.0497
Random Effects	**Variable**	**Standard Deviation**		
	(Intercept)	0.286		
	Residual	0.140		

* Relative to Facility: No Facility

Table 6.8 Mixed Effects Model for log(NO_x Concentration)

	Variable	Estimate	Standard Error	p-Value
Fixed Effects	(Intercept)	4.728	0.106	0
	log(Hourly Traffic)	0.027	0.001	0
	Facility: Separated*	-0.147	0.009	0
	Facility: Bus Lane*	0.319	0.009	0
	Facility: Road Marking*	0.243	0.007	0
	Temperature	-	-	-
	RH	-0.008	0.001	0
	Wind	-	-	-
Random Effects	**Variable**	**Standard Deviation**		
	(Intercept)	0.508		
	Residual	0.532		

* Relative to Facility: No Facility

Table 6.9 Mixed Effects Model for Noise

	Variable	Estimate	Standard Error	p-Value
Fixed Effects	(Intercept)	62.662	1.003	0
	Hourly Traffic	0.001	4.54E-05	0
	Facility: Separated*	0.769	0.112	0
	Facility: Bus Lane*	1.558	0.109	0
	Facility: Road Marking*	2.293	0.084	0
	Temperature	-	-	-
	RH	0.028	0.010	0.0079
	Wind	0.143	0.048	0.0029
Random Effects	**Variable**	**Standard Deviation**		
	(Intercept)	1.667		
	Residual	5.381		

Table 6.10 Mixed Effects Model for log($PM_{2.5}$ Concentration)

	Variable	Estimate	Standard Error	p-Value
Fixed Effects	(Intercept)	1.334	0.269	0
	log(Hourly Traffic)	0.002	0.001	0.0451
	Facility: Separated*	-0.016	0.007	0.0261
	Facility: Bus Lane*	-0.013	0.007	0.0706
	Facility: Road Marking*	-0.029	0.006	0
	Temperature	0.062	0.010	0
	RH	-0.011	0.002	0
	Wind	-	-	-
Random Effects	**Variable**	**Standard Deviation**		
	(Intercept)	0.4809742		
	Residual	0.3908196		

Table 6.11 Mixed Effects Model for log(CO Intake)

	Variable	Estimate	Standard Error	p-Value
Fixed Effects	(Intercept)	0.953	0.267	0.0004
	Hourly Traffic	1.04E-05	2.83E-06	0.0002
	Facility: Separated	0.063	0.007	0
	Facility: Bus Lane	0.025	0.007	0.0003
	Facility: Road Marking	0.122	0.006	0
	Cycle Speed	0.031	0.000	0
	Temperature	-0.042	0.010	0
	RH	-0.0048433	0.00181731	0.0077
	Wind	-	-	-
Random Effects	**Variable**	**Standard Deviation**		
	(Intercept)	0.673		
	Residual	0.392		

Table 6.12 Mixed Effects Model for log(NO_x Intake)

	Variable	Estimate	Standard Error	p-Value
Fixed Effects	(Intercept)	-1.401	0.032	0
	Hourly Traffic	0.000	0.000	0
	Facility: Separated	0.152	0.015	0
	Facility: Bus Lane	0.612	0.016	0
	Facility: Road Marking	0.506	0.012	0
	Cycle Speed	0.048	0.001	0
	Temperature	-	-	-
	RH	-0.010	3.59E-04	0
	Wind	-0.024	0.001	0

Table 6.13 Mixed Effects Model for log($PM_{2.5}$ Intake)

	Variable	Estimate	Standard Error	p-Value
Fixed Effects	(Intercept)	-4.854	0.161	0
	Hourly Traffic	0.000	0.000	0
	Facility: Separated	0.094	0.010	0
	Facility: Bus Lane	-0.041	0.010	0
	Facility: Road Marking	0.055	0.008	0
	Cycle Speed	0.030	0.001	0
	Temperature	-	-	-
	RH	-0.011	0.001	0
	Wind	-	-	-
Random Effects	**Variable**	**Standard Deviation**		
	(Intercept)	0.865		
	Residual	0.533		

As expected, Hourly Traffic was positively associated with all exposure variables. For the three pollutant concentration variables, logged traffic was included but for Noise and the three pollutant intake variables, unlogged Traffic was more appropriate based on the BIC of the models. For the models with logged dependent variables and logged traffic, the effect on the exposure variable of increasing traffic by x% could be estimated by taking (1+x) to the power of the coefficient of log(Traffic). Based on the models, it can therefore be estimated that increasing the traffic on a link by 10% increases NO_x concentrations on that link by 0.3%, CO concentrations by 0.03% and PM2.5 concentrations by 0.02%. For the models with logged dependent variable and unlogged traffic, the effect of increasing traffic by x vehicles/hour can be found by

exponentiating the coefficient of Traffic multiplied by x. Therefore, based on the models, it is estimated that adding 100 additional vehicles/hour to a link increases NO_x intake by 1%, CO intake by 0.1% and $PM_{2.5}$ intake by 0.2%. For the Noise model where both the dependent variable and traffic variable are unlogged, the effect of adding 100 additional vehicles/hour to a link is estimated to increase noise exposure by 0.1dBA.

The presence of cycling facilities also influenced all exposure variables. Concentrations of CO were reduced by 4% and concentrations of NO_x were reduced by 14% on separated facilities relative to no facility. On bus lanes, concentrations of CO were increased by 5% and concentrations of NO_x were increased by 37%. These results are consistent with the results of the pilot study. On adjacent lanes, CO concentrations were increased by 3% and and NO_x concentrations were increased by 27%. This is in contrast to the results of the pilot study which showed that on-road cycle lanes significantly reduced exposure concentrations of NO_x. However, in the pilot study, the observations on adjacent lanes were restricted to a single short segment on one route. This segment was adjacent to the river Liffey as it widens near to Dublin port and so it may have been the location rather than the facility type which caused the lower exposure concentrations on adjacent cycle lanes in the pilot study. The intake dose per sampling period of both CO and NO_x was lowest when no cycling facility was present. Even cycling on segregated lanes increased the rate of intake of the gaseous pollutants compared to no facility. This is likely because, as shown in Table 6.6, when no cycling facility was present, cycling speeds and therefore heart rates and breathing rates were lowest. The lower speeds and exertion can be expected as the cyclist must navigate through motor vehicle traffic. It should be noted that due to the lower cycling speed when cycling on no facility, the cyclist may spend a longer time in traffic and ultimately have a higher intake. The total intakes would also depend on the lengths of the respective routes however. Bus lanes were associated with the greatest increase in NOx intake and roadside lanes were associated with the greatest increase in CO intake. Noise levels were higher for all facility types than for no facility. This is surprising as separated lanes, at least, would be expected to have lower noise levels due to the increased distance from traffic. However, it may be that motor vehicles were more likely to overtake a cyclist in a cycle lane than one sharing the road. Overtaking cars would be expected to significantly increase the noise exposure of the cyclists. $PM_{2.5}$ concentrations were lower on separated lanes and adjacent lanes compared to no facility. Bus lanes were also associated with a decrease in $PM_{2.5}$ concentrations compared to no facility but the effect was not statistically significant. $PM_{2.5}$ intakes were higher on roadside lanes and segregated lanes compared to no facility and this can again be explained by the cycling speeds and breathing rates. However, $PM_{2.5}$ intake rates were lower for bus lanes

than for no facility. Cycling speed was positively associated with intake rates of all pollutant due to the correlation between heart rate and breathing rate.

All weather variables which were considered had some influence on the exposure variables. RH was negatively associated with exposure concentrations and intakes of all air pollutants. RH was also positively associated with noise exposure. This is as expected because atmospheric attenuation of sound is influenced by humidity. Temperature was negatively associated with concentrations and intakes of CO and positively associated with concentrations of $PM_{2.5}$. Wind speed was negatively associated with CO concentrations and with NO_x intake. This is inconsistent with the results of the pilot study but consistent with the results of many other studies which have shown that wind decreases pollution levels through increased dispersion (Kaur et al., 2007) . The results of the pilot study may have been biased by the weather conditions which occurred during the small number of sampling days. Wind was also positively associated with Noise. This is to be expected as the wind shield used with the microphone could not eliminate 100% of wind noise.

Both fixed and random intercept terms were included for all models apart from the NO_x Intake model. For this model, when the random intercept was introduced, the intercept term became non-significant. For the rest of the models, the standard deviations of the random intercept terms are sufficiently large to indicate that there were unobserved differences in the background pollution levels between the different trips. Unfortunately, background concentrations were not available to include in the models and so it is unclear whether or not the random intercept terms would still be significant if background concentrations were included as explanatory variables.

6.4 Conclusions

In this chapter, the environmental exposures of cyclists in Dublin were studied using a custom environmental sensing platform. Two studies were carried out, a pilot study and a full scale study, and some but not all of the findings were consistent across both studies. The inconsistencies between the two studies can be attributed to issues with the sample size and choice of routes in the pilot study.

This chapter built on previous studies of in-travel pollution exposure in a number of ways. Firstly, measurements of a number of different exposures were measured simultaneously, including NO_x concentrations, which had been neglected in the studies to date. This work also showed that time-resolved link traffic volumes are positively associated with all the negative

environmental exposures experienced by cyclists on those links. Although some previous studies have shown similar associations, most of these studies were based on aggregate measures such as AADT. As discussed in Chapter 2, the few studies which considered temporally and spatially resolved traffic volumes were inconsistent in their findings in this regard. In the full scale study, participants cycled on their regular routes rather than a predesignated route. All previous studies which analysed the factors influencing cyclist exposures used predefined routes, except for Dons et al. (2013) where cycle facilities were not considered. Studying the influence of cycling facilities is easier to do using predefined routes as this avoids the difficulty of assigning facility types to measurements after they are recorded. However, in this study GPS measurements were combined with a GIS shape file of cycle facilities in the study area in order to assign facility types to recorded data without difficulty. In this way, it was found that cycling on separated cycling facilities can reduce the air pollution exposure concentrations to which cyclists are exposed. However, cycling on bus lanes or on roadside cycle lanes without segregation actually increases exposure to air pollution. Also, since cyclists tend to increase their speed and effort when using cycling facilities, their rate of intake of pollution with respect to time increases when using cycling facilities, even if they are segregated. However, this study does not consider pollution intake at a route level and it is possible that a route which includes segregated lanes will decrease total intake because the cyclist will cycle faster and spend less time in the polluted environment. If the use of a segregated facility does not significantly reduce travel time, it is likely to increase pollution intake. The levels of noise exposure were also higher on cycling facilities than on roads with no facilities.

Overall these findings suggest that cycling facilities, and particularly those without physical separation from traffic, do not provide as much protection against environmental exposures as previously thought. Multiple studies have found that in terms of cycling infrastructure, there is a hierarchy of cyclist preferences, with segregated facilities generally being preferred over on-road facilities (Buehler and Dill, 2016; Buehler and Pucher, 2012; Tilahun et al., 2007). This work has shown that segregated facilities also provide significantly greater protection from environmental exposures than other types of facilities. This strengthens the case for providing segregated cycling facilities whenever possible rather than roadside cycling facilities. The higher pollution exposures in bus lanes compared to on-road cycling may be an indication of the level of pollution produced by buses in Dublin city. However, in recent years, the fleet of Dublin Bus—the metro bus operator in Dublin city—has been upgraded significantly. The first buses to meet the Euro 6 standard were introduced to the fleet in 2014 and these now make up almost 30% of

the fleet (Dublin Bus, 2017). If the technology of buses in Dublin continues to be upgraded, the exposures experienced by cyclists in bus lanes may decrease significantly.

A number of limitations of these studies are noteworthy. Firstly, spatial and temporal autocorrelation of observations were not considered in this work and the existence of such autocorrelations could potentially have inflated the test statistics and increased the likelihood of type 1 errors. However, since almost all of the significant p-values were highly significant (<0.01), it is highly unlikely that non-significant associations would have been found had the observations been serially independent. Secondly, as discussed in Chapter 5, the accuracy of the $PM_{2.5}$ sensor used in this chapter was questionable and so, the results pertaining to this particular pollutant should be treated with caution. Since the pollution exposure models used in Chapters 3 and 4 were based on $PM_{2.5}$ exposure, the insights from this chapter can't be used directly to improve the accuracy of these models. However, it has been shown that there traffic volumes and presence of cycling facilities significantly influence intra-urban pollution exposures of cyclists and so, further exposure studies using more reliable $PM_{2.5}$ monitors are needed in order to improve studies of the benefits and risks of urban cycling.

Chapter 7: A Cycling Cost Function; development, validation and calibration

In Chapter 3, a framework was developed for quantifying the benefits and risks resulting from cycling where the amount of cycling taking place could be known or hypothesised. Chapters 4 and 5 analysed one particular risk of cycling—exposure to traffic-related air and noise pollution—in more detail in order to allow the risk to be quantified more accurately in this framework. However, as noted in Chapter 3, the usefulness of this framework is limited by the need for actual or hypothesised data on cycling. In many situations, for example, when considering building a new piece of cycling infrastructure, it would be more useful to predict the benefits and risks resulting from this decision. To enable this, it must be possible to estimate the change in cycling patterns that would result from a change in infrastructure. In the context of motor traffic modelling, similar predictions have been made for decades using macroscopic transport models. These models can be extended to other modes of transport but only if a cost function for that mode is available. As discussed in chapter 2, cycling has typically been ignored in transport models or else modelled using very simplistic models, often assuming that all cyclists take the shortest path with arbitrary average speeds (Subhani et al., 2013). In this chapter, a more realistic and useful cost function for cyclists will be developed and calibrated for the Dublin transport network.

Calibration of the cycling cost function will be carried out using the Inverse Combined Mode Choice and Traffic Assignment Problem (I-CMC-TAP). Before discussing the ITAP, however, it is necessary to describe the Combined Mode Choice and Traffic Assignment Problem (CMC-TAP). 0 will describe the CMC-TAP and 7.2 will propose a cycling cost function which can be used within this CMC-TAP formulation. Sections 7.3 and 7.4 will describe the proposed I-CMC-TAP and solution algorithm. Section 7.5 will present a numerical experiment which demonstrates the efficacy of the proposed I-CMC-TAP using a theoretical problem and section 7.6 will report the calibration of the proposed cost function with the ITAP using data from the Dublin city network. The notation used in the rest of the chapter is defined in Table 7.1 to Table 7.4 below.

Table 7.1 Notation: Travel modes

Notation	Definition
m	mode
a	auto mode
b	bus mode
c	bicycle mode

Table 7.2 Notation: Sets

Notation	Definition
S	set of all links in transport network
$\hat{S}$	set of links in S where flows are observed
W	set of O-D pairs
P_w^m	set of route alternatives between O-D pair w by mode m
M	set of possible modes in network
$\hat{M}$	set of modes for which flows are observed on links $s \in \hat{S}$

Table 7.3 Notation: Variables

Notation	Definition
h_p^m	flow of mode m on route p
q_w	travel demand between O-D pair w
$\boldsymbol{Q}$	vector of all O-D travel demands $q_w \forall w \in W$
q_w^m	travel demand for mode m between O-D pair w
$\boldsymbol{q}$	vector of all modal O-D demands $q_w^m \ \forall w \in W, m \in M$
t_s^m	travel time by mode m on link s
t_s^{m0}	free-flow travel time by mode m on link s
u_p^m	disutility of travel on route p by mode m
$r^{c,0}$	baseline modal bias factor associated with choosing bicycle as travel mode
σ	parameter which determines the scale of the impact of link congestion on cycling link cost
τ	parameter which determines the degree of nonlinearity of the relationship between link congestion and cycling link cost.
x_s^m	modelled flow of mode m on link s
x_s^{c-m}	modelled flow of mode m with which cyclists on link s interact
$\bar{x}_s^m$	observed flow of mode m on link s
λ_w^m	expected travel disutility by mode m between O-D pair w
λ_w	expected travel disutility between O-D pair w
$\boldsymbol{\lambda}$	vector of all dual variables $\lambda_w^m, \forall m \in M, w \in W$ and $\lambda_w, \forall w \in W$
PS_p^m	path size of path p by mode m

Table 7.4 Notation–constants

Notation	Definition
K_s	total capacity of link s in PCU.
$\boldsymbol{K}$	vector of total link capacities $K_s, \forall s \in S$
K_s^c	capacity of segregated link *s* for mode *m*.
q_w^0	potential (latent) travel demand between O-D pair w
$\overline{v_s^m}$	average free-flow speed of mode *m* on link *s*.
$\bar{v}$	vector of all free-flow speeds $\overline{v_s^m}, \forall s \in S, m \in M$
d_s^m	length of link *s* for mode *m*
$\boldsymbol{d}$	vector of link lengths $d_s^m, \forall s \in S, m \in M$
Γ_p	length of route p
Γ_s	length of link s
α_t	value of travel time
θ_1, θ_2	Logit model parameters representing the importance of travel disutility in route and mode choices respectively
η	parameter that reflects O-D demand sensitivity to O-D travel disutility
ρ, β	parameters that reflect the importance of traffic volumes to travel times (in the BPR function)
$\boldsymbol{\Phi}$	Vector of calibration parameters in the ITAP
ψ	step-size for MPEC descent-type solution algorithm
ι	tolerance for convergence of MPEC solution algorithm
δ_{sp}	indicator variable; if link s is on route p $\delta_{sp} = 1$, 0 otherwise
Δ_{sp}	link-path incidence matrix; entry in row *s*, column *p* will be 1 if link s is on route *p*, 0 otherwise
Δ_{wm-p}	OD mode-path incidence matrix; entry in row *wm*, column *p* will be 1 if path *p* is associated with OD-mode pair *wm*, 0 otherwise.
Δ_{w-mw}	OD-OD mode incidence matrix; entry in row *w*, column *wm* will be 1 if O-D mode pair *mw* is associated with OD-mode pair *w*, 0 otherwise.

7.1 The Combined Mode Choice and Traffic Assignment Problem

The traffic assignment problem is concerned with finding the equilibrium traffic flows over a given urban transportation network. The basic formulation is based on the behavioural assumption that all users of the transport network aim to minimise their own travel cost. There are, however, several common variations and extensions to this basic formulation. Those which are relevant to this chapter will briefly be described below.

There are two main conditions which are alternately used in the literature to describe the route choice behaviour in a transport network: deterministic user equilibrium (DUE) and stochastic user equilibrium (SUE). DUE is the condition which corresponds to Wardrops's First Principal which states "The journey times on all routes actually used are equal, and less than those which

would be experienced by a single vehicle on any unused route." (Patriksson, 1994). A way to relax the DUE condition and to make it more realistic is to allow some portion of O-D flow to be "dispersed" to higher cost routes. This can be achieved by allowing route flows between each O-D to be allocated to different routes according to a logit or probit choice model. In the case of the logit model, the logit parameter can be thought of as a measure of user knowledge about route costs or as an inverse measure of the dispersion. The simple logit model for route choice can be expressed as follows:

$$h_p{}^m = q_w^m \frac{exp\left(-\theta_1 u_p^m\right)}{\sum_{q \in P_w^m} exp\left(-\theta_1 u_q^m\right)}, \forall m \in M,\ p \in P_w^m,\ w \in W \qquad \text{Eq. (7.1)}$$

A limitation of the simple logit model for route choice is that it cannot account for similarities between alternate routes. Several extensions of the logit model have been developed to address this limitation. The Path-Size logit model uses the notion of "size" from the theory of aggregate alternatives. The model is formed by adding the log of the path size to the path utility (Bekhor et al., 2006):

$$h_p^m = q_w^m \frac{exp(-\theta_1(u_p^m) + ln(PS_p{}^m))}{\sum_{q \in P_w^m} exp(-\theta_1(u_q^m) + ln(PS_p{}^m))}, \forall m \in M,\ p \in P_w^m,\ w \in W \qquad \text{Eq. (7.2)}$$

Where $PS_p{}^m$, the path size of path *p* by mode *m* is defined as:

$$PS_p{}^m = \sum_{s \in S} \delta_{sp} \left(\frac{\Gamma_s}{\Gamma_p}\right)\left(\frac{1}{\sum_{q \in P_w^m} \delta_{sq}}\right) \qquad \text{Eq. (7.3)}$$

The TAP can be extended to the CMC-TAP which also considers mode choice. The choice of mode can be modelled by a logit model:

$$q_w^m = q_w \frac{exp(-\theta_2 \lambda_w^m)}{\sum_{n \in M} exp(-\theta_2 \lambda_w^n)}, \forall m \in M, w \in W \qquad \text{Eq. (7.4)}$$

Where

$$\lambda_w^m = \frac{-1}{\theta_1} ln(\sum_{p \in P_w^m} exp\left(-\theta_1\left(u_p^m\right) + ln\left(PS_p{}^m\right)\right)), \forall m \in M, w \in W \qquad \text{Eq. (7.5)}$$

The CMC-TAP may also allow the demand for travel between each origin-destination (O-D) pair to vary as a decreasing function of the total expected travel disutility between the O-D pair. One

such function is given below, where η is a parameter which would need to be calibrated by survey data:

$$q_w = q_w{}^0 \exp\left(-\eta \lambda_w\right), \forall\, w \in W \qquad \text{Eq. (7.6)}$$

Where

$$\lambda_w = \frac{-1}{\theta_2} ln\left(\sum_{m \in M} exp\left(-\theta_2 \lambda_w^m\right)\right), \forall w \in W \qquad \text{Eq. (7.7)}$$

The solution to the CMC-TAP with path-size logit-based route choice, logit-based mode choice and elastic demand is, therefore, the flow pattern which satisfies eqt. Eq. (7.2) to Eq. (7.7).

7.2 The Disutility of Cycling (DOC) Function

In Eq. (7.2) and Eq. (7.5), the route disutility, $u_p^m(\boldsymbol{x})$ must be calculated using a cost function which estimates the cost of travel by mode m on route p based on the network flow pattern $\boldsymbol{x}$. An example of a commonly used cost function for motor vehicles is the Bureau of Public Roads (BPR) function which estimates the congested travel time for motor vehicles on a link based on the total flow of motor vehicles on that link (US Department of Commerce and Bureau of Public Roads, 1964):

$$t_s(x_s) = t_s^0 \left(1 + \rho \left(\frac{x_s}{K_s}\right)^\beta\right) \qquad \text{Eq. (7.8)}$$

Where t_s and t_s^0 are the congested and free-flow travel time for motor vehicles on link *s*, x_s is the total motor vehicle traffic on link *s* and K_s is the capacity for motor vehicles on link *s*. ρ and β are parameters of the function whose values may vary by application. The travel cost for a link can then be calculated by multiplying the travel time by the Value of Time (VoT). The travel cost for a route can be found by summing the individual travel costs for each link on the route and adding any fixed costs such as tolls or operating costs. The BPR function is parameterised by two parameters, ρ and β which can be adjusted to suit a particular transport network.

No suitable cost function exists for cycling. In this chapter, we propose such a cycling cost function. Based on the existing literature on link cost functions and route preferences of cyclists discussed in Chapter 2, it was concluded that a cost function for cyclists should have the following characteristics:

1. It should allow the type of cycling facility to influence disutility, independently of any effect on travel time or distance (Winters and Teschke, 2010).

2. The link cost should be monotonically increasing with bicycle traffic volumes (TRB, 2000).

3. Unless the link is a fully segregated cycle lane, the link cost should be monotonically increasing with volume of motor vehicle traffic with which the cyclist interacts on the corresponding auto and bus links (Sener et al., 2009).

4. In order to be widely useful, the function should exclude parameters which are unlikely to be readily available to transport authorities.

A new cost function for cycling—the Disutility of Cycling (DOC) function—is proposed as follows:

$$c_s^c = \alpha_t * \frac{d_s^c}{\bar{v}_s^c} * r_s^c \qquad \text{Eq. (7.9)}$$

Where c_s^c is the cost of cycling on link s, d_s^c is the length of bicycle link s, $\bar{v}_s^c$ is the average cycling speed on link s and r_s^c is the discomfort factor associated with cycling on link s. It can be seen from equation 9 that if, for example r_s^c were equal to 1, there would be no discomfort cost and if r_s^c were equal to 2, the discomfort cost would constitute half of the total link cost. The discomfort factor can be calculated as follows:

$$r_s^c = r^{c,0} + \sigma \left(\frac{x_s^{c-a} + x_s^{c-b} + x_s^c}{K_s} \right)^{\tau} \qquad \text{Eq. (7.10)}$$

Where $r^{c,0}$ is a baseline modal bias factor associated with cycling, σ is a parameter which determines the scale of the impact of link congestion of cycling link cost and τ is a parameter which determines the degree of nonlinearity of the relationship between link congestion and cycling link cost. x_s^{c-a} and x_s^{c-b} are the flows of private cars and buses respectively with which cyclists on link s interact in passenger car units (PCU). x_s^c is the flow of cyclists on link s and K_s is the capacity of link s in PCU. The travel cost, u_p^c, of travel by bicycle on a route p can be calculated by simply summing the individual travel costs for each link on the route. This cost function meets each of the requirements specified above. Since the cycling link cost is influenced only by other vehicles with which the cyclist interacts, the separation from traffic afforded by

separated cycle lanes will influence link costs. Requirement 1 is therefore satisfied. The link cost function is increasing with cyclist volumes on the link so requirement 2 is satisfied. On links which are shared with motor vehicle traffic, cyclist link cost is increasing with car and bus volumes so requirement 3 is satisfied. Finally, the only input data required for the function are the VoT, traffic volumes of other modes—which would be solved for simultaneously in a multi-modal traffic model—and the link capacities which would be readily available to transport planners and researchers. An additional attractive feature of this function is its similarity to the BPR function.

The parameters $r^{c,0}$, σ and τ of Eq. (7.10) must be calibrated before the function can be used in practice. As discussed in Chapter 2, there are two main approaches in the literature for calibrating the parameters of link cost functions (Garcia-Rodenas and Verastegui-Rayo, 2013). The first approach is calibration based on link data whereby links are considered in isolation in order to determine their speed-flow relationships. The second approach is calibration based on network data using the ITAP. The network-based approach is more appropriate for the current problem. This is because estimating parameters based on link data requires that the costs can be observed directly. This is not a problem for traditional link cost functions for motor vehicles as the cost to be observed is simply the travel time. However, since the DOC function of Eq. (7.9) and Eq. (7.10) assumes that cycling link costs are influenced by an unobservable discomfort factor, the link-based method cannot be used. Conversely, in the network-based approach, there is no need to directly observe the travel costs on the links; it is only necessary to observe the network utilisation at a macroscopic level.

7.3 The Inverse Combined Mode Choice and Traffic Assignment Problem (I-CMC-TAP)

Whereas the CMC-TAP aims to find the network flow pattern resulting from a network model, given a set of assumptions and parameters, the I-CMC-TAP aims to find values of the network model parameters which lead to the best possible agreement between the modelled flows and a set of corresponding network observations. In this study, the network parameters to be estimated are the parameters of the DOC function and the network observations are observed link flows on a subset of links in the network. This I-CMC-TAP can be modelled as a Mathematical Programme with Equilibrium Constraints (MPEC). The general form of the MPEC will now be introduced and then an MPEC will be proposed to model an I-CMC-TAP for to calibrating the parameters of the DOC function.

The general form of a MPEC can be expressed as follows (Colson et al., 2007):

$$\begin{aligned} &min_{x,y} \quad F(x,y) \\ &s.t. \qquad (x,y) \in Z \quad and \quad y \in V(x) \end{aligned} \qquad \text{Eq. (7.11)}$$

Where $F(x,y)$ is the objective function, x and y are the decision variable and dependent variables respectively, $Z \subseteq \mathbb{R}^{n1+n2}$ is a non-empty closed set and $V(x)$ is the solution set of the following parameterised variational inequality (VI) defined over the closed convex set $C(x) \subset \mathbb{R}^{n2}$

$$y \in V(x) \quad \Leftrightarrow \quad y \in C(x) \quad and \quad (v-y)^T f(x,y) \geq 0 \quad \forall v \in C(x) \qquad \text{Eq. (7.12)}$$

The following MPEC is proposed to model the I-CMC-TAP in this study:

$$\begin{aligned} &min_{\phi} \quad \sum_{m \in \hat{M}} \sum_{s \in \hat{S}} \left(\bar{x}_s^m - x_s^m(\boldsymbol{\Phi}) \right)^2 \\ &s.t. \qquad x_s = \sum_{p \in P} h_p^m \delta_{sp}, \forall s \in S \\ &\boldsymbol{\Phi} \in \Omega_1, \quad \mathrm{h} \in V(\boldsymbol{\Phi}) \end{aligned} \qquad \text{Eq. (7.13)}$$

Where $\boldsymbol{\Phi} = \left[r^{c,0}, \sigma, \tau, \theta_2 \right]^T$ is the vector of network parameters to be calibrated, Ω_1 defines the constraints on the decision variable and $V(\boldsymbol{\Phi})$ is the solution set of the following parameterised VI:

$$\begin{aligned} h^* \in V(\boldsymbol{\Phi}) \Leftrightarrow & \sum_{w \in W} \sum_{m \in M} \sum_{p \in P} \left(u_p^m(\boldsymbol{\Phi}) + \frac{1}{\theta_1} \ln \left(\frac{1}{PS_p{}^m} \frac{h_p^{m*}}{q_w^{m*}} \right) \right) \left(h_p^m - h_p^{m*} \right) \\ & + \sum_{w \in W} \sum_{m \in M} \frac{1}{\theta_2} \ln \left(\frac{q_w^{m*}}{q_w^*} \right) \left(q_w^m - q_w^{m*} \right) \\ & + \sum_{w \in W} \frac{1}{\eta} \ln \left(\frac{q_w}{q_w{}^0} \right) \left(q_w - q_w{}^* \right) \geq 0, \ \forall \left(h_p^m, q_w^m, q_w^m \right) \in \Omega_2 \end{aligned} \qquad \text{Eq. (7.14)}$$

The feasible set, Ω_2 is defined by the following constraints:

$$q_w^m = \sum_{p \in P_w^m} h_p^m, \forall w \in W, m \in M$$

$$q_w = \sum_{m \in M} q_w^m, \forall w \in W$$

$$h_p^m \geq 0, \forall p \in P_w^m, w \in W, m \in M \qquad \text{Eq. (7.15)}$$

$$q_w^m \geq 0, \forall w \in W, m \in M$$

$$q_w \geq 0, \forall w \in W$$

The objective is to minimise the sum of squared differences between the modelled link flows, x_s and the observed link flows, $\overline{x}_s$. The VI ensures that the solution satisfies the combined mode and traffic assignment conditions described by Eq. (7.2) to Eq. (7.7). It can be easily shown that the Karush-Kuhn-Tucker (KKT) conditions of the VI, described by Eq. (7.14) and Eq. (7.15), are equivalent to Eq. (7.2) to Eq. (7.7). A similar proof is given by (Li et al., 2015), where route choice is governed by a simple logit model rather than a PS logit model.

7.4 Solving the I-CMC-TAP

7.4.1 Descent Method

The proposed solution algorithm for estimating network model parameters in the current study is a descent algorithm. Descent algorithms are a class of algorithms for the solution of MPECs which rely on derivative information about the VI with respect to the decision variables. In order to use such an algorithm to solve the current problem, it must be possible to compute the derivatives of the equilibrium link flows with respect to the network parameters being calibrated. This is not trivial but can be achieved using an adaptation of the sensitivity analysis described by Tobin and Friesz (Tobin, 1986). This sensitivity analysis will be described in detail in section 7.5.2.2.

Assuming that the aforementioned derivatives are available, the MPEC can be solved using a descent algorithm as follows. Starting from any given feasible solution, $\boldsymbol{\Phi}^0$, we can find a local approximation of the objective function by using a Taylor expansion:

$$F(\boldsymbol{\Phi}) = \sum_{m \in \hat{M}} \sum_{s \in \hat{S}} \left(\bar{\boldsymbol{x}}_s^{\,m} - \hat{\boldsymbol{x}}_s^{\,m}(\boldsymbol{\Phi}) \right)^2 \qquad \text{Eq. (7.16)}$$

Where

$$\hat{\boldsymbol{x}}(\boldsymbol{\Phi}) = \boldsymbol{x}(\boldsymbol{\Phi}^0) + \left(\nabla_{\boldsymbol{\Phi}} \boldsymbol{x}(\boldsymbol{\Phi}^0)\right)^T (\boldsymbol{\Phi} - \boldsymbol{\Phi}^0) \quad \text{Eq. (7.17)}$$

Where $\nabla_{\Phi} \boldsymbol{x}$ is the Jacobian matrix of the modelled flows with respect to the vector of network calibration parameters. By replacing the objective function of the MPEC described by Eq. (7.13) with this approximation, the MPEC is reformulated as a single level optimisation problem. The solution of this single level optimisation problem (or an arbitrary number of iterations of the single level problem) can then be input into the VI of the MPEC. By alternating between solving the VI and optimising the approximated objective function, a locally optimal solution to the MPEC can be reached (Si et al., 2011). In the next section, this process will be demonstrated in detail using a numerical example.

7.5 Numerical Experiment

A numerical experiment was carried out using the Sioux Falls network in order to test the calibration process described in section 7.4. The purpose of this numerical experiment was not to validate the form of a particular cycling cost function but to determine whether or not the parameters of a cycling cost function can be effectively calibrated using the I-CMC-TAP described—assuming that a suitable model form is chosen. The Sioux Falls network (LeBlanc et al., 1975), shown in Figure 7.1, was used for the experiment. This network is a simplification of the road network of the real city of Sioux Falls and is commonly used for testing transport models. A map of Sioux Falls is provided in Figure 7.2. Two modes of travel are considered in this experiment: private auto and bicycle. The experiment can be described in three stages: simulation, calibration and prediction. The simulation stage simulates a traffic survey being taken on a subset of links on a real multi-modal network. In the calibration stage, the I-CMC-TAP described in section 7.3 is used to work backwards from the observed flows to find the model parameters which best reproduce these observed flows. Finally, in the prediction stage, the calibrated model parameters are used to make link flow predictions for those links where simulated counters were not present. The assumptions underlying the experiment will now be described, followed by a more detailed description of the methodology and reporting of the results.

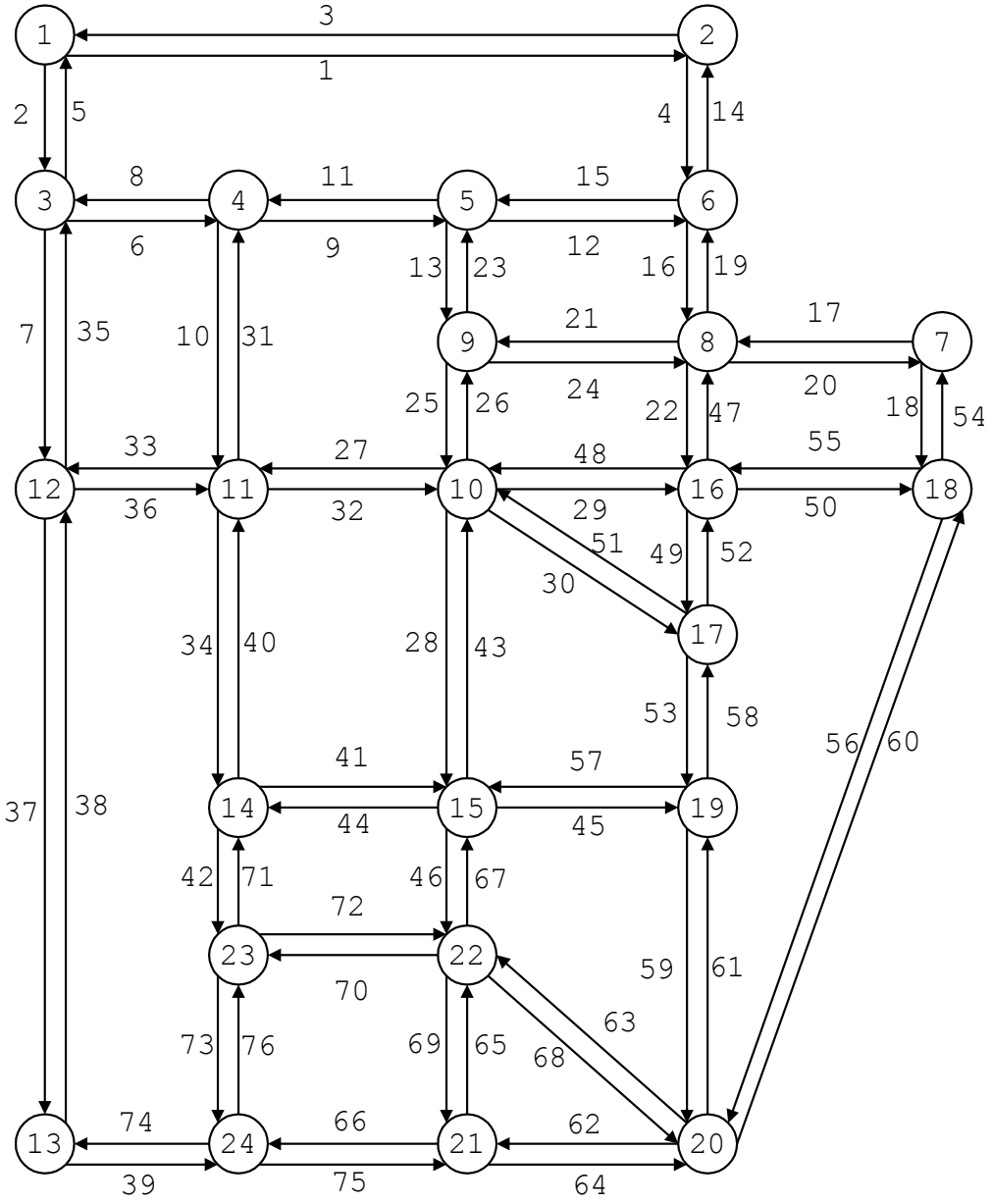

Figure 7.1 Sioux Falls Test Network

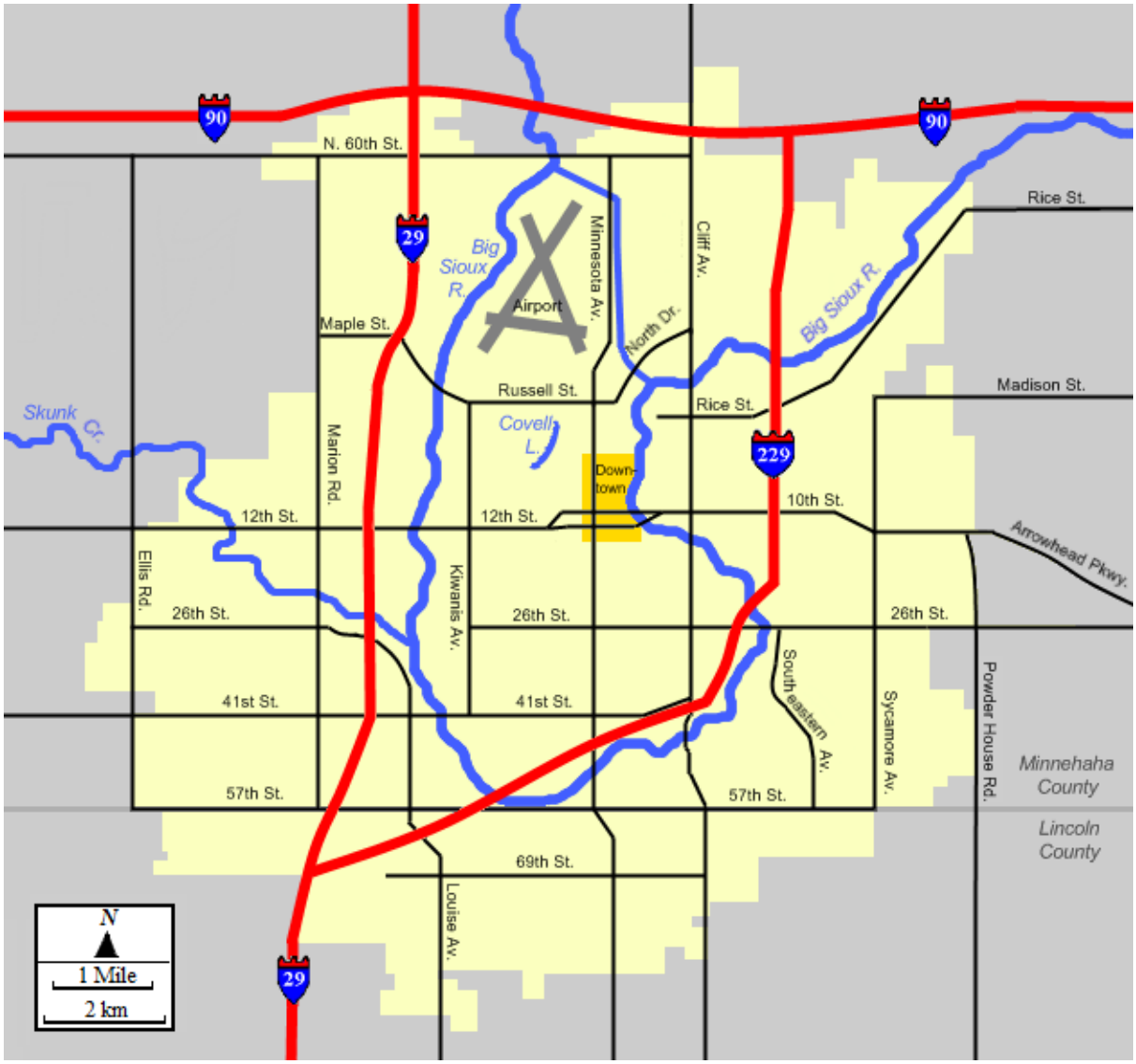

Figure 7.2 Map of Sioux Falls

7.5.1 Modelling Assumptions

For the purposes of this numerical experiment, it is assumed that the behaviour of users of the test network is governed by Eq. (7.2) to Eq. (7.7). The travel cost of cyclists is assumed to be described by the DOC function given by Eq. (7.9) and Eq. (7.10). The travel costs of private car drivers are assumed to be consistent with the BPR function, Eq. (7.8), with no fixed costs or tolls. Cyclists are allowed to travel on every link in the network but there are no segregated cycling facilities on any of these links. It is also assumed that the only unknown parameters in the model are the parameters of the DOC function, $r^{c,0}$, σ and τ and the modal split dispersion parameter, θ_2. Since the goal of this procedure is to allow an existing transport model to be extended in order to include cyclists, it can be assumed that the parameters which do not relate specifically to cycling or to modal choice are known. The values of the other modelling

parameters used in the experiment were as follows: $\overline{v}_s^c$ =15km/hr, $\overline{v}_s^a$ =30km/hr, θ_1 =0.2 , η =0.01, ρ =0.15, β =4 and α_t =20€/hr.

7.5.2 Methodology

7.5.2.1 Simulation

The first stage of the experiment, the simulation stage, simulated a traffic survey being taken on a subset of links on a real multi-modal network. First, "true" values of the model parameters were arbitrarily chosen and then the equilibrium link flows for the network corresponding to the modelling assumptions and the chosen values of the parameters were found. The arbitrarily chosen "true" values of the model parameters were as follows: $r^{c,0} = 1.1,\ \sigma = 0.1,\ \tau = 2\ \ and\ \ \theta_2 = 0.2$. For both the simulation and calibration stages, it was necessary to generate a choice set of route alternatives for each combination of mode and O-D pair. The choice set generation algorithm used in this study was a simulation algorithm which generated up to five alternative routes for each mode-O-D combination. For each alternative, link travel times for each link were drawn from a normal distribution centred at the free flow travel time with coefficient of variation of 0.5. The Floyd-Warshall algorithm (Cormen, 2009) was then used to find the shortest path between each O-D pair by each mode. A method for finding the equilibrium of the elastic-demand multi-modal network with SUE assignment was also required in the simulation and calibration stages. The Guass-Siedel decomposition approach with the Method of Successive averages (described in detail in Li et al. (2015)) was used for this.

Having solved for the equilibrium link flows in the network, half of the links were randomly allocated as the counter links and the auto and bicycle flows on these links became the "observed" flows. The resulting flows on the rest of the links were the "unobserved" flows.

7.5.2.2 Calibration

In the calibration stage, the MPEC model described section 7.3 was solved using the descent algorithm in order find the model parameters which best reproduce the observed flows. Since the solution algorithm described here only aims to find local optima, the descent algorithm was repeated multiple times with different initial values for all of the model parameters. These initial values were sampled from uniform distributions between the upper and lower limits of each parameter. The upper and lower limits, shown in Table 7.5, were chosen to include a reasonable range of possible values. After each run, the final parameters and the final value of the objective function were recorded and after all runs were completed, the set of model parameters corresponding to the lowest objective function value was chosen as the ultimate solution. As

described in section 7.4.1, the descent algorithm requires calculation of the Jacobian matrix of the modelled flows with respect to the vector of network calibration parameters. This was achieved using an adaptation of the sensitivity analysis described by Tobin (1986). Tobin (1986) describes a method of analysing the sensitivity of the solution to a VI to perturbations in the parameters of the model. The output of this analysis is $\nabla_{\varepsilon}\mathrm{y}$, a matrix of derivatives of each variable of the VI with respect to a vector of model perturbation parameters $\boldsymbol{\varepsilon}$. The matrix can be found as follows:

$$\nabla_{\varepsilon}\mathrm{y} = -\left(\mathrm{J}_{y}^{*}\right)^{-1}\mathrm{J}_{\varepsilon}^{*} \qquad \text{Eq. (7.18)}$$

Where y is the vector of equilibrium variables and dual variables, J_{y}^{*} is the Jacobian matrix of the KKT conditions of the problem with respect to y and $\mathrm{J}_{\varepsilon}^{*}$ is the Jacobian matrix of the KKT conditions of the problem with respect to the perturbation parameters. Tobin and Friesz (1988) demonstrate this analysis for a simple transport network with a single mode, fixed O-D demands and DUE assignment. This sensitivity analysis has not previously been presented for the network equilibrium model with elastic demand, logit based modal split and path-size logit SUE route assignment before. This sensitivity analysis will now be described.

According to Facchinei and Pang (2007), the KKT conditions of a $VI(K,F)$, where the feasible set, *K* is defined by $h(x)=0$ and $g(x)\geq 0$ are:

$$F(x)+\nabla_{x}h(x)^{T}\lambda+\nabla_{x}g(x)^{T}\mu=0$$

$$h(x)=0 \qquad \text{Eq. (7.19)}$$

$$0\leq g(x)\perp\lambda\geq 0$$

Where λ and μ are the dual variables associated with the equality and inequality constraints respectively. The KKT conditions for the VI represented by equations Eq. (7.14) and Eq. (7.15) are as follows. Since all variables in the model must be positive at optimal, it is not necessary to consider the non-negativity constraints or the associated dual variables (Fiacco, 1983) (Yang and Chen, 2009):

$$\mu_{p}^{m}(\Phi)+\frac{1}{\theta_{1}}ln\left(\frac{1}{PS_{p}^{m}}\frac{h_{p}^{m}}{q_{w}^{m}}\right)-\lambda_{w}^{m}=0, \qquad \forall m\,\epsilon\,M, p\,\epsilon\,P_{w}^{m}, w\,\epsilon\,W \qquad \text{Eq. (7.20)}$$

$$\frac{1}{\theta_2} ln \frac{q_w^m}{q_w} + \lambda_w^m - \lambda_w = 0, \qquad \forall m \epsilon M, w \epsilon W$$

$$\frac{1}{\eta} log\left(\frac{q_w}{q_w^0}\right) + \lambda_w = 0, \qquad \forall w \epsilon W$$

$$q_w^m = \sum_{p \epsilon P_w^m} h_p^m, \qquad \forall\, w \epsilon W, m \epsilon M$$

$$q_w = \sum_{m \epsilon M} q_w^m, \qquad \forall\, w \epsilon W$$

The Jacobian of this system of equations with respect to the vector of equilibrium variables and dual variables, $\boldsymbol{y} = \left[\boldsymbol{h}, \boldsymbol{q}, \boldsymbol{Q}, \boldsymbol{\lambda}\right]^T$ is below. The non-zero elements are detailed in the Appendix of the thesis.

$$\nabla_y KKT = \begin{bmatrix} \nabla_h KKT_1 & \nabla_q KKT_1 & 0 & -\Delta_{wm-p}{}^T & 0 \\ 0 & \nabla_q KKT & \nabla_Q KKT_2 & I & -\Delta_{w-wm}{}^T \\ 0 & 0 & \nabla_Q KKT_3 & 0 & I \\ -\Delta_{wm-p} & I & 0 & 0 & 0 \\ 0 & -\Delta_{w-mw} & I & 0 & 0 \end{bmatrix}$$

Where

$$KKT = \begin{bmatrix} KKT_1 \\ KKT_2 \\ KKT_3 \\ KKT_4 \\ KKT_5 \end{bmatrix} = \begin{bmatrix} \left[\left(\mu_p^m(\Phi) + \frac{1}{\theta_1} \ln\left(\frac{1}{PS_p^m} \frac{h_p^m}{q_w^m}\right) - \lambda_w^m\right) \ \forall\, p \epsilon P_w^m, m \epsilon M, \ w \epsilon W\right]^T \\ \left[\left(\frac{1}{\theta_2} \ln\left(\frac{q_w^m}{q_w}\right) + \lambda_w^m - \lambda_w\right) \ \ \forall m \epsilon M, w \epsilon W\right]^T \\ \left[\left(\frac{1}{\eta} \log\left(\frac{q_w}{q_w^0}\right) + \lambda_w\right) \ \ \forall\, w \epsilon W\right]^T \\ \left[\left(q_w^m - \sum_{p \epsilon P_w^m} h_p^m\right) \ \ \forall\, w \epsilon W, m \epsilon M\right]^T \\ \left[\left(q_w - \sum_{m \epsilon M} q_w^m\right) \ \ \forall\, w \epsilon W\right]^T \end{bmatrix} \qquad \text{Eq. (7.21)}$$

The Jacobian of the system of KKT equations with respect to the vector of calibration parameters, $\boldsymbol{\Phi} = \left[r^{c,0} \ \ \sigma \ \ \tau \ \ \theta_2\right]$ *is* below. The non-zero elements are detailed in the Appendix of the thesis.

$$\nabla_{\boldsymbol{\Phi}} KKT = \begin{bmatrix} \nabla_{r^{c,0}} KKT_1 & \nabla_{\sigma} KKT_1 & \nabla_{\tau} KKT_1 & 0 \\ 0 & 0 & 0 & \nabla_{\theta_2} KKT_2 \\ 0 & 0 & 0 & 0 \\ 0 & 0 & 0 & 0 \\ 0 & 0 & 0 & 0 \end{bmatrix} \qquad \text{Eq. (7.22)}$$

Based on Eq. (7.18), we can then find the Jacobian of the equilibrium variables with respect to the vector of calibration parameters, $\boldsymbol{\Phi}$:

$$\nabla_{\boldsymbol{\Phi}} \boldsymbol{y} = \begin{bmatrix} \nabla_{\boldsymbol{\Phi}} \boldsymbol{h} \\ \nabla_{\boldsymbol{\Phi}} \boldsymbol{q} \\ \nabla_{\boldsymbol{\Phi}} \boldsymbol{Q} \\ \nabla_{\boldsymbol{\Phi}} \boldsymbol{\lambda} \end{bmatrix} = -\nabla_{y} KKT^{-1} * \nabla_{\boldsymbol{\Phi}} KKT \qquad \text{Eq. (7.23)}$$

The Jacobian of the link flows with respect to $\boldsymbol{\Phi}$ can then easily by found:

$$\nabla_{\boldsymbol{\Phi}} \boldsymbol{x} = \Delta_{\text{sp}} \nabla_{\boldsymbol{\Phi}} \boldsymbol{h} \qquad \text{Eq. (7.24)}$$

This gives us the required gradients in order to carry out the descent algorithm. The full descent algorithm used in the calibration stage of this numerical experiment is summarised in Table 7.6. The values used for the algorithmic parameters in Table 7.6 were $\psi = 10^{-7}$, $\iota = 10^{-11}$ and $Iteration\ Limit = 300$.

Table 7.5 Upper and lower limits of each calibration parameter in the numerical experiment.

Parameter	Min	Max
$r^{c,0}$	0.5	2
σ	0.1	1
τ	1	3
θ_2	0.01	0.99

Table 7.6 Solving the I-CMC-TAP using the descent algorithm with sensitivity analysis

Step 0: Initialise each of the calibration parameters, $\boldsymbol{\Phi}^0$. Set $k = 0$

Step 1: Find the equilibrium link flows $\boldsymbol{x}^k$ corresponding to $\boldsymbol{\Phi}^k$ using Gauss-Seidel Decomposition with the Method of Successive Averages

Step 2: Use sensitivity analysis to find the Jacobian of the link flows with respect to $\boldsymbol{\Phi}^0$:

$$\nabla_{\boldsymbol{\Phi}} y = \left[\nabla_{\boldsymbol{\Phi}} \boldsymbol{h} \quad \nabla_{\boldsymbol{\Phi}} \boldsymbol{q} \quad \nabla_{\boldsymbol{\Phi}} \boldsymbol{Q} \quad \nabla_{\boldsymbol{\Phi}} \boldsymbol{\lambda}\right]^T = -\nabla_y KKT^{-1} * \nabla_{\boldsymbol{\Phi}} KKT$$

$$\nabla_{\boldsymbol{\Phi}} \boldsymbol{x} = \Delta_{\text{sp}} * \nabla_{\boldsymbol{\Phi}} \boldsymbol{h}$$

Step 3: Construct a local approximation to the objective function:

$$\hat{F}\left(\boldsymbol{\Phi}\right) = \sum_{s \in \hat{S}} \left(\bar{\boldsymbol{x}}_s - \hat{\boldsymbol{x}}_s\left(\boldsymbol{\Phi}\right)\right)^2$$

Where $\hat{\boldsymbol{x}} = \boldsymbol{x}\left(\boldsymbol{\Phi}^k\right) + \left(\nabla_{\phi} \boldsymbol{x}\left(\boldsymbol{\Phi}^k\right)\right)^T \left(\boldsymbol{\Phi} - \boldsymbol{\Phi}^k\right)$

Step 4: Find $\hat{\boldsymbol{v}}^{\boldsymbol{k}}$, the direction of steepest descent of $\hat{F}\left(\boldsymbol{\Phi}\right)$

Step 5: Update the model parameters:

$$\boldsymbol{\Phi}^{k+1} = \boldsymbol{\Phi}^k + \psi * \hat{\boldsymbol{v}}^{\boldsymbol{k}}$$

where $0 < \psi < 1$ is a step-size parameter.

Step 6: Ensure feasibility of the calibration parameters:

If	$\phi_i^{k+1} > \phi_i^u$,	$\phi_i^{k+1} = \phi_i^u$
Else if	$\phi_i^{k+1} < \phi_i^l$,	$\phi_i^{k+1} = \phi_i^l$

$\forall \phi_i^{k+1} \in \boldsymbol{\Phi}^{k+1}$

Step 7: Check convergence:

If	$\left(\boldsymbol{\Phi}^{k+1} - \boldsymbol{\Phi}^k\right)^T * \left(\boldsymbol{\Phi}^{k+1} - \boldsymbol{\Phi}^k\right) < \iota$,	
Or	*k>Iteration limit*	terminate
Otherwise,	*k*=*k*+1 Return to Step 1	

Where ε is a small constant

7.5.2.3 Prediction

Finally, in the prediction stage, the calibrated model parameters are used to make link flow predictions for those links where counters were not present. The correlation coefficient between the predicted and "actual" flows is used as a measure of the accuracy of the predictions and the effectiveness of the calibration.

7.5.3 Results

The calibration algorithm was run 10 times from different starting points as described and the results of each run are shown in Table 7.7. The lowest value of the objective function was recorded on run 10. The wide range of final objective function values achieved in each run demonstrate the existence of many local optima for this problem and importance of using multiple starting points. The final parameter values for run 10 were $r^{c,0} = 1.09$, σ=0.17, τ =2.27, and θ_2=0.1. There were significant differences between the final calibrated parameter values and the "true" parameter values set in the simulation stage. In particular, $r^{c,0}$ was underestimated by 17% while τ was overestimated by 13%.

Despite these errors in the calibrated parameters, the calibrated model was capable of making highly accurate flow predictions. These parameter values of run 10 were used to make flow predictions on the unobserved links and the correlation coefficient between the actual and predicted flows was 0.9997. The Mean Absolute Percentage Error (MAPE) of the predictions was 1.5%. Figure 7.3 shows that there was a strong linear relationship between the actual and predicted flows. The reason for the errors in calibrated parameters despite the high prediction accuracy is likely that the form of the DOC function was more complex than required for the relatively simple network used in this experiment. This, along with the flexibility of the function allowed errors in each parameter to compensate for one another so that the behaviour of the calibrated function very closely matched the behaviour of the function with the "true" parameter values. This simple experiment validates the methodology and algorithm described in this paper for network-based calibration of a cycling link cost function based on a multi-modal transport model. The next step will be to apply this methodology to a real transport network using actual traffic counts. This will determine (i) whether good prediction accuracies and acceptable computation times can still be achieved using a larger network with real data and (ii) whether the form of the DOC function can accurately capture urban cycling behaviour.

Table 7.7 Calibration results of the numerical experiment

	$\boldsymbol{r}^{c,0}$		σ		τ		θ_2			
Run	Initial	Final	Initial	Final	Initial	Final	Initial	Final	Final F	Iterations
1	1.13	1.02	0.75	0.62	1.00	0.98	0.32	0.07	1.81E+06	227
2	1.15	0.95	0.12	0.15	2.10	2.10	0.44	0.14	3.29E+05	300
3	1.33	1.19	0.74	0.51	1.58	1.52	0.51	0.06	1.75E+06	300
4	1.95	1.94	0.59	0.59	2.95	2.95	0.69	0.67	3.72E+08	41
5	0.83	0.83	0.88	0.88	1.41	1.41	0.88	0.88	3.68E+08	19
6	1.84	1.80	0.40	0.30	2.64	2.62	0.09	0.04	8.12E+06	22
7	0.61	0.89	0.80	0.17	1.88	1.67	0.70	0.17	5.63E+06	300
8	1.81	1.79	0.97	0.96	2.74	2.74	0.53	0.46	3.71E+08	37
9	0.52	0.82	0.55	0.32	1.99	1.83	0.17	0.11	1.23E+07	300
10	**1.66**	**1.09**	**0.12**	**0.17**	**2.27**	**2.27**	**0.72**	**0.10**	**2.90E+05**	**227**

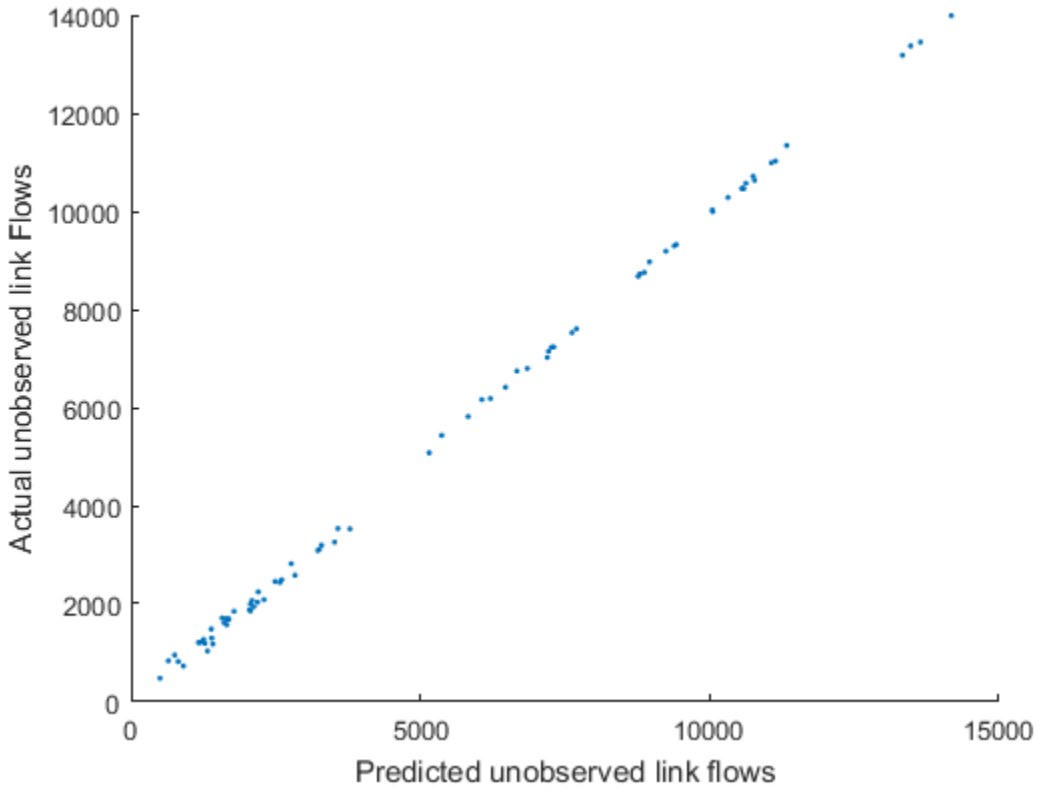

Figure 7.3 Predicted and actual flows on unobserved links

7.6 Calibration of cost function for Dublin city network

The last piece of work in this chapter is concerned with using the theory and algorithm developed earlier in the chapter to validate the DOC function proposed in section 7.2 and calibrate its parameters. This is done using data from the actual transport network of Dublin, Ireland. An ITAP is modelled as an MPEC where the equilibrium problem is a TAP for cyclists

only, using a model of the road network of the Greater Dublin Area (GDA) including segregated cycle lanes. The ITAP seeks values for network parameters—including the parameters of the DOC function—which induce the greatest agreement between modelled flows and actual observations of cyclist flows on a sub-set of links in the Dublin city network. The accuracy of the calibrated model is tested by comparing link flow predictions to actual observations on links not used in the calibration process. All analysis is carried out using Matlab R2016b (The MathWorks Inc., 2016).

For context, the transport model currently in use in Dublin by the National Transport Authority (NTA) is briefly described next. The model inputs and assumptions used in the ITAP are then described, followed by the methodology used and the results of the experiment.

7.6.1 Transport Models for the Greater Dublin Area

The macroscopic transport model which has been used in recent years for the Greater Dublin Area (GDA) is the GDA Transport Model of the NTA (National Transport Authority, 2011b). The geographical area covered by this model includes the county of Dublin as well as the adjacent counties of Kildare, Meath and Wicklow in the mid-east of Ireland, as shown in Figure 7.4 (National Transport Authority, 2015a). Both a "Peak" model for the morning peak hours between 7am and 10am and an "Off-Peak" model exist. The components of the "Peak" model are illustrated in Figure 7.5 (National Transport Authority, 2011b). After the demands are divided into "Car Available" trips and "Car Not Available" trips, they are further divided into Slow Modes (SM) and Mechanised modes (Mech). It can be seen that, for "Slow Modes" which include walking and cycling, no further modelling takes place. For cars, assignment to the road network takes place in Saturn (Hall and WILLUMSEN, 1980). The GDA transport model was not used directly in this study but did provide some model inputs for the ITAP which are discussed in the next section.

The NTA has recently developed a new macroscopic transport model, the Eastern Regional Model (National Transport Authority, 2015a), which encompasses an area including the GDA. The Eastern Regional Model was used to support the development and assessment of the proposed GDA Transport Strategy 2015 – 2035 (National Transport Authority, 2015a). Unlike the GDA model, the Eastern Regional Model includes an Active Modes Model which assigns active modes (walking and cycling) to the network. However, all trips undertaken by active modes are assumed to simply take the shortest path between the trip origin and trip destination.

Figure 7.4 The Greater Dublin Area (National Transport Authority, 2015a)

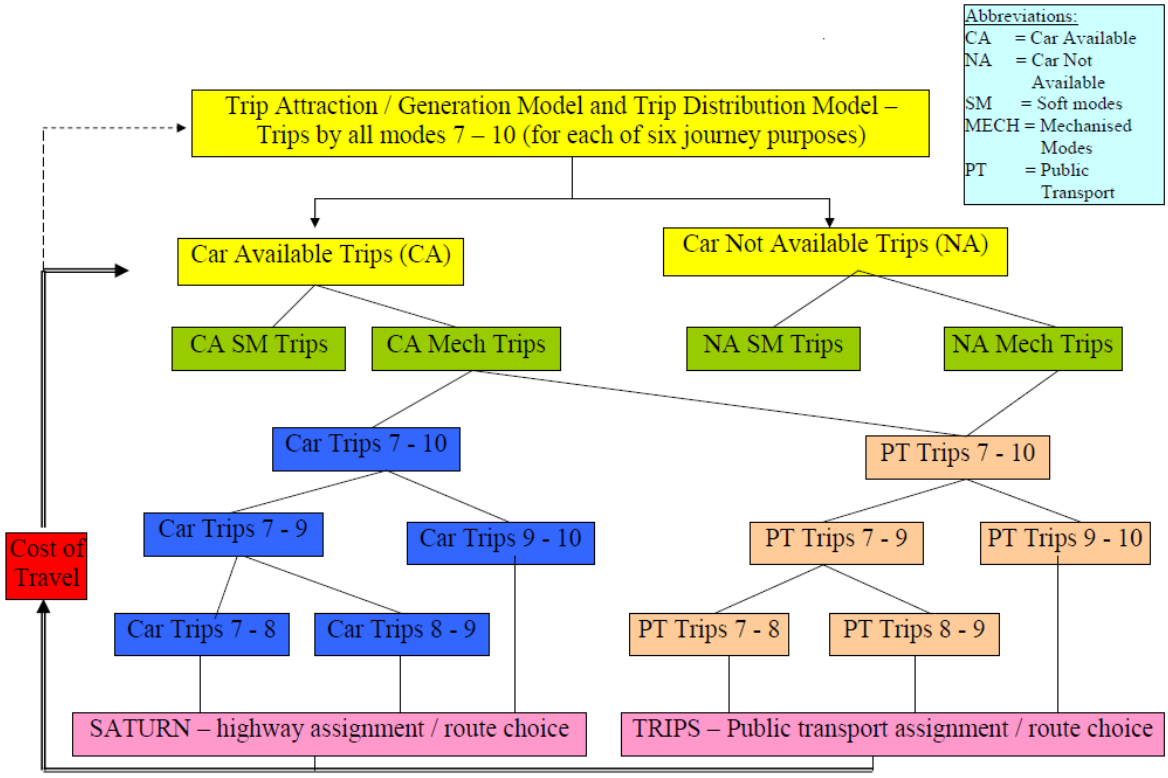

Figure 7.5 Components of the NTA Peak GDA Model (National Transport Authority, 2011b)

7.6.2 Model Inputs and Assumptions

Similarly to the GDA Peak Transport Model, the time period considered in this study was the morning peak period between 7am and 10am. All data corresponded to the years of 2011 or 2012.

7.6.2.1 Cycling Demand

The demand data for cycling trips between each origin and destination in the study period were obtained from the POWSCAR (Place of Work, School or College – Census of Anonymised Records), 2011 data (Central Statistics Office, 2011a; Central Statistics Office, 2011b). This dataset includes details of commuter trips made by all persons over the age of 4, resident in Ireland on 10/Apr/2011, including home and work/school/college locations, journey times and journey modes. This dataset only contains trips going to and from work, school or college. However, it was assumed that during the morning peak period, the effect of recreational cycling trips on city centre traffic would be negligible. The POWSCAR data include a field indicating the time at which the individual usually begins their journey to work in 30 minute intervals. The time period between 6:30am and 9:30m was chosen as the most appropriate time period to represent the demand contributing to traffic in the city centre during the peak period of 7am to 10am. Trips leaving outside of this time interval were ignored. For the sake of parsimony, it was

also assumed that only cycling trips which begin or end in the city centre would significantly affect cycling traffic in the city centre during the morning rush hour and so, all other trips were ignored. The POWSCAR data include the residence location and work/school/college location of each individual at the level of Small Areas as set out by the Central Statistics Office (CSO). The GDA Transport model, on the other hand, divides the GDA into 666 “zones” which are coarser than the CSO Small Areas. These GDA zones were used to represent origins and destinations in the current study and so, before the O-D demand matrices could be created, the Small Area level origins and destinations needed to be mapped to zones. This was done by finding the centroid of each Small Area and each zone and matching each Small Area centroid to the closest zone centroid. A 666*666 O-D demand matrix was then produced from the trip data with 12,447 non-zero entries. Figure 7.6 compares the CSO Small Areas with the NTA zones.

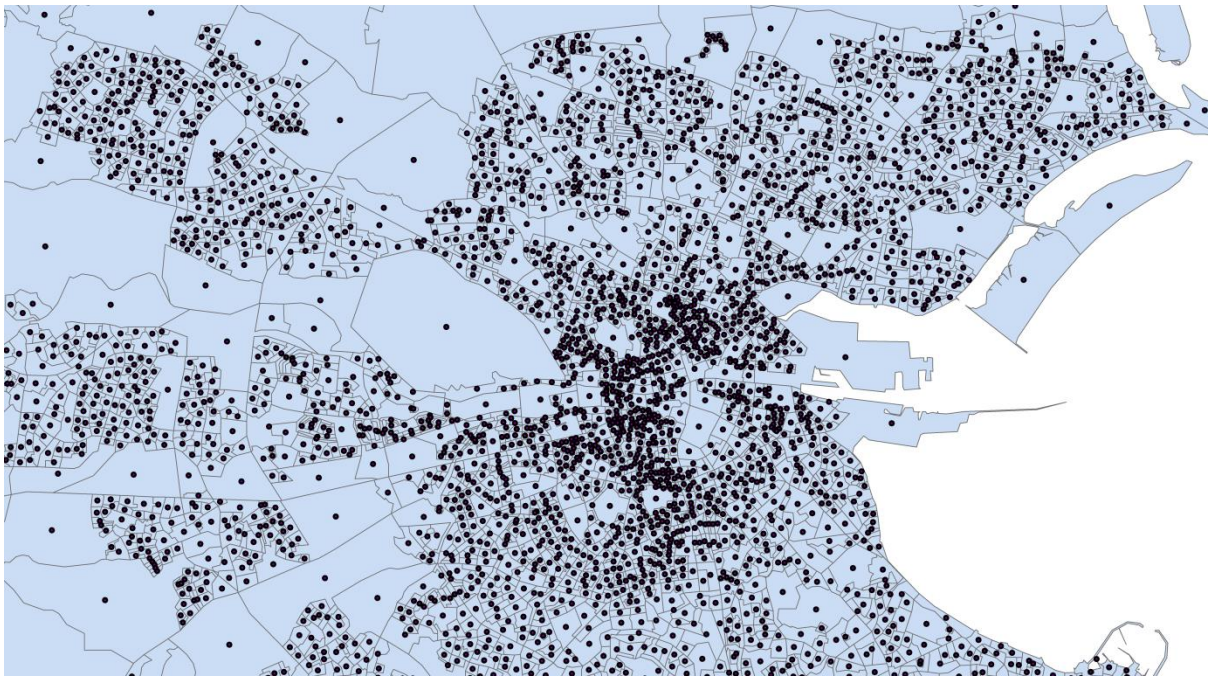

(a)

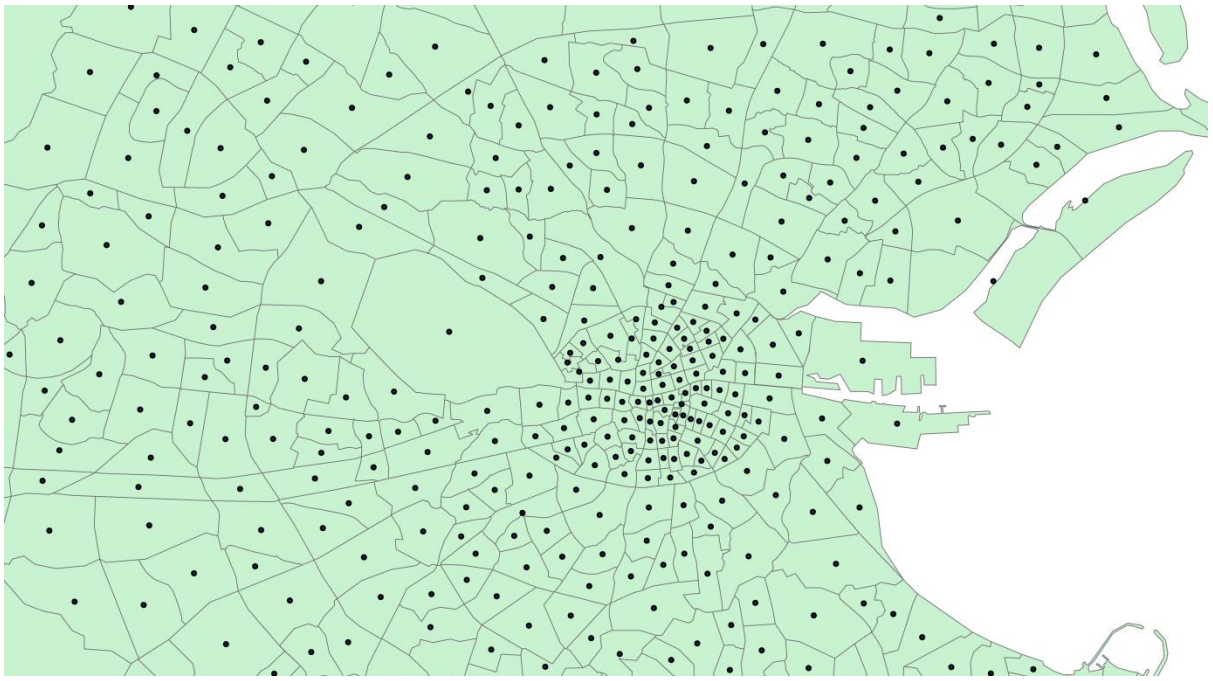

(b)

Figure 7.6 Comparison of (a) CSO Small Areas and (b) NTA zones and their centroids

7.6.2.2 Transport Network

The network model used in this study was composed of four sub-networks: the motor vehicle network, the centroid connectors, the segregated cycle lane network and the super-connectors joining the motor vehicle and segregated cycle lane networks. The motor vehicle network and the centroid connectors were obtained from the highway assignment component of the NTA GDA model (National Transport Authority, 2011b) which is implemented in Saturn (Hall and WILLUMSEN, 1980) .The motor vehicle network and centroid connector network were composed of 5,834 and 3,518 links respectively. It was assumed that cyclists could cycle on the road network with the direction of traffic. However, since cycling on motorways is not permitted in Ireland, the motorways were removed from the network (Road Safety Authority, 2012). The centroid connectors joined the GDA zones to the motor vehicle network and could only be used as the first and last links on a route. The segregated cycle lane network was modelled from a GIS shape file of cycle facilities in Dublin as of 2012, provided by the NTA. The information in the shape file was processed into a suitable format using Matlab, producing 5,591 links. Maps of the combined motor vehicle network and segregated cycle networks for the whole GDA and the Dublin city centre are shown in Figure 7.7 and Figure 7.8. In order to allow cyclists to use routes comprising links in both the motor vehicle and segregated cycle networks, super-connectors were added to join any pair of nodes in the two networks which were closer than 50m. The length assigned to each super-connector was equal to the straight-line distance between the car node and segregated cycle node. 325 super-connectors were added in total.

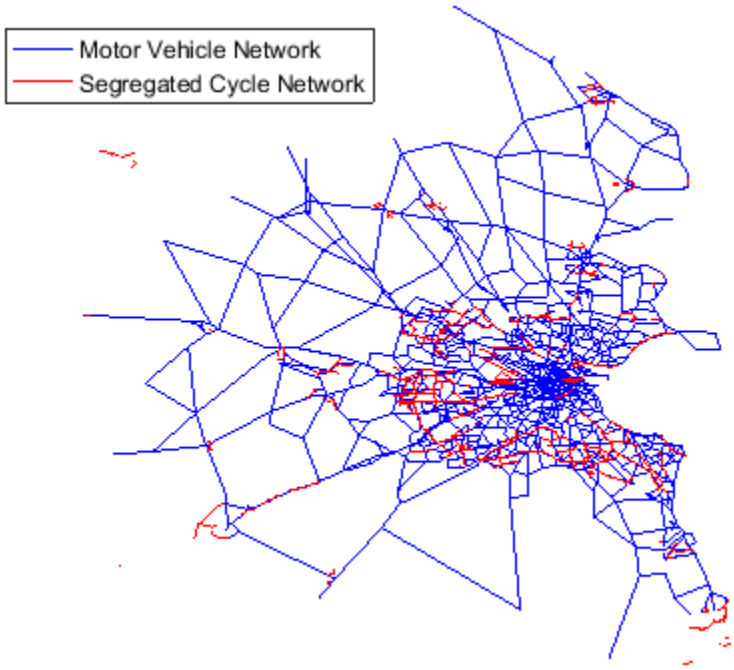

Figure 7.7 Motor vehicle network and segregated cycle network of GDA

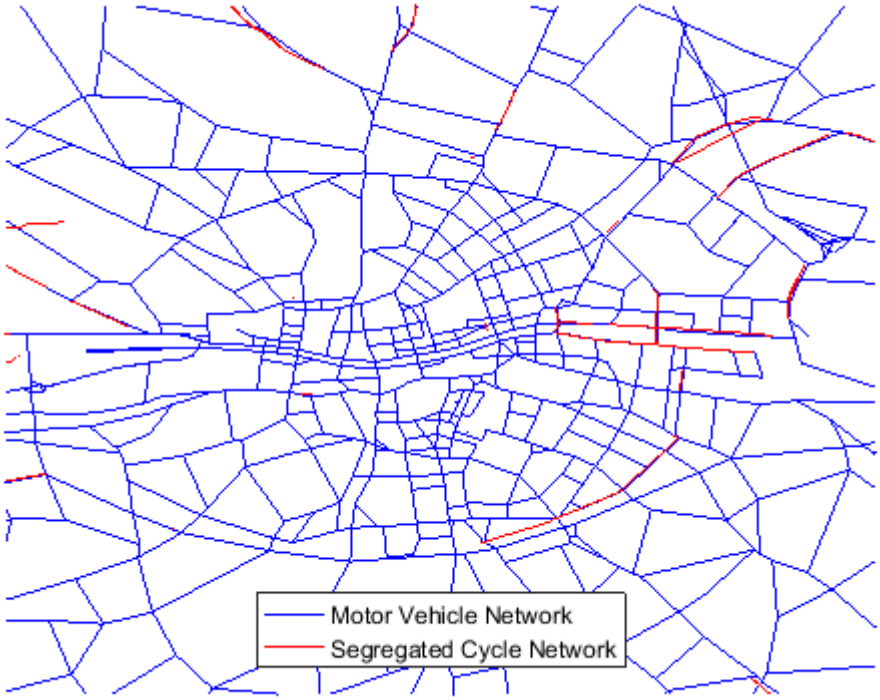

Figure 7.8 Motor vehicle network and segregated cycle network of Dublin city centre.

7.6.2.3 Link Flow Observations

Similarly to the numerical experiment of section 7.5, network observations were used to calibrate the network parameters and then test the prediction accuracy of the calibrated model. However, in this case, the observations were not simulated flows but actual cyclist flow

observations from the Dublin city network. Cyclist flows for the 7am to 10am weekday peak period were gathered from a number of sources. The first source was the 2012 canal cordon count carried out by Dublin City Council (DCC) which recorded cyclist flows during several days in November, 2012 at 33 locations around the cordon formed by the Royal Canal and Grand Canal. This survey was designed to ensure that any person entering or leaving must pass through one of the survey locations. The second source was another traffic survey carried out by DCC in May, 2012 which included counts along the bridges crossing the river Liffey in the city centre. The third source was traffic counts provided by the NTA at 35 junctions close to the city centre on days during March and May, 2012. Finally, continuous cyclist counts from a cyclist-specific inductive loop detector beside the Grand Canal were available from 1/Oct/2011 to 1/Oct/2012: the counts between 7am and 10am on all weekdays were averaged to give a single flow observation in each direction. Since the NTA model is a simplified representation of the Dublin network, there were a number of links for which observations were available but which either did not exist or were over-simplified in the model. These link observations were excluded from the calibration and predictions. In total, valid cyclist flow observations were available for 249 directional links which are shown in Figure 7.9.

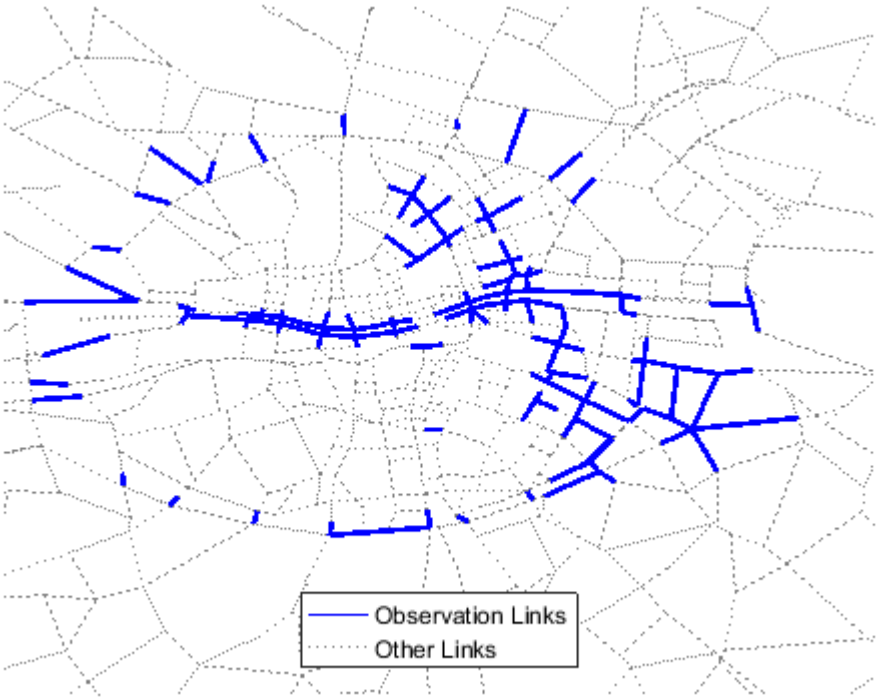

Figure 7.9 Links in city centre for which flow observations were available

7.6.2.4 ITAP formulation

Since data were available on the actual mode-specific travel demands in the Dublin network, there was no need to model modal choice in the ITAP. Also, since the demands were actual demands rather than potential demands, there was no need to model elasticity of demand. The equilibrium constraint TAP then, was subject to the following flow conservation constraint:

$$q_w^c = \sum\nolimits_{p \in P_w^c} h_p^c, \forall w \in W \qquad \text{Eq. (7.25)}$$

Similarly to the model used for the numerical experiment of section 7.5, traffic assignment was assumed to follow the SUE principal, governed by the path-size logit model described by Eq. (7.2) and Eq. (7.3). It was hypothesised that the travel costs of cyclists in the Dublin city network can be modelled by the DOC function described by Eq. (7.9) and Eq. (7.10). Since motor vehicle traffic was not modelled, estimates of x_s^a and x_s^b, the flows of cars and buses in PCU on each link *s* of the motor vehicle network during the morning peak period, were obtained from the GDA Peak Transport Model. Since modal choice was not modelled in this experiment, it would not have been appropriate to calibrate the modal bias parameter, $r^{c,0}$. This parameter was therefore assigned a fixed value of 1, implying no bias for or against cycling. The only unknown parameters then were σ, τ and θ_1. The ITAP could be represented by the following MPEC:

$$\begin{aligned} & min_{\phi} \quad \sum\nolimits_{s \in \hat{S}} \left(\overline{x}_s^c - x_s^c\left(\boldsymbol{\Phi}\right) \right)^2 \\ & s.t. \qquad x_s = \sum\nolimits_{p \in P} h_p^m \delta_{sp}, \forall s \in S \qquad \text{Eq. (7.26)} \\ & \boldsymbol{\Phi} \in \Omega_1, \quad \boldsymbol{h} \in V\left(\boldsymbol{\Phi}\right) \end{aligned}$$

Where $\boldsymbol{\Phi} = \left[\sigma, \tau, \theta_1\right]^T$ is the vector of network parameters to be calibrated, Ω_1 defines the constraints on the network parameters and $V\left(\boldsymbol{\Phi}\right)$ is the solution set of the following parameterised VI:

$$h^* \in V(\phi) \Leftrightarrow \sum\nolimits_{w \in W} \sum\nolimits_{p \in P} \left(u_p^c\left(\boldsymbol{\phi}\right) + \frac{1}{\theta_1} \ln\left(\frac{1}{PS_p{}^m} \frac{h_p^{c*}}{q_w^c} \right) \right) \left(h_p^c - h_p^{c*} \right) \geq 0, \ \forall h_p^c \in \Omega_2 \qquad \text{Eq. (7.27)}$$

The feasible set, Ω_2 is defined by the following constraints:

$$q_w^c = \sum_{p \in P_w^c} h_p^c, \forall w \in W$$

$$h_p^c \geq 0, \forall p \in P_w^c, w \in W$$

Eq. (7.28)

7.6.3 Methodology

The methodology was similar to the methodology of the numerical experiment in section 7.5. However, since actual observations from the Dublin network were used for calibration and validation, there was no simulation stage. 2/3 of the link observations were randomly allocated to a training set and the other 1/3 were allocated to the test set. In the calibration stage, the MPEC of Eq. (7.26) was solved using the descent method described in section 7.4, which was run 10 times from different starting points, sampled from uniform distributions. The upper and lower limits set for each calibration parameter are shown in Table 7.8. The method of finding derivative information based on sensitivity analysis described in section 7.5.2.2, was found to be inefficient for this problem due to the large number of possible routes. In particular, the matrix inversion in step 2 of the algorithm described in Table 7.6 was computationally expensive. It was found to be more efficient to simply calculate the derivatives of the objective function with respect to each of the parameters empirically. At each iteration of the descent algorithm, the empirical gradients and direction of steepest descent of the objective function could be calculated as follows:

$$\hat{\boldsymbol{v}}^{\boldsymbol{k}} = -\left[\frac{dF}{d\sigma}^k, \quad \frac{dF}{d\tau}^k, \quad \frac{dF}{d\theta_1}^k \right]$$

where $$F(\boldsymbol{x}) = \sum_{s \in S} \left(\bar{x}_s^c - x_s^c(\boldsymbol{\Phi}) \right)^2$$

and $$\frac{dF}{dz}^k = \frac{F(\boldsymbol{x}^{z'k}) - F(\boldsymbol{x}^k)}{dz}$$

such that $$x_s^{z'k} = \sum_{p \in P} h_p^c \delta_{sp}, \forall s \in \bar{S}$$

$$\boldsymbol{h} \in V(\boldsymbol{\Phi}^{z'k})$$

$$\begin{aligned}
&if \quad z == \sigma, \quad \boldsymbol{\Phi}^{z'k} = \left[\sigma^k + d\sigma, \quad \tau^k, \quad \theta_1^k \right] \\
&if \quad z == \tau, \quad \boldsymbol{\Phi}^{z'k} = \left[\sigma^k, \quad \tau^k + d\tau, \quad \theta_1^k \right] \\
&if \quad z == \theta_1, \quad \boldsymbol{\Phi}^{z'k} = \left[\sigma^k, \quad \tau^k, \quad \theta_1^k + d\theta_1 \right]
\end{aligned}$$

Eq. (7.29)

Table 7.8 Upper and lower limits on model parameters.

Parameter	Min	Max
σ	0.01	2
τ	1	5
θ_1	0.01	1.6

In order to ensure that the empirically calculated gradient vectors were in agreement with the gradient vectors which would be calculated using sensitivity analysis, both methods were used to calculate gradients for a random sample of 50 points within the feasible region of the MPEC. A value of 0.01 was used for all three perturbations, $d\sigma$, $d\tau$ and $d\theta_1$, as it was deemed that the interval should be 2 orders of magnitude smaller than the expected value of each parameter. The agreement of each pair of gradient vectors was compared by computing the dot product of the normalised vectors. A result of 0 would indicate perpendicular gradients while a value of 1 would indicate parallel gradients. The mean of the dot products over the 50 samples was 0.91 with a standard deviation of 0.13, showing that there was good agreement between the gradients calculated with both methods. Therefore, the more efficient empirical calculation was used in the descent algorithm.

The descent algorithm with empirical derivatives can be summarised by Table 7.9. The chosen values of the algorithmic parameters were $d\sigma$=0.01, $d\tau$=0.01 , $d\theta_1$=0.01, ψ = 1E-7 and ι=1E-11. After the calibration process was completed and the best set of parameters was chosen, the accuracy of the calibration was tested by comparing the predicted and observed cyclist flows on the links in the test set.

Table 7.9 Solving the ITAP using the descent algorithm with empirical gradients

Step 0: Initialise each of the calibration parameters, $\boldsymbol{\Phi}^0$. Set $k = 0$

Step 1: Find the equilibrium link flows $\boldsymbol{x}^k$ corresponding to $\boldsymbol{\Phi}^k$ using the Method of Successive Averages.

Step 2: Evaluate the objective function, $F\left(x^k\right)$, corresponding to $\boldsymbol{x}^k$:

$$F\left(x^k\right) = \sum_{s \in S} \left(\bar{x}_s^c - x_s^{ck}\right)^2$$

Step 3: For each parameter, z, in $\boldsymbol{\Phi}$, add a perturbation, dz, to z and find the equilibrium link flows $x^{z'k}$ corresponding to the perturbed parameter vector $\boldsymbol{\Phi}^{z'k}$

Step 4: For each parameter, z, in $\boldsymbol{\Phi}$, evaluate the perturbed objective function, $F\left(x^{z'k}\right)$

Step 5: Evaluate the empirical gradients of the upper objective function with respect to each z in $\boldsymbol{\Phi}$:

$$\frac{dF^k}{dz} = \frac{F\left(x^{z'k}\right) - F\left(x^k\right)}{dz}$$

Step 6: Find $\hat{\boldsymbol{v}}^{\boldsymbol{k}}$, the direction of steepest descent of $F\left(x^k\right)$:

$$\hat{\boldsymbol{v}}^{\boldsymbol{k}} = -\left[\frac{dF^k}{d\sigma}, \quad \frac{dF^k}{d\tau}, \quad \frac{dF^k}{d\theta_1}\right]$$

Step 7: Update the model parameters:

$$\boldsymbol{\Phi}^{k+1} = \boldsymbol{\Phi}^k + \psi * \hat{\boldsymbol{v}}^{\boldsymbol{k}}$$

where $0 < \psi < 1$ is a step-size parameter.

Step 8: Ensure feasibility of the calibration parameters:

If $\phi_i^{k+1} > \phi_i^u$, $\quad \phi_i^{k+1} = \phi_i^u$

Else if $\phi_i^{k+1} < \phi_i^l$, $\quad \phi_i^{k+1} = \phi_i^l$

$\forall \phi_i^{k+1} \in \boldsymbol{\Phi}^{k+1}$

Step 9: Check convergence:

If $\left(\boldsymbol{\Phi}^{k+1} - \boldsymbol{\Phi}^k\right)^T * \left(\boldsymbol{\Phi}^{k+1} - \boldsymbol{\Phi}^k\right) < \iota$, where ι small

Otherwise, k=k+1, Return to Step 1

7.6.4 Results

The results of each run of the descent algorithm are shown in Table 7.10. The lowest value of the objective function was recorded on run 4 and so the values of the network parameters at the local optimum of run 4 were chosen as the final parameters. The final parameters were σ = 0.68, τ =4.46 and θ_1 =1.37. A different local optima was found in each run of the descent algorithm but the values of σ and θ_1 were relatively consistent across each of these points. All results for σ were reasonably close to the final value of 0.68 except for run 7 and run 10. Similarly, all results for θ_1 were reasonably close to the final value of 1.37 except for run 7. The values of τ , however, were not as consistent. The final value for τ of 4.46 represents a strong non-linearity in the relationship between congestion level and increase in travel cost. It implies that at low or moderate levels of congestion, the cost of cycling does not increase significantly but as the traffic on a link approaches full capacity, the cost of cycling increases sharply. The final value for σ of 0.68 implies that a cyclist

on a shared link which is at full capacity has an average perceived travel cost of 62% higher than a cyclist on an empty link or segregated lane. These values seem reasonable with respect to previous research into the perceived travel costs of cyclists. For example, a Swedish study (Börjesson and Eliasson, 2012) has estimated that the value of time while cycling on a cycle lane to be approximately 45% higher than the value of time while cycling on the street. A reasonably high coefficient of correlation of 0.82 was found between the predicted and observed flow observations on the links assigned to the test set. The level of agreement between the predicted and observed flows is also shown by the linear pattern of the scatterplot in Figure 7.10. The spatial distribution of the prediction errors is illustrated in Figure 7.11. Two of the largest errors were close to another in space but apart from this there were no clear spatial patterns in the error distributions.

In order to provide context for the prediction results, a shortest-path assignment was carried out using the same network model and O-D demand matrices. This assignment model simply assigned all cycling trips to the shortest path between the trip origin and destination. Figure 7.12 compares the absolute percentage errors on the test links from both assignment models by means of their cumulative distributions functions (CDF). It can be seen that the CDF from the assignment using the DOC function is entirely to the right of the CDF from the shortest path assignment. This shows that for any given level of 'acceptable' error, a higher proportion of acceptable link flow predictions were achieved with the DOC function than with the shortest path assignment. The MAPE on the test set using the shortest path assignment was 67.6% while

the MAPE on the test set using the DOC function was 48.6%. This is a significant improvement considering the simplicity of the cost function and the small number of link observations which were available for the calibration process. This has important implications for transport modelling in Ireland, where the NTA is in the process of adopting a new transport model, the Regional Modelling System (National Transport Authority, 2015a). This model uses a simple shortest path assignment for cycling. While shortest-path assignment is an improvement on the previous GDA model which did not assign cycling trips to the network at all, the results of this study show that more accurate assignments could be achieved by using the DOC function. Moreover, it is likely that further iteration on the form of the DOC function would lead to further improvements in accuracy.

The calibrated parameters reported here are specific to the Dublin network and so it is uncertain whether they would generalise well to other transport networks. However, the methodology and/or form of the DOC function could easily be adopted in order to calibrate a cycling cost function for any other network where observations of cyclist traffic volumes are available.

Table 7.10 Calibration of DOC function results

	σ		τ		θ_1			
Run	Initial	Final	Initial	Final	Initial	Final	Final F	Iterations
1	0.84	0.76	3.88	3.85	0.01	1.35	4.18E+06	39
2	0.88	0.99	1.10	1.22	0.88	1.17	4.16E+06	33
3	1.11	0.82	3.83	3.76	0.47	1.35	4.08E+06	49
4	**0.45**	**0.68**	**4.48**	**4.46**	**0.34**	**1.37**	**4.06E+06**	**44**
5	0.16	0.67	4.12	4.12	0.71	1.37	4.09E+06	38
6	0.03	0.70	3.01	3.04	0.80	1.34	4.23E+06	36
7	1.54	1.54	1.08	1.08	1.02	1.03	4.21E+06	26
8	0.37	0.76	1.08	1.22	0.75	1.22	4.14E+06	36
9	0.32	0.70	3.96	3.95	0.43	1.36	4.10E+06	42
10	1.70	1.36	1.72	1.72	0.10	1.18	4.20E+06	51

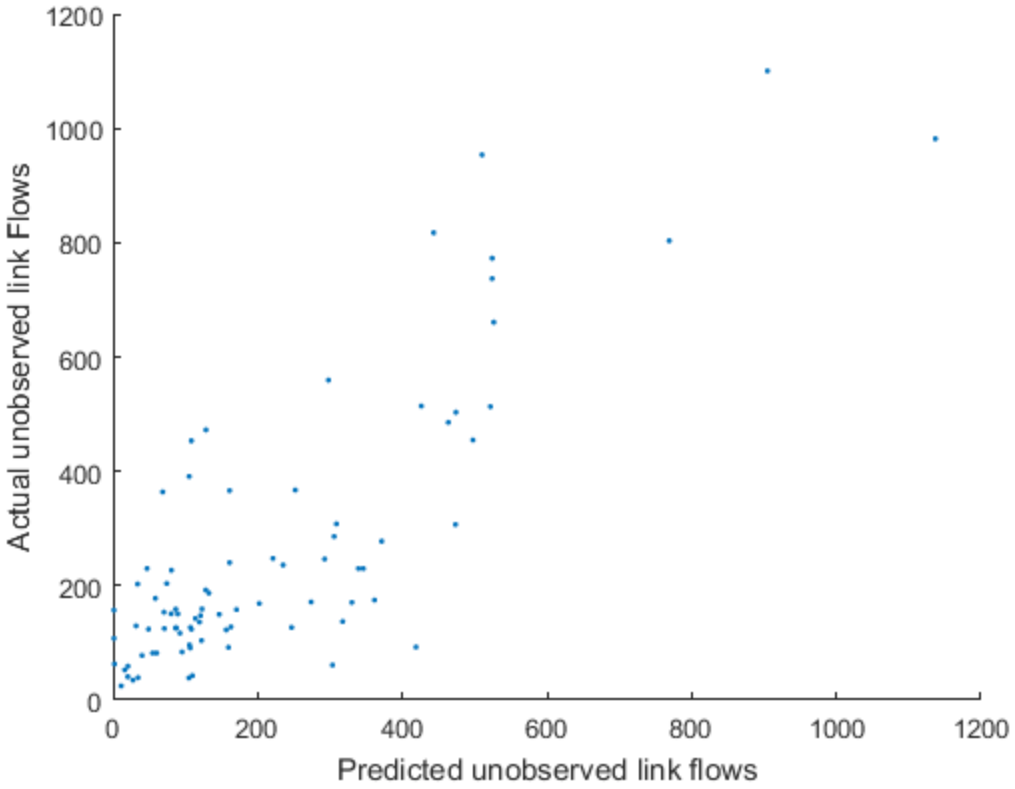

Figure 7.10 Scatterplot of predicted vs observed flows on the links of the test set.

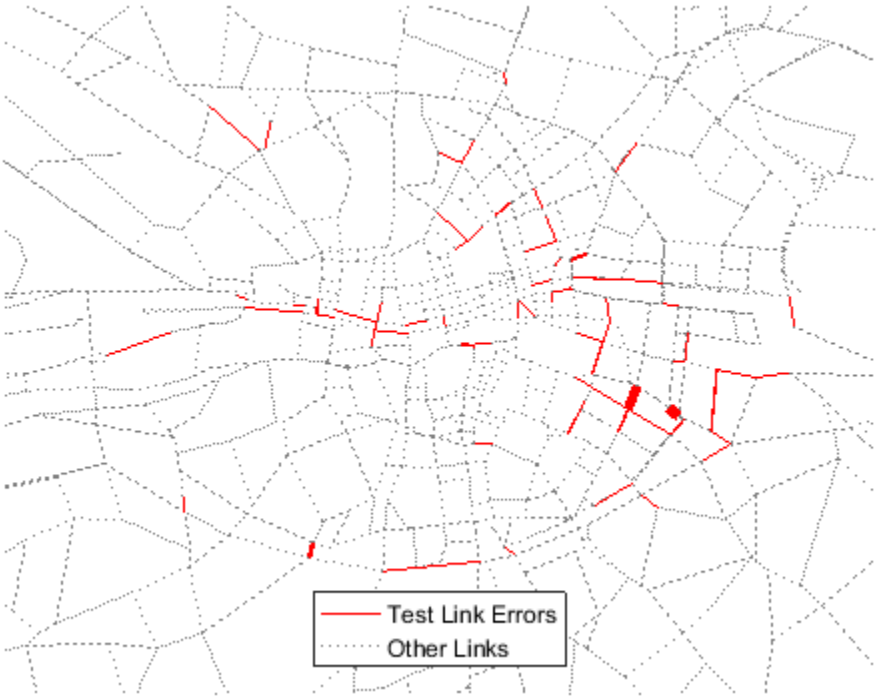

Figure 7.11 Prediction errors on test links; link widths shown are proportional to absolute percentage errors.

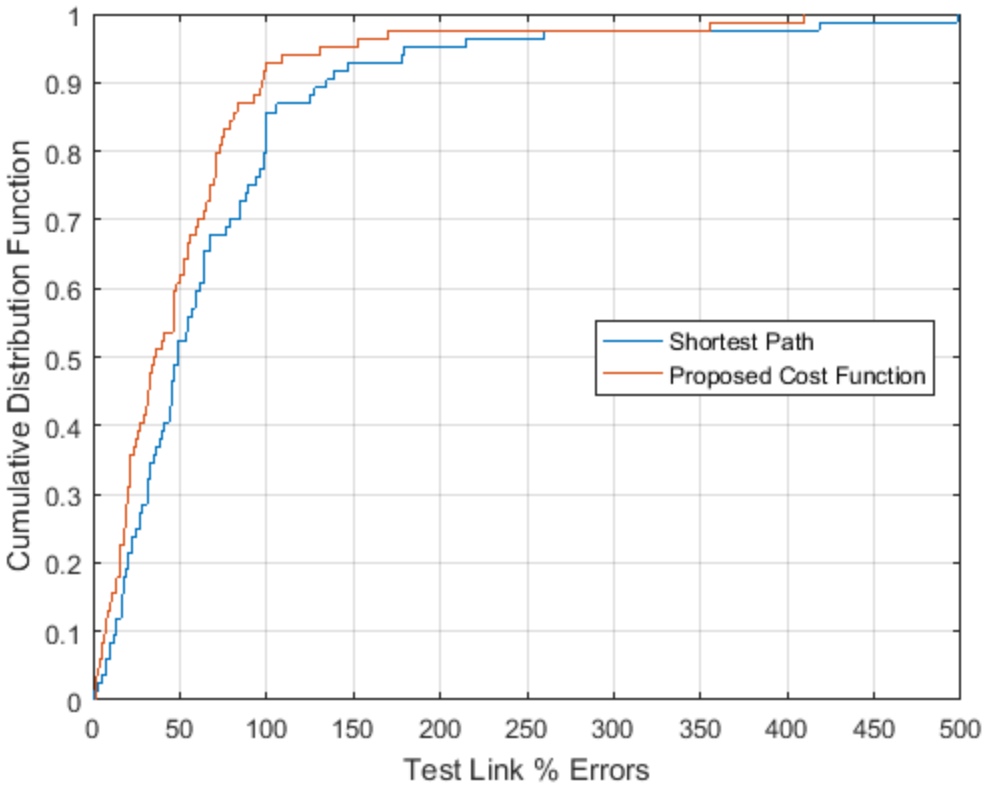

Figure 7.12 Empirical CDFs of absolute percentage errors on the test set using (i) shortest path assignment and (ii) assignment using the Disutility of Cycling (DOC) function.

7.7 Conclusions

In this chapter, it has been demonstrated that cycling cost functions can be calibrated using the ITAP by formulating the ITAP as a MPEC and solving it using a descent method. It has further been shown that the gradient information required by the MPEC can be obtained either by sensitivity analysis or an empirical method, both of which provide similar gradient directions. The sensitivity analysis method appears to work more efficiently for small network problems but for larger problems, the empirical method is more efficient. Furthermore, a particular form of a cycling cost function has been suggested and, using the descent algorithm described, it has been shown that even when calibrated using a small number of network observations, it outperforms shortest path assignment. It should be noted that the cost function chosen in this chapter was simple and did not taken into account many other potentially important variables such as hills, turn frequency and route aesthetics. It is therefore likely that further iterations of cost functions calibrated using this method will produce better predictions, particularly if larger numbers of link observations are available.

The inclusion of cycling in the NTA Regional Modelling System was an important step towards improved planning for cycling. However, the model of cycling behaviour used is based on a principle which has been shown by many studies to be inadequate and so the results of the model with respect to cycling are unlikely to be of much value. Such modelling may even have a negative impact on the planning process by giving a false sense of precision to highly simplistic predictions of cyclist behaviour. This chapter has also shown that transport authorities could significantly improve models of cycling behaviour by replacing shortest path assignment with assignment based on a disutility function which accounts for motorised traffic levels and cycling facilities—even if this disutility function is still relatively simple. Transport authorities and policymakers wishing to include cyclists in strategic transport modelling should consider using a more realistic disutility function such as the DOC function to model cyclist behaviour.

Chapter 8: Optimal design of cycle networks

8.1 Introduction

In the second chapter of this thesis, it was noted that although many studies in the past ten years have quantified the health and environmental impacts of cycling, most of the methodologies had limited value for evaluating real-world transport policies. This is because they were based on hypothetical scenarios where increased cycling takes place but gave no consideration to the courses of action which may help policymakers to achieve the scenarios. Similarly, in Chapters 3 and 4 of this thesis, the impacts of cycling in Dublin were evaluated with reference to hypothetical increases in cycling. A useful extension to this framework would be one which allowed a user to find the optimal infrastructure design and/or policies which would maximise total societal benefit, taking into account the health and environmental impacts of cycling.

The tool which is used in the literature for optimising the decisions of transport authorities in general is the Network Design Problem (NDP) (Boyce, 1984). This problem is generally formulated as a bilevel optimisation problem whereby the objectives and decisions of the transport authority are represented by the upper level and the behavioural responses of the users within the network are represented by the lower level. If the network equilibrium is represented as a VI instead of an optimisation, the NDP can be formulated as an MPEC. As described in Chapter 2, very few studies have experimented with using the NDP to design cycling infrastructure layouts. Cycle network design is instead based on evaluation of alternatives, sometimes making use of tools such as evaluation matrices. A limitation of these approaches is that they can only reveal the value of an existing design but cannot find the optimal or near-optimal design, nor can they determine whether the existing design is optimal. Even in an unrealistically small network of 20 links where a cycle lane can be either built or not built on each link, the number of possible alternatives would be over a million. Clearly, for even a very small transport network, it is highly unlikely that the optimal cycle network would be found through evaluation of alternative designs. Although in recent years a small number of studies have used the NDP to design cycle networks, no study to date has considered the health and environmental impacts of cycling in the objective of a NDP. Additionally, the models of network equilibrium in the lower level optimisation have tended to be overly simple.

In order to formulate a NDP to optimise a cycle network, taking into account the health and environmental benefits of cycling, it must be possible to (i) quantify the net benefit of given amounts of cycling and motorised transport and (ii) predict the amounts of cycling and motorised transport which would result from any possible design of a cycle network. Chapters 3 to 6 and chapter 7 of this thesis addressed the first and second tasks respectively. This chapter will draw on elements from all of the work up to this point in the thesis in order to develop a NDP for systematically designing cycling network layouts in order to maximise the net benefits to the network users and society. The rest of the chapter is organised as follows. The model formulation will first be described, followed by a Genetic Algorithm (GA) which may be used to solve the problem. A simple numerical example will then be given to demonstrate the process and the chapter will be concluded with some discussion of the significance of this work.

8.2 Methodology

This section describes a mathematical model and solution algorithm for allowing a transport authority to identify the links in an existing transport network where cycle facilities should be introduced in order to maximise societal benefit (SB). The SB is a function of travel costs, infrastructure costs, health impacts, traffic collisions and environmental impacts. The SB is influenced by the decisions of the both the transport authority and the network users.

The decision making process which must be represented by the model is complex. The transport planner first decides where in the network the facilities should be introduced and in response to this decision, the network users choose their travel behaviour in order to maximise their own perceived benefits. However, the transport planner would also like to anticipate the travel responses of the network users and make decisions such that when the network users choose their travel behaviour, the resulting SB is as high as possible. Since the transport planner makes decisions before the network users, the decision making process can be thought of as a Stackelberg game where the transport authority is the leader and the network users are the followers (Colson et al., 2007). The decision making process can therefore be represented by a Mathematical Programme with Equilibrium Constrains (MPEC) and this MPEC can be solved to find the optimal design of the cycle network to maximise the SB. The MPEC, as described in Chapter 7 is a generalisation of the bilevel optimisation framework which allows the lower level optimisation to be replaced with a variational inequality (VI).

The rest of this section describes the formulation of the MPEC to represent this decision making process and the solution algorithm which can find a near-optimal strategy for the transport authority.

8.2.1 Model Formulation

8.2.1.1 Equilibrium constraints: multi-modal network equilibrium

The equilibrium constraints of the MPEC in this study represent the travel choices of the network users who are assumed to try to maximise their own utility in response to the decisions of the transport authority. The behaviours of the cyclists and motorists in the network are assumed to be governed by the network equilibrium model described in Chapter 7 with path-size logit-based route choice, logit-based mode choice and elastic demand. The equilibrium flow pattern therefore must satisfy Eq. 7.2 to Eq. 7.7. These conditions are equivalent to the Karush-Kuhn-Tucker (KKT) conditions of the following variational inequality (VI):

$$h^* \in V(\gamma) \Leftrightarrow \sum_{w\in W}\sum_{m\in M}\sum_{p\in P}\left(u_p^m(\gamma)+\frac{1}{\theta_1}\ln\left(\frac{1}{PS_p{}^m}\frac{h_p^{m*}}{q_w^{m*}}\right)\right)\left(h_p^m-h_p^{m*}\right)$$
$$+\sum_{w\in W}\sum_{m\in M}\frac{1}{\theta_2}\ln\left(\frac{q_w^{m*}}{q_w^{*}}\right)\left(q_w^m-q_w^{m*}\right) \qquad \text{Eq. (8.1)}$$
$$+\sum_{w\in W}\frac{1}{\eta}\ln\left(\frac{q_w}{q_w{}^0}\right)\left(q_w-q_w{}^*\right)\geq 0,\ \forall\left(h_p^m,q_w^m,q_w^m\right)\in\Omega_2$$

Where γ is the vector of decision variables of the transport authority and all other variables have the same meaning as in Chapter 7.The equilibrium path flow vector h^* can depend on the vector of decision variables γ due to the influence of γ on the mode-path disutilities, $u_p^m(\gamma)$. For example, the cycling cost function could depend on the traffic with which the cyclist interacts, as is the case with the DOC function. Also, the addition of a cycle lane can be assumed to decrease the road capacity available to motor vehicles. If, for example, the BPR function is used to model driver disutility, the addition of the cycle lane would increase driver disutility on that link.

8.2.1.2 Objective function: system optimal network design

The objective function of the MPEC represents the decision making process of the transport authority. The transport authority is assumed to be concerned with maximising total SB for both the users of the transport network and the surrounding population. The total is quantified by an objective function which includes the cost of the infrastructure and all of the benefits and risks of travel considered in Chapter 3: health impacts of physical activity and pollution exposure, societal impacts of environmental emissions, traffic collisions and travel costs. Additionally, since elasticity of demand will be considered, the total number of trips will not be fixed and so the benefits of travel itself must be included. The transport authority must decide which cycling

facility, if any, to place on each existing link in the network in order to maximise this . This optimisation problem is represented as follows:

$$\begin{aligned} &\max_{\gamma} \quad SB(x,\gamma) \\ &s.t. \quad x_s = \sum_{p\in P} h_p^m \delta_{sp}, \forall s \in S \\ &\qquad \mathrm{h} \in V(\gamma) \\ &\qquad \gamma_s^f \in \{0,1\}, \forall f \in F, s \in \tilde{S} \\ &\qquad \sum_{f\in F} \gamma_s^f = 1, \forall s \in \tilde{S} \\ &\qquad \gamma_s^{nf} = 1, \forall s \in S \setminus \tilde{S} \end{aligned} \qquad \text{Eq. (8.2)}$$

Where $SB(x,\gamma)$ is the , γ_s^f is a binary decision variable indicating whether or not link *s* is assigned to facility type *f*, F is the set of possible facility-types, γ is the vector of all decision variables γ_s^f , $\tilde{S}$ is the set of all links where a cycle facility could be added and $nf \subset F$ indicates no cycling facility. The constraints ensure that no more than one type of cycling facility can be added to each link and no cycling facilities can be added to links not contained in $\tilde{S}$. The equilibrium constraints also ensure that at any feasible point, the network equilibrium problem, parameterised by γ, is satisfied. In the framework of this study, the over a given time period can be defined as follows:

$$SB(x,\gamma) = PA - AP_{In} - TC - AP_{Ex} - GHG - N_{Ex} + S_C - C_I \qquad \text{Eq. (8.3)}$$

Where PA is the value of the physical activity health impact, AP_{In} is the cost of the traveller pollution exposure health impact, TC is the cost of traffic collisions, AP_{Ex} is the cost of air pollution emissions, GHG is the cost of greenhouse gas emissions, N_{Ex} is the cost of noise pollution, S_C is the consumer surplus and C_I is the cost of the cycling facilities.

8.2.2 Solution Algorithm

As discussed in Chapter 7, MPECs are intrinsically hard problems, particularly if a guaranteed global optimum is required. The research focus to date has been on efficient procedures for finding near-optimal solutions. The descent based approach used to solve the MPEC in Chapter 7

would not be appropriate for the current problem as the decision variables are discrete and therefore it would be impossible to estimate gradients with respect to them. Genetic algorithms (GA) are a class of algorithms which are applicable to a wide range of problems as they don't require the computation of gradients or Hessians (Chong and Zak, 2013). Yin (2000) also showed that GAs can be used to solve common bilevel programmes in transportation system planning and recently Mesbah et al. (2012) used a GA to solve a cycle network design problem, with some structural similarity to the one presented in this chapter. For these reasons, a GA was used to solve the MPEC in this study.

GAs aim to generate progressively better solutions to an optimisation problem by a process resembling biological evolution. The process involves first generating an initial pool of candidate solutions known as chromosomes. The attractiveness of each of these candidates is then evaluated by means of a fitness function. A new pool of candidates is formed by selecting candidates from the old pool with a selection probability proportional to their fitness. Some of the chromosomes are then modified using operations known as crossovers and mutations to create the next generation of candidate solutions. This process continues iteratively until the algorithm converges to an acceptable solution. Because GAs search from a population of candidate solutions rather than a single point, they are less likely to get stuck at a local optimum. The use of probabilistic transition rules also contributes the robustness and globality of the solutions found by GAs (Yin, 2000).

The first step in applying a GA to the solution of the MPEC in this study was to define the representation scheme which maps the vector of decision variables γ to a string of symbols. Each symbol is referred to as a gene and the string of genes is referred to as a chromosome. The chromosome used to represent the layout of cycle facilities in a transport network was a string of genes Ψ_s of length *L* where *L* was the number of links in the network. The set of possible values of each gene was the set F. Each gene Ψ_s in the chromosome represented the type of facility on link *s* such that $\Psi_s = f \Leftrightarrow \gamma_s^f = 1 \& \gamma_s^g = 0, \forall g \neq f$. Having defined the representation scheme, the rest of the steps of the GA could then be carried out. These steps are summarised in Table 8.1 and explained in detail below. In the *Initialisation* step, an initial population of chromosomes of size, *N*, is created where each gene of each chromosome is randomly assigned a value from the set *F*. In the *Evaluation* step, the value of the objective function corresponding to each chromosome must be calculated. Since the objective function is parameterised by the dependent variable ***x***, the VI must be first be solved by finding the network

equilibrium corresponding to the network design represented by the chromosome. The equilibrium link flow pattern $\boldsymbol{x}$ is found by combining diagonalization and the method of successive averages as discussed in Chapter 7. The value of the objective function $SB(\boldsymbol{x},\boldsymbol{\gamma})$ is then calculated and its value becomes the fitness of the chromosome. In the *Crossover* step, pairs of chromosomes are randomly selected from the mating pool without replacement such that the proportion of chromosomes selected is equal to the predetermined crossover probability, P_c. For each pair of chromosomes selected, a crossing site is randomly selected between 1 and *L*-1 according to a uniform distribution. The crossover operation exchanges the substrings to one side of the crossing site between the two parents to create two new offspring chromosomes which replace the parents in the mating pool. In the mutation step, each gene in each chromosome is taken and with a pre-determined probability, P_m, is randomly assigned a new value from the set, *F*. In the *Evolution* step, this evolved mating pool becomes the new population. If a predetermined stopping criterion is met, the algorithm terminates. Otherwise, it returns to the *Evaluation* step with the new population.

During each iteration of the GA; the best-so-far chromosome—the chromosome with the highest fitness function in any iteration so far—is tracked. As long as the best-so-far fitness is increasing over time, the algorithm is working effectively. When the algorithm terminates, the best-so-far solution becomes the ultimate solution to the MPEC.

Table 8.1 Steps of the Genetic Algorithm for solving the MPEC

Step	**Description**
Initialisation	Set $k=0$ Create initial population of chromosomes $P(k)$.
Evaluation	Evaluate the fitness of each chromosome in $P(k)$.
Selection	Create a mating pool $M(k)$ of chromosomes by selecting chromosomes from $P(k)$ (with replacement) where the probability of selection is in proportion to the fitness of the chromosome.
Crossover	Perform the crossover operation on pairs of parent chromosomes randomly chosen from $M(k)$ such that the probability of any chromosome being chosen is a predetermined value, P_c.
Mutation	Perform the mutation operation on randomly chosen genes from $M(k)$ such that the probability of any gene being chosen is a predetermined value, P_m.
Evolution	Assign the altered $M(k)$ to become the new population $P(k+1)$
Iteration	If stopping criterion has been met, terminate algorithm. Otherwise, increment k and return to the *Evaluation* step

8.3 Numerical Example

In this section, the model formulation and solution are demonstrated using a numerical example on a test network. For simplicity, travel is modelled during a single time period which is assumed to representative of the total average traffic per day. In practical applications, it would most likely be necessary to model several periods of the day and days of the week.

8.3.1 Test network

The test network used in this example is based on the simple network presented in Li et al. (2015). The network is shown in Figure 8.1. It has 9 nodes, 12 links, 2 origins and 1 destination. The details of the links are summarised in Table 8.2. In this example, there are three possible facility types for each link: no facility, kerbside cycle lane and segregated cycle lane. It is assumed that if a cycle facility is introduced on a link, the capacity for motor vehicles on that link is reduced. Therefore, each car link has three possible capacities according to the cycle facility which is present. The car capacities for all links with no cycle lanes, roadside cycle lanes and segregated cycle lanes are 5000, 4000 and 3000 respectively. As in Chapter 7, it was assumed that cyclists on segregated cycle lanes do not experience any increase in disutility due to increased cyclist traffic and so the capacities of segregated cycle lanes can be considered to be effectively unlimited. The first O-D pair is from node 1 to node 9 and the second O-D pair is from node 5 to node 9. There are six possible routes between O-D pair (1,9) and 2 possible routes between O-D pair (5,9) and these are detailed in Table 8.3. The same routes are available to both cyclists and drivers. The potential travel demand, q_w^0, was 10000 for each O-D pair.

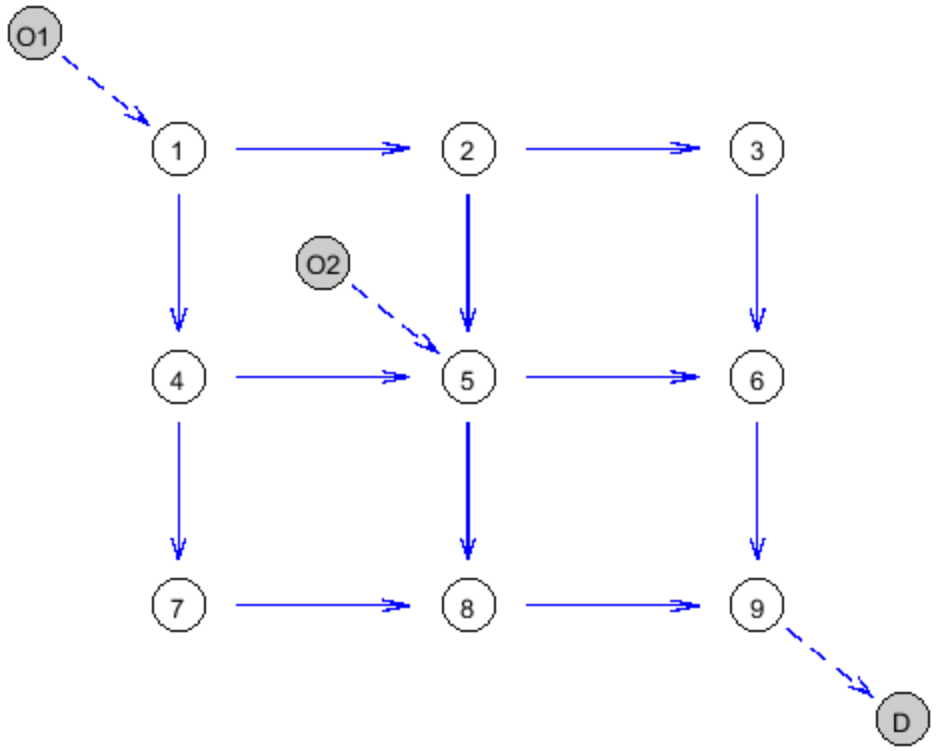

Figure 8.1 Test network

Table 8.2 Link characteristics of test network

Link	A Node	B Node	Length (km)
1	1	2	3
2	2	3	6
3	1	4	4
4	2	5	6
5	3	6	3
6	4	5	7
7	5	6	5
8	4	7	6
9	5	8	5
10	6	9	5
11	7	8	4
12	8	9	4

Table 8.3 Route characteristics of test network

OD	Route	Links
(1,9)	1	1,2,5,10
(1,9)	2	1,4,7,10
(1,9)	3	1,4,9,12
(1,9)	4	3,6,7,10
(1,9)	5	3,6,9,12
(1,9)	6	3,8,11,12
(5,9)	7	7,10
(5,9)	8	9,12

Since the test network is a simple "toy" network, the choice of parameters used in the problem can be considered to be arbitrary. However, as discussed below, parameter values which are relevant to Ireland and/or Europe were used wherever possible.

The disutility of motorists is governed by the BPR function with the same parameters as in Chapter 7. A fixed operating cost of €10 per driving trip also applies. The disutility of cyclists is governed by the DOC function. For on-road cycling, the calibrated parameters from Chapter 7 are used: σ = 0.68 and τ =4.46. Cyclists using roadside lanes are assumed to experience a real or perceived interaction with traffic and so their disutility increases with motor vehicle traffic on the link. However, it can be expected that the increase in disutility would not be as great as if they were cycling on a road without any lane. Since kerbside lanes were not modelled in Chapter 7, for the purpose of this demonstration it is assumed that the cyclists on roadside lanes experience an increase in disutility due to link congestion equal to half that which would be experienced if no lane were present. This is a somewhat arbitrary value. However, multiple studies have shown that the perceived benefit of roadside lanes to cyclists lies somewhere between the benefit of segregated lanes and no cycling facility (Buehler and Dill, 2016). Therefore, sigma is given a value of 0.34 for cycling on roads with a kerbside lane. The values of the other network parameters were $\theta_1 = 0.2$, $\theta_2 = 0.2$, $\alpha_t = €10/hr$, $\bar{v}_s^c = 14\text{km}/hr$, $\bar{v}_s^a = 40\text{km}/hr$.

8.3.2 Calculating Societal Benefit

Societal benefit, which defined in Eq. 8.1, was evaluated by drawing from the finding of Chapters 2 to 6. C_I is the only component of the SB which occurs at a single point in time. For all other impacts, the benefit/cost over a timeframe of ten years was calculated. This was done by first calculating the annual value and then calculating the Net Present Value (NPV) over ten years with a discount rate of 5%—the rate recommended by the World Health Organisation (WHO) for

calculating NPV of cycling using the Health Economic Assessment Tool (HEAT) (WHO, 2014). For the impacts associated with chronic illnesses of the travellers themselves- PA and AP_{In} - a linear build-up period of 5 years for the health impacts to take effect was also assumed. This is consistent with the approach recommended by the WHO (WHO, 2014).

The annual benefits due to physical activity were calculated using the same models as described in Chapter 3. It was assumed that the type of cycling facility did not influence the quality or intensity of physical activity. The dose response function (DRF) required estimation of the baseline physical activity levels. Since this numerical example was based on simulated individuals rather than census data, the baseline DALY rates and proportions of individuals with low, moderate and high activity levels were simply assumed to be the same as for the general population of Ireland (IPSOS MRBI, 2015).

The change in annual DALYs lost due to air pollution was estimated using similar models to Chapter 3 with one important difference. It was shown in Chapter 6 that the presence of cycling facilities affects cyclist exposure to air pollution. Therefore in addition to the mode-specific scaling factor, additional facility-specific scaling factors were used to correct for the effect of cycling facilities on pollution exposure. Based on the results of Chapter 6, the scaling factors used for on-road cycling, kerbside cycle lanes and segregated cycle lanes were 1, 1.15 and 0.91 respectively based on the average of the impacts of these facilities on CO concentrations and NO_x concentrations.

The costs associated with fatal, serious and minor injuries were estimated using the same non-linear collision model and collision data as in Chapter 3. In this numerical example, the effect of cycle lanes on actual collision risk of cyclists was not modelled as there was insufficient quantitative evidence regarding the level of protection offered by cycling facilities. Although the collision risks while cycling on a segregated facility may appear to be minimal, many collisions in reality occur during manoeuvres at junctions where the segregation breaks. A difference in collisions risks for different facility types can be easily included in future studies if sufficient collision data are available.

The costs of noise pollution and GHG emissions were calculated based on the IMPACT 2014 handbook, similarly to Chapter 3. However, in this study, instead of estimating the avoided emissions costs attributable to the replacement of driving trips by cycling trips, the emissions costs due to the driving that did take place were calculated. This means that it was required to use average unit costs rather than marginal unit costs. For air pollution and GHG costs, the

average and marginal costs can be considered to be equal (Korzhenevych et al., 2014). However, for noise pollution, the marginal costs tend to be lower than the average costs. The IMPACT 2014 handbook only gives marginal noise costs of driving. However, the IMPACT 2008 handbook gives an average per-km noise cost for driving in European urban areas and so this estimate was used instead.

The consumer surplus represents the difference between the benefits of travel and the costs of travel as perceived by the network users themselves. For the network model with exponential demand function described by Eq. 8.1, the consumer surplus for a single modelled time period can be expressed as q_w/η (Li et al., 2015).

The infrastructure cost could be calculated as follows assuming constant per-km costs for each facility type:

$$C_I = \sum_{f \in F} \sum_{s \in S} \gamma_s^f \times d_s \times c^f \qquad \text{Eq. (8.4)}$$

Where d_s is the length of link *s* and c^f is the construction cost per km of cycle facility type *f*. The construction costs of roadside cycle lanes and segregated cycle lanes were based on estimates for the UK (Sustrans). The middle values of the cost range estimates for "Cycle lane with few junctions " and "Segregated path with minor junctions" were used. The values given in 2007 GBP were converted from GBP to Euro and corrected for inflation to 2015 to give values of €59,787/km and €298,935/km for roadside cycle lanes and segregated cycle lanes respectively.

8.3.3 Baseline

In order to establish a baseline, the network equilibrium was first found for the case where there are no cycle facilities on any links and the SB corresponding to this case was evaluated. The link flows of cyclists and motor vehicles are illustrated by Figure 8.2, Figure 8.3 and Table 8.4. Since node 9 is the destination node for all trips, the traffic volumes were highest on links in its vicinity. The total 10-year value of SB in the base case was €28.96M. As shown in Figure 8.4, this figure is dominated by the health benefits of physical activity, the health cost of traffic collisions and the greenhouse gas emission costs.

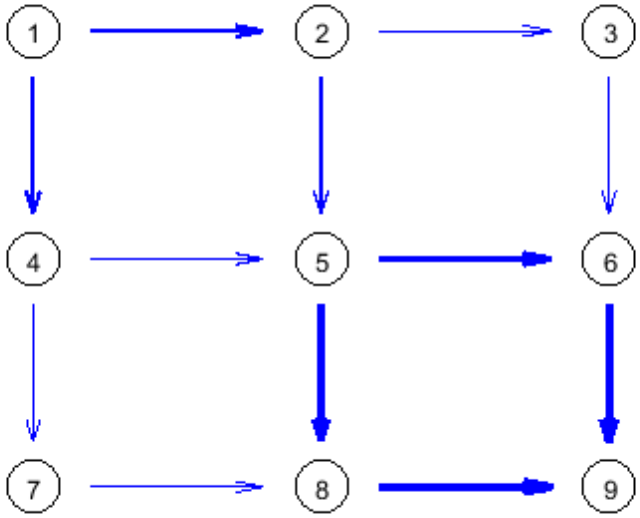

Figure 8.2 Car traffic in base case (no cycling facilities). Link thickness is proportional to traffic volume.

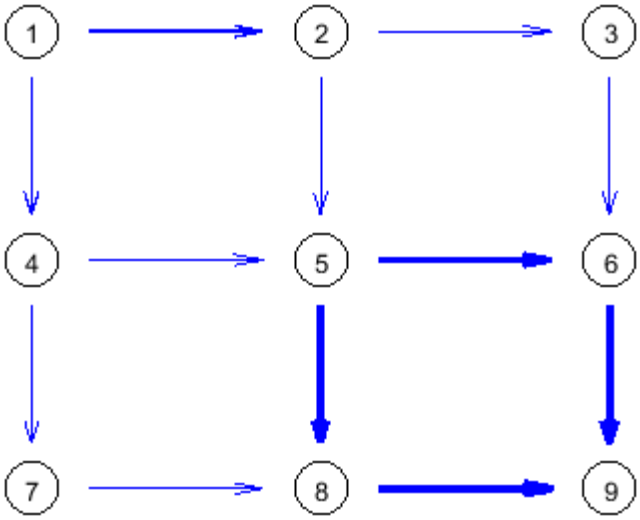

Figure 8.3 Bicycle traffic in base case (no cycling facilities). Link thickness is proportional to traffic volume.

Table 8.4 Link traffic volumes in base case (no cycle facilities)

Link	A Node	B Node	Length (km)	Car Traffic	Cyclist Traffic
1	1	2	3	1707	900
2	2	3	6	787	498
3	1	4	4	1597	738
4	2	5	6	919	402
5	3	6	3	787	498
6	4	5	7	829	294
7	5	6	5	2193	1857
8	4	7	6	768	444
9	5	8	5	2316	2050
10	6	9	5	2981	2355
11	7	8	4	768	444
12	8	9	4	3085	2494

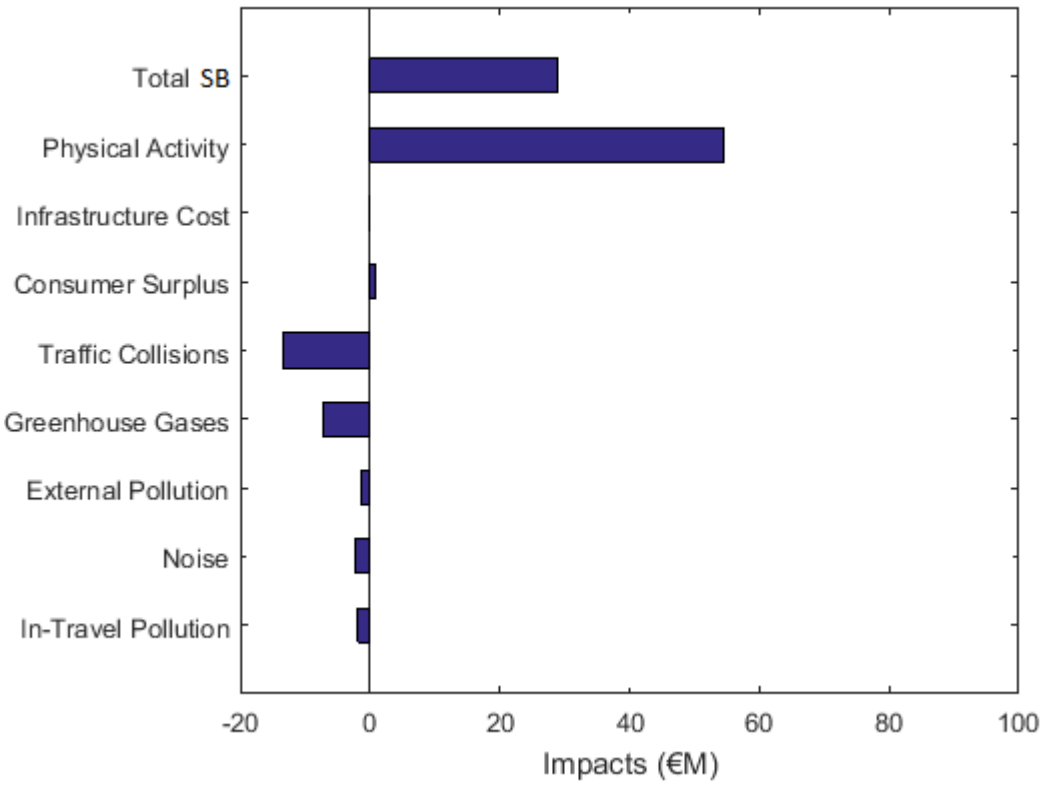

Figure 8.4 Societal benefit values at baseline (no cycle facilities)

8.3.4 Initial Results of GA

For the initial run of the GA algorithm, the algorithmic parameters, P_c, P_m, and N were given arbitrary values based previous on a previous study (Yin, 2000). In the next section, the impact of varying these parameters will be explored. The values chosen for the initial run were

$P_c = 0.6, P_m = 0.033, N = 30$. As a stopping criterion, an iteration limit of 300 was chosen. Figure 8.5 shows the evolution of the best-so-far fitness in each iteration. The highest fitness was found on iteration 263 which was close to the chosen iteration limit of 300. However, the algorithm was run again with an iteration limit of 600 and the fitness did not improve after iteration 263, indicating that the iteration limit of 300 is likely to be high enough for this example. The final value of the fitness function was a SB of €62.6M. The cycle network design which led to this SB value is shown in Figure 8.6. The segregated lanes have been introduced mainly on the links close to the destination node 9, which had the highest traffic of both cyclists and drivers. Only one roadside cycle lane was introduced and this linked node 1, one of the two origin nodes, to node 4. The placement of segregated lanes on the busiest links makes intuitive sense in that it creates the greatest reduction in travel costs for cyclists. However, the decrease in capacity for cars would also affect the travel times of a large number of drivers and so, even in this simple example, the best design was not clear in advance. The values of each component of the SB are shown in Figure 8.7. The biggest change from the baseline values was the increase in the physical activity benefit. This is due to an increase in cycling demand caused by the introduction of cycle facilities. The other positive changes were reductions in greenhouse gases, noise and external pollution. The negative impacts included an increase in traffic collisions and the cost of the infrastructure. These changes in societal benefit resulting from the introduction of cycle facilities are similar to the results of increasing modal share of cycling found in Chapter 3.

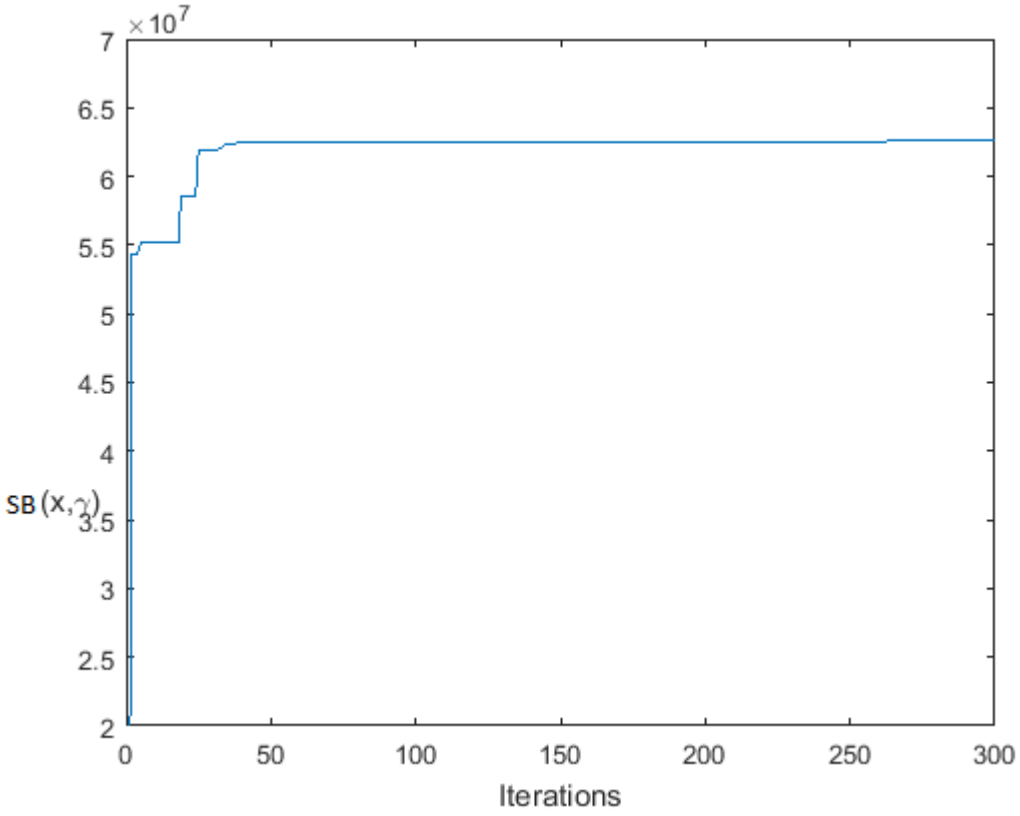

Figure 8.5 Evolution of best-so-far fitness in initial run of GA

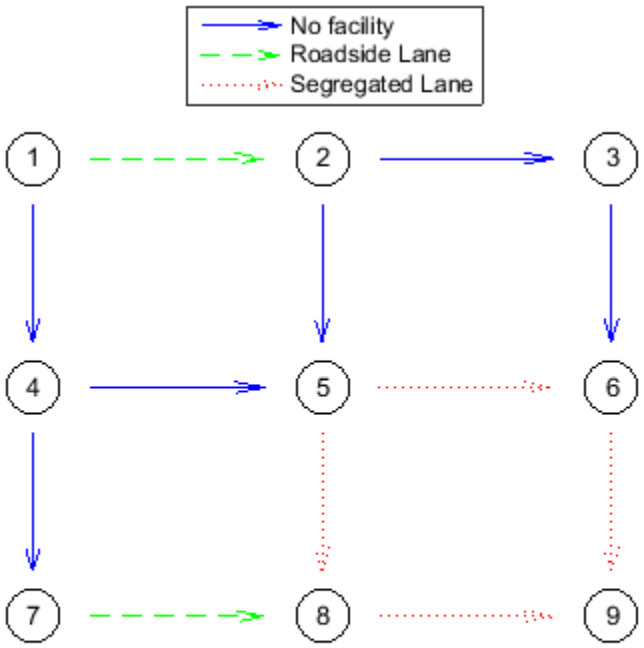

Figure 8.6 Cycle network design suggested by initial run of GA

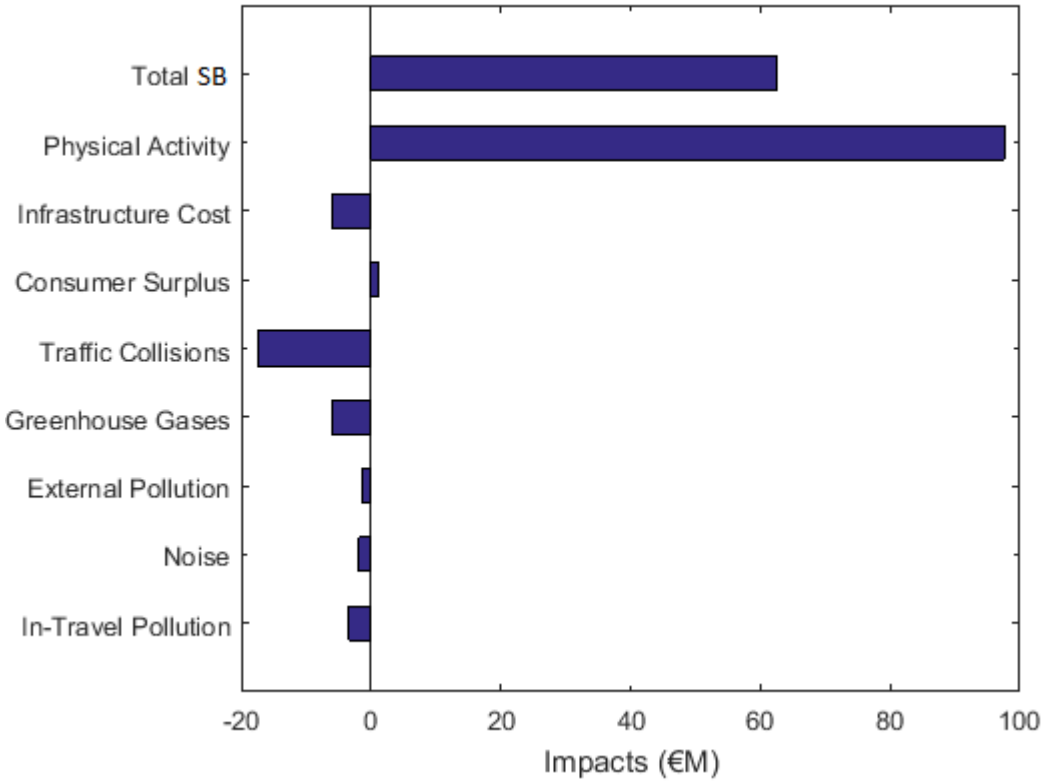

Figure 8.7 Societal benefit values resulting from solution of initial GA run

8.3.5 Effect of GA parameters

Some additional experiments were run in order to test whether the solution found by the GA was influenced by the values of the GA parameters: P_c and P_m. The GA was run in a nested loop, varying the value of P_c between 0 and 1 in steps of 0.04 and varying the value of P_m between 0 and 0.2 in steps of 0.008. This resulted in 625 runs in total. Of interest were the SB associated with the best solution found in each run and the number of iterations required to find the best solution in each run. As shown in Figure 8.8, there was no clear relationship between P_c and the ultimate SB or the number of iterations required. P_m also did not seem to influence the number of iterations required. However, the maximum societal benefit tended to increase with the value of P_m until P_m reached a value of about 0.05. Above this value, the value of P_m did not seem to have a strong influence on maximum SB. In general, low values of P_m in a GA increase the risk of the algorithm getting stuck at local optima but high values of P_m disturb the search direction too much so that the candidate solutions do not move towards better solutions. Since increasing P_m results in a slight increase in computation time, a P_m of about 0.1 would

seem to be an appropriate value for this example in order to avoid local optima without increasing computation time unnecessarily. The highest SB found across all 625 runs was a value of €62.83M, marginally higher than the highest SB found in the initial run of the GA. The design corresponding to this SB is shown in Figure 8.9. This same solution was found in 61 of the 625 runs. Since almost 10% of the runs of the GA produced the solution shown in Figure 8.9 and no better solutions were found, it is likely that this is the globally optimal solution to the problem. The values of P_c and P_m at which this solution was found are plotted in Figure 8.10. The figure does not show a strong pattern in the values of P_c and P_m which produced the best solution. This and the small difference between the initial best solution and the ultimate best solution suggest that, for this example, the efficacy of the algorithm is affected only slightly by the choice of these parameters. Even without tuning of the parameters, a solution to this problem which was very close to the global optimum could be found. However, it can be seen in Figure 8.10 that a relatively high number of the globally optimal solutions were found with $0.25 < P_c \leq 0.5$ and $0.04 < P_m \leq 0.08$ and so this is suggested as an appropriate range of these parameters for this problem.

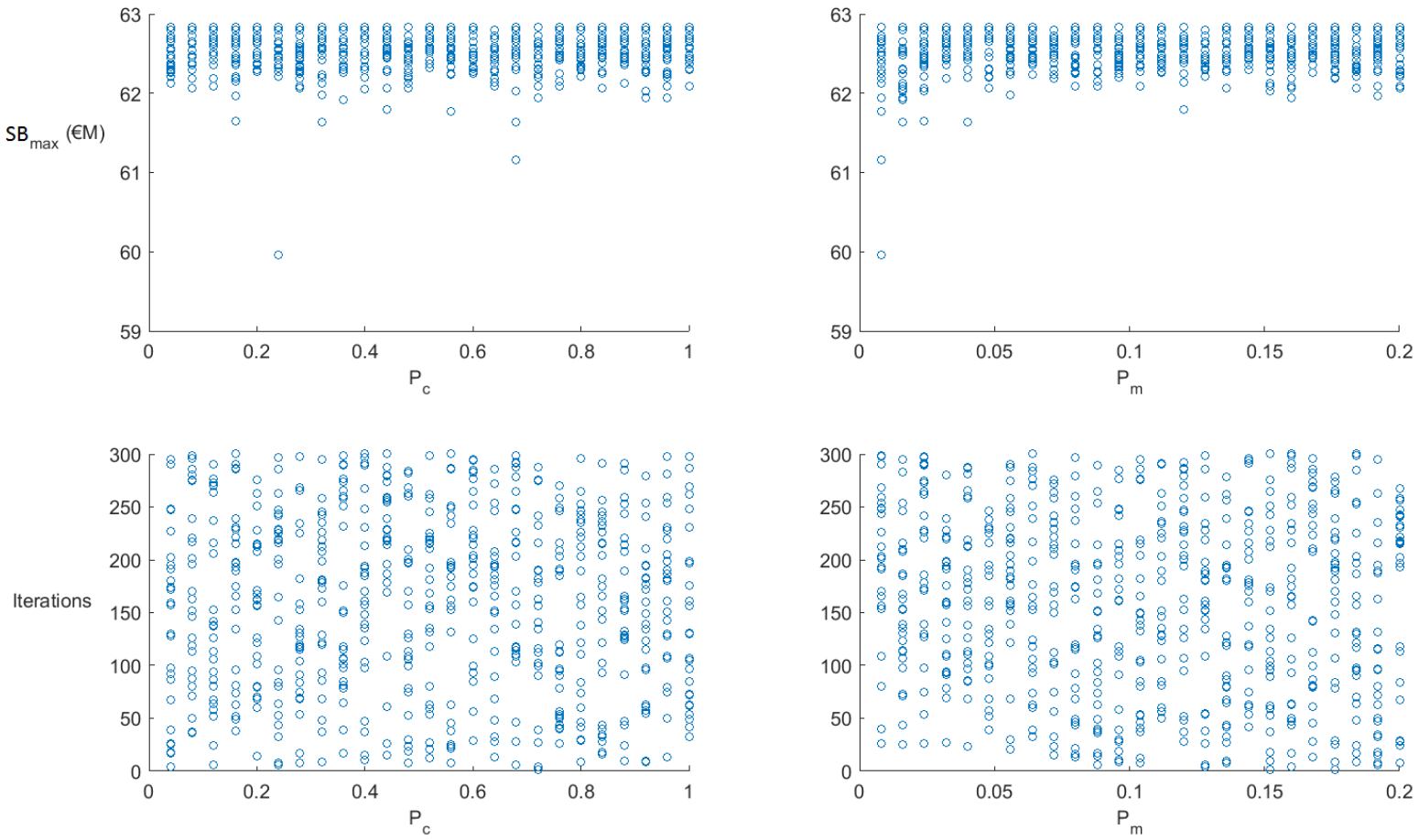

Figure 8.8 Influence of GA parameters P_c and P_m on the optimum SB value found by the GA and the iterations taken to find it.

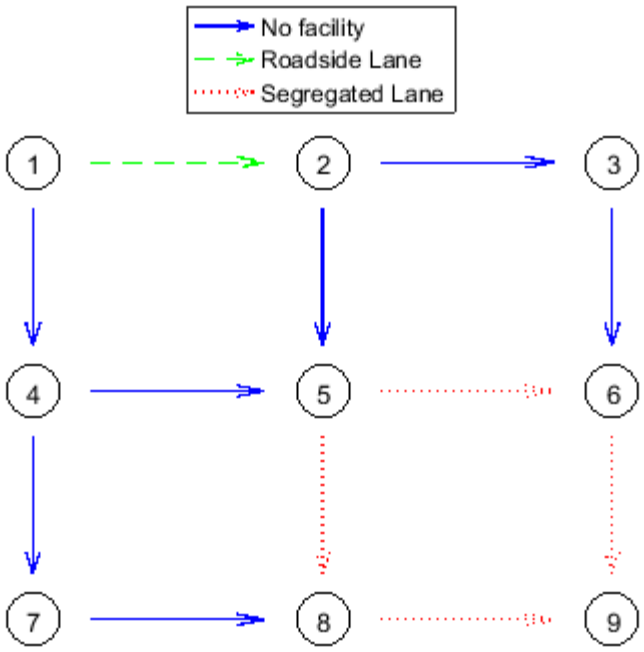

Figure 8.9 Best cycle network design found across all runs of GA

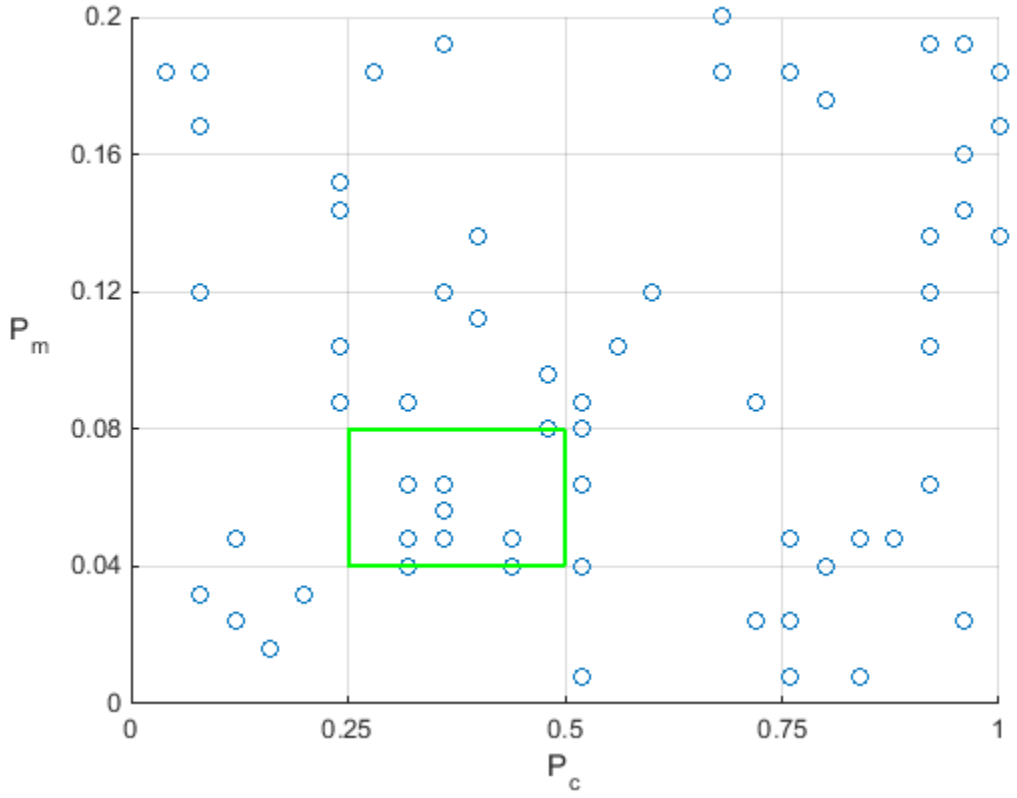

Figure 8.10 Value of P_c and P_m for the GA runs which found the overall best solution. The highlighted box shows the suggested interval.

8.4 Conclusions

This study has combined traditional transport network optimisation tools with recent research into the health and environmental impacts of active travel to develop a useful tool for maximising the societal benefits of investments in cycling infrastructure. A MPEC formulation and solution algorithm were developed which can identify the best design of a cycle network in order to optimise public health, environmental impacts and travel benefits and costs at the societal level. This adds to growing area of research which aims to develop software based tools to aid in the design of cycle networks. Studies such as (Lovelace et al. (2015)) and (Vandenbulcke et al. (2011)) had previously developed tools to identify areas or O-D pairs with high potential for increased cycling. The tool presented in this chapter builds on this work in a number of ways. While previous tools could identify potential for cycling at the O-D or municipal level, this tool identifies interventions at the level of individual streets. Previous tools were ultimately concerned only with increasing levels of cycling. This tool aims to find the optimum investment in order to maximise the net benefit to society taking into account health and environmental impacts, travel costs and infrastructure costs. The intervention which maximises this combination of impacts will not necessarily be the intervention which would maximise the increase in cycling. The tool presented in this chapter also has advantages over traditional appraisal methodologies such as the CAF (Department of Transport, 2016) or WebTAG (Department of Transport, 2013) as they are only suitable for evaluation of a small number of predefined designs. They cannot suggest new designs or find the optimal design. A few previous studies had presented cycle network optimisation models but none of these had considered health impacts which are an important driver of investment in cycling infrastructure. Previous optimisation based tools had also used very simple models of driving and cycling behaviour which could not be expected to accurately capture the changes in behaviour of cyclists and drivers in response to an intervention. Using the foundations built by the previous chapters of this thesis, this study included more aspects of societal benefit and modelled driver and cyclist behaviour more realistically than any previous studies. It has been shown that the model and algorithm presented can efficiently find optimal or near-optimal solutions to the cycle network design problem. By tuning the algorithmic parameters, the globality of the solution could be ensured but this would not necessary in order to find a near-optimal solution. The algorithm presented is robust as it does not depend on gradients or Hessian information. This means that the objective function and equilibrium formulations of the model can easily be changed without numerical difficulties. This framework can be applied to case studies of real transport networks if data such as baseline DALY rates and traffic collision risks and calibrated disutility functions for

each transport mode are available. The calibration approach introduced in Chapter 7 can be used to calibrate a cycling cost function if needed.

Chapter 9: Conclusions

The main objective of this thesis was to develop methods for quantifying the benefits and risks of urban cycling and for optimising a cycle network with regard to these benefits and risks. This has been achieved through use of statistical models, analysis of data collected using a custom sensing node and development of optimisation models and solution algorithms.

This chapter concludes the thesis by summarising the main contributions, providing a critical assessment of the work carried out, discussing the implications of the findings and suggesting directions for future research.

9.1 Main Contributions

The main contributions of this thesis can be discussed under three themes: quantification of the benefits and risks of urban cycling, measuring and analysing the environmental exposures of urban cyclists and development of tools for modelling and optimisation of cycling in multi-modal transport networks. Each of these areas will now be discussed in turn.

Chapter 2 of this thesis, among other contributions, provided a critical assessment of the existing methodologies for quantifying the health benefits and risks of cycling at the societal level. It was found that there were significant heterogeneities in the approaches taken by different studies in recent years and that these differences in approaches, could significantly influence the results. In particular, the physical activity impacts could vary widely—the BOD approach being more conservative than mortality based approaches. Based on the findings of this review, a framework for quantifying the benefits and risks of cycling was developed in Chapter 3, which was conservative, realistic and included a comprehensive analysis of uncertainties. This framework was applied to a case study of Dublin and it was found that the net health and environmental impacts of increasing the modal share of cycling in Dublin would be strongly positive, largely due to the health benefits of physical activity. This was the first study to quantify the health and environmental impacts of cycling alongside the change in travel costs to both the cyclists and the rest of the network. When the costs of travel itself were also included, the central estimate of net impact was similar but the uncertainty increased significantly—mainly due to the uncertainty with regard to the disutility of travel by bicycle. A limitation of the approach taken in this chapter, shared with all previous studies in this area was that in reporting total impacts, the potential for negative health impacts to some individuals may be masked by the health benefits to others. Chapter 4 therefore extended this modelling framework in order

to carry out the first study to estimate the distribution of the health impacts which can be expected as a result cycling at an individual level. This methodology was also applied to a case study of Dublin and it was found that, contrary to popular belief, there may be certain demographic groups for whom the expected health impacts of cycling are negative. In particular, male cyclists between the ages of 20 and 30 may experience negative health impacts on average. If the benefits and risks of cycling are only studied at a more aggregate level, these negative impacts can be expected to be masked by the positive health impacts experienced by other groups of cyclists and by non-cyclists.

Chapters 5 and 6 aimed to analyse the factors influencing the environmental exposures experienced by urban cyclists in Dublin. First, an environmental sensing node, the BEE node, was developed which is capable of being easily carried by a cyclist in a backpack and measuring their exposure to air and noise pollution. The BEE node included low-cost electrochemical gas sensors which were validated to a high degree of accuracy through comparisons with much more expensive and bulky equipment. The node also incorporated a low-cost particulate matter sensor but the accuracy of this sensor could not be validated to the same degree of accuracy. Previous research into the pollution exposures of cyclists had shown that traffic volumes and facilities were likely to be significant factors but most studies were based on aggregate measures of traffic such as ADT and the studies which considered temporally and spatially resolved traffic volumes were inconsistent in their findings. Also, none of these studies had considered exposure NO_x. The study described in Chapter 6 found that temporally resolved link traffic volumes were positively associated with all the negative environmental exposures experienced by cyclists on those links. This study also found that cycling on separated cycling facilities can reduce the air pollution exposure concentrations to which cyclists are exposed but cycling on bus lanes or on roadside cycle lanes without segregation actually increases exposure to air pollution. The levels of noise exposure were also higher on cycling facilities than on roads with no facilities. Overall these findings suggest that adjacent traffic volumes are strongly correlated with all environmental exposures and that the only cycling facilities which provide protection from environmental exposures are segregated facilities.

Chapters 7 and 8 were aimed at extending the models of Chapters 3 and 4 in order to allow the potential health and environmental impacts of cycling to drive the design process of cycle networks. In order to achieve this, it was necessary to develop, calibrate and validate a disutility function for cyclists. Although disutility functions are an essential tool in transportation planning, no study to date had attempted this, possibly because the link-based calibration methods used

for motor vehicle disutility functions are not suitable for cycling. Chapter 7 proposed a Disutility of Cycling (DOC) which incorporates factors which have been previously shown to affect the route choices of cyclists such as intensity of vehicle traffic and the protection afforded by cycling facilities. The calibration is performed by formulating the problem as a Mathematical Programme with Equilibrium Constraints (MPEC) and solving the MPEC using a descent method. The DOC function significantly outperformed route choice predictions based on cyclists seeking the shortest path. Perhaps more importantly, by developing a suitable calibration method, this chapter lay the foundations for future studies to explore different functional forms which may be even more accurate than the DOC function proposed in this thesis. The final contribution of this thesis brought together all of the contributions of the previous chapters in the development of an optimisation model for optimal design of cycle networks, taking into account the health and environmental impacts of cycling and driving. A solution algorithm was proposed and the efficacy of the method was demonstrated using a simple network example. The solution algorithm is robust as it does not depend on gradients or Hessian information. This means that the objective function and equilibrium formulations of the MPEC can be changed without changing the solution algorithm. This tool allows cycle network design and investment to be driven by the potential health and environmental impacts of cycling and driving.

9.2 Critical Assessment

The strengths and weaknesses of the thesis will be discussed in terms of the same three themes used above.

The level of uncertainty analysis was a strength of Chapters 3 and 4. Although many previous studied had addressed uncertainty in the parameters of the models they used, Chapter 3 took an additional step by comparing the estimates of different models for the same impact. This was an important step due to the aforementioned heterogeneity evident in the results of these models. Chapter 4 also addressed uncertainty in the model parameters by using stochastic sampling of parameters. This allowed distributions of impacts to be produced rather than just central, upper and lower estimates. A further strength of Chapter 4 was the novelty and timeliness of the individual-level analysis of the benefits and risks of cycling. Both Chapter 3 and Chapter 4 were largely based on local data. This can be seen as a strength in terms of the accuracy of the results but also as a weakness as it is unclear how well these results would generalise to a different setting. For example, in an urban environment where cycling rates are high and collision rates for cyclists are low, the expected net health benefits may turn out to be positive for all. Another limitation of these chapters is that there are likely to be other physical benefits of cycling which

were not accounted for such as improved fitness and agility. There may also be mental benefits such as improved focus, confidence and happiness. Finally, the models used for quantifying the impact of individual pollution exposure ignored many potential sources of variation and this was part of the motivation for Chapters 5 and 6.

The BEE node developed in Chapter 5 was based on low-cost sensors and electronics and so the node could be easily and cheaply replicated by other researchers. The node was also shown to have a high degree of accuracy in measuring gaseous pollutants when compared to much larger and more expensive devices. However, the accuracy of the particulate matter sensor could not be validated to a high degree of accuracy in the Dublin environment. The ambient particulate matter concentrations are low in Dublin and so it is possible that the accuracy would be higher when measuring higher concentrations. Due to the high sampling rate of the BEE node, a large number of data points could be collected. Additionally, the data collection in the full scale study was carried out by a group of volunteers completing their normal commute rather than a course decided by the researchers. This allowed for a large sample of realistic exposure data to be collected and analysed.

Chapter 7 addresses the problem of modelling of cyclist behaviour in a comprehensive way by suggesting a functional form for the model, developing a framework for the calibration problem and developing and testing the solution algorithm using a test network as well as an actual city network. The accuracy of the calibrated function was better than that of the most commonly used alternative but still left much room for improvement. This may be because only a single type of disutility function was tested and there may be many other aspects of cyclist behaviour not reflected by this model. However, another strength of this work is the calibration process can easily be adapted to other functional forms and so the foundation has been lain for future studies to propose and test other disutility functions. The methodology described in Chapter 8 could be used in practice to help transport planners to achieve a goal which is becoming increasingly relevant. Also, the solution algorithm does not depend on the equilibrium formulation or the objective function having any particular form and so it is very robust. A weakness of Chapter 8 is that the genetic algorithm is not guaranteed to find global solution. Also, the method was only tested on small network and so it is not clear how efficient it will be for networks of higher complexity. However, this will continue to become less of an issue with the increasing availability of cheap commoditised computing power; especially since genetic algorithms are particularly well suited to parallelisation.

9.3 Policy Implications and Directions for Future Research

The results of Chapters 2 and 3 have this have added to the evidence basing showing that the total net benefits of modal shifts in favour of cycling are strongly positive. However, it has also been demonstrated in Chapter 4 that younger demographics are less likely to experience a net benefit from cycling than older people as they do not benefit as much from the physical activity and their risk of traffic collision is higher. In light of the positive impacts for the local population and for the majority of cyclists, it remains important to promote cycling as an alternative to driving, particularly for short trips. However, promotion of cycling should be accompanied by measures to mitigate risks to the cyclists themselves to ensure that the overall health benefits do not come at the expense of a small group of cyclists. Since traffic collisions are the only significant health risk to cyclists, measures which mitigate traffic collision risk such as such as traffic calming in residential areas and segregated facilities in urban areas are of particular importance.

The studies in this thesis were based on the population and transportation system of Dublin and the vast majority of the other studies which have quantified the health and environmental impacts of cycling have been carried out in a European context. It is unclear if the same conclusions would be reached for different environments. For example, in a city with higher baseline collision rates of cyclists, the promotion of cycling could lead to less positive health impacts. Future research in other environments with different levels of economic development, congestion, air pollution and traffic collision risk would add to the evidence base.

The results of Chapter 6 suggest that cycling facilities do not protect cyclists from environmental exposures as much as previously thought. However, this does not mean that transport planners should not try to provide cycling facilities or that cyclists should not use them. As shown in Chapters 3 and 4, the risk of traffic collisions is a more significant health hazard than air pollution exposure and it is still likely that cycling facilities, especially separated cycle lanes, reduce the risk of traffic collision for cyclists. A similar exposure study with more reliable measurement of coarse, fine and ultrafine particulate matter would be necessary to reliably test whether the conclusions of this thesis apply specifically to particulate matter. Segregated facilities were shown to decrease environmental exposures of cyclists more effectively than roadside lanes or bus lanes. This superiority of segregated lanes over other facility types adds to previous evidence indicating that cyclists prefer segregated lanes over other types of facilities (Buehler and Dill, 2016) and that roadside lanes do little to reduce risk perceptions of cyclists (Parkin et al., 2007). Transport planners wishing to encourage cycling should therefore endeavour to provide cycling

facilities with physical separation from traffic wherever possible, especially on highly trafficked roads. The National Cycle Manual of Ireland refers to roadside cycle lanes as “Standard Cycle Tracks” but the results of this thesis as well as previous work suggest that lanes with physical segregation should become the standard cycling facility.

The NTA, by incorporating cycling assignment into the new Regional Modelling System has demonstrated an intention to take cyclists into account in strategic transport models. However, the model still relies on the assumption that cyclists take the shortest path without any regard for levels of motorised traffic or available facilities. Assignment of cyclists to a network using the shortest path method is unrealistic and this thesis has shown that superior accuracy can be achieved by using a function which takes account of volumes of motor vehicle traffic and presence of cycling facilities. Transport authorities such as the NTA should consider more realistic models of cyclist behaviour in order to ensure that any insights or strategies generated through modelling efforts are based on a reasonable approximation to reality. Future research in this area should also test different forms of disutility function for cyclists in order to arrive at a widely accepted disutility function such as the BPR function for motorised traffic.

Finally, this thesis has shown that is possible to take a rigorous and systematic approach to designing cycle facilities in order to maximise societal benefit. In the approaches currently taken by government bodies to appraise transportation projects, only a small number of options can be considered in detail, due to the time and resources required for each appraisal. These options are generally chosen from a larger group using tools such as Multi-Criteria Analysis as recommended by the CAF. Multi Criteria Analysis involves the decision maker subjectively assigning scores and weights to various impacts (Department of Transport, 2016). Taking a rigorous optimisation based approach towards appraisals would make the process less resource-intensive, more objective and make it less likely for appraisals to become “case-making” exercises. Some further research is required to make this approach ready for practical applications as the model and algorithm presented in this thesis have not yet been tested on a realistic sized network. However, if this method can be validated for realistic problems it should be possible to implement it in practical situations with very little adaptation. This would provide a valuable decision support tool for transportation planners and policymakers.

Chapter 10: Appendices

10.1 Jacobians of KKT equations

For the TAP described by Eq. (7.2) to Eq. (7.7), the Jacobian of the KKT equations with respect to the equilibrium variables and dual variables is given by Eq. (7.21). For the case where there are two possible modes—private car and bicycle—with disutilities described by the BPR function and DOC function respectively, the non-zero elements of Eq. (7.21) are detailed below.

$$\nabla_h KKT_1 = \nabla_h \boldsymbol{u} + \begin{bmatrix} \frac{1}{\theta_1 h_1} & 0 & \dots & 0 \\ 0 & \frac{1}{\theta_1 h_2} & 0 & \vdots \\ \vdots & 0 & \ddots & 0 \\ 0 & \dots & 0 & \frac{1}{\theta_1 h_{|P|}} \end{bmatrix}$$

Where

$$\nabla_h \boldsymbol{u} = \begin{bmatrix} \frac{dc_1^a}{dx_1^a} & 0 & \dots & 0 & 0 & 0 & \dots & 0 \\ \vdots & \frac{dc_2^a}{dx_2^a} & & \vdots & 0 & 0 & \dots & 0 \\ 0 & 0 & \ddots & 0 & \vdots & \vdots & \ddots & \vdots \\ 0 & \dots & 0 & \frac{dc_{|S|}^a}{dx_{|S|}^a} & 0 & 0 & \dots & 0 \\ \frac{dc_1^c}{dx_1^a} & 0 & \dots & 0 & \frac{dc_1^c}{dx_1^c} & 0 & \dots & 0 \\ \vdots & \frac{dc_2^c}{dx_2^a} & & \vdots & 0 & \frac{dc_2^c}{dx_2^c} & & \vdots \\ 0 & & \ddots & 0 & \vdots & & \ddots & 0 \\ 0 & 0 & \dots & \frac{dc_{|S|}^c}{dx_{|S|}^a} & 0 & \dots & 0 & \frac{dc_{|S|}^c}{dx_{|S|}^c} \end{bmatrix} \quad \text{Eq. (A1)}$$

And

$$\frac{dc_s^a}{dx_s^a} = \frac{\alpha_t t_s^{c0} \rho \beta \left(\frac{x_s^c}{K_s}\right)^{\beta-1}}{K_s}$$

$$\frac{dc_s^c}{dx_s^c} = \frac{\alpha_t \frac{d_s^m}{\bar{v}_s^m} \tau \sigma \left(\frac{v_s^{a-c} + v_s^c}{K_s}\right)^{\beta-1}}{K_s}$$

$$\frac{dc_s^c}{dx_s^a} = \frac{\alpha_t \frac{d_s^m}{\bar{v}_s^m} \tau\sigma \left(\frac{v_s^{a-c} + v_s^c}{K_s}\right)^{\beta-1}}{K_s}$$

$$\nabla_q KKT_1 = \left[\left[\frac{d}{dq_v^n}\left(\mu_p^m(\Phi) + \frac{1}{\theta_1}\ln\left(\frac{1}{PS_p^m}\frac{h_p^m}{q_w^m}\right) - \lambda_w^m\right) \;\forall\; p \epsilon P_w^m, m \epsilon M, w \epsilon W\right]^T\right] \quad \forall\, n \epsilon M, v \epsilon W$$

Where

Eq. (A2)

$$\frac{d}{dq_v^n}\left(\mu_p^m(\Phi) + \frac{1}{\theta_1}\ln\left(\frac{1}{PS_p^m}\frac{h_p^m}{q_w^m}\right) - \lambda_w^m\right) = \begin{cases} \frac{-1}{\theta_1 q_w^m} & if\ m = n, w = v \\ 0 & otherwise \end{cases}$$

$$\nabla_q KKT_2 = \left[\left[\frac{d}{dq_v^n}\left(\frac{1}{\theta_2}\ln\left(\frac{q_w^m}{q_w}\right) + \lambda_w^m - \lambda_w\right) \;\forall m \epsilon M, w \epsilon W\right]^T\right] \quad \forall\, n \epsilon M, v \epsilon W$$

Where

Eq. (A3)

$$\frac{d}{dq_v^n}\left(\frac{1}{\theta_2}\ln\left(\frac{q_w^m}{q_w}\right) + \lambda_w^m - \lambda_w\right) = \begin{cases} \frac{1}{\theta_2 q_w^m} & if\ m = n, w = v \\ 0 & otherwise \end{cases}$$

$$\nabla_Q KKT_2 = \left[\left[\frac{d}{dq_v}\left(\frac{1}{\theta_2}\ln\left(\frac{q_w^m}{q_w}\right) + \lambda_w^m - \lambda_w\right) \;\forall m \epsilon M, w \epsilon W\right]^T\right] \quad \forall\, v \epsilon W$$

Eq. (A4)

Where

$$\frac{d}{dq_v}\left(\frac{1}{\theta_2}\ln\left(\frac{q_w^m}{q_w}\right)+\lambda_w^m-\lambda_w\right)=\begin{cases}\dfrac{-1}{\theta_2 q_w} & if\ w=v\\ 0 & otherwise\end{cases}$$

$$\nabla_Q KKT_3=\begin{bmatrix}\dfrac{1}{\eta q_1} & 0 & \dots & 0\\ 0 & \dfrac{1}{\eta q_2} & 0 & \vdots\\ \vdots & 0 & \ddots & 0\\ 0 & \dots & 0 & \dfrac{1}{\eta q_{|W|}}\end{bmatrix} \qquad \text{Eq. (A5)}$$

The Jacobian of the KKT equations with respect to the calibration parameters is given by Eq. (7.22). The non-zero elements of Eq. (7.22) are detailed below.

$$\nabla_{r^{c,0}} KKT_1=\left[\frac{d}{dr^{c,0}}\left(\mu_p^m(\Phi)+\frac{1}{\theta_1}\ln\left(\frac{1}{PS_p^m}\frac{h_p^m}{q_w^m}\right)-\lambda_w^m\right)\ \forall\ p\in P_w^m, m\in M, w\in W\right]^T \qquad \text{Eq. (A6)}$$

Where

$$\frac{d}{dr^{c,0}}\left(\mu_p^m(\Phi)+\frac{1}{\theta_1}\ln\left(\frac{1}{PS_p^m}\frac{h_p^m}{q_w^m}\right)-\lambda_w^m\right)=\begin{cases}\alpha_t\displaystyle\sum_{s\in S}\delta_{sp}\frac{d_s^m}{\bar{v}_s^m} & if\ m=c\\ 0 & otherwise\end{cases}$$

$$\nabla_\sigma KKT_1=\left[\frac{d}{d\sigma}\left(\mu_p^m(\Phi)+\frac{1}{\theta_1}\ln\left(\frac{1}{PS_p^m}\frac{h_p^m}{q_w^m}\right)-\lambda_w^m\right)\ \forall\ p\in P_w^m, m\in M, w\in W\right]^T \qquad \text{Eq. (A7)}$$

Where

$$\frac{d}{d\sigma}\left(\mu_p^m(\Phi)+\frac{1}{\theta_1}\ln\left(\frac{1}{PS_p^m}\frac{h_p^m}{q_w^m}\right)-\lambda_w^m\right) = \begin{cases}\alpha_t\sum_{s\in S}\delta_{sp}\frac{d_s^m}{\bar{v}_s^m}\left(\frac{v_{a-c}+v_{a-b}+v_c}{K_s}\right)^{\tau} & if\ m=c\\ 0 & otherwise\end{cases}$$

$$\nabla_\tau KKT_1=\left[\frac{d}{d\tau}\left(\mu_p^m(\Phi)+\frac{1}{\theta_1}\ln\left(\frac{1}{PS_p^m}\frac{h_p^m}{q_w^m}\right)-\lambda_w^m\right)\ \forall\ p\in P_w^m, m\in M, w\in W\right]^T$$

Where

$$\frac{d}{d\tau}\left(\mu_p^m(\Phi)+\frac{1}{\theta_1}\ln\left(\frac{1}{PS_p^m}\frac{h_p^m}{q_w^m}\right)-\lambda_w^m\right) = \begin{cases}\alpha_t\sigma\,\tau\sum_{s\in S}\delta_{sp}\frac{d_s^m}{\bar{v}_s^m}\left(\frac{v_{a-c}+v_{a-b}+v_c}{K_s}\right)^{\tau-1} & if\ m=c\\ 0 & otherwise\end{cases} \quad \text{Eq. (A8)}$$

$$\nabla_{\theta_2}KKT_2=\left[\frac{d}{d\theta_2}\left(\frac{1}{\theta_2}\ln\left(\frac{q_w^m}{q_w}\right)+\lambda_w^m-\lambda_w\right)\ \ \forall m\in M, w\in W\right]^T$$

Eq. (A9)

Where

$$\frac{d}{d\theta_2}\left(\frac{1}{\theta_2}\ln\left(\frac{q_w^m}{q_w}\right)+\lambda_w^m-\lambda_w\right)=\ -ln\left(\frac{q_w^m}{q_w}\right)\left(\frac{1}{{\theta_2}^2}\right)$$

10.2 Dissemination from thesis

The contributions of this thesis have been published in the following international peer-reviewed journal articles.

Doorley, R., Pakrashi, V. and Ghosh, B., 2017. Health impacts of cycling in Dublin on individual cyclists and on the local population. Journal of Transport & Health.

Doorley, R., Pakrashi, V. and Ghosh, B., 2015. Quantifying the health impacts of active travel: assessment of methodologies. Transport Reviews, 35(5), pp.559-582.

Doorley, R., Pakrashi, V. and Ghosh, B., 2015. Quantification of the Potential Health and Environmental Impacts of Active Travel in Dublin, Ireland. Transportation Research Record: Journal of the Transportation Research Board, (2531), pp.129-136.

Contributions from the thesis have also been presented at the following conferences.

R. Doorley, V. Pakrashi and B. Ghosh, "Designing cycle networks to maximise health, environmental and travel time impacts: an optimisation-based approach" in Universities' Transport Study Group 49th Annual Conference, 2017

R. Doorley, V. Pakrashi, C. de Courcy, F. Pilla and B. Ghosh, " Intake of Air Pollutants by Cyclists in Urban Environments: Characterization Using Low-Cost Mobile Monitoring" in Transportation Research Board, 95th Annual Meeting, 2016

R. Doorley, V. Pakrashi and B. Ghosh, " Quantification of the potential health and environmental impacts of active travel in Dublin" in Irish Transportation Research Network Conference, 2014

10.3 Participant Information and Consent Form

Introduction

This research aims to quantify the benefits and risks of active travel by means of a field measurement study. Study participants will carry out their regular commute by bicycle while carrying a backpack containing a number of sensors which will provide information about the physical hazards to which they are exposed as well as the amount and intensity of physical activity. This research is being conducted as part of PhD degree project in Trinity College, Dublin.

Procedure

You will be one of 20-25 participants who will complete their commutes as usual by bicycle while wearing a backpack containing an environmental sensing platform and wearing a heart rate monitor. You will carry out measurements during 2-4 commutes. You may use your own bicycle if available or, if not, you may use the project bicycle. Before starting your first measurement session, you will be trained in the use of the equipment by the research team. You will also be provided with a document which will explain the steps to be taken in carrying out the measurements. Before starting each session, you will switch on the equipment, ensure that all instruments are working correctly and continue with your commute as normal while wearing the backpack. After reaching your destination, you will turn off the equipment and prepare the equipment for the next measurement session. The data which will be recorded during each commute are:

- Concentrations of airborne particulate matter (PM1, PM2.5, PM10)
- Concentrations of carbon monoxide (CO), nitrogen dioxide (NO_2) and nitrogen oxides (NO_x)
- Sound Pressure Level
- Heart Rate
- GPS location

Benefits

You find out how much you are benefiting (or harming) your health and the environment by cycling instead of driving. The benefits of physical exercise as well as reductions in emissions of CO_2 and toxic pollutants will be quantified and weighed against your personal exposures to air pollution and noise pollution. We can also provide estimates of the percentage reduction in risk of mortality you will be experience if the same programme of cycling is sustained in the long term. If you are interested in learning more about the outcomes of the research project we can arrange to give you this information upon the project's completion.

Inclusion Criteria

You must be over the age of 18 and in good health to participate in this study.

Confidentiality

The identities of all participants will remain confidential. Names will not be published and will not be disclosed to anyone outside the study group. Only non-personally identifiable information will be used in analysis, publication and presentation of resulting data and findings. The data may be published in such a way that the participants remain anonymous. The data will be retained after the study is completed.

Voluntary Participation

You have volunteered to participate in this study and you may quit at any time. You have the right to omit information without penalty. Choosing to limit certain information may reduce the accuracy of the reported results.

Risks

You understand and appreciate the risks involved in urban cycling and voluntarily assume those risks. You will be responsible for your own welfare and personal property.

Stopping the study

You understand that the investigators may stop your participation in the study at any time without your consent.

Conflict of Interest

The study organisers might take advantage of their existing relationships (friends and colleagues) to recruit study participants, and thereby make progress in their research.

Further information

You can get further information about the study, your participation in the study, and/or your rights, by contacting the investigators: Mr. Ronan Doorley (0871214006/ doorleyr@tcd.ie) or Dr

Bidisha Ghosh (bghosh@tcd.ie). If the study team learns of important new information that might affect your desire to remain in the study, you will be informed at once.

Please Initial Box

I confirm that I have read and understand the information form for this study.	☐
I understand that my participation is voluntary and that I am free to withdraw at any time, without giving reason.	☐
I agree to take part in this study.	☐

Name of Participant	Date	Signature
_____	_____	_____

REFERENCES

ABDULAAL, M. & LEBLANC, L. J. 1979. Methods for combining modal split and equilibrium assignment models. *Transportation Science,* 13**,** 292-314.

ABRAHAMSSON, T. & LUNDQVIST, L. 1999. Formulation and estimation of combined network equilibrium models with applications to Stockholm. *Transportation Science,* 33**,** 80-100.

ADAMS, H., NIEUWENHUIJSEN, M. J., COLVILE, R., OLDER, M. & KENDALL, M. 2002. Assessment of road users' elemental carbon personal exposure levels, London, UK. *Atmospheric Environment,* 36**,** 5335-5342.

ADAMS, H. S., NIEUWENHUIJSEN, M. J., COLVILE, R. N., MCMULLEN, M. A. S. & KHANDELWAL, P. 2001. Fine particle (PM2.5) personal exposure levels in transport microenvironments, London, UK. *Science of the Total Environment,* 279**,** 29-44.

AINSWORTH, B. E., HASKELL, W. L., HERRMANN, S. D., MECKES, N., BASSETT, D. R., JR., TUDOR-LOCKE, C., GREER, J. L., VEZINA, J., WHITT-GLOVER, M. C. & LEON, A. S. 2011. 2011 Compendium of Physical Activities: A Second Update of Codes and MET Values. *Medicine and Science in Sports and Exercise,* 43**,** 1575-1581.

ALLEN, R. W., DAVIES, H., COHEN, M. A., MALLACH, G., KAUFMAN, J. D. & ADAR, S. D. 2009. The spatial relationship between traffic-generated air pollution and noise in 2 US cities. *Environmental Research,* 109**,** 334-342.

ALPHASENSE. 2015a. *NO2-B42F Nitrogen Dioxide Sensor 4-electrode Data Sheet* [Online]. Available: http://www.alphasense.com/index.php/products/nitrogen-dioxide-2/ [Accessed 30 July 2015].

ALPHASENSE 2015b. OPC-N2 Particle Monitor.

ANDERSEN, Z. J., LOFT, S., KETZEL, M., STAGE, M., SCHEIKE, T., HERMANSEN, M. N. & BISGAARD, H. 2008. Ambient air pollution triggers wheezing symptoms in infants. *Thorax,* 63**,** 710-6.

ARMITAGE, C. J. & CONNER, M. 2001. Efficacy of the Theory of Planned Behaviour: A meta-analytic review. *British Journal of Social Psychology,* 40**,** 471-499.

AXHAUSEN, K. W. & GÄRLING, T. 1992. Activity-based approaches to travel analysis: conceptual frameworks, models, and research problems. *Transport Reviews,* 12**,** 323-341.

BABISCH, W. 2014. Updated exposure-response relationship between road traffic noise and coronary heart diseases: A meta-analysis. *Noise and Health,* 16**,** 1.

BAGLOEE, S. A., SARVI, M. & WALLACE, M. 2016. Bicycle lane priority: Promoting bicycle as a green mode even in congested urban area. *Transportation Research Part A: Policy and Practice,* 87**,** 102-121.

BAMBERG, S., AJZEN, I. & SCHMIDT, P. 2003. Choice of Travel Mode in the Theory of Planned Behaviour: The Roles of Past Behaviour, Habit, and Reasoned Action. *Basic and Applied Social Psychology,* 25**,** 175-187.

BEAN, T., CARSLAW, N., ASHMORE, M., GILLAH, A. & PARKINSON, C. 2011. How does exposure to nitrogen dioxide compare between on-road and off-road cycle routes? *Journal of Environmental Monitoring,* 13**,** 1039-1045.

BECKMANN, M., MCGUIRE, C. & WINSTEN, C. B. 1956. Studies in the Economics of Transportation.

BEELEN, R., HOEK, G., VAN DEN BRANDT, P. A., GOLDBOHM, R. A., FISCHER, P., SCHOUTEN, L. J., JERRETT, M., HUGHES, E., ARMSTRONG, B. & BRUNEKREEF, B. 2008a. Long-term effects of traffic-related air pollution on mortality in a Dutch cohort (NLCS-AIR study). *Environmental Health Perspectives,* 116**,** 196-202.

BEELEN, R., HOEK, G., VAN DEN BRANDT, P. A., GOLDBOHM, R. A., FISCHER, P., SCHOUTEN, L. J., JERRETT, M., HUGHES, E., ARMSTRONG, B. &

BRUNEKREEF, B. 2008b. Long-term effects of traffic-related air pollution on mortality in a Dutch cohort (NLCS-AIR study). *Environmental health perspectives,* 116**,** 196.
BEKHOR, S., BEN-AKIVA, M. E. & RAMMING, M. S. 2006. Evaluation of choice set generation algorithms for route choice models. *Annals of Operations Research,* 144**,** 235-247.
BELL, M. G. & IIDA, Y. 1997. *Transportation network analysis*.
BERGAMASCHI, E., BRUSTOLIN, A., DE PALMA, G., MANINI, P., MOZZONI, P., ANDREOLI, R., CAVAZZINI, S. & MUTTI, A. 1999. Biomarkers of dose and susceptibility in cyclists exposed to monoaromatic hydrocarbons. *Toxicology letters,* 108**,** 241-247.
BHALLA, K., EZZATI, M., MAHAL, A., SALOMON, J. & REICH, M. 2007. A risk-based method for modeling traffic fatalities. *Risk Analysis,* 27**,** 125-136.
BHATIA, R. & WIER, M. 2011. "Safety in Numbers" re-examined: Can we make valid or practical inferences from available evidence? *Accident Analysis & Prevention,* 43**,** 235-240.
BICKEL, P., FRIEDRICH, R., BURGESS, A., FAGIANI, P., HUNT, A., JONG, G. D., LAIRD, J., LIEB, C. & LINDBERG, G. 2006. Developing Harmonised European Approaches forTransport Costing and Project Assessment *HEATCO (Ed.).*
BIGAZZI, A. Y., BROACH, J. & DILL, J. 2016. Bicycle route preference and pollution inhalation dose: Comparing exposure and distance trade-offs. *Journal of Transport & Health,* 3**,** 107-113.
BIGAZZI, A. Y. & FIGLIOZZI, M. A. 2014. Review of Urban Bicyclists' Intake and Uptake of Traffic-Related Air Pollution. *Transport Reviews,* 34**,** 221-245.
BIGAZZI, A. Y. & FIGLIOZZI, M. A. 2015a. Roadway determinants of bicyclist exposure to volatile organic compounds and carbon monoxide. *Transportation Research Part D: Transport and Environment,* 41**,** 13-23.
BIGAZZI, A. Y. & FIGLIOZZI, M. A. 2015b. Roadway Determinants of Bicyclist Multi-pollutant Exposure Concentrations.
BLUHM, G. L., BERGLIND, N., NORDLING, E. & ROSENLUND, M. 2007. Road traffic noise and hypertension. *Occupational and Environmental Medicine,* 64**,** 122-126.
BOLDO, E., MEDINA, S., LE TERTRE, A., HURLEY, F., MÜCKE, H.-G., BALLESTER, F. & AGUILERA, I. 2006. Apheis: Health impact assessment of long-term exposure to PM2. 5 in 23 European cities. *European journal of epidemiology,* 21**,** 449-458.
BOOGAARD, H., BORGMAN, F., KAMMINGA, J. & HOEK, G. 2009. Exposure to ultrafine and fine particles and noise during cycling and driving in 11 Dutch cities. *Atmospheric Environment,* 43**,** 4234-4242.
BÖRJESSON, M. & ELIASSON, J. 2012. The value of time and external benefits in bicycle appraisal. *Transportation Research Part A: Policy and Practice,* 46**,** 673-683.
BOYCE, D. & BAR-GERA, H. 2004. Multiclass combined models for urban travel forecasting. *Networks and Spatial Economics,* 4**,** 115-124.
BOYCE, D. E. 1984. Urban transportation network-equilibrium and design models: recent achievements and future prospects. *Environment and Planning A,* 16**,** 1445-1474.
BREEMERSCH, T., CEUSTER, G. D., CHIFFI, C., FIORELLO, D., NTZIACHRISTOS, L., KOURIDIS, C. & KNÖRR, W. 2010. Update and further development of transport model TREMOVE. Brussels.
BROACH, J., DILL, J. & GLIEBE, J. 2012. Where do cyclists ride? A route choice model developed with revealed preference GPS data. *Transportation Research Part a-Policy and Practice,* 46**,** 1730-1740.
BROOK, R. D., RAJAGOPALAN, S., POPE, C. A., BROOK, J. R., BHATNAGAR, A., DIEZ-ROUX, A. V., HOLGUIN, F., HONG, Y. L., LUEPKER, R. V., MITTLEMAN,

M. A., PETERS, A., SISCOVICK, D., SMITH, S. C., WHITSEL, L., KAUFMAN, J. D., AMER HEART ASSOC COUNCIL, E., COUNCIL KIDNEY CARDIOVASC, D. & COUNCIL NUTR PHYS ACTIVITY, M. 2010. Particulate Matter Air Pollution and Cardiovascular Disease An Update to the Scientific Statement From the American Heart Association. *Circulation,* 121**,** 2331-2378.
BRUYNOOGHE, M., GIBERT, A. & SAKAROVITCH, M. Une methode d'affectation du trafic. Proceedings of the 4th International Symposium on the Theory of Road Traffic, 1969. Bundesminister fur Verkehr, Abt. Strassenbau, Bonn, Germany, 198-204.
BUEHLER, R. & DILL, J. 2016. Bikeway networks: A review of effects on cycling. *Transport Reviews,* 36**,** 9-27.
BUEHLER, R. & PUCHER, J. 2012. Cycling to work in 90 large American cities: new evidence on the role of bike paths and lanes. *Transportation,* 39**,** 409-432.
BUEKERS, J., DONS, E., ELEN, B. & INT PANIS, L. 2015. Health impact model for modal shift from car use to cycling or walking in Flanders: application to two bicycle highways. *Journal of Transport & Health,* 2**,** 549-562.
BULL, F. C., ARMSTRONG, T. P., DIXON, T., HAM, S., NEIMAN, A. & PRATT, M. 2004. Physical inactivity, Comparative Quantification of Health Risks. WHO.
CAN, A., RADEMAKER, M., VAN RENTERGHEM, T., MISHRA, V., VAN POPPEL, M., TOUHAFI, A., THEUNIS, J., DE BAETS, B. & BOTTELDOOREN, D. 2011. Correlation analysis of noise and ultrafine particle counts in a street canyon. *Science of The Total Environment,* 409**,** 564-572.
CENTRAL STATISTICS OFFICE 2006. POWCAR.
CENTRAL STATISTICS OFFICE 2009. Irish Life Tables No. 15.
CENTRAL STATISTICS OFFICE 2011a. Census 2011 Reports.
CENTRAL STATISTICS OFFICE 2011b. POWSCAR 2011.
CENTRAL STATISTICS OFFICE 2012. Environmental Indicators Ireland. Dublin: Central Statistics Office, Ireland.
CHAKRABARTI, B., FINE, P. M., DELFINO, R. & SIOUTAS, C. 2004. Performance evaluation of the active-flow personal DataRAM PM2.5 mass monitor (Thermo Anderson pDR-1200) designed for continuous personal exposure measurements. *Atmospheric Environment,* 38**,** 3329-3340.
CHAU, C. K., TU, E. Y., CHAN, D. W. T. & BURNETT, J. 2002. Estimating the total exposure to air pollutants for different population age groups in Hong Kong. *Environment International,* 27**,** 617-630.
CHEN, H., GOLDBERG, M. S. & VILLENEUVE, P. J. 2008. A Systematic Review of the Relation Between Long-Term Exposure to Ambient Air Pollution and Chronic Diseases. *Reviews on Environmental Health,* 23**,** 243-297.
CHERTOK, M., VOUKELATOS, A., SHEPPEARD, V. & RISSEL, C. 2004. Comparison of air pollution exposure for five commuting modes in Sydney-car, train, bus, bicycle and walking. *Health promotion journal of Australia,* 15**,** 63-67.
CHONG, E. K. & ZAK, S. H. 2013. *An introduction to optimization*, John Wiley & Sons.
CHOWDHURY, A. K., DEBSARKAR, A. & CHAKRABARTY, S. 2015. Novel Methods for Assessing Urban Air Quality: Combined Air and Noise Pollution Approach. *Journal of Atmospheric Pollution,* 3**,** 1-8.
CLANCY, L., GOODMAN, P., SINCLAIR, H. & DOCKERY, D. W. 2002. Effect of air-pollution control on death rates in Dublin, Ireland: an intervention study. *Lancet,* 360**,** 1210-1214.
COLE-HUNTER, T., JAYARATNE, R., STEWART, I., HADAWAY, M., MORAWSKA, L. & SOLOMON, C. 2013a. Utility of an alternative bicycle commute route of lower proximity to motorised traffic in decreasing exposure to ultra-fine particles, respiratory symptoms and airway inflammation–a structured exposure experiment. *Environmental health,* 12**,** 1.

COLE-HUNTER, T., JAYARATNE, R., STEWART, I., HADAWAY, M., MORAWSKA, L. & SOLOMON, C. 2013b. Utility of an alternative bicycle commute route of lower proximity to motorised traffic in decreasing exposure to ultra-fine particles, respiratory symptoms and airway inflammation - a structured exposure experiment. *Environmental Health,* 12**,** 29.
COLSON, B., MARCOTTE, P. & SAVARD, G. 2007. An overview of bilevel optimization. *Annals of Operations Research,* 153**,** 235-256.
COMEAP 2015. Statement on the evidence for the effects of nitrogen dioxide on health.
CORMEN, T. H. 2009. *Introduction to Algorithms*, MIT Press.
CROW 2007. Design manual for bicycle traffic.
CSO 2015. CSO Statistical Release; Irish Life Tables 2010-2012.
DAFERMOS, S. C. 1971. An extended traffic assignment model with applications to two-way traffic. *Transportation Science,* 5**,** 366-389.
DAVIES, H. & VAN KAMP, I. 2012. Noise and cardiovascular disease: A review of the literature 2008-2011. *Noise & Health,* 14**,** 287-291.
DE NAZELLE, A., FRUIN, S., WESTERDAHL, D., MARTINEZ, D., RIPOLL, A., KUBESCH, N. & NIEUWENHUIJSEN, M. 2012. A travel mode comparison of commuters' exposures to air pollutants in Barcelona. *Atmospheric Environment,* 59**,** 151-159.
DE NAZELLE, A., NIEUWENHUIJSEN, M., PEREZ, L., KUZLI, N. & LOBO, A. 2008. Pilot Study of Barcelona Commuters' Exposure to Particulate Matter. *Epidemiology,* 19**,** S130-S131.
DE NAZELLE, A., NIEUWENHUIJSEN, M. J., ANTO, J. M., BRAUER, M., BRIGGS, D., BRAUN-FAHRLANDER, C., CAVILL, N., COOPER, A. R., DESQUEYROUX, H., FRUIN, S., HOEK, G., PANIS, L. I., JANSSEN, N., JERRETT, M., JOFFE, M., ANDERSEN, Z. J., VAN KEMPEN, E., KINGHAM, S., KUBESCH, N., LEYDEN, K. M., MARSHALL, J. D., MATAMALA, J., MELLIOS, G., MENDEZ, M., NASSIF, H., OGILVIE, D., PEIRO, R., PEREZ, K., RABL, A., RAGETTLI, M., RODRIGUEZ, D., ROJAS, D., RUIZ, P., SALLIS, J. F., TERWOERT, J., TOUSSAINT, J. F., TUOMISTO, J., ZUURBIER, M. & LEBRET, E. 2011. Improving health through policies that promote active travel: A review of evidence to support integrated health impact assessment. *Environment International,* 37**,** 766-777.
DE NAZELLE, A., RODRIGUEZ, D. A. & CRAWFORD-BROWN, D. 2009. The built environment and health: Impacts of pedestrian-friendly designs on air pollution exposure. *Science of the Total Environment,* 407**,** 2525-2535.
DEENIHAN, G. & CAULFIELD, B. 2014. Estimating the health economic benefits of cycling. *Journal of Transport & Health,* 1**,** 141-149.
DEKONINCK, L., BOTTELDOOREN, D. & INT PANIS, L. 2013. An instantaneous spatiotemporal model to predict a bicyclist's Black Carbon exposure based on mobile noise measurements. *Atmospheric Environment,* 79**,** 623-631.
DELOITTE ACCESS ECONOMICS 2011. The economic impact of vision impairment and blindness in the Republic of Ireland. National Council for the Blind of Ireland.
DEPARTMENT FOR TRANSPORT 2017. TAG Unit M2 Variable Demand Modelling. *Transport Analysis Guidance (TAG).* London.
DEPARTMENT OF TRANSPORT. 2013. *Transport Analysis Guidance: WebTAG* [Online]. Available: https://www.gov.uk/guidance/transport-analysis-guidance-webtag [Accessed 12 Sep 2017].
DEPARTMENT OF TRANSPORT, T. A. S., IRELAND,. 2016. *Common Appraisal Framework for Transport Projects and Programmes* [Online]. Available: http://www.dttas.ie/sites/default/files/publications/corporate/english/common-appraisal-framework-2016-complete-document/common-appraisal-framework.pdf [Accessed 12/Sep 2017].

DEPARTMENT OF TRANSPORT TOURISM AND SPORT IRELAND 2012. Irish Bulletin of Vehicle and Driver Statistics.
DESAIGUES, B., AMI, D., BARTCZAK, A., BRAUN-KOHLOVA, M., CHILTON, S., CZAJKOWSKI, M., FARRERAS, V., HUNT, A., HUTCHISON, M., JEANRENAUD, C., KADERJAK, P., MACA, V., MARKIEWICZ, O., MARKOWSKA, A., METCALF, H., NAVRUD, S., NIELSEN, J. S., ORTIZ, R., PELLEGRINI, S., RABL, A., RIERA, R., SCASNY, M., STOECKEL, M. E., SZANTO, R. & URBAN, J. 2011. Economic valuation of air pollution mortality: A 9-country contingent valuation survey of value of a life year (VOLY). *Ecological Indicators,* 11**,** 902-910.
DHONDT, S., BECKX, C., DEGRAEUWE, B., LEFEBVRE, W., KOCHAN, B., BELLEMANS, T., INT PANIS, L., MACHARIS, C. & PUTMAN, K. 2012a. Health impact assessment of air pollution using a dynamic exposure profile: Implications for exposure and health impact estimates. *Environmental Impact Assessment Review,* 36**,** 42-51.
DHONDT, S., KOCHAN, B., BECKX, C., LEFEBVRE, W., PIRDAVANI, A., DEGRAEUWE, B., BELLEMANS, T., PANIS, L. I., MACHARIS, C. & PUTMAN, K. 2013. Integrated health impact assessment of travel behaviour: Model exploration and application to a fuel price increase. *Environment International,* 51**,** 45-58.
DHONDT, S., PIRDAVANI, A., MACHARIS, C., BELLEMANS, T. & PUTMAN, K. 2012b. Translating road safety into health outcomes using a quantitative impact assessment model. *Injury Prevention,* 18**,** 413-420.
DILL, J. 2009. Bicycling for Transportation and Health: The Role of Infrastructure. *Journal of Public Health Policy,* 30**,** S95-S110.
DILL, J. & VOROS, K. 2007. Factors affecting bicycling demand - Initial survey findings from the Portland, Oregon, Region. *Transportation Research Record***,** 9-17.
DOHERTY, S. T., AULTMAN-HALL, L. & SWAYNOS, J. 2000. Commuter cyclist accident patterns in Toronto and Ottawa. *Journal of Transportation Engineering-Asce,* 126**,** 21-26.
DONS, E., PANIS, L. I., VAN POPPEL, M., THEUNIS, J. & WETS, G. 2012. Personal exposure to black carbon in transport microenvironments. *Atmospheric Environment,* 55**,** 392-398.
DONS, E., TEMMERMAN, P., VAN POPPEL, M., BELLEMANS, T., WETS, G. & PANIS, L. I. 2013. Street characteristics and traffic factors determining road users' exposure to black carbon. *Science of the Total Environment,* 447**,** 72-79.
DOORLEY, R., PAKRASHI, V. & GHOSH, B. 2015a. Quantification of the Potential Health and Environmental Impacts of Active Travel in Dublin. *Transportation Research Record*.
DOORLEY, R., PAKRASHI, V. & GHOSH, B. 2015b. Quantifying the Health Impacts of Active Travel: Assessment of Methodologies. *Transport Reviews***,** 1-24.
DOORLEY, R., PAKRASHI, V. & GHOSH, B. 2017. Health impacts of cycling in Dublin on individual cyclists and on the local population. *Journal of Transport & Health*.
DUBLIN BUS. 2017. *Dublin Bus Fleet* [Online]. Available: https://www.dublinbus.ie/About-Us/Dublin-Bus-Fleet/ [Accessed 6 Sep 2017].
DUTHIE, J. & UNNIKRISHNAN, A. 2014. Optimization Framework for Bicycle Network Design. *Journal of Transportation Engineering,* 140.
DZHAMBOV, A. M. 2015. Long-term noise exposure and the risk for type 2 diabetes: A meta-analysis. *Noise and Health,* 17**,** 23.
EDWARDS, R. D. & MASON, C. N. 2014. Spinning the wheels and rolling the dice: Life-cycle risks and benefits of bicycle commuting in the US. *Preventive medicine,* 64**,** 8-13.
ELVIK, R. 2009. The non-linearity of risk and the promotion of environmentally sustainable transport. *Accident Analysis and Prevention,* 41**,** 849-855.

ELVIK, R. & BJØRNSKAU, T. 2017. Safety-in-numbers: A systematic review and meta-analysis of evidence. *Safety Science,* 92**,** 274-282.
ENVIRONMENTAL PROTECTION AGENCY 2012. Air Quality in Ireland 2012, Key Indicators of Ambient Air Quality.
ENVIRONMENTAL PROTECTION AGENCY 2015. Air Quality in Ireland 2014; Key Indicators of Ambient Air Quality.
ENVIRONMENTAL PROTECTION AGENCY 2016. Air Quality in Ireland 2015; Key Indicators of Ambient Air Quality.
EUROPEAN COMMISSION 1999. Cycling - The way ahead for towns and cities. *DG XI — Environment, Nuclear Safety and Civil Protection.*
EUROPEAN COMMISSION 2014. Update of the Handbook on External Costs of Transport. London: European Commission – DG Mobility and Transport.
FACCHINEI, F. & PANG, J.-S. 2007. *Finite-dimensional variational inequalities and complementarity problems*, Springer Science & Business Media.
FERNANDEZ-CAMACHO, R., CABEZA, I. B., AROBA, J., GOMEZ-BRAVO, F., RODRIGUEZ, S. & DE LA ROSA, J. 2015. Assessment of ultrafine particles and noise measurements using fuzzy logic and data mining techniques. *Science of the Total Environment,* 512**,** 103-113.
FIACCO, A. 1983. Introduction to sensitivity and stability analysis in nonlinear programming, Acad. Press.
FISHER, G., KJELLSTROM, T., KINGHAM, S., HALES, S. & SHRESTHA, R. 2007. Health and Air Pollution in New Zealand (HAPiNZ). Wellington (NZ): Health Research Council of New Zealand.
FISHMAN, E. 2011. *Benefits of public bicycle schemes must be evaluated carefully*.
FISHMAN, E., WASHINGTON, S. & HAWORTH, N. L. An evaluation framework for assessing the impact of public bicycle share schemes. Transportation Research Board (TRB) 91st Annual Meeting, 22-26 Jan 2012, 2012 Marriott Wardman Park, Washington, D.C.
FLORIAN, M., WU, J. H. & HE, S. 2002. *A multi-class multi-mode variable demand network equilibrium model with hierarchical logit structures*, Springer.
GARBER, C. E., BLISSMER, B., DESCHENES, M. R., FRANKLIN, B. A., LAMONTE, M. J., LEE, I. M., NIEMAN, D. C., SWAIN, D. P. & AMER COLL SPORTS, M. 2011. Quantity and Quality of Exercise for Developing and Maintaining Cardiorespiratory, Musculoskeletal, and Neuromotor Fitness in Apparently Healthy Adults: Guidance for Prescribing Exercise. *Medicine and Science in Sports and Exercise,* 43**,** 1334-1359.
GARCÍA-RÓDENAS, R. & MARÍN, Á. 2009. Simultaneous estimation of the origin–destination matrices and the parameters of a nested logit model in a combined network equilibrium model. *European Journal of Operational Research,* 197**,** 320-331.
GARCIA-RODENAS, R. & VERASTEGUI-RAYO, D. 2013. Adjustment of the link travel-time functions in traffic equilibrium assignment models. *Transportmetrica a-Transport Science,* 9**,** 798-824.
GATERSLEBEN, B. & APPLETON, K. M. 2007. Contemplating cycling to work: Attitudes and perceptions in different stages of change. *Transportation Research Part A: Policy and Practice,* 41**,** 302-312.
GKATZOFLIAS, D., KOURIDIS, C. & NLZIACHRISTOS, L. 2007. COPERT 4: Computer Programme to Calculate Emissions from Road Transport. Brussels: European Environmental Agency.
GOEL, R., GANI, S., GUTTIKUNDA, S. K., WILSON, D. & TIWARI, G. 2015. On-road PM 2.5 pollution exposure in multiple transport microenvironments in Delhi. *Atmospheric Environment,* 123**,** 129-138.
GOOGLE MAPS. 2014. *Street View of 51 R148* [Online]. Available: https://goo.gl/maps/GiSmMcktiGS2 [Accessed 11 Nov 2015.

GOOGLE MAPS. 2015. *Dublin City, Ireland* [Online]. Available: https://www.google.ie/maps/@53.3484336,-6.2601236,14z [Accessed 13 July, 2015.
GOTSCHI, T. 2011. Costs and Benefits of Bicycling Investments in Portland, Oregon. *Journal of Physical Activity & Health,* 8**,** S49-S58.
GRABOW, M. L., SPAK, S. N., HOLLOWAY, T., STONE, B., MEDNICK, A. C. & PATZ, J. A. 2012. Air Quality and Exercise-Related Health Benefits from Reduced Car Travel in the Midwestern United States. *Environmental Health Perspectives,* 120**,** 68-76.
GREAVES, S., ISSARAYANGYUN, T. & LIU, Q. 2008. Exploring variability in pedestrian exposure to fine particulates (PM2.5) along a busy road. *Atmospheric Environment,* 42**,** 1665-1676.
GULLIVER, J. & BRIGGS, D. J. 2004. Personal exposure to particulate air pollution in transport microenvironments. *Atmospheric Environment,* 38**,** 1-8.
HAAGSMA, J. A., POLINDER, S., LYONS, R. A., LUND, J., DITSUWAN, V., PRINSLOO, M., VEERMAN, J. L. & VAN BEECK, E. F. 2012. Improved and standardized method for assessing years lived with disability after injury. *Bulletin of the World Health Organization,* 90**,** 513-521.
HALL, M. & WILLUMSEN, L. 1980. SATURN-a simulation-assignment model for the evaluation of traffic management schemes. *Traffic Engineering & Control,* 21.
HALL, R. M., HEITBRINK, W. A. & REED, L. D. 2002. Evaluation of a tractor cab using real-time aerosol counting instrumentation. *Applied occupational and environmental hygiene,* 17**,** 47-54.
HANKEY, S. & MARSHALL, J. D. 2015. On-bicycle exposure to particulate air pollution: Particle number, black carbon, PM 2.5, and particle size. *Atmospheric Environment,* 122**,** 65-73.
HANSEN, C. H. & SEHRNDT, C. 2001. Fundamentals of acoustics. *Occupational Exposure to Noise: Evaluation, Prevention and Control. World Health Organization*.
HARKEY, D. L., REINFURT, D. W., KNUIMAN, M. & NRC 1998. Development of the bicycle compatibility index. *Bicycle and Pedestrian Research 1998.*
HARTOG, J. J. D., BOOGAARD, H., NIJLAND, H. & HOEK, G. 2011. Do the health benefits of cycling outweigh the risks? *Ciencia & saude coletiva,* 16**,** 4731-44.
HATZOPOULOU, M., WEICHENTHAL, S., DUGUM, H., PICKETT, G., MIRANDA-MORENO, L., KULKA, R., ANDERSEN, R. & GOLDBERG, M. 2013. The impact of traffic volume, composition, and road geometry on personal air pollution exposures among cyclists in Montreal, Cananda. *J Expo Sci Environ Epidemiol,* 23.
HEINEN, E., VAN WEE, B. & MAAT, K. 2010. Commuting by Bicycle: An Overview of the Literature. *Transport Reviews,* 30**,** 59-96.
HOEK, G., KRISHNAN, R. M., BEELEN, R., PETERS, A., OSTRO, B., BRUNEKREEF, B. & KAUFMAN, J. D. 2013a. Long-term air pollution exposure and cardio-respiratory mortality: a review. *Environmental Health,* 12.
HOEK, G., KRISHNAN, R. M., BEELEN, R., PETERS, A., OSTRO, B., BRUNEKREEF, B. & KAUFMAN, J. D. 2013b. Long-term air pollution exposure and cardio-respiratory mortality: a review. *Environ Health,* 12.
HOLM, A. L., GLUMER, C. & DIDERICHSEN, F. 2012. Health Impact Assessment of increased cycling to place of work or education in Copenhagen. *Bmj Open,* 2**,** 8.
HOLMES, N. S. & MORAWSKA, L. 2006. A review of dispersion modelling and its application to the dispersion of particles: An overview of different dispersion models available. *Atmospheric Environment,* 40**,** 5902-5928.
HONG, E.-S. & BAE, C.-H. 2012. Exposure of Bicyclists to Air Pollution in Seattle, Washington Hybrid: Analysis Using Personal Monitoring and Land Use

Regression. *Transportation Research Record: Journal of the Transportation Research Board*, 59-66.
HOOD, J., SALL, E. & CHARLTON, B. 2011. A GPS-based bicycle route choice model for San Francisco, California. *Transportation Letters-the International Journal of Transportation Research,* 3, 63-75.
HUANG, J., DENG, F., WU, S. & GUO, X. 2012. Comparisons of personal exposure to PM 2.5 and CO by different commuting modes in Beijing, China. *Science of the Total Environment,* 425, 52-59.
IPAQ RESEARCH COMMITTEE 2005. Guidelines for data processing and analysis of the International Physical Activity Questionnaire (IPAQ)–short and long forms. *Retrieved September,* 17, 2008.
IPSOS MRBI 2015. Healthy Ireland Survey 2015; Summary of Findings. Dublin.
JACOBSEN, P. L. 2003. Safety in numbers: more walkers and bicyclists, safer walking and bicycling. *Injury Prevention,* 9, 205-209.
JARJOUR, S., JERRETT, M., WESTERDAHL, D., DE NAZELLE, A., HANNING, C., DALY, L., LIPSITT, J. & BALMES, J. 2013. Cyclist route choice, traffic-related air pollution, and lung function: a scripted exposure study. *Environmental Health,* 12, 1.
JARRETT, J., WOODCOCK, J., GRIFFITHS, U. K., CHALABI, Z., EDWARDS, P., ROBERTS, I. & HAINES, A. 2012. Effect of increasing active travel in urban England and Wales on costs to the National Health Service. *The Lancet,* 379, 2198-2205.
JERRETT, M., ARAIN, A., KANAROGLOU, P., BECKERMAN, B., POTOGLOU, D., SAHSUVAROGLU, T., MORRISON, J. & GIOVIS, C. 2005. A review and evaluation of intraurban air pollution exposure models. *Journal of Exposure Analysis and Environmental Epidemiology,* 15, 185-204.
JONKERS, S. & VANHOVE, F. 2010. CAR-Vlaanderen V2. 0: Handleiding. *Transport & Mobility Leuven, Leuven*, 69.
KAUR, S. & NIEUWENHUIJSEN, M. 2009. Determinants of personal exposure to PM2. 5, ultrafine particle counts, and CO in a transport microenvironment. *Environmental Science & Technology,* 43, 4737-4743.
KAUR, S., NIEUWENHUIJSEN, M. & COLVILE, R. 2005a. Personal exposure of street canyon intersection users to PM 2.5, ultrafine particle counts and carbon monoxide in Central London, UK. *Atmospheric Environment,* 39, 3629-3641.
KAUR, S., NIEUWENHUIJSEN, M. J. & COLVILE, R. N. 2005b. Pedestrian exposure to air pollution along a major road in Central London, UK. *Atmospheric Environment,* 39, 7307-7320.
KAUR, S., NIEUWENHUIJSEN, M. J. & COLVILE, R. N. 2007. Fine particulate matter and carbon monoxide exposure concentrations in urban street transport microenvironments. *Atmospheric Environment,* 41, 4781-4810.
KELLY, P., KAHLMEIER, S., GÖTSCHI, T., ORSINI, N., RICHARDS, J., ROBERTS, N., SCARBOROUGH, P. & FOSTER, C. 2014. Systematic review and meta-analysis of reduction in all-cause mortality from walking and cycling and shape of dose response relationship. *International Journal of Behavioral Nutrition and Physical Activity,* 11, 132.
KINGHAM, S., LONGLEY, I., SALMOND, J., PATTINSON, W. & SHRESTHA, K. 2013. Variations in exposure to traffic pollution while travelling by different modes in a low density, less congested city. *Environmental Pollution,* 181, 211-218.
KINGHAM, S., MEATON, J., SHEARD, A. & LAWRENSON, O. 1998. Assessment of exposure to traffic-related fumes during the journey to work. *Transportation Research Part D: Transport and Environment,* 3, 271-274.
KLEINER, B. C. & SPENGLER, J. D. 1976. Carbon monoxide exposures of Boston bicyclists. *Journal of the Air Pollution Control Association,* 26, 147-149.

KLOBUCAR, M. S. & FRICKER, J. D. 2007. Network evaluation tool to improve real and perceived bicycle safety. *Transportation Research Record***,** 25-33.
KOLSTAD, C. D. 1985. Review of the literature on bi-level mathematical programming.
KORZHENEVYCH, A., DEHNEN, N., BRÖCKER, J., HOLTKAMP, M., MEIER, H., GIBSON, G., VARMA, A. & COX, V. 2014. Update of the handbook on external costs of transport. *European Commission DG MOVE*.
KOUSOULIDOU, M., NTZIACHRISTOS, L., MELLIOS, G. & SAMARAS, Z. 2008. Road-transport emission projections to 2020 in European urban environments. *Atmospheric Environment,* 42**,** 7465-7475.
KREWSKI, D., JERRETT, M., BURNETT, R. T., MA, R., HUGHES, E., SHI, Y., TURNER, M. C., POPE, C. A., 3RD, THURSTON, G., CALLE, E. E., THUN, M. J., BECKERMAN, B., DELUCA, P., FINKELSTEIN, N., ITO, K., MOORE, D. K., NEWBOLD, K. B., RAMSAY, T., ROSS, Z., SHIN, H. & TEMPALSKI, B. 2009. Extended follow-up and spatial analysis of the American Cancer Society study linking particulate air pollution and mortality. *Research report (Health Effects Institute)***,** 5-114; discussion 115-36.
KUMAR, P., MORAWSKA, L., MARTANI, C., BISKOS, G., NEOPHYTOU, M., DI SABATINO, S., BELL, M., NORFORD, L. & BRITTER, R. 2015. The rise of low-cost sensing for managing air pollution in cities. *Environment International,* 75**,** 199-205.
LANDIS, B., VATTIKUTI, V. & BRANNICK, M. 1997. Real-time human perceptions: toward a bicycle level of service. *Transportation Research Record***,** 119-126.
LAWSON, A. 2015. *An Analysis of Cycling Safety Perceptions and Development of a Bicycle Trip Assignment Methodology.* PhD, Trinity College, Dublin.
LAWSON, A. R., PAKRASHI, V., GHOSH, B. & SZETO, W. V. 2013. Perception of safety of cyclists in Dublin City. *Accident Analysis and Prevention,* 50**,** 499-511.
LEBLANC, L. J., MORLOK, E. K. & PIERSKALLA, W. P. 1975. An efficient approach to solving the road network equilibrium traffic assignment problem. *Transportation Research,* 9**,** 309-318.
LI, Z.-C., YAO, M.-Z., LAM, W. H. K., SUMALEE, A. & CHOI, K. 2015. Modeling the Effects of Public Bicycle Schemes in a Congested Multi-Modal Road Network. *International Journal of Sustainable Transportation,* 9**,** 282-297.
LIN, J.-J. & LIAO, R.-Y. 2014. Sustainability SI: Bikeway Network Design Model for Recreational Bicycling in Scenic Areas. *Networks and Spatial Economics,* 16**,** 9-31.
LIN, J.-J. & YU, C.-J. 2012. A bikeway network design model for urban areas. *Transportation,* 40**,** 45-68.
LIN, J.-R. & YANG, T.-H. 2011. Strategic design of public bicycle sharing systems with service level constraints. *Transportation research part E: logistics and transportation review,* 47**,** 284-294.
LINDSAY, G., MACMILLAN, A. & WOODWARD, A. 2011. Moving urban trips from cars to bicycles: impact on health and emissions. *Australian and New Zealand Journal of Public Health,* 35**,** 54-60.
LOVELACE, R., GOODMAN, A., ALDRED, R., BERKOFF, N., ABBAS, A. & WOODCOCK, J. 2015. The Propensity to Cycle Tool: An open source online system for sustainable transport planning. *arXiv preprint arXiv:1509.04425*.
LUO, Z.-Q., PANG, J.-S. & RALPH, D. 1996. *Mathematical programs with equilibrium constraints*, Cambridge University Press.
MACKIE, P., WORSLEY, T. & ELIASSON, J. 2014. Transport appraisal revisited. *Research in Transportation Economics,* 47**,** 3-18.
MACMILLAN, A., CONNOR, J., WITTEN, K., KEARNS, R., REES, D. & WOODWARD, A. 2014. The Societal Costs and Benefits of Commuter Bicycling: Simulating the Effects of Specific Policies Using System Dynamics Modeling. *Environmental Health Perspectives,* 122**,** 335-344.

MAIZLISH, N., WOODCOCK, J., CO, S., OSTRO, B., FANAI, A. & FAIRLEY, D. 2013. Health cobenefits and transportation-related reductions in greenhouse gas emissions in the San Francisco Bay area. *American journal of public health,* 103**,** 703-9.
MANKIW, N. G. 2011. *Principles of economics*, South-Western Cengage Learning.
MCNABOLA, A., BRODERICK, B. M. & GILL, L. W. 2008. Relative exposure to fine particulate matter and VOCs between transport microenvironments in Dublin: Personal exposure and uptake. *Atmospheric Environment,* 42**,** 6496-6512.
MCNABOLA, A., BRODERICK, B. M. & GILL, L. W. 2009. A principal components analysis of the factors effecting personal exposure to air pollution in urban commuters in Dublin, Ireland. *Journal of Environmental Science and Health Part a-Toxic/Hazardous Substances & Environmental Engineering,* 44**,** 1219-1226.
MENG, Q., LEE, D.-H. & CHEU, L. A bilevel programming approach to simultaneously estimate OD matrix and calibrate link travel time functions from observed link flows. Proceedings of the international conference on applications of advanced technologies in transportation engineering, 2004. 56-60.
MESBAH, M., THOMPSON, R. & MORIDPOUR, S. 2012. Bilevel Optimization Approach to Design of Network of Bike Lanes. *Transportation Research Record***,** 21-28.
MET ÉIREANN. 2016. *Historical Data* [Online]. Available: http://www.met.ie/climate-request/ [Accessed 6/Sep 2017].
MINDELL, J. S., LESLIE, D. & WARDLAW, M. 2012. Exposure-based,'like-for-like'assessment of road safety by travel mode using routine health data. *PloS one,* 7**,** e50606.
MUELLER, N., ROJAS-RUEDA, D., COLE-HUNTER, T., DE NAZELLE, A., DONS, E., GERIKE, R., GÖTSCHI, T., INT PANIS, L., KAHLMEIER, S. & NIEUWENHUIJSEN, M. 2015. Health impact assessment of active transportation: A systematic review. *Preventive Medicine,* 76**,** 103-114.
MURRAY, C. J. L. & ACHARYA, A. K. 1997. Understanding DALYs. *Journal of Health Economics,* 16**,** 703-730.
NAGURNEY, A. 1993. *Network economics: a variational inequality approach,* New York, Springer Science+Business Media, LLC.
NAMDEO, A., BALLARE, S., JOB, H. & NAMDEO, D. 2014. Commuter exposure to air pollution in Newcastle, UK, and Mumbai, India. *Journal of Hazardous, Toxic, and Radioactive Waste,* 20**,** A4014004.
NATIONAL ROADS AUTHORITY 2012. Expansion Factors for Short Period Traffic Counts. *Project Appraisal Guidelines.* Dublin: NRA.
NATIONAL ROADS AUTHORITY 2014. National Transport Model; Model Development Report.
NATIONAL TRANSPORT AUTHORITY 2011a. National Cycle Manual.
NATIONAL TRANSPORT AUTHORITY 2011b. Transport Modelling Report, Greater Dublin Area.
NATIONAL TRANSPORT AUTHORITY 2013. National Household Travel Survey 2012.
NATIONAL TRANSPORT AUTHORITY 2015a. Draft Transport Strategy for the Greater Dublin Area; Transport Modelling Report.
NATIONAL TRANSPORT AUTHORITY 2015b. National Household Travel Survey 2014.
NWOKORO, C., EWIN, C., HARRISON, C., IBRAHIM, M., DUNDAS, I., DICKSON, I., MUSHTAQ, N. & GRIGG, J. 2012. Cycling to work in London and inhaled dose of black carbon. *European Respiratory Journal,* 40**,** 1091-1097.
NYHAN, M., MCNABOLA, A. & MISSTEAR, B. 2014. Comparison of particulate matter dose and acute heart rate variability response in cyclists, pedestrians, bus and train passengers. *Science of The Total Environment,* 468–469**,** 821-831.
OECD DATA. 2016. *Gross Domestic Product (GDP)* [Online]. Available: https://data.oecd.org/gdp/gross-domestic-product-gdp.htm [Accessed 20/June 2016].

OLABARRIA, M., PEREZ, K., SANTAMARINA-RUBIO, E., NOVOA, A. M. & RACIOPPI, F. 2013. Health impact of motorised trips that could be replaced by walking. *European Journal of Public Health,* 23**,** 217-222.
OSTRO, B. 2004. Outdoor air pollution: Assessing the environmental burden of disease at national and local levels. *Environmental Burden of Disease Series, No. 5.* Geneva.
OTT, W. R., STEINEMANN, A. C. & WALLACE, L. A. 2006. *Exposure analysis*, CRC Press.
PANIS, L. I., DE GEUS, B., VANDENBULCKE, G., WILLEMS, H., DEGRAEUWE, B., BLEUX, N., MISHRA, V., THOMAS, I. & MEEUSEN, R. 2010. Exposure to particulate matter in traffic: A comparison of cyclists and car passengers. *Atmospheric Environment,* 44**,** 2263-2270.
PARKIN, J., WARDMAN, M. & PAGE, M. 2007. Models of perceived cycling risk and route acceptability. *Accident Analysis & Prevention,* 39**,** 364-371.
PARKIN, J., WARDMAN, M. & PAGE, M. 2008. Estimation of the determinants of bicycle mode share for the journey to work using census data. *Transportation,* 35**,** 93-109.
PATRIKSSON, P. 1994. *The traffic assignment problem: models and methods*.
PETERS, A., DOCKERY, D. W., MULLER, J. E. & MITTLEMAN, M. A. 2001. Increased particulate air pollution and the triggering of myocardial infarction. *Circulation,* 103**,** 2810-2815.
PINHEIRO, J. C. & BATES, D. M. 2000. *Mixed-Effects Models in S and S-PLUS,* New York, Springer.
POOLEY, C. G., HORTON, D., SCHELDEMAN, G., MULLEN, C., JONES, T., TIGHT, M., JOPSON, A. & CHISHOLM, A. 2013. Policies for promoting walking and cycling in England: A view from the street. *Transport Policy,* 27**,** 66-72.
POPE, C. A., BURNETT, R. T., THUN, M. J., CALLE, E. E., KREWSKI, D., ITO, K. & THURSTON, G. D. 2002. Lung cancer, cardiopulmonary mortality, and long-term exposure to fine particulate air pollution. *Jama-Journal of the American Medical Association,* 287**,** 1132-1141.
POPE, C. A. & DOCKERY, D. W. 2006. Health effects of fine particulate air pollution: Lines that connect. *Journal of the Air & Waste Management Association,* 56**,** 709-742.
PUCHER, J. & BUEHLER, R. 2008. Making cycling irresistible: Lessons from the Netherlands, Denmark and Germany. *Transport Reviews,* 28**,** 495-528.
PUCHER, J. & DIJKSTRA, L. 2003. Promoting safe walking and cycling to improve public health: lessons from the Netherlands and Germany. *American journal of public health,* 93**,** 1509-1516.
PUCHER, J., DILL, J. & HANDY, S. 2010. Infrastructure, programs, and policies to increase bicycling: An international review. *Preventive Medicine,* 50**,** S106-S125.
QUIROS, D. C., LEE, E. S., WANG, R. & ZHU, Y. 2013. Ultrafine particle exposures while walking, cycling, and driving along an urban residential roadway. *Atmospheric Environment,* 73**,** 185-194.
RABL, A. & DE NAZELLE, A. 2012. Benefits of shift from car to active transport. *Transport Policy,* 19**,** 121-131.
RAGETTLI, M. S., CORRADI, E., BRAUN-FAHRLÄNDER, C., SCHINDLER, C., DE NAZELLE, A., JERRETT, M., DUCRET-STICH, R. E., KÜNZLI, N. & PHULERIA, H. C. 2013. Commuter exposure to ultrafine particles in different urban locations, transportation modes and routes. *Atmospheric Environment,* 77**,** 376-384.
RAKOWSKA, A., WONG, K. C., TOWNSEND, T., CHAN, K. L., WESTERDAHL, D., NG, S., MOČNIK, G., DRINOVEC, L. & NING, Z. 2014. Impact of traffic volume and composition on the air quality and pedestrian exposure in urban street canyon. *Atmospheric Environment,* 98**,** 260-270.

RAMOS, C. A., WOLTERBEEK, H. T. & ALMEIDA, S. M. 2016. Air pollutant exposure and inhaled dose during urban commuting: a comparison between cycling and motorized modes. *Air Quality, Atmosphere & Health*, 1-13.
RASPBERRY PI. 2016. *Raspberry Pi 1 Model B* [Online]. Available: https://www.raspberrypi.org/products/model-b/ [Accessed 29/Sep/2016.
RICHARDSON, G. P. 2011. Reflections on the foundations of system dynamics. *System Dynamics Review,* 27, 219-243.
ROAD SAFETY AUTHORITY 2011, 2012. Road Collision Facts Ireland 2011, 2012.
ROAD SAFETY AUTHORITY 2012. Motorway Driving.
ROBINSON, D. L. 2005. Safety in numbers in Australia: more walkers and bicyclists, safer walking and bicycling. *Health promotion journal of Australia : official journal of Australian Association of Health Promotion Professionals,* 16, 47-51.
ROJAS-RUEDA, D., DE NAZELLE, A., ANDERSEN, Z. J., BRAUN-FAHRLÄNDER, C., BRUHA, J., BRUHOVA-FOLTYNOVA, H., DESQUEYROUX, H., PRAZNOCZY, C., RAGETTLI, M. S. & TAINIO, M. 2016. Health impacts of active transportation in Europe. *PloS one,* 11, e0149990.
ROJAS-RUEDA, D., DE NAZELLE, A., TAINIO, M. & NIEUWENHUIJSEN, M. J. 2011. The health risks and benefits of cycling in urban environments compared with car use: health impact assessment study. *British Medical Journal,* 343, 8.
ROJAS-RUEDA, D., DE NAZELLE, A., TEIXIDO, O. & NIEUWENHUIJSEN, M. J. 2012. Replacing car trips by increasing bike and public transport in the greater Barcelona metropolitan area: A health impact assessment study. *Environment International,* 49, 100-109.
ROJAS-RUEDA, D., DE NAZELLE, A., TEIXIDÓ, O. & NIEUWENHUIJSEN, M. J. 2013. Health impact assessment of increasing public transport and cycling use in Barcelona: A morbidity and burden of disease approach. *Preventive Medicine,* 57, 573-579.
RUTTER, H., CAVILL, N., RACIOPPI, F., DINSDALE, H., OJA, P. & KAHLMEIER, S. 2013. Economic Impact of Reduced Mortality Due to Increased Cycling. *American Journal of Preventive Medicine,* 44, 89-92.
SAMOLI, E., TOULOUMI, G., SCHWARTZ, J., ANDERSON, H. R., SCHINDLER, C., FORSBERG, B., VIGOTTI, M. A., VONK, J., KOŠNIK, M. & SKORKOVSKY, J. 2007. Short-term effects of carbon monoxide on mortality: an analysis within the APHEA project. *Environmental Health Perspectives*, 1578-1583.
SCHEPERS, P., FISHMAN, E., BEELEN, R., HEINEN, E., WIJNEN, W. & PARKIN, J. 2015. The mortality impact of bicycle paths and lanes related to physical activity, air pollution exposure and road safety. *Journal of Transport & Health,* 2, 460-473.
SEATON, A., CHERRIE, J., DENNEKAMP, M., DONALDSON, K., HURLEY, J. F. & TRAN, C. L. 2005. The London Underground: dust and hazards to health. *Occupational and Environmental Medicine,* 62, 355-362.
SENER, I. N., ELURU, N. & BHAT, C. R. 2009. An analysis of bicycle route choice preferences in Texas, US. *Transportation,* 36, 511-539.
SHEFFI, Y. 1985. *Urban Transportation Networks: Equilibrium Analysis with Mathematical Programming Methods,* Englewood Cliffs, N. Prentice Hall.
SHORT, J. & CAULFIELD, B. 2014. The safety challenge of increased cycling. *Transport Policy,* 33, 154-165.
SI, B., YAN, X., SUN, H., YANG, X. & GAO, Z. 2012. Travel Demand-Based Assignment Model for Multimodal and Multiuser Transportation System. *Journal of Applied Mathematics,* 2012, 22.
SI, B., ZHANG, H., ZHONG, M. & YANG, X. 2011. Multi-criterion system optimization model for urban multimodal traffic network. *Science China Technological Sciences,* 54, 947-954.
SMARTER TRAVEL 2009. National Cycle Policy Framework 2009-2020. Department of Transport, Tourism and Sport.

SMITH, H. L. & HAGHANI, A. A mathematical optimization model for a bicycle network design considering bicycle level of service. Transportation Research Board 91st Annual Meeting, 2012.
SMITH, M. J. 1979. Existence, uniqueness and stability of traffic equilibria. *Transportation Research Part B-Methodological,* 13**,** 295-304.
SNYDER, E. G., WATKINS, T. H., SOLOMON, P. A., THOMA, E. D., WILLIAMS, R. W., HAGLER, G. S. W., SHELOW, D., HINDIN, D. A., KILARU, V. J. & PREUSS, P. W. 2013. The Changing Paradigm of Air Pollution Monitoring. *Environmental Science & Technology,* 47**,** 11369-11377.
SPADARO, J. V. & RABL, A. 2008. Estimating the uncertainty of damage costs of pollution: A simple transparent method and typical results. *Environmental Impact Assessment Review,* 28**,** 166-183.
STEINLE, S., REIS, S. & SABEL, C. E. 2013. Quantifying human exposure to air pollution—Moving from static monitoring to spatio-temporally resolved personal exposure assessment. *Science of The Total Environment,* 443**,** 184-193.
STEINLE, S., REIS, S., SABEL, C. E., SEMPLE, S., TWIGG, M. M., BRABAN, C. F., LEESON, S. R., HEAL, M. R., HARRISON, D., LIN, C. & WU, H. 2015. Personal exposure monitoring of PM2.5 in indoor and outdoor microenvironments. *Science of The Total Environment,* 508**,** 383-394.
STIEB, D. M., JUDEK, S. & BURNETT, R. T. 2002. Meta-analysis of time-series studies of air pollution and mortality: Effects of gases and particles and the influence of cause of death, age, and season. *Journal of the Air & Waste Management Association,* 52**,** 470-484.
SUBHANI, A., STEPHENS, D., KUMAR, R. & VOVSHA, P. 2013. Incorporating Cycling in Ottawa - Gatineau Travel Forecasting Model. *Conference of the Transportation Association of Canada.* Winnipeg, Manitoba.
SUH, S. & KIM, T. J. 1989. Solving nonlinear bilevel programming models of the equilibrium network design problem: A comparative review. *Annals of Operations Research,* 34**,** 203-218.
SUH, S., PARK, C.-H. & KIM, T. J. 1990. A highway capacity function in Korea: Measurement and calibration. *Transportation Research Part A: General,* 24**,** 177-186.
SUSTAINABLE ENERGY AUTHORITY OF IRELAND 2016. Energy-Related Emissions from Fuel Combustion 2016 Report. *In:* UNIT, E. P. S. S. (ed.).
SUSTRANS Costs and sources of funding. *Connect2 Greenways Guide.*
SUSTRANS 2014. Handbook for cycle-friendly design. *Sustrans Design Manual.*
TAINIO, M., OLKOWICZ, D., TERESIŃSKI, G., DE NAZELLE, A. & NIEUWENHUIJSEN, M. J. 2014. Severity of injuries in different modes of transport, expressed with disability-adjusted life years (DALYs). *BMC public health,* 14**,** 1.
TAPP, A. & PARKIN, J. 2015. The use of social marketing in promoting cycling. *Cycling Futures: From Research into Practice.* Farnham, Surrey, UK: Ashgate.
TEIKARI, M., LINNAINMAA, M., LAITINEN, J., KALLIOKOSKI, P., VINCENT, J., TIITTA, P. & RAUNEMAA, T. 2003. Laboratory and field testing of particle size-selective sampling methods for mineral dusts. *AIHA Journal,* 64**,** 312-318.
THE MATHWORKS INC. 2016. Matlab R2016b. Natick, MA: The MathWorks Inc.
TILAHUN, N. Y., LEVINSON, D. M. & KRIZEK, K. J. 2007. Trails, lanes, or traffic: Valuing bicycle facilities with an adaptive stated preference survey. *Transportation Research Part A-Policy and Practice,* 41**,** 287-301.
TIWARY, A., ROBINS, A., NAMDEO, A. & BELL, M. 2011. Air flow and concentration fields at urban road intersections for improved understanding of personal exposure. *Environment International,* 37**,** 1005-1018.
TOBÍAS, A., DÍAZ, J., SAEZ, M. & ALBERDI, J. C. 2001. Use of Poisson regression and Box–Jenkins models to evaluate the short-term effects of environmental noise

levels on daily emergency admissions in Madrid, Spain. *European journal of epidemiology,* 17**,** 765-771.
TOBIN, R. L. 1986. Sensitivity analysis for variational inequalities. *Journal of Optimization Theory and Applications,* 48**,** 191-204.
TOBIN, R. L. & FRIESZ, T. L. 1988. Sensitivity analysis for equilibrium network flow. *Transportation Science,* 22**,** 242-250.
TRB, H. C. M. 2000. Transportation Research Board. *Washington, DC*.
TURNER, S., HUGHES, T., ALLATT, T., WOOD, G. & LUO, Q. W. 2010. Cycle safety - measuring the crash risk. *Road & Transport Research,* 19**,** 20-31.
U.S. DEPARTMENT OF COMMERCE AND BUREAU OF PUBLIC ROADS 1964. Traffic Assignment Manual. Washington, D.C.
US DEPARTMENT OF COMMERCE AND BUREAU OF PUBLIC ROADS 1964. Traffic Assignment Manual.
US EPA. *National Trends in Sulfur Dioxide Levels* [Online]. Available: http://www.epa.gov/air/airtrends/sulfur.html [Accessed 14/Jan/14.
VAN RENTERGHEM, T., THOMAS, P., DOMINGUEZ, F., DAUWE, S., TOUHAFI, A., DHOEDT, B. & BOTTELDOOREN, D. 2011. On the ability of consumer electronics microphones for environmental noise monitoring. *Journal of Environmental Monitoring,* 13**,** 544-552.
VANDENBULCKE, G., DUJARDIN, C., THOMAS, I., DE GEUS, B., DEGRAEUWE, B., MEEUSEN, R. & PANIS, L. I. 2011. Cycle commuting in Belgium: spatial determinants and 're-cycling'strategies. *Transportation research part A: policy and practice,* 45**,** 118-137.
VANWIJNEN, J. H., VERHOEFF, A. P., JANS, H. W. A. & VANBRUGGEN, M. 1995. THE EXPOSURE OF CYCLISTS, CAR DRIVERS AND PEDESTRIANS TO TRAFFIC RELATED AIR-POLLUTANTS. *International Archives of Occupational and Environmental Health,* 67**,** 187-193.
VLACHOKOSTAS, C., ACHILLAS, C., MICHAILIDOU, A. V. & MOUSSIOPOULOS, N. 2012. Measuring combined exposure to environmental pressures in urban areas: An air quality and noise pollution assessment approach. *Environment International,* 39**,** 8-18.
WALDMAN, M., WEISS, S. & ARTICOLA, W. 1977. A study of the health effects of bicycling in an urban atmosphere.
WARDMAN, M., TIGHT, M. & PAGE, M. 2007. Factors influencing the propensity to cycle to work. *Transportation Research Part A: Policy and Practice,* 41**,** 339-350.
WEICHENTHAL, S., KULKA, R., DUBEAU, A., MARTIN, C., WANG, D. & DALES, R. 2011. Traffic-related air pollution and acute changes in heart rate variability and respiratory function in urban cyclists. *Environ Health Perspect,* 119.
WHO. *WHO Mortality Database* [Online]. Available: http://www.who.int/healthinfo/mortality_data/en/ [Accessed 20/June 2016].
WHO. 2005. *Air Quality Guidelines, Global Update* [Online]. Available: http://www.euro.who.int/__data/assets/pdf_file/0005/78638/E90038.pdf [Accessed 14/Jan/14.
WHO 2010. Global Recommendations on Physical Activity for Health. Geneva: World Health Organization.
WHO. 2011. *Health Economic Assessment Tools (HEAT) for Walking and for Cycling. Methodology and User Guide* [Online]. Available: http://www.euro.who.int/__data/assets/pdf_file/0003/155631/E96097rev.pdf [Accessed 18 Mar 2014].
WHO 2014. Health economic assessment tools (HEAT) for walking and for cycling; Methods and user guide, 2014 update.
WINTERS, M. & TESCHKE, K. 2010. Route Preferences Among Adults in the Near Market for Bicycling: Findings of the Cycling in Cities Study. *American Journal of Health Promotion,* 25**,** 40-47.

WOODCOCK, J., EDWARDS, P., TONNE, C., ARMSTRONG, B. G., ASHIRU, O., BANISTER, D., BEEVERS, S., CHALABI, Z., CHOWDHURY, Z., COHEN, A., FRANCO, O. H., HAINES, A., HICKMAN, R., LINDSAY, G., MITTAL, I., MOHAN, D., TIWARI, G., WOODWARD, A. & ROBERTS, I. 2009. Health and Climate Change 2 Public health benefits of strategies to reduce greenhouse-gas emissions: urban land transport. *Lancet,* 374**,** 1930-1943.

WOODCOCK, J., FRANCO, O. H., ORSINI, N. & ROBERTS, I. 2011. Non-vigorous physical activity and all-cause mortality: systematic review and meta-analysis of cohort studies. *International Journal of Epidemiology,* 40**,** 121-138.

WOODCOCK, J., GIVONI, M. & MORGAN, A. S. 2013. Health Impact Modelling of Active Travel Visions for England and Wales Using an Integrated Transport and Health Impact Modelling Tool (ITHIM). *Plos One,* 8**,** 17.

WOODCOCK, J., TAINIO, M., CHESHIRE, J., O'BRIEN, O. & GOODMAN, A. 2014. Health effects of the London bicycle sharing system: health impact modelling study. *BMJ,* 348.

WORLD HEALTH ORGANISATION. 2013. *WHO methods and data sources for global burden of disease estimates 2000-2011* [Online]. Geneva: Department of Health Statistics and Information Systems, WHO. Available: http://www.who.int/healthinfo/global_burden_disease/estimates/en/index2.html [Accessed 1/Dec/2016 2016].

WORLD HEALTH ORGANIZATION 2014. WHO Methods and Data Sources for Country-level Causes of Death 2000–2012. *Global Health Estimates Technical Paper WHO/HIS/HSI/GHE/2014.7. Geneva: Department of Health Statistics and Information Systems, World Health Organization*.

XU, G., LAM, W. & CHAN, K. 2004. Integrated approach for trip matrix updating and network calibration. *Journal of transportation engineering,* 130**,** 231-244.

XU, X., CHEN, A. & YANG, C. 2016. A review of sustainable network design for road networks. *KSCE Journal of Civil Engineering,* 20**,** 1084-1098.

YANG, C. & CHEN, A. 2009. Sensitivity analysis of the combined travel demand model with applications. *European Journal of Operational Research,* 198**,** 909-921.

YANG, H., MENG, Q. & BELL, M. G. H. 2001. Simultaneous estimation of the origin-destination matrices and travel-cost coefficient for congested networks in a stochastic user equilibrium. *Transportation Science,* 35**,** 107-123.

YIN, Y. F. 2000. Genetic-algorithms-based approach for bilevel programming models. *Journal of Transportation Engineering-Asce,* 126**,** 115-120.

YU, Q., LU, Y., XIAO, S., SHEN, J., LI, X., MA, W. & CHEN, L. 2012. Commuters' exposure to PM 1 by common travel modes in Shanghai. *Atmospheric environment,* 59**,** 39-46.

ZUURBIER, M., HOEK, G., OLDENWENING, M., LENTERS, V., MELIEFSTE, K., VAN DEN HAZE, P. & BRUNEKREEF, B. 2010. Commuters' Exposure to Particulate Matter Air Pollution Is Affected by Mode of Transport, Fuel Type, and Route. *Environmental Health Perspectives,* 118**,** 783-789.

ZUURBIER, M., HOEK, G., VAN DEN HAZEL, P. & BRUNEKREEF, B. 2009. Minute ventilation of cyclists, car and bus passengers: an experimental study. *Environmental Health,* 8**,** 10.